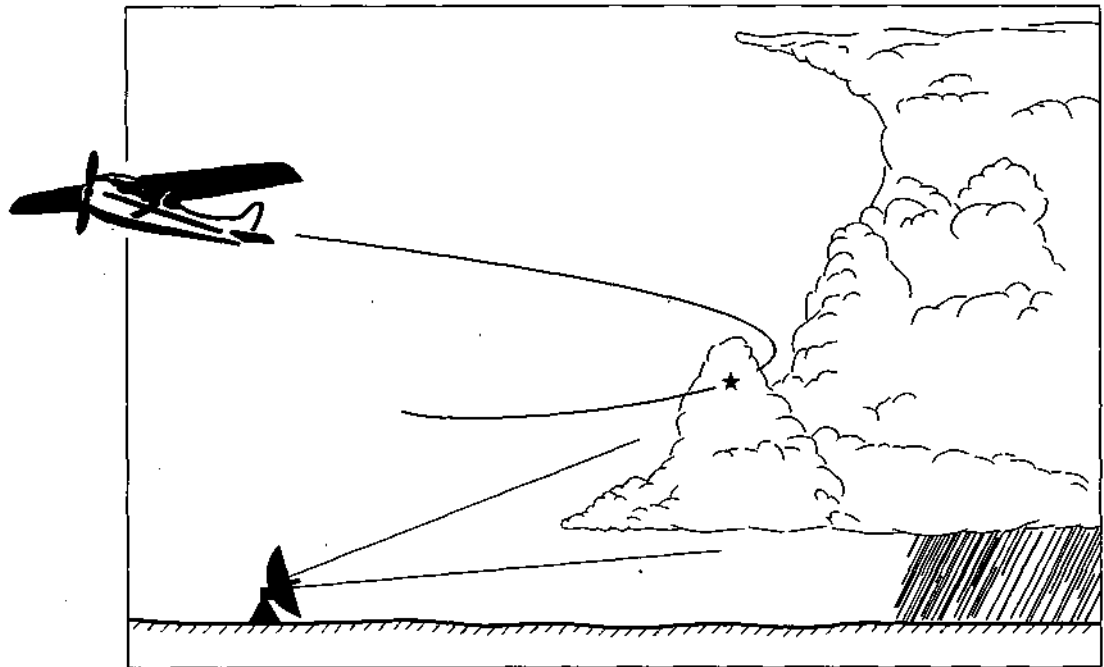


BULLETIN 72

Results from the 1989 Exploratory Cloud Seeding Experiment in Illinois

by
Robert R. Czys, Stanley A. Changnon, K. Ruben Gabriel
Mary Schoen Petersen, Robert W. Scott, and Nancy E. Westcott



Illinois State Water Survey
Department of Energy and Natural Resources

1993

BULLETIN 72



Results from the 1989 Exploratory Cloud Seeding Experiment in Illinois

by

Robert R. Czys, Stanley A. Changnon, K. Ruben Gabriel,
Mary Schoen Petersen, Robert W. Scott, and Nancy E. Westcott

Title: Results from the 1989 Exploratory Cloud Seeding Experiment in Illinois.

Abstract: An exploratory cloud seeding experiment designed to modify clouds to augment rainfall was conducted in Illinois during the summer of 1989. This field experiment was carried out as part of the Precipitation Augmentation for Crops Experiment (PACE) initiated by the Illinois State Water Survey in 1978 with support from the National Oceanic and Atmospheric Administration. Findings after adjusting for sample bias indicate visual evidence for seeding effects on cloud tops; no evidence of enhancement in echo size or growth from seeding; and a weak suggestion of a possible rain increase in cloud groups that had been treated with silver iodide. This report also considers the implications that the results pose for the design and direction of future weather modification research, as well as for the practical use of cloud seeding in Illinois.

Reference: Czys, R.R., S.A. Changnon, K.R. Gabriel, M.S. Petersen, R.W. Scott, and N.E. Westcott, Results from the 1989 Exploratory Cloud Seeding Experiment in Illinois, Illinois State Water Survey, Champaign, Bulletin 72.

Indexing Terms: Cloud seeding, weather modification, precipitation enhancement, dynamic seeding hypothesis, cloud physics, radar meteorology, forecasting, predictor variables, response variables, sample bias, radar-estimated rainfall.

**STATE OF ILLINOIS
HON. JIM EDGAR, Governor**

**DEPARTMENT OF ENERGY AND NATURAL RESOURCES
John S. Moore, B.S., Director**

BOARD OF NATURAL RESOURCES AND CONSERVATION

John S. Moore, B.S., Chair
Robert H. Benton, B.S.C.E., Engineering
Donna M. Jurdy, Ph.D., Geology
H.S. Gutowsky, Ph.D., Chemistry
Roy L Taylor, Ph.D., Plant Biology
Robert I_ Metcalf, Ph.D., Biology
W.R. (Reg) Gomes, Ph.D.
University of Illinois
John H. Yopp, Ph.D.
Southern Illinois University

**STATE WATER SURVEY DIVISION
Mark E. Peden, Acting Chief**

**2204 GRIFFITH DRIVE
CHAMPAIGN, ILLINOIS 61820-7495**

1993

ISSN 0360-9804

*Funds derived from grants and contracts administered by
the University of Illinois were used to produce this report.*

This report was printed on recycled and recyclable papers.

Printed by authority of the State of Illinois (10-93-150)

CONTENTS

	Page
1. Introduction	2
Preface	2
Background	2
Modification Hypothesis	5
The 1989 Field Project	6
Epilogue	8
Acknowledgments	8
Figures and Tables for Chapter 1	9
2. Data Assessment and Comparison of Predictor and Response Variables	15
Overview	15
The Data Set	15
Rerandomization Procedure	16
Comparison of Predictors and Responses	16
Atmospheric Variability during the Experiment	17
Targeting of Seeding Material	18
Conclusions	18
Figures and Tables for Chapter 2	19
3. Visual Assessment of Seeding Effects	39
Introduction	39
Analysis of the Results	39
Summary	39
Tables for Chapter 3	41
4. Evaluation Based on Synoptic Weather Conditions	43
Introduction	43
Data and Analysis	44
Weather Conditions	46
Comparison of Echo Properties of Cold-Front and Air-Mass Cases	47
Evaluation of Potential Seeding Effects	49
Variability within Day and within Synoptic Category	50
Summary and Conclusions	51
Figures and Tables for Chapter 4	53
5. Evaluation Utilizing a Seedability Index	75
Introduction	75
Development of the Seedability Index	75
Determination of SI Ratings	76
Application of the Seedability Index	77
Key Findings	77
Discussion	79
Conclusions	80
Figures and Tables for Chapter 5	81
6. Statistical Significance of the Effects of Seeding Individual Illinois Clouds in Illinois in 1989	99
Design of the 1989 Experiment	99
The Data	99
Methods of Analysis	99
Analysis of Individual Predictors and Responses	100

Analysis of Responses Adjusted for Some of the Predictors.100
Conclusions100
Tables for Chapter 6.101
7. Comparison of Cloud Seeding Results from Illinois and Texas.105
Introduction105
Experimental Design, Data, and Analysis.105
Echo Characteristics at Treatment108
Assessment of Sampling Bias.108
Comparison of Echo Responses to Treatment109
Comparison of Experimental Unit Rainfall111
Conclusions.112
Figures and Tables for Chapter 7.115
8. Rainfall Assessment125
Introduction125
Data and Analyses.125
Regional Rainfall Conditions.125
Evaluation of Seeded Rainfall Amounts.126
Summary.127
Figures and Tables for Chapter 8.129
9. Summary, Conclusions, and Recommendations.139
Summary.139
A Possible Alternative Hypothesis.141
Conclusions.142
Recommendations.142
Appendix A. Synoptic Variables, Abbreviations and Definitions.145
Appendix B. Radar Variables, Abbreviations and Definitions.146
Appendix C. Aircraft Variables, Abbreviations and Definitions.149
References.151

RESULTS FROM THE 1989 EXPLORATORY CLOUD SEEDING EXPERIMENT IN ILLINOIS

Executive Summary

A randomized exploratory cloud seeding experiment was conducted in Illinois from mid-May through July 1989. The experiment was designed around the dynamic seeding hypothesis with the intent to investigate whether silver iodide seeding near the tops of growing cumulus clouds increased individual cloud growth and/or longevity and enhanced cloud system rainfall. Treatment randomization was based on a "floating" experimental unit encompassing the cloud system to obtain a 50/50 split between clouds and cloud systems that received silver iodide treatment and those that received sand treatment as a placebo. Allocation and delivery of the seeding material was devised so that project scientists and other personnel were unaware of the type of treatment used.

During the course of the experiment, 82 clouds were treated, 36 with sand (in six experimental units) and 46 with silver iodide (also in six units). Most findings from the summer experiment are based on analysis of 67 clouds that produced trackable radar echo cores, 35 treated with silver iodide and 32 treated with sand. The analysis focused on 13 predictor variables that described the synoptic, in-cloud, and radar properties prior to and at treatment, and 11 response variables based on radar measurements. Comparison of predictor variable means and extremes revealed a statistically significant sample difference between silver iodide and control clouds, even though every effort was made to randomly select "similar" clouds according to a strict set of visual and in-cloud criteria. Thus, the 1989 experiment resulted in a classic example of the "bad draw."

In spite of the sample bias, the experiment produced a number of important findings about cloud and rainfall modification in Illinois. These findings relate to effects on clouds that could be seen, effects measured by the radar properties of individual echo cores, and effects on radar-estimated rainfall. To test whether seeding effects could be observed in outward cloud appearance, the pilot and the flight meteorologist kept independent records of what type of effect they thought occurred in each experimental unit. This test revealed a very high level of skill for the cloud seeding pilot and marginal skill for the flight meteorologist in assessing seeding effects in outward cloud appearance. This finding implies that treatment dosages were large enough to enhance cloud glaciation, and thus alter cloud appearances.

Analyses used to eliminate the sample bias revealed that no conclusion could be drawn for seeding effects in clouds that developed under cold-front conditions. Analysis of clouds that developed during air-mass conditions revealed essentially no seeding effect. Further analysis and comparison among clouds with high suitability for dynamic seeding indicated that if seeding had any effect at all, it negatively affected echo-core height, area, and reflectivity. Curiously, clouds characterized by low seeding suitability showed weak evidence of positive seeding effects. These findings are generally not expected to occur from the dynamic seeding technique, and taken alone, they suggest that its use does not produce desired results in echo-core behavior.

An analysis using median radar-estimated rainfall suggested that precipitation enhancement may have occurred at the scale of the rain cloud system, in spite of possible negative effects on individual clouds. However, sample size was too small to draw firm conclusions.

When taken together, the results raise questions about the validity of using the dynamic seeding hypothesis in Illinois. The findings are sufficiently negative to call for either a major revision in the modification hypothesis or rejection of the dynamic hypothesis in favor of an alternative seeding technique. They also suggest that the present technology needs advancement for the practical use of cloud seeding in Illinois to produce more than marginal benefits.

1. INTRODUCTION

by

Robert R. Czys and Stanley A. Changnon

Preface

An exploratory cloud seeding experiment designed to modify clouds to augment rainfall was conducted in Illinois during the summer of 1989. The project resulted in several key findings about clouds and rainfall modification in Illinois, and they are presented in this report. This field experiment was conducted as part of the ongoing Precipitation Augmentation for Crops Experiment (PACE), which was initiated by the Illinois State Water Survey (ISWS) in 1978.

Background

The 1989 cloud and precipitation modification experiment represented a major step forward in the long-term weather research program of the ISWS. Study of the possibility of increasing rainfall for agricultural benefit in Illinois is rooted in a major Water Survey research program initiated in the 1950s. At that time, a broad goal of the Survey's endeavors was "water for Illinois agriculture." Areas of investigation developed as part of this broad goal have included:

1. The suppression of pond and lake evaporation and the reduction of evapotranspiration from growing crops.
2. The use of irrigation and its development across Illinois.
3. Weather modification to serve agricultural purposes.

The history of the Water Survey's weather modification research includes studies in planned weather modification and inadvertent or accidental weather modification due to human activities. (For additional information about PACE see Changnon, 1979, 1980a; and Changnon et al., 1991a).

Weather modification-related research began in 1959 with climatic studies of possible urban modification of precipitation. Farmers in the Vandalia area experiencing a localized drought in 1963-1964 raised funds and hired commercial cloud seeding services. The county Extension agents asked Water Survey scientists to provide scientific and technical advice and to evaluate the potential outcome, either more rain or less. This event led Water Survey scientists into further studies of Illinois rainfall data to evaluate potential shifts in rainfall due to purposeful modification endeavors.

During 1969-1970, a federal grant enabled Water Survey scientists to join with agricultural economists at the University of Illinois to launch the state's first multidisciplinary study related to weather modification. This study focused on the development of methods using Illinois data to estimate the effects of additional rainfall on corn and soybean yields, including the

economic outcomes from different levels of rainfall change. This research demonstrated that enhancement of summer rainfall, depending on the amount of change and the season, could benefit Illinois agriculture (Huff and Changnon, 1972).

This effort, coupled with the scientific capabilities of the Survey, led to a major multiyear program in 1970, the Precipitation Enhancement Project (PEP), which was funded by the U.S. Bureau of Reclamation. It was designed to answer two questions: 1) can summer rainfall in Illinois be enhanced, and 2) how would enhanced summer rainfall affect the environment and the state's economy? The resulting social, economic, and environmental analyses of 1971-1973 pointed to the viability of summer rainfall enhancement for Illinois agriculture. It further illustrated the need for extensive public information about such research and experimentation, and the need for a law that regulated cloud seeding projects in Illinois.

In 1973, with the support of the Illinois Farm Bureau, legislation was passed regulating the use of weather modification in Illinois (Ackerman et al., 1974), and the new Illinois statute became a model state law for this purpose [Weather Modification Advisory Board (WMAB) 1978]. However, PEP ended suddenly in 1973 with a reduction in federal spending for weather modification as the result of territorial disagreements among federal agencies that were funding and conducting weather modification activities (Changnon, 1973).

In the meantime, 1967-1970, Water Survey scientists were aggressively pursuing studies of urban effects on clouds and precipitation. Water Survey researchers reviewed historical data that indicated that large cities like St. Louis and Chicago produce increases in warm-season rainfall. These studies fostered considerable public and scientific interest at the state and national levels. This national interest led Water Survey scientists, in conjunction with scientists of several other institutions, to plan the Metropolitan Meteorological Experiment (METROMEX). This large field program was conducted in the St. Louis area from 1971 through 1975, and involved 100 scientists and a large variety of meteorological field instruments, including 250 recording raingages, meteorological aircraft, and six radar systems. METROMEX results demonstrated how a large metropolitan area affects clouds and enhances summer rainfall and storms (Changnon et al., 1981), and it produced unique information about the modification of atmospheric processes relating to summer rainfall (ibid.).

In 1975, the U.S. Bureau of Reclamation asked Water Survey scientists to design a national weather modification experiment to be conducted in the High Plains region of the country, reflecting the breadth and quality of staff skills in this

area. The High Plains Experiment (HIPLEX) was designed during 1976-1977.

Another series of important activities also began in 1976 in Illinois. Farmers and agribusinesses in a five-county area centered on Mattoon raised funds, hired a cloud seeding firm, and launched a summer cloud seeding project to produce more rain to improve yields. The Water Survey became an adviser in the process, both in its licensing through the state; and by scientifically evaluating the project. Additional seeding projects developed in Illinois in the next six years. By the end of 1981, eight projects had been conducted in the state; and during two years, cloud seeding was conducted over 10 percent of the state's total area to enhance summer rainfall. Analyses provided some weak indication that in the more carefully conducted projects, the seeded areas received more rain than surrounding areas (Changnon and Hsu, 1981). Unfortunately, though, the "seed-everything" approach of these nonexperimental projects makes it impossible to establish cause and effect.

Cloud seeding by agricultural interests in several Illinois locations during the late 1970s was accompanied by similar seeding projects in Michigan and Indiana. Collectively, these projects raised fundamental information/guidance questions for the agricultural scientific communities in these states, as well as at the University of Illinois.

As a result of the rapidly growing interest in this new technology, the Illinois State Water Survey joined with the Colleges of Agriculture at the University of Illinois, Michigan State University, Purdue University, and Ohio State University to plan a major multiyear research program to assess the feasibility and potential effects of summer rain enhancement in the Midwest.

These five groups, under the leadership of the Water Survey, developed the proposal for the PACE program. It was submitted to the Weather Modification Program Office of the National Oceanic and Atmospheric Administration (NOAA) in 1978. At that time, NOAA was conducting a major cloud seeding research project in Florida (FACE) and was also funding other weather modification research. NOAA provided limited funding to initiate the weather research at the Water Survey, but not the impacts studies. Impact research in this five-group proposal was largely to be conducted at the four state universities. With this limited funding, PACE began a series of meteorological background studies in Illinois during 1978-1979.

A flow diagram (figure 1) shows the dimensions of PACE as envisioned at that time. PACE was designed as a three-phase project, and as shown, each phase included meteorological studies and impact studies. Phase 1, launched in 1979, was the pre-experiment phase. It was designed to collect enough data to determine if there was a testable hypothesis for modifying summer rainfall and a rationale to justify launching experimental field trials to modify clouds and rainfall. Phase 2, the experiment phase, consisted of two parts: the cloud group

experiment and the area rain experiment. Part A, the cloud experimentation, was to focus on exploratory research of clouds and cloud groups, the evaluation of seeding effects on these clouds, and continuing hypothesis refinement. As shown in figure 1, part A incorporated a major decision as to whether results were sufficiently positive to proceed into a more elaborate area, confirmation-type experiment.

The funding obtained from NOAA for the pre-experimental work during 1978-1981 was much less than requested, limiting the meteorological research and delaying the impact research. Suddenly, and for the second time in ten years, NOAA terminated federal support for the Water Survey's multiyear weather modification project in 1981. This termination was related to a decision at NOAA to end all weather modification research, an action related to the new administration's desire to reduce support for applied scientific research (Changnon, 1973; Changnon and Lambright, 1987).

Illinois joined with weather research groups in three other states, whose research support was also terminated by NOAA, to seek congressional restoration of the funding. In 1983 Congress restored the funding for the resumption of Illinois' PACE and for research endeavors in three other states (North Dakota, Nevada, and Utah).

During 1983-1985, the pre-experiment phase of PACE was completed and a testable hypothesis was developed, along with the design of a field experiment, which would be phase 2 of PACE (Ackerman, 1986). The results indicated that "the dynamic seeding hypothesis" could be used to enhance summer cumulus clouds in Illinois (Bethwait et al., 1966; Simpson et al., 1967; Dennis and Koscielski, 1972; Ackerman et al., 1979; Cooper and Lawson, 1984; Morrison et al., 1986; Ackerman, 1986; Kraus et al., 1987; Rosenfeld and Woodley, 1989; Hudak and List, 1988). The hypothesis is described later in this chapter.

The first field experiment was launched in 1986, but data collection was limited because dry conditions prevailed during the two-month operational season. However, sufficient data were collected to improve the design for the next experiment, scheduled for 1988. Annual efforts were needed to get congressional restoration of the project support, since the administration refused to allocate federal budget funds for weather modification research. This process led to frequent delays in the receipt of annual funding from NOAA and continuing problems related to NOAA's efforts to redirect funding for in-house purposes. Such delays kept the Water Survey from conducting the field experiment planned for the summer of 1988. It was rescheduled after many administrative problems and finally conducted during the summer of 1989. This experiment, the data it produced, and the ensuing analyses are the major focus of this report.

Other key events in recent years have shaped the dimensions of weather modification research at the Water Survey. The 1980s witnessed growing scientific awareness of the potential for a global climate change. Interestingly, much of the

scientific belief in the human factors in climate change stemmed from earlier Water Survey findings on how St. Louis and Chicago change their local/regional climates. New interests and concerns about inadvertent climate modification developed around influences such as jet aircraft and large-scale land use changes. Thus, in 1987, the scope of the research under PACE was broadened to include studies of inadvertent weather modification.

The inability to obtain NOAA funding during 1978-1981 for studies of the impacts of altered weather, which had been planned for PACE, limited such endeavors. Hence, with the resumption of funding through Congress in 1983, essential research could begin in this area. Work with agricultural economists at the University of Illinois over a three-year period led to the development of a national econometric model that allowed estimates of the effects of changed weather on the feed/livestock complex. These estimates led in turn to calculations of the economic benefits at the state, regional, and national levels (Garcia et al., 1990). This model revealed that enhanced summer rainfall in certain crop districts in Illinois would have sizable regional and national benefits.

A second major area of impact research related to the development of a basin-scale hydrologic model by Water Survey hydrologists. This detailed model made it possible to measure the distribution of additional rainfall through the hydrologic cycle in wet and dry years (Knapp et al., 1988).

Of singular importance in the renewed impacts research was definitive information on the effects of altered rainfall on Illinois' two major crops, corn and soybeans, under current management practices. To this end, staff scientists and University of Illinois agronomists began field research at the University of Illinois farms in 1987. These interesting results are also the subject of a Water Survey report (Hollinger and Changnon, 1993).

By 1989, the dimensions of PACE included cloud seeding research, inadvertent weather modification research, and impacts research. A new and revised program with broader goals was initiated, the Illinois Precipitation, Cloud Changes and Impact Project (PreCCIP). Its two general goals were to assess how clouds and precipitation were being modified in Illinois (either accidentally or purposefully) and to assess the potential impacts of these changes on Illinois, with a focus on agriculture and water resources.

Goals of this Report

The 1989 field experiment obtained sufficient cloud and precipitation data to allow exploration of a few of the critical questions related to cloud modification as a means of testing certain steps in the dynamic cloud modification hypothesis.

The description of phase 2 (figure 1) shows that part A is a cloud experiment whose objectives were to 1) continue the evaluation of seeding effects, emphasizing physical param-

eters; and 2) refine the hypothesis and redesign future experimentation. The high costs of field experimentation in weather modification and the broadening of the PreCCIP program to other areas, including inadvertent weather modification and weather change impacts, made it imperative to assess the totality of the 1989 results. These results will determine the need for and type of future experimentation in cloud and rainfall modification in Illinois. This report presents, in great detail, the results thus far obtained in order to help make well-informed decisions about future research.

Scope of the Report

Chapter 1 presents the purpose and scope of the report and includes a discussion of the relevant history behind the 1989 cloud and rain modification experiment. Also included is a discussion of the modification hypothesis under assessment, along with a description of the 1989 field project.

Chapter 2 presents information on the data collected during the 1989 experiment, including the randomization procedure used for the treatment of clouds with silver iodide (AgI) or placebos. Assessments of the total cloud sample and the predictor and response variables are also presented.

Chapter 3 discusses attempts to assess cloud seeding effects visually. A formal test was based on the observations of the seeding aircraft pilot and the project meteorologist.

Chapter 4 is a comparative analysis of the seeded and nonseeded clouds, separated according to the synoptic weather conditions producing the rain events. The seeded and nonseeded clouds associated with cold-front and air-mass conditions are compared.

Chapter 5 presents the results of cloud analyses based on the selection of a special set of clouds. The evaluation of the total data sample (chapter 2) revealed that a bias had occurred accidentally in the choice of clouds for silver iodide and placebo treatment. This problem was addressed by developing "seedability" criteria to reclassify the clouds and minimize the effects of the bias.

Chapter 6 presents a statistical assessment of the 1989 clouds with complete data histories.

Chapter 7 compares the Illinois results with those from a comparable Texas experiment using the same modification hypothesis and seeding method.

Chapter 8 presents the rainfall results from 1989, including a comparison of the rainfall from the silver iodide- and placebo-treated experimental units.

Chapter 9 summarizes and interprets the major findings presented in this report and assesses the types of research that could be pursued.

This project created a large number of extensive databases that support the findings presented herein. These data have been assembled in a separate Water Survey report, The PACE 1989 Data Book (Czys et al., 1993).

Terminology

Treatment refers to the application of flares filled with silver iodide or sand (the placebo) in clouds.

Large clouds (A clouds) grew to heights greater than 30,000 feet.

Small clouds (B clouds) never exceeded 30,000 feet.

Cloud groups (clusters) were groups of two or more cumuliform clouds that produced radar echoes, moved as an entity, and were visually and physically interrelated.

Experimental unit was a cloud group in which one or more cumulus congestus clouds were treated with the same material.

Control clouds (nonseeded clouds) received sand treatment.

Seeded clouds received AgI treatment.

Extended area was defined as a square, 240 x 240 kilometers (km), centered on the Champaign radars.

Study area was a circular area in Illinois within a 160-km (100-mile) radius of the Champaign radars.

Echo core is a three-dimensional entity defined by radar reflectivity data and associated with a single growing cumulus congestus in a multicelled cloud group. Many echo cores were attached to other echo cores at the time of treatment. Echo cores were separated from one another by a trough of minimum reflectivity values in three-dimensional space.

Modification Hypothesis

As part of the phase 1 assessment of existing data, two broad categories of seeding strategies were considered. The first was "static" mode seeding, in which the primary objective was to initiate precipitation from clouds that would not naturally be expected to produce precipitation-size particles. The second strategy was "dynamic" mode seeding, in which the primary objective was to augment precipitation from clouds or cloud systems that would probably produce rain regardless of seeding. Partly on the basis of observations (see for example Battan, 1953; Braham and Dungey, 1978) that typical Illinois clouds have prolific coalescence processes that often produce rain soon after cloud initiation, it was concluded that dynamic mode seeding was the appropriate strategy to follow (Woodley, 1970; Simpson and Woodley, 1971; Orville, 1986; and Simpson, 1980). That is, a dynamic response could be elicited: a cloud or group of clouds could be invigorated by a latent heat release due to seeding, thus converting supercooled water to ice earlier than would occur naturally. This stimulation may cause the treated clouds to grow larger, last longer, process more water vapor, merge, or some combination thereof, ultimately producing more rain than if there had been no seeding.

The sequence of events believed to occur as a result of seeding is summarized in figure 2. Events begin by targeting the seeding agent to the main updraft region of an echo core or cloud. This must occur very early in the cloud life cycle, when supercooled condensate is abundant and before natural freezing

processes have had sufficient time to operate. This action is supposed to speed the conversion of supercooled condensate to nearly total ice particles at a lower altitude in the cloud than would occur naturally. If the seeding material is targeted properly, freezing of the liquid condensate produces a net buoyancy enhancement in the updraft region. The effect of buoyancy enhancement may range from reducing net deceleration in most instances, to increasing the updraft and enhancing acceleration in some instances (Politovich and Reinking, 1987). To achieve any of these effects, the cloud's vertical circulation must be organized, implying a minimum main updraft diameter. Cumulus clouds composed of several small updrafts probably do not have well-organized circulation, and thus may not benefit from a latent heat release. Poorly organized circulation may, in fact, suffer from seeding with an unorganized release of latent heat, reflected in increased turbulence and further dissipation of the cloud's vertical motions.

Assuming that seeding results in some type of buoyancy enhancement, the cloud top may reach higher maximum altitudes than it would naturally. In the presence of limiting conditions such as mid-level dry layers and/or inversions, the cloud top may be sufficiently invigorated to overcome them and grow much taller than it would naturally. This could then condition the atmosphere by erosion of unfavorable mid-level conditions, permitting subsequent untreated clouds to grow taller than they would in a natural cloud environment. In either event, cloud mergers are encouraged by the presence of larger clouds and increased vertical (upward and downward) circulations (Simpson, 1980).

Buoyancy enhancement may also be translated throughout the entire cloud depth, resulting in increased moisture convergence below the cloud base. Overall vertical motion, including falling air, may boost the development of subsequent clouds. The resulting invigorated cloud system should occupy larger horizontal and vertical areas with a concurrent proportional increase in updraft and downdraft diameters.

As convective clouds grow larger, gain longer life, or both, they should produce more rain because their precipitation mechanisms operate over larger volumes or longer times, or both. Consequently, net rainfall reaching the surface will be augmented, even though precipitation efficiency and/or intensity may not be appreciably different than if the cloud system had received no treatments at all.

Phase 2 of PACE involved exploratory seeding trials to test certain aspects of the dynamic seeding hypothesis. The first efforts involved designing initial experimental seeding trials. The principal elements of Illinois field projects during the summers of 1986 and 1989 included an operational forecasting effort, the use of meteorological and seeding aircraft, weather radars, and special thermodynamic soundings from the National Center for Atmospheric Research/Cross-Chain Loran Atmospheric Sounding System (NCAR/CLASS). Although the 1986 sample was limited to 23 clouds in July and only 20 in

August due to the lack of daytime convective cloud activity, the results encouraged further field testing of the seeding hypothesis, which was done in 1989 (Westcott, 1990; Czys, 1991). The 1989 experiments are the subject of this report. Further experimentation depends heavily on how the results of this research are interpreted.

The 1989 Field Project

The 1989 Illinois field experiment studied natural cloud behavior and cloud reactions to silver iodide seeding. Operations began on May 8 and ended on August 11, and were divided into two periods. Period 1, May 8-31, was devoted to monitoring the conversion of water to ice in clouds treated within experimental units with either AgI or sand. Period 2, June 1 - August 7, addressed the seeding reactions of clouds and cloud systems within experimental units.

Operations were based at the ISWS facilities at the University of Illinois' Willard Airport. As shown in figure 3, the study area included the region within a 160-km radius of Champaign. The study area was approximately 19,500 km², bounded to the north by Joliet, to the west by Peoria and Springfield, and to the south by Salem. Almost all seeding missions were conducted between the hours of 1300 and 1900 local time (LT), and no treatments were delivered over Indiana airspace.

Facilities

The plane used for cloud physics and cloud seeding was a twin-engine Beechcraft Baron leased from Colorado International Corporation, Boulder. The aircraft was used to make in-cloud measurements of cumulus congestus as their cloud tops reached the -10 to -15°C levels, and to simultaneously release cloud treatment flares (either AgI or sand placebos) according to a predetermined randomization scheme. The airplane was equipped to measure Rosemont and reverse-flow temperature, cooled-mirror dew point, pressure, vertical winds, Johnson-Williams hot-wire liquid water content, cloud droplet spectra using a forward scattering spectrometer probe (FSSP), and precipitation-size particles using two-dimensional cloud (2D C) and two-dimensional precipitation (2D P) optical array probe imaging. The airplane also carried a rack containing 200 pyrotechnic flares used for cloud treatments.

The T-28 aircraft of the South Dakota School of Mines and Technology was used to monitor water-to-ice conversions at constant temperatures as a cloud evolved. Being armored, the aircraft could penetrate into cloud regions containing hail and severe turbulence. Thus, it provided in-cloud data on more mature and potentially severe cloud stages, which were not safely accessible to the twin-engine cloud seeding/measurement airplane. Results based on data collected during the T-28 flights will be the subject of other scientific papers.

Two radars were involved in the 1989 PACE field program: the CHILL radar and the ISWS HOT radar. Both are capable of

measuring reflectivity and Doppler velocity. They transmit at 10-centimeter (cm) wavelengths with a beam width of 1 degree for the CHILL radar and 1.5 degrees for the HOT radar.

Organization

More than 30 people were involved in the day-to-day activities of the 1989 field experiment, including scientists, engineers, technicians, and students. A large staff was also involved in the postexperiment data analysis. Field personnel were organized around five primary activities: radar operations, aircraft operations, forecasting and nowcasting, randomization and flare management, and data archiving.

Radar operations were directed by a radar meteorologist who identified and monitored experimental units during missions and directed radar antenna scanning strategies. The radar meteorologist also monitored quality control of the radar data. After the experiment, the radar meteorologist was responsible for the reduction and analysis of the radar data. The radar group also included three radar software/hardware engineers and two support engineers who were responsible for radar maintenance.

Aircraft operations were directed by a cloud physicist/physical meteorologist. This individual was responsible for directing the aircraft in flight and for selecting clouds for treatment and delivering cloud treatments. The aircraft group also included a pilot experienced in commercial weather modification operations and an in-flight instruments engineer. Another staff member monitored the aircraft data; served as the radio communications officer during missions; coordinated aircraft and radar maneuvers; and relayed information on clouds, treatments, and echo behavior between the in-flight meteorologist and the radar meteorologist.

Forecasting operations were conducted by a staff forecaster and a graduate meteorology student who served as a forecaster/nowcaster. Forecasting was conducted seven days a week through the ten-week project to ensure that no days suitable for experimentation were missed. In general, operations were conducted on all days when supercooled cumuli were in the experiment area. The forecasting group was responsible for a daily weather briefing (at 1000 LT) and for making subjective and objective forecasts on the potential development of clouds and cloud systems suitable for treatment. The forecasting group was also responsible for obtaining special vertical atmospheric readings and for nowcasting during seeding operations. An important purpose of the nowcasting effort was to identify areas of simple rain and thunderstorm activity that could turn into severe weather and to signal the need to terminate the seeding mission for safety reasons.

Randomization and flare management followed seeding schedules developed well in advance of experimentation. Personnel loaded and unloaded flares to and from the aircraft for each mission and managed flares after the flights. Only three members of the randomization group knew about the specific flare loading for a mission, so that the remainder of the

personnel were "blind" as to the treatment type for each experimental unit.

The data management group cataloged data received from each of the other four groups. The data management officer ascertained that data were properly logged, archived, and accessible to all other members of the field and analysis teams.

The 1989 field experiment would not have been possible without the cooperation and coordination of several state and federal agencies. These included, but are not limited to, the Federal Aviation Administration; the ISWS Office of the Chief and the Office of Financial and Human Resources; the University of Illinois Department of Atmospheric Sciences, Purchasing Division, and Telecommunications Office; the National Center for Atmospheric Research; and NOAA under Cooperative Agreement COMM NA89 RAH-09086.

Design

The field project was designed to achieve two primary objectives: 1) to obtain data on the largest possible sample of clouds (seeded and natural), and 2) to test some of the early steps of the dynamic seeding hypothesis by focusing on initial cloud reactions. Operational procedures were designed around five weather, cloud, and facility readiness situations. The five experiments fell into two general classes: 1) the collection of data about natural cloud and precipitation processes by the project aircraft and/or through the radar(s) when seeding was inappropriate for various reasons, or 2) the randomized treatment of clouds (using AgI or placebos) under three experimental variations that differed according to cloud sizes and/or the equipment available.

Within the second class were two top-priority experiments. The first involved randomized treatment of cumulus congestus clouds expected to reach at least 30,000 feet or 9,145 meters (m) in height. In this "large cloud experiment," the cumulus congestus cloud towers were either forming individually or in association with a larger, sustaining cloud system. The large cloud experiment included simultaneous collection of radar and aircraft data on treated clouds.

The second experiment, the "small cloud experiment," involved randomized treatment of cumulus congestus clouds, typically growing alone above 20,000 feet (6,095 m), but not surpassing 30,000 feet (9,145 m) in height. This experiment included simultaneous collection of radar and aircraft data on treated clouds. All of the procedures of the large cloud experiment were followed in the small cloud experiment, except that small clouds were penetrated at least once after treatment to obtain limited, direct measurements of the effect of the seeding agent on in-cloud conditions. Initial results of randomized large cloud treatments are the primary subject of this report.

Randomization

Randomization was used because it is considered essential to gathering trustworthy data when individuals are involved in

making critical analytical choices and assessments. Ejectable AgI flares were chosen as best to target the seeding materials toward the updraft regions of the clouds, a necessity within the framework of the dynamic seeding hypothesis. The treatment randomization was based on "floating" experimental units, initially defined as a single congestus cloud or a group of congestus clouds behaving as an entity (see figure 4).

The concept of a "floating" experimental unit was adapted from that used in cloud seeding operations in Texas (Rosenfeld and Woodley, 1989). The radius of each treated cloud group was set at 28 km from an initial cloud treatment point. Each unit typically swept out an oblate-shaped area during its lifetime. All clouds in the unit received the same seeding material, and the design allowed selection of up to four units during any operational period of up to three hours (limited by the on-station time of the airplane). An annular buffer area of another 28 km around the treatment area was maintained to minimize any physical and chemical interactions between units. Radar observations were initiated well in advance of cloud treatments and continued until all of the treated cloud systems either dissipated or moved out of the viewing range of the radar.

A 50/50 randomization was set on experimental units rather than on individual clouds. Flights through two or more experimental units included at least one AgI and one sand unit. Separate randomization schedules were used for the large and small cloud experiments to further maintain balance. The in-flight meteorologist who selected the clouds (and hence the experimental units) was blind to the type of treatment being applied. Analysis, processing, and quality control of aircraft, radar, and synoptic data were completed prior to releasing information about the type of treatment used in any of the experimental units.

Flight Procedure and Choice of Clouds

In the large cloud experiment, aircraft and radar operations were launched at the time of the first satellite, radar, and/or visual indication of cumulus initiation. On these days, the morning forecast predicted clouds to be warm-based (preferably around 16°C) and to grow to at least 30,000 feet (9,145 m). Seeding trials were conducted on typical Illinois rain/thunderstorm systems that were readily available for daytime cloud seeding activities. The cloud/cloud systems were not special cases. When the aircraft arrived at a potential seeding area, a candidate cloud was selected on the basis of visual criteria. It must have appeared to a) have a cloud top just passing 20,000 feet, with potential for reaching 30,000 feet and beyond; b) have a cumulus congestus (hard, blocky) appearance; c) be at least 2 km in diameter; and d) show little or no vertical tilt. These clouds would have produced rain naturally.

Test penetration of a candidate cloud helped establish whether neighboring clouds could be considered suitable for treatment. In-cloud properties consistent with requirements of the seeding hypothesis had to include: 1) moderate updrafts,

preferably 2 to 4 meters per second (m s^{-1}); 2) large amounts of supercooled water, about 1 to 6 grams per cubic meter (g m^{-3}); 3) supercooled drizzle and raindrops in the updrafts; and 4) little or no indication of ice, particularly in the updrafts.

If the candidate cloud passed these in-cloud criteria, an experimental unit was declared otherwise another candidate cloud was sought. Usually, the first candidate cloud tested met the in-cloud selection criteria. Once an experimental unit was declared, all clouds in the unit received the same treatment at approximately the -10°C level, as specified by the predetermined randomization schedule. Treatment flares containing either AgI or sand were delivered, and every attempt was made to release flares only in the updraft regions at a rate of approximately one flare every 5 to 10 seconds, or at approximately every 500 to 1,000 meters of cloud updraft. The aircraft was *always* positioned between 1,000 and 5,000 feet (300 to 1,500 m) below the cloud top, in order to release at least 20 g of seeding material into the volume of the cloud updraft in the levels of -10 to -3°C . In no case was there more than 5,000 feet of cloud above the altitude of the aircraft during treatment.

During these operations, the radars were operated in sector scanning mode to obtain detailed three-dimensional portrayals of the echoes. A sector scan was completed about once every 1.5 to 4 minutes, followed by one or two 360-degree, low-elevation scans. If ten or more clouds were treated, a decision was made either to remain with or leave the experimental unit for another. Typically, the experimental unit was abandoned and another one was usually sought with the aid of radar information.

Epilogue

In all, 19 flight missions were carried out in 1989, and 25 experimental units were treated in both large and small cloud experiments. The experiment was successful at meeting its two primary objectives: to obtain sufficient data to test some of the early steps of the dynamic seeding hypothesis and to develop analytical procedures to evaluate for seeding effects.

Tables 1 and 2 summarize pertinent features of the large cloud (denoted as " α ") and small cloud experiments, in addition to several missions conducted as part of the other three weather/facility-dependent experiments, which were denoted as " β " when cloud treatments were delivered. The randomization schedule worked well at producing numerical balance between AgI and placebo treatments. As shown in the tables, 12 experimental units were treated with AgI and 13 units were treated with sand. Overall, 118 clouds were penetrated. Sand flares were released in 52, and AgI flares were released in 66. The 118 cloud penetrations produced a total of 87 radar echoes for analysis, of which 41 received sand and 46 received AgI. In

addition, a large number of nontreated clouds was also measured, usually when seeding was terminated because severe weather safety limits were exceeded.

The randomization schemes also produced good overall numerical balance in the number of flares used. Over the course of the 25 missions, 682 flares were released, 375 AgI and 367 sand. In the large cloud experiment, 451 flares were released, 249 AgI and 202 sand.

Of the 82 large clouds treated, 36 received sand flares and 46 received AgI flares. Of the 82 clouds, 71 were identifiable and tracked as part of the radar analysis. The difference between the 82 treated clouds and the 71 echo cores can largely be attributed to an inability to identify a different echo core at the time of treatment. Sounding data from Peoria were available for every large cloud experiment, while CLASS soundings launched from Champaign were only available for about half the units.

Thirteen units were classified as β experiments (see table 2). Seven received sand treatments, while six received AgI treatment. Because flight procedures in the small cloud experiments were designed for multiple cloud penetrations, table 2 lists the number of clouds treated as well as repenetrations. Thirty-six treatments were delivered to 32 clouds (20 AgI and 16 sand).

The remainder of this report focuses on data analyses of seeding effects in the large cloud experiment. This report does not discuss natural in-cloud conditions and precipitation processes, studies of natural behavior at the rain storm scale, or the details of the effects of the small cloud seeding experiments. These data will require further attention.

Acknowledgments

This report is part of an annual report to the National Oceanic and Atmospheric Administration under Cooperative Agreement NA 90AA-H-04175. Several Water Survey staff members assisted in the analyses, including Carl Lonquist, Julia Chen, and Robin Shealy. Linda Hascall assisted in preparation of the illustrations, Laurie Talkington edited and formatted the report, and Joyce Fringer provided word processing support.

Dr. William Woodley supplied Texas data, and his comments were very helpful in chapter 7 and elsewhere in the report. The National Center for Supercomputing Applications at the University of Illinois provided considerable support essential to the radar data analysis.

This research was conducted as part of the duties of the staff of the Illinois State Water Survey, and this report was prepared under the general administrative guidance of Mark E. Peden, Acting Chief.

FIGURES AND TABLES FOR CHAPTER 1

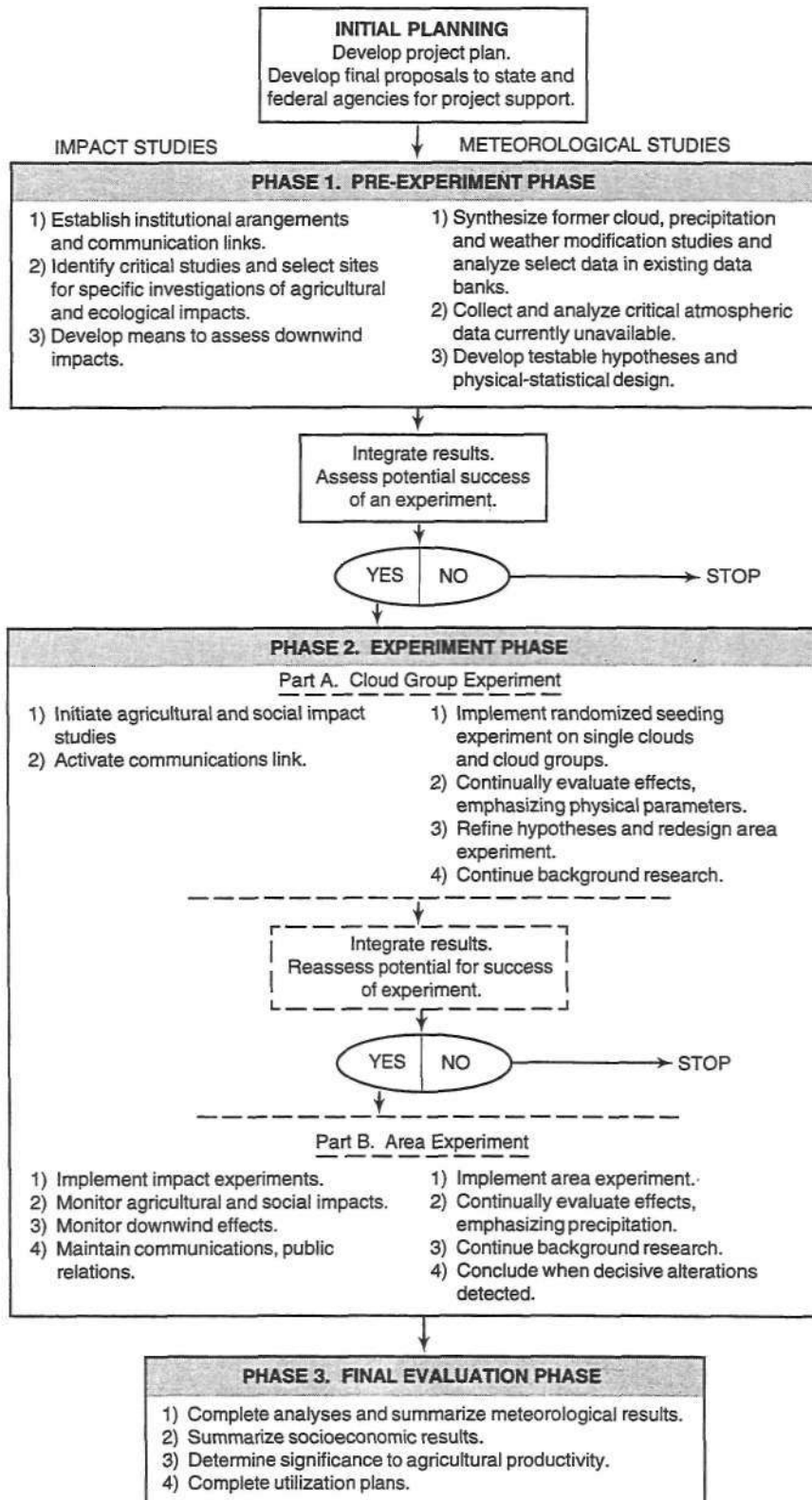


Figure 1. Flow chart for the Illinois research program on planned weather modifications

MAJOR STEPS INVOLVED IN THE DYNAMIC SEEDING
HYPOTHESIS ADOPTED FOR ILLINOIS CLOUDS

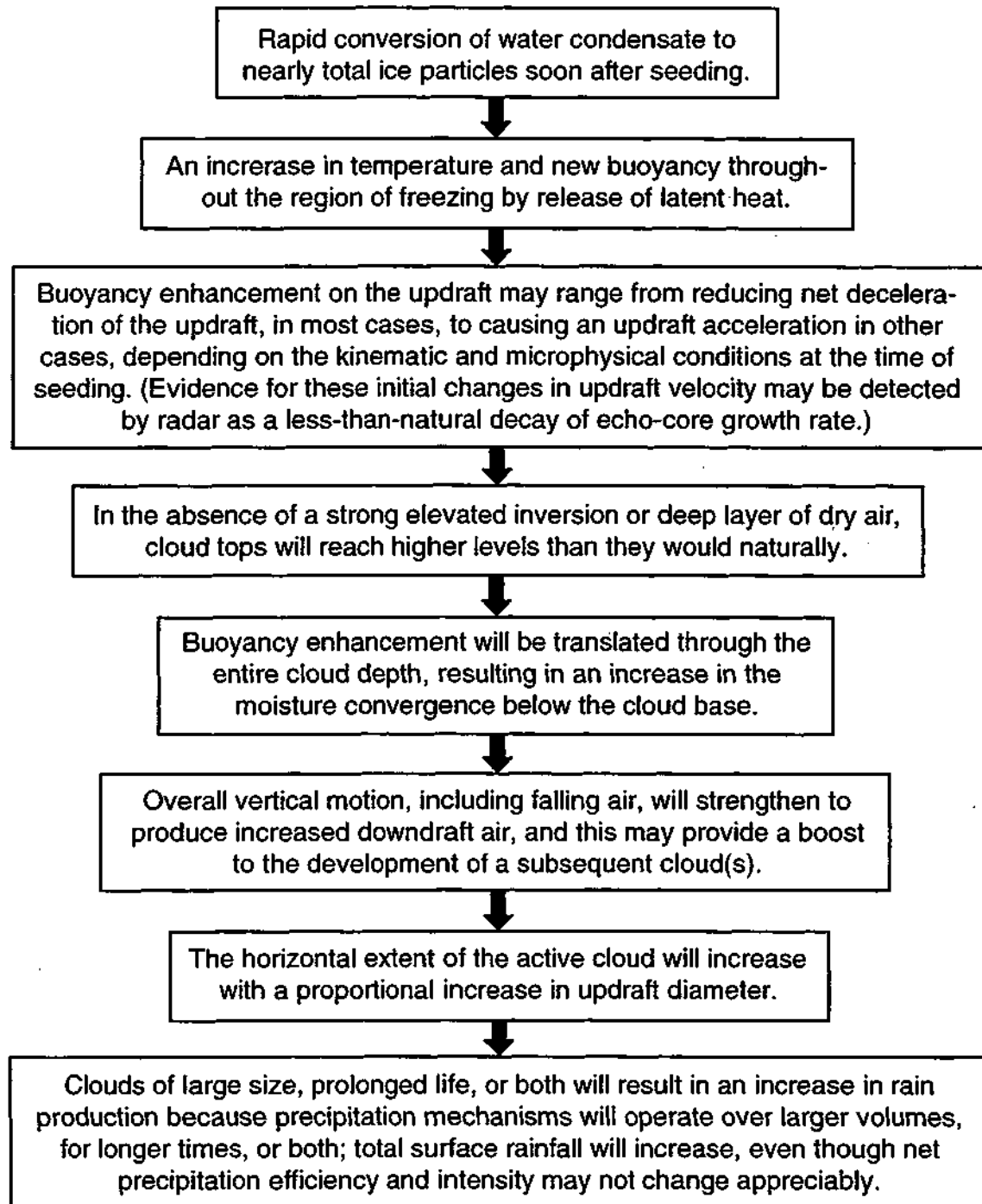


Figure 2. The dynamic seeding hypothesis as adopted for the exploratory PACE seeding trials

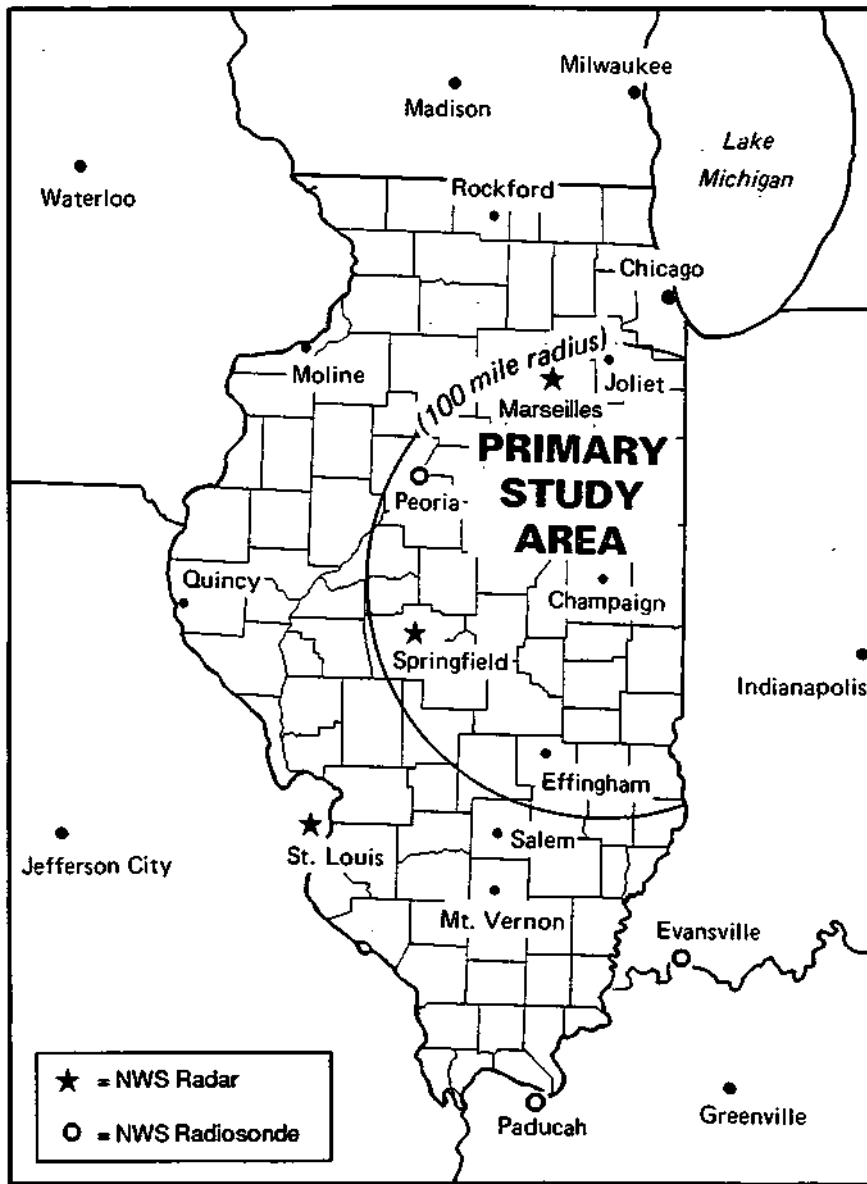


Figure 3. Study area for the 1989 PACE field project

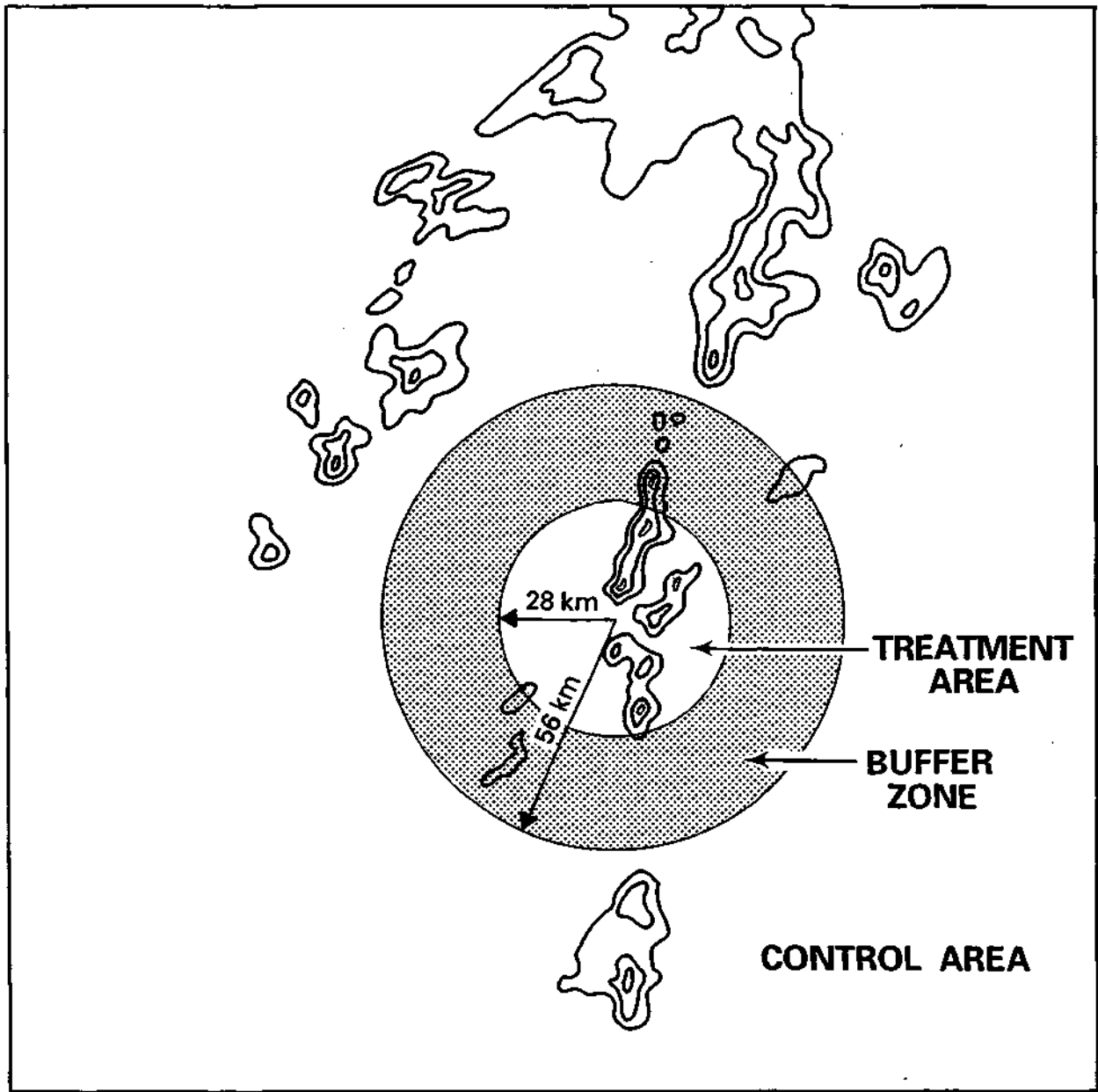


Figure 4. Experimental unit geometry

Table 1. Summary of the In-Target Large Cloud (a) Missions

<i>Date (mission)¹</i>	<i>Experimental unit number</i>	<i>Treatment material</i>	<i>Treated clouds</i>	<i>Nontreated clouds</i>	<i>Radar echoes analyzed</i>	<i>Source of sounding data²</i>
May 19 (b)	2	Sand	5	8	4	PIA
June 1	5	AgI	4	27	4	PIA & CMI
June 23 (a)	11	AgI	10	7	7	PIA & CMI
June 23(b)	13	Sand	8	1	7	PIA & CMI
July 8	17	Sand	5	2	5	PIA & CMI
July 8	18	AgI	8	3	7	PIA & CMI
July 11	19	AgI	7	6	7	PIA & CMI
July 19 (a)	20	Sand	4	3	3	PIA & CMI
July 23	22	AgI	13	3	10	PIA
July 24	23	Sand	6	4	5	PIA
July 25	24	Sand	8	5	8	PIA
July 25	25	AgI	4	2	4	PIA
Totals: 9 days	12	6 Sand 6 AgI	82	71	71	

Notes: ¹(a) or (b) following the date of a mission denotes the first (a) or second (b) mission on that date.

² PIA = Peoria, IL; CMI = Champaign, IL.

Table 2. Summary of the Out-of-Target and Small Cloud, (B) Missions

<i>Date (mission)¹</i>	<i>Experimental unit number</i>	<i>Treatment material</i>	<i>Penetrations treated</i>	<i>Clouds treated</i>	<i>Penetrations not treated</i>	<i>Clouds not treated</i>	<i>Radar echoes analyzed</i>	<i>Source of sounding data²</i>
May 19 (a)	1	AgI	1	1	5	3	0	PIA
May 25	3 ³	Sand	~2 ⁵	~2	~4	~2	0	PIA & CMI
May 30	4	Sand	2	2	4	3	0	PIA & CMI
June 3	6	Sand	1	1	11	7	2	PIA & CMI
June 3	7 ⁴	AgI	2	2	14	7	0	PIA & CMI
June 12	8	AgI	4	2	8	2	3	PIA & CMI
June 12	9	Sand	2	1	2	2	1	PIA & CMI
June 18	10 ³	Sand	~4	~4	~15	~5	0	PIA & CMI
June 23(b)	12 ³	AgI	5	5	3	3	0	PIA & CMI
June 27	14	Sand	3	3	8	4	3	PIA & CMI
June 27	15	AgI	3	3	7	3	4	PIA & CMI
July 2	16	Sand	2	2	16	12	3	PIA & CMI
July 19(b)	21 ⁴	AgI	~5	~4	~7	~1	0	PIA & CMI
Totals: 10 days	13	7 Sand 6 AgI	36	32	108	54	16	

Notes: ¹ (a) or (b) following the date of a mission denotes the First (a) or second (b) mission on that date.

² PIA = Peoria, IL; CMI = Champaign, IL.

³ Out of target

⁴ No radar data

⁵ Approximate signs indicate that numbers were taken directly from field notes and not later verified.

2. DATA ASSESSMENT AND COMPARISON OF PREDICTOR AND RESPONSE VARIABLES

by

Mary Schoen Petersen, Robert R. Czys, and Robert W. Scott

Overview

This chapter summarizes the data collected during the 1989 PACE field program. It discusses the process used to select key predictor and response variables for many of the analyses covered in other chapters in this report. Most importantly, this chapter draws attention to the fact that in many ways the placebo-treated and AgI-treated clouds differed in character and behavior before and at treatment. This precluded a direct comparison of cloud responses to ascertain possible seeding effects. Finally, because seeding results are sensitive to a large set of uncontrolled variables, the 1989 experiment is viewed within the context of synoptic/mesoscale conditions, how these changed over the course of the experiment, and how these changes were manifested in the variability of conditions at the microphysical and echo-core scales.

The Data Set

Three primary data sources were used in the 1989 Illinois exploratory cloud seeding experiment: 1) meteorological data from the National Weather Service (NWS), the Illinois State Water Survey and other observing stations used in forecasting; 2) data obtained from the ISWS/National Science Foundation (NSF) CHILL 10-cm Doppler radar in use at the time; and 3) measurements of in-cloud conditions obtained from the cloud seeding aircraft, which was specially equipped with a full range of cloud physics equipment. Measurements of in-cloud conditions in intense regions of cumulonimbus systems were also obtained using the T-28 armored aircraft of the South Dakota School of Mines and Technology. Analyses in this report are primarily based on data from forecasting operations, the CHILL radar, and the cloud physics/cloud seeding aircraft.

The summer forecasting effort used basic weadier data received via satellite from Zephyr Weadier Service. They included 1) meteorological charts prepared by the National Meteorological Center (NMC) received via the DIFAX line, and 2) verbal and coded weadier information from the NWS Domestic Plus weadier circuit. Important data from this NWS weadier line consisted of twice-daily upper air soundings, hourly surface observations, and hourly radar reports from across the United States. A special NCAR CLASS rawinsonde was also used at Champaign, the radar location (see figure 3).

The CHILL radar collected reflectivity, velocity, and differential reflectivity measurements throughout the summer. The radar scanning procedure was devised 1) to obtain high-resolution time and spatial data on clouds and cloud systems

(complete sampling within two to four minutes per sector scan), 2) to top (rise above) the echoes of interest, 3) to obtain ZDR measurements, and 4) to collect reflectivity measurements.

As described in chapter 1, the seeding aircraft was equipped to measure various parameters, such as temperature, pressure, vertical wind, liquid water content, and precipitation-size particles. The aircraft continuously recorded these data in all clouds, but this report includes analyses of only those clouds that received treatment flares and for which there are analyzed radar data. The aircraft data are unique in that each treatment penetration was accompanied by a detailed set of coincident in-cloud conditions at the time of seeding.

The processing, quality control, and digitization of the raw data from these three sources (synoptic, radar, and aircraft) resulted in a large set of directly measured and derived variables, yielding a total of 190. They describe the state of the cloud, the environment around treatment time, or the cloud's subsequent behavior. These variables and their definitions are given in appendixes A, B, and C. The 40 synoptic variables generally describe the morning environment in the target area on the day of a mission. The 57 aircraft parameters depict the conditions of the individual clouds as the aircraft flew through them and released flares, and they describe in great detail the conditions in the main or broadest updraft of the cloud. Of the 93 radar variables, 57 describe the conditions of the cloud at the time of first echo (FE) or at the time of treatment, while 36 variables relate to the echo's behavior after the treatment material had been released.

The term "predictor" has been used for the variables that describe the conditions at or before treatment; response is used to describe the variables that measure behavior after treatment. The large cloud analysis database includes 154 predictor variables and 36 response variables. The response variables were derived from the radar echo data.

Because many of the 154 predictor and 36 response variables were closely interrelated or redundant, the data set was reduced to a few key variables closely associated with 1) initial conditions desired for dynamic seeding; 2) initial conditions that could be related to future cloud growth; and 3) responses expected due to dynamic seeding, most notably changes in vertical and horizontal size or cloud lifetime. The selection of key responses addressed three fundamental questions about dynamic cloud seeding: did AgI-treated clouds grow bigger, last longer, or both?

As one of the first steps in the analysis, the number of predictor variables used to assess cloud cores was reduced to 11:

three synoptic, four radar, and four aircraft variables. Their definitions and abbreviations are given in table 3. The response variables were reduced to eight, and these are listed in table 4. Most of the approaches to discerning cloud seeding effects centered on these key predictor and response variables.

Note that the analyses of the experimental units also included calculation of the units' rainfall production over time, based on radar data. This too became a key response variable. Synoptic weather conditions were also employed in which each rain event was considered a key predictor variable.

Rerandomization Procedure

The 1989 field program used a treatment randomization scheme intended to meet three objectives: 1) to produce an approximate 50/50 split between AgI- and sand-treated experimental units (and ideally a 50/50 split in the number of AgI- and sand-treated clouds); 2) to avoid having more than two experimental units in a row receive the same treatment type; and 3) to treat experimental units alternately (one sand, one AgI) if two units were declared during a single flight

Based on the above objectives, randomization schedules were developed well in advance of the experiment. One was used in the large cloud experiment, and the other was used during small cloud and other seeding missions. Two randomizations were used to avoid the possibility that a majority of large clouds might receive one type of treatment, while clouds on the other missions would receive the other treatment. Moreover, the randomization made it impossible for more than two experimental units in a row to receive the same treatment, thus avoiding the chance that a majority of the units encountered early in the summer would receive one type of treatment and those later in the summer receive the other type of treatment. The randomization scheme required that either a large cloud or a small cloud/other seeding experiment be declared during flight based on predefined visual and in-cloud criteria. Specifics of the randomization scheme and how it was followed are given in the 1989 PACE Data Book (Czys et al., 1993) and the 1989 PACE Operations Manual (Changnon et al., 1989). Other than the seeding officers and their technician, no one else involved in the project had knowledge of the treatments or the details of the randomization plan until all the data were quality controlled and digitized.

Unless otherwise stated, the results of statistical tests covered in this report are based on the rerandomization of the experiment. Rerandomized P-values were computed following the procedure intended by the original randomization scheme developed for the 1989 experiment. But this procedure produced permutations that precluded more than two treatments of the same type in a row, and always switched treatments when two large cloud experimental units were declared on a single flight. Based on a simple recursive relationship, it can be shown that only 208 permutations are possible if these requirements

are imposed. For each individual variable of interest a t or Z statistic was computed for each permutation. P-values were then computed as a fraction of the total permutations (208) that were greater than the t or Z statistic, based on the actual sequence of AgI and sand treatments.

Comparison of Predictors and Responses

The next step in the analysis was to compare the properties of the sand- and AgI-treated clouds at the time of treatment to determine the physical similarities of the two samples. Table 5 lists statistics on the key predictor variables for all (N=71) sand- and AgI-treated clouds. They are grouped by synoptic, radar, and aircraft variables. Means, standard deviations, sample size, and the results of the rerandomized t test for differences in means (0 and the Wilcoxon sum rank test for shifts between distributions (W) are listed in table 5. Dark shading of P-values indicates significance levels between 0 and 5 percent; light shading indicates significance between 5 and 10 percent. Histograms for each variable are shown in figures 5-7.

Between five and six of the predictor variables were found to be significantly different at less than 10 percent, depending on the statistical test; 39 of the 154 predictor variables were also found to be significantly different at less than 10 percent. Assuming that these differences did not happen by chance, the data in table 5 were interpreted to mean that more sand-treated clouds than AgI-treated clouds developed on days with slightly slower upward vertical motions (as indicated by pb). But otherwise similar atmospheric conditions prevailed for cloud-base temperature and shear. The aircraft data indicated that the net buoyancy of the AgI-treated clouds may have been more negative; that the potential buoyancy enhancement was different (presumably less); that the main updraft may have been slower, and that the fraction of the condensate in ice was probably about the same as in the sand-treated clouds. Hence, the sand-treated clouds were more vigorous than the AgI-treated clouds and could have been expected to result in bigger clouds.

Inspection of the radar variables in table 5 shows that the sand-treated clouds were wider, taller, more reflective, and possibly older at treatment than the AgI-treated clouds. These large differences in initial conditions mean that the sand-treated clouds should grow bigger, last longer, or both, than the AgI-treated clouds, unless the effects of AgI seeding overcame the growth and size advantages of the sand-treated clouds.

Each of the treated echo cores was tracked in three dimensions using an interactive echo tracking program developed specifically for analysis of the 1989 radar data. In the tracking procedure, the radar data were interpolated to a 1 x 1-km CAPPI grid at each elevation for which radar data were available. Next, an echo core was identified at treatment as well as each of the horizontal and vertical grid points that composed the echo. These marked grid points made it possible to determine the

radar characteristics of the echo core. The echo core was then tracked back in time until first echo (FE), and then forward in time from treatment until the echo core dissipated or until it lost its individuality by merger with an echo structure. Generally, most echo tracking was terminated because of echo merger.

Statistics on the key response variables in table 6 indicate that on the average, the sand-treated clouds became taller, wider, and more reflective than the AgI-treated clouds. Figures 8, 9, and 10 show composite diagrams of echo-core behavior for height, area, and reflectivity, respectively, which were derived from the data set produced by the echo tracking programs. Together they demonstrate the nature of the bias in the 1989 cloud sample. Two methods have been used to compute population behavior. The top graph of each figure was computed using only the echo-core data in existence at each interpolated observation time. Hence sample size varies with time, as shown at the bottom of the graphs. The bottom diagrams are means based on the entire sample, including zero values used for echo cores not in existence at any of the observation times.

Each graph shows that the behaviors of the sand-treated clouds and the AgI-treated clouds differed prior to and at treatment (as did the values in table 5). It is interesting to note that for both treatments, post-treatment echo behavior did not appear to differ from that expected, based on behavior prior to treatment. Hence, with respect to height, area, and reflectivity, the AgI seeding did not produce anomalous deviations in cloud behavior based on expectations prior to treatment. Three possible conclusions can be drawn. First, the signal-to-noise ratio was very low. Second, the AgI was not effective in overcoming the bias in cloud conditions. And third, an acceptable method of addressing the bias was needed before a seeding effect could be detected.

Atmospheric Variability during the Experiment

A major difference between meteorological experiments conducted in the laboratory and in the field is that field experiments are subject to much uncontrolled variability. This variability has long been recognized as a major source of uncertainty in cloud seeding experiments and has often hampered attempts to arrive at definitive conclusions (Changnon, 1976). Experimental control procedures such as randomization of treatment and rigorous cloud selection criteria are often used to reduce the influence of natural variability at many atmospheric scales. Therefore, even though experimental precautions were taken, such as randomization between units, it was still important to know how atmospheric conditions varied during the course of experimentation. Potential seeding effects were considered critically, depending on existing conditions each day that experimental units were declared.

For this report three primary synoptic variables were chosen to illustrate how meteorological conditions varied during the course of the experiment: temperature of the convective

condensation level, potential buoyancy, and bulk Richardson number. The temperature of the convective condensation level, which is closely related to cloud-base height, was chosen as an indicator of boundary layer moisture. Potential buoyancy, similar to lifted index, was selected as an indicator of updraft strength. These two synoptic variables, in combination, are very good indicators of the vigor of the coalescence processes that produce supercooled drizzle and raindrops before the cloud top reaches the seeding level (Mather et al., 1986a; Scott and Czys, 1992). Hence, they provided a link between mesoscale and in-cloud conditions. The bulk Richardson number, expressed as the ratio between the convective available potential energy (CAPE, the positive area of a thermodynamic sounding) and the density-weighted wind shear, demonstrates how instability varies. The bulk Richardson number is most widely recognized as being correlated with the development of single and multicelled mesoscale convective systems (Weisman and Klemp, 1982, 1984).

Figure 11 shows how the temperature of the convective condensation level varied from mission to mission during the 1989 experiment. While mission-to-mission differences were as large as 5°C, the plot shows a general trend for cloud-base temperatures to increase, implying a decrease in the height of the cloud base as the experiment progressed into July. This trend is consistent with the northern retreat of the so-called "polar front" with the arrival of Gulf moisture in the Midwest.

Classification of each mission by synoptic weather type showed that many of the early missions were associated with cold fronts, while many of the later missions were associated with air-mass conditions. Hence, the trend displayed in figure 11, as will be shown for the other selected synoptic variables, is consistent with a general shift in season from that typical of late spring/early summer to late summer.

Potential buoyancy also changed in a manner consistent with a change from cold-front to air-mass conditions. Figure 12 shows that the early part of the experiment was associated with relatively high values of potential buoyancy (>5°C), while the last few experimental units were associated with more moderate potential buoyancy (~4°C).

The relative changes in tccl and pb over the course of the experiment have several implications. First, the May and June experimental clouds should have had more vigorous updrafts. This is documented in figure 13, which shows the mean vertical velocity of the main updraft. Secondly, those clouds treated early in the experiment, with cold cloud bases and strong vertical motion, should not have had the optimal time required for coalescence to operate. Hence, the liquid water content for large drops, those with diameters greater than 300 micrometers (μm) should be less than for drops in clouds encountered later in the experiment, when cloud bases were warmer and potential buoyancy moderate. This is supported by figure 14, which shows only intermittent presence of LWCD for clouds 1 to 41, while clouds 42 to 71 usually had some measurable LWCD.

Finally, the changes shown in figure 11 and figure 14 suggest that first echo heights should be higher, with cooler tcl and higherpb; and that the development of radar-detectable scattering from cloud particles should take longer if cloud bases are warmer and potential buoyancy is moderate. Figure 15 shows data for the top height of first echoes and is consistent with this physical reasoning.

Also consistent with the transition from spring to summer meteorological conditions is the change of bulk Richardson number over the course of the experiment (figure 16). With the exception of experimental units that occurred on July 11 and July 19, bulk Richardson number generally increased through the summer. Bulk Richardson number can increase with increasing CAPE and constant shear, with constant CAPE and decreasing shear, or with simultaneously increasing CAPE and decreasing shear. Figures 17 and 18 show how CAPE and the vertical shear of the horizontal wind (VSHR) varied during the 1989 experiment. Although the mission-to-mission variability of CAPE was large in certain instances (almost 1,400 from May 19 to June 1, and about 1,000 from July 11 to July 19), a comparative inspection shows that almost all the increase in bulk Richardson number can be associated with decreasing shear as spring progressed into summer. Thus, the changes are consistent with reduced flow aloft.

Because the location of the treated clouds relative to the radar directly contributes to measurement uncertainty in the radar echo data, the variability of this parameter was also taken into consideration. Figure 19 shows the distance of the seeding aircraft (and hence the echoes) from the CHILL radar at the University of Illinois Willard Airport. Best measures of echo-core behavior are obtained when echoes occur approximately 40 to 100 km from the radar. Figure 19 shows that a group of echoes, treated on July 11, 19, and 23, were located just beyond the outermost limit. Hence, due to problems associated with beam spreading and filling, measurement of these echoes had generally poorer resolution and lower accuracy than the other observations. It should be noted that the 1989 radar data have been range-corrected.

Targeting of Seeding Material

The targeting of seeding material into the updraft was assessed because the dynamic seeding hypothesis requires that the glaciation occur in the updraft. This becomes critical information in evaluating the outcome of the seeding.

Figure 20 shows the percentage of flares placed in the updrafts for each of the treated clouds. They varied considerably from one cloud to the next, reflecting the difficulty of identifying updraft regions when positive vertical motions are weak.

It is also evident in figure 20 that the targeting of the seeding material did not favor any particular group of clouds in an experimental unit. So in this respect, all the clouds were treated similarly. Although the cloud-to-cloud dosage variabil-

ity is large, the seeding material was well targeted. Of the 71 clouds, flares were deposited completely outside the updraft regions in only eight. Of these, an updraft could not be detected in seven, either because the motion was below threshold values or because the cloud had neutral to negative vertical motions at the treatment level. In contrast, the seeding material was perfectly targeted in 25 of the 71 clouds; in 42 clouds, at least two-thirds of the seeding material was delivered to the updraft.

Clearly, better targeting of the seeding material would have been desirable, and the exact impact of the targeting on the results could not be precisely determined. However, seeding material was well targeted in most of the clouds, and no group of clouds was more favorably targeted than any other (either with sand or AgI). Therefore, the samples were considered comparable.

Conclusions

The most important finding from the examination of the cloud-echo data presented in this chapter was that the sand-treated clouds differed in many ways from the AgI-treated clouds, both before and at treatment. Thus, the sand- and AgI-treated populations probably would not have followed similar, natural growth trajectories. Hence, evidence of a classic "bad draw" was revealed by this analysis: the sand-treated clouds were more vigorous at treatment (larger size, stronger vertical motion, more reflective), so a straightforward comparison of response would perhaps lead to an erroneous conclusion that AgI had a negative (undesired) effect on initial cloud growth. This finding necessitated the development of other approaches to account for the bias and to search for the presence of seeding effects.

The 1989 experiment produced a sizable set of data on the meteorological conditions relevant to the life cycle of treated clouds in the experimental units. The 190 variables led to the selection of a few key predictor and response variables closely related to the dynamic seeding hypothesis. These key variables would likely serve well in a future exploratory or confirmatory experiment. However, refinement of the list would be justified as gaps in knowledge are reduced.

Examination of the temporal variation of a number of synoptic/mesoscale variables revealed that the 1989 experiment was subject to uncontrollable seasonal trends in spite of randomization and cloud selection criteria. The trends were found to be consistent with a transition from early spring to late summer meteorological conditions. Moreover, the analysis showed that mesoscale conditions and trends also manifested themselves in concurrent trends in echo-core and in-cloud conditions. The "bad draw" was not strictly related to these trends; it was just an unfortunate selection of clouds. This finding points to the need to monitor predictor variables more closely in future experimentation, and perhaps to devise operational procedures to objectively adjust for the development of sample bias.

FIGURES AND TABLES FOR CHAPTER 2

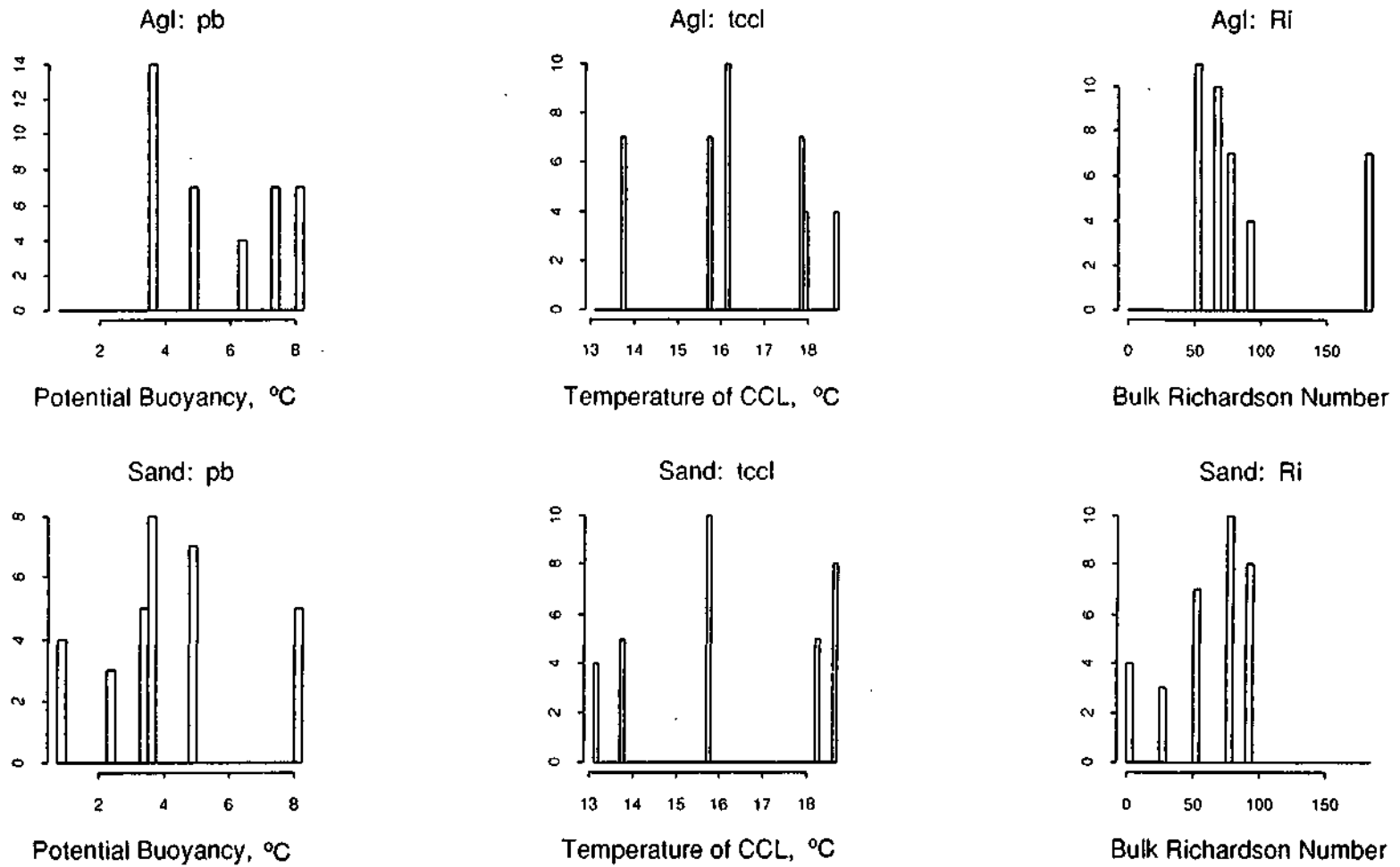


Figure 5. Histograms of potential buoyancy, temperature of the CCL, and Richardson number for the Agl-treated clouds (top) and the sand-treated clouds (bottom) based on 71 clouds

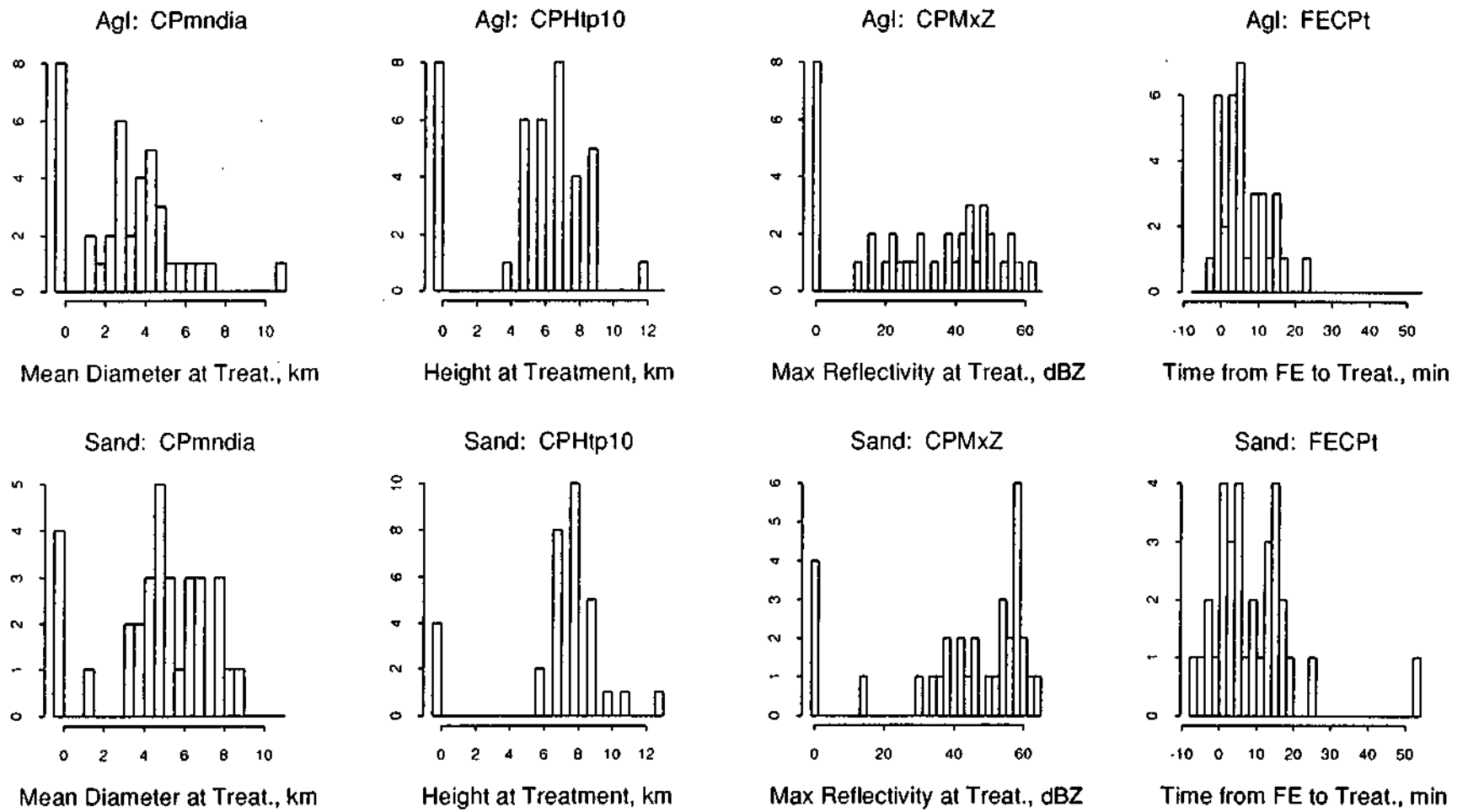


Figure 6. Histograms of mean echo diameter at treatment, top height of the 10-dBZ contour at treatment, maximum reflectivity at treatment, and time from first echo (FE) to treatment for the Agl-treated clouds (top) and the sand-treated clouds (bottom) based on 71 clouds

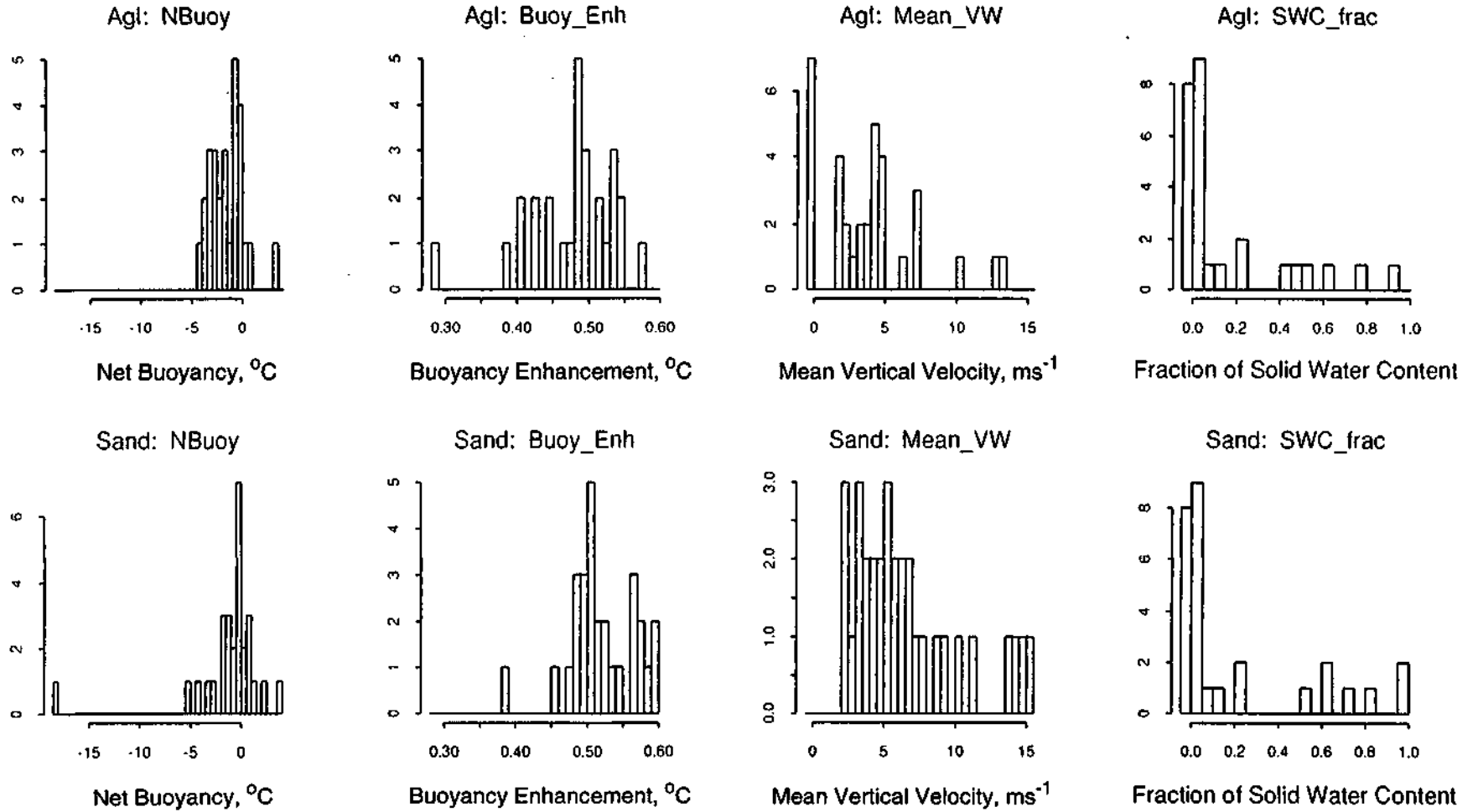


Figure 7. Histograms of net buoyancy, buoyancy enhancement, mean vertical velocity, and fraction of solid water content for the AgI-treated clouds (top) and the sand-treated clouds (bottom) based on 71 clouds

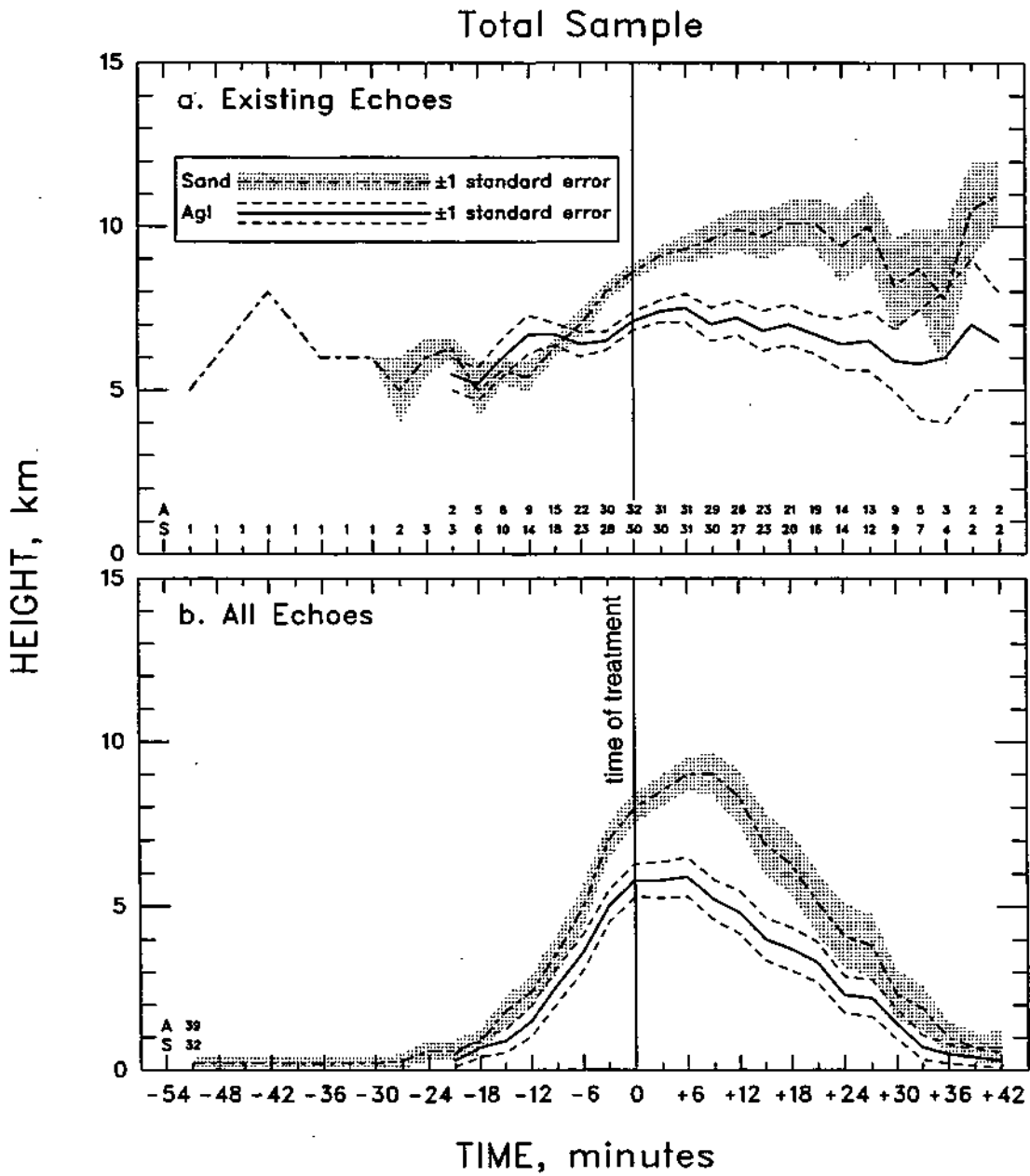


Figure 8. Variation with time of the means of the 10-dBZ echo-top heights for sand- and AgI-treated echoes in existence at each interpolated volume scan (a) and for all treated echoes (b)

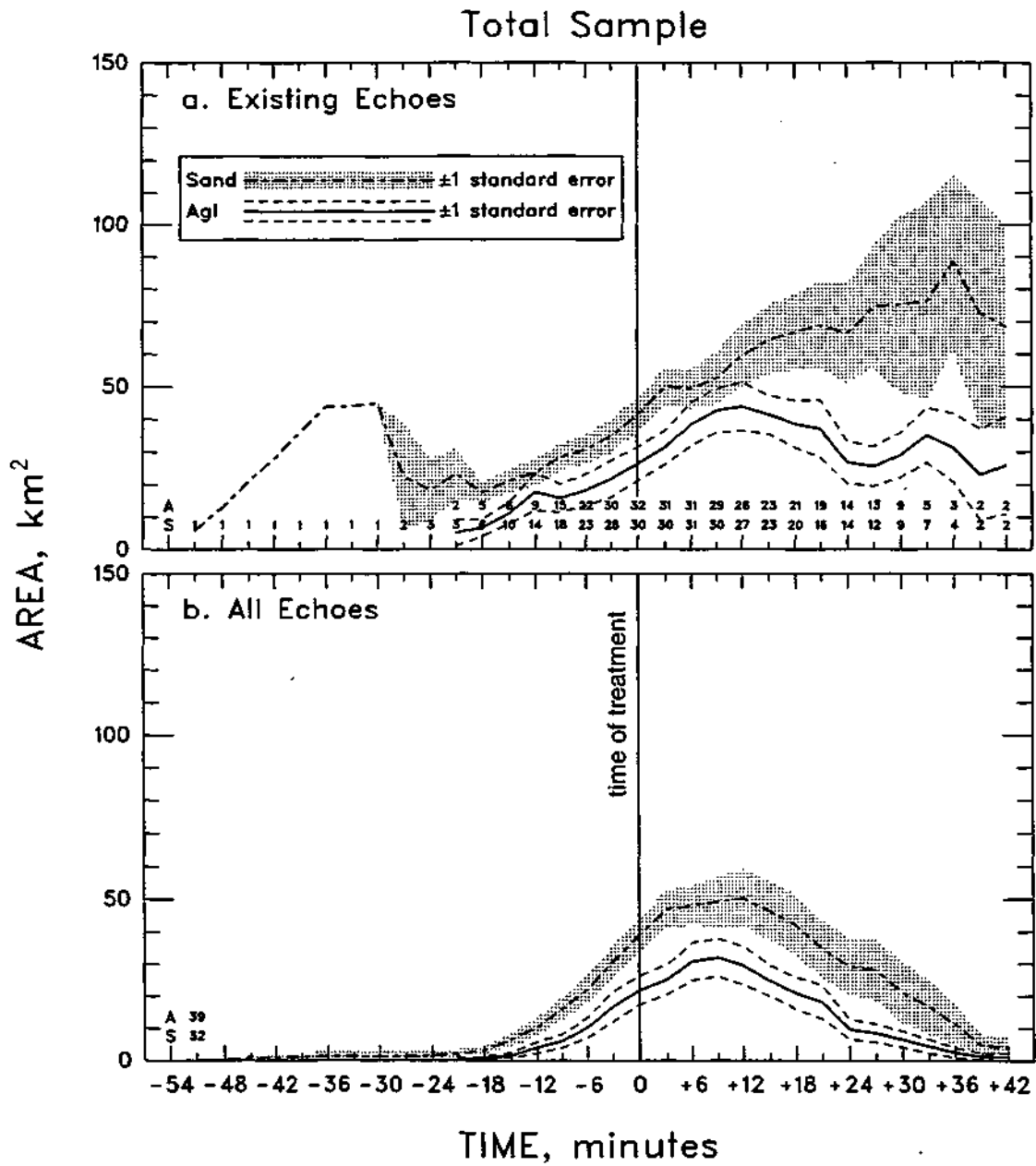


Figure 9. Variation with time of the means of the 10-dBZ echo areas for sand- and AgI-treated echoes in existence at each interpolated volume scan (a) and for all treated echoes (b)

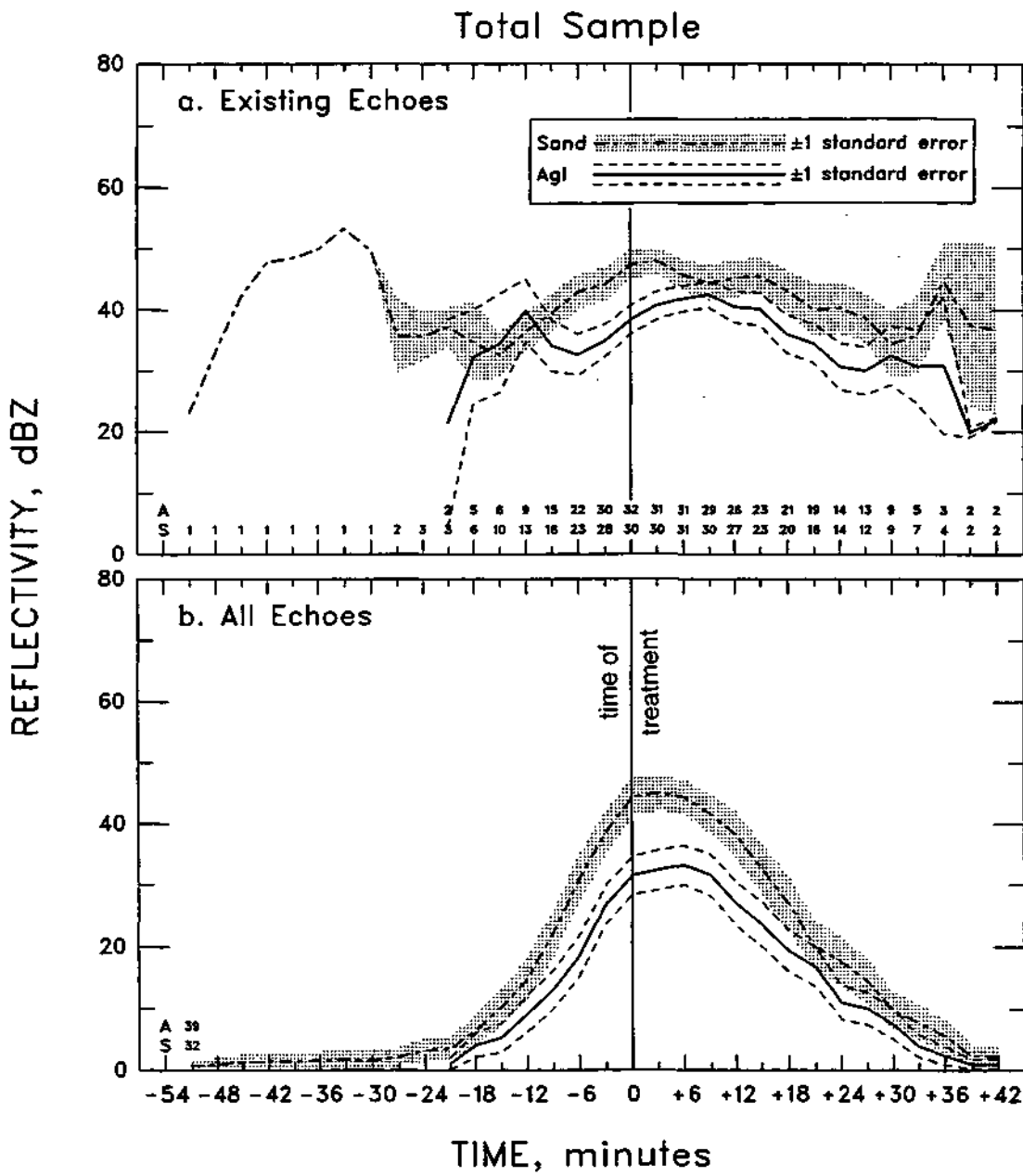


Figure 10. Variation with time of the means of the maximum reflectivities for sand- and AgI-treated echoes in existence at each interpolated volume scan (a) and for all treated echoes (b)

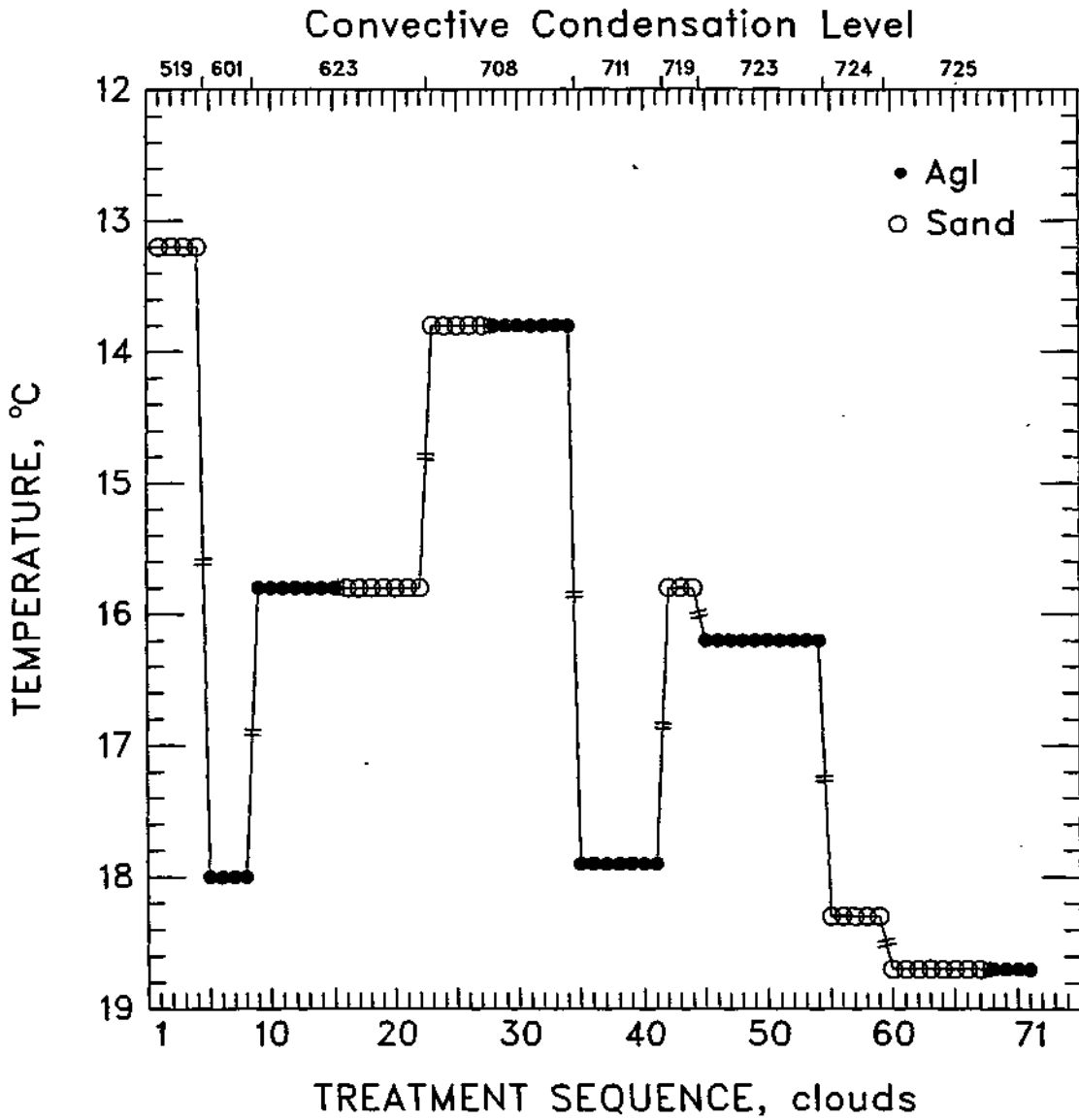


Figure 11. Temperature of the convective condensation level through the operational period

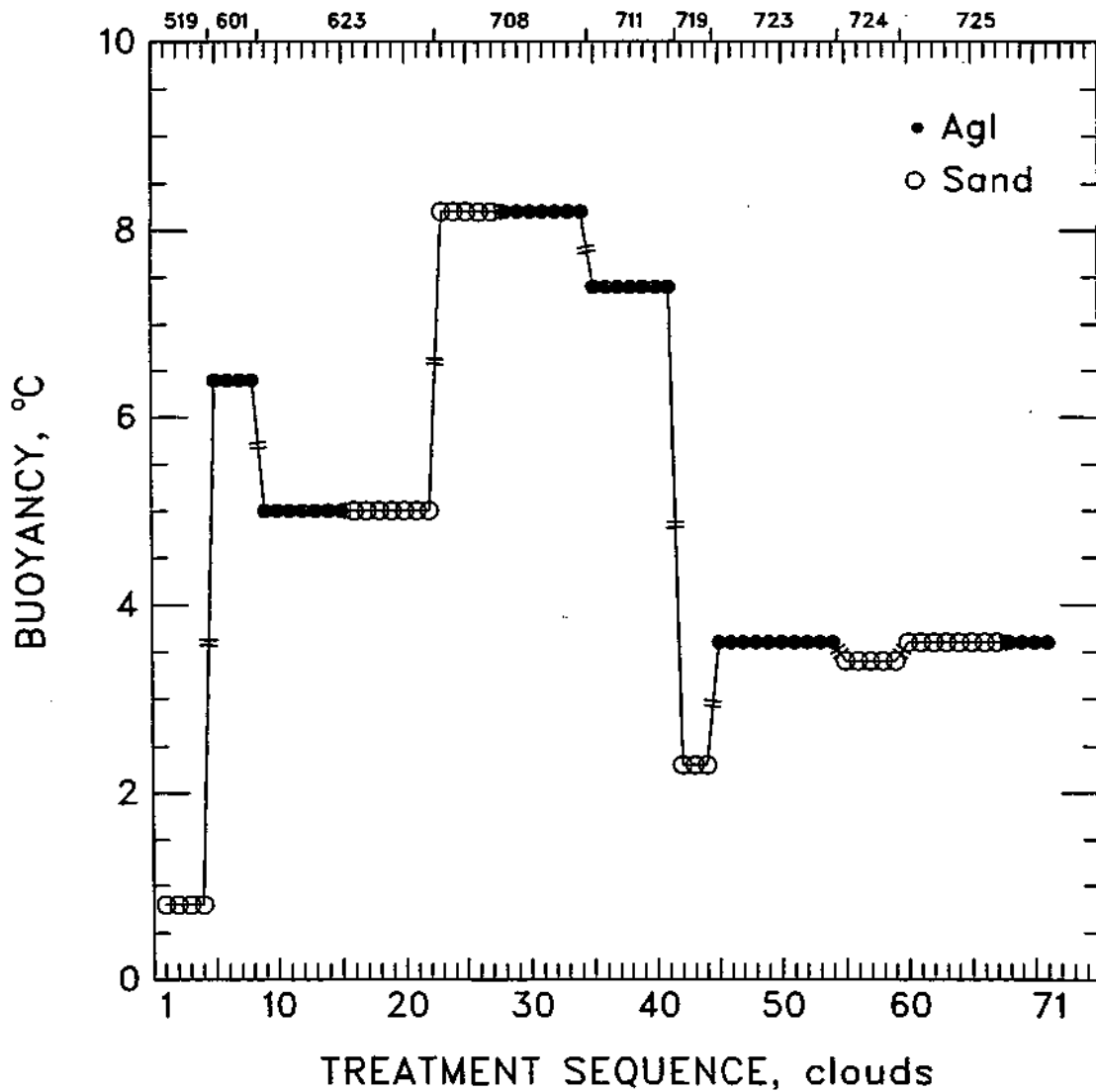


Figure 12. Potential buoyancy through the operational period

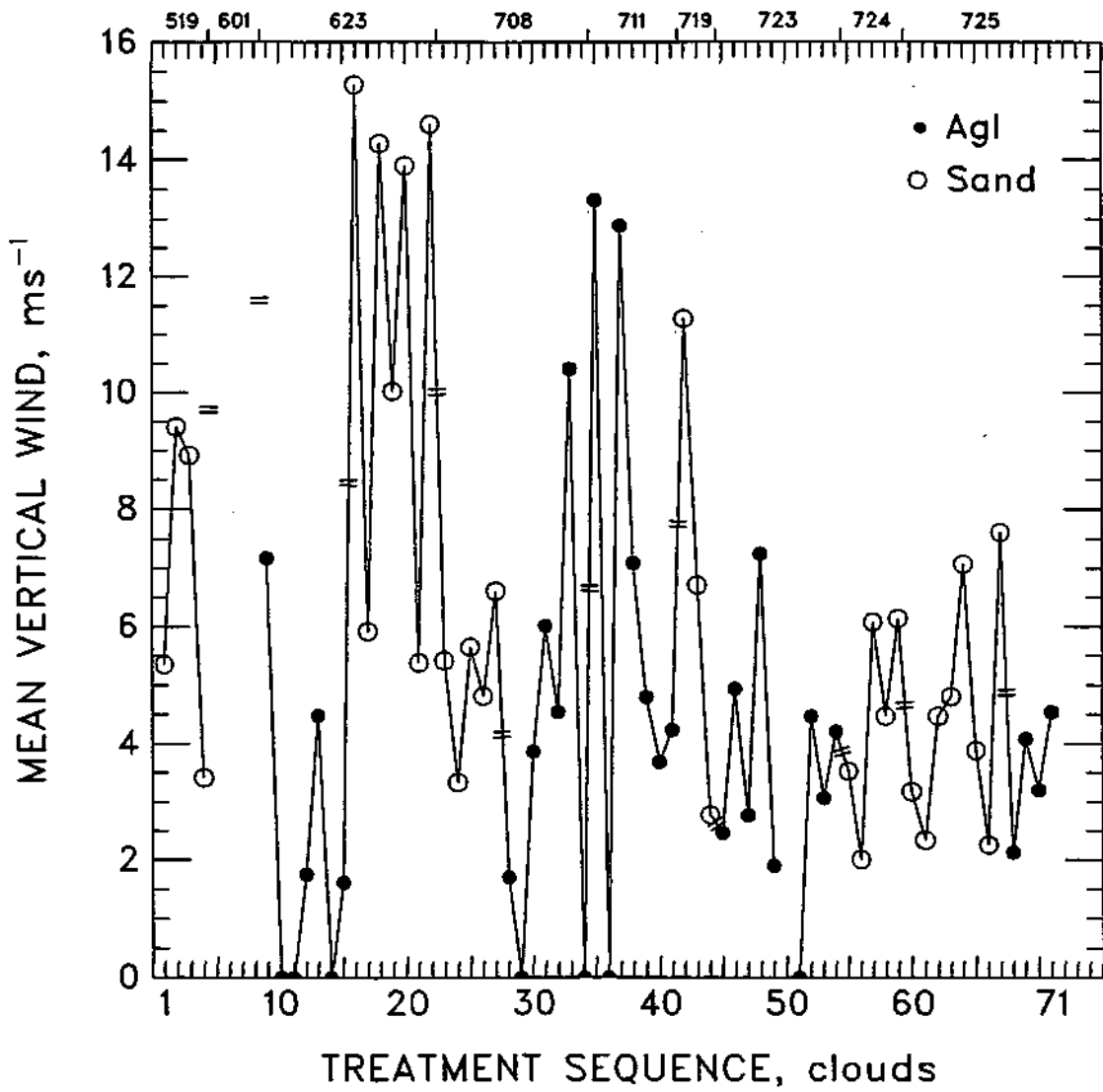


Figure 13. Mean vertical velocity or vertical wind of the main updraft through the operational period

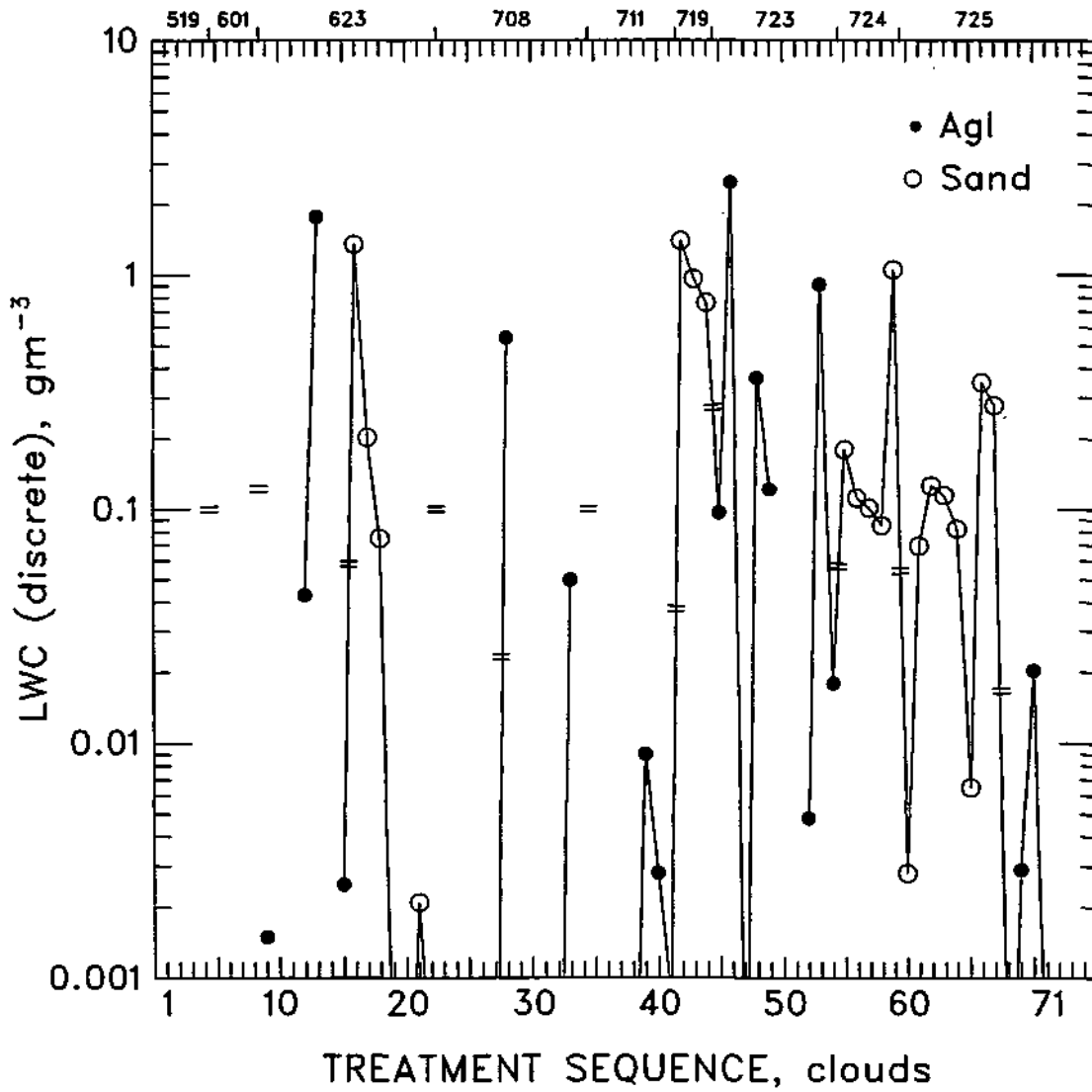


Figure 14. Liquid water content by method I (discrete), calculated for the main updraft through the operational period

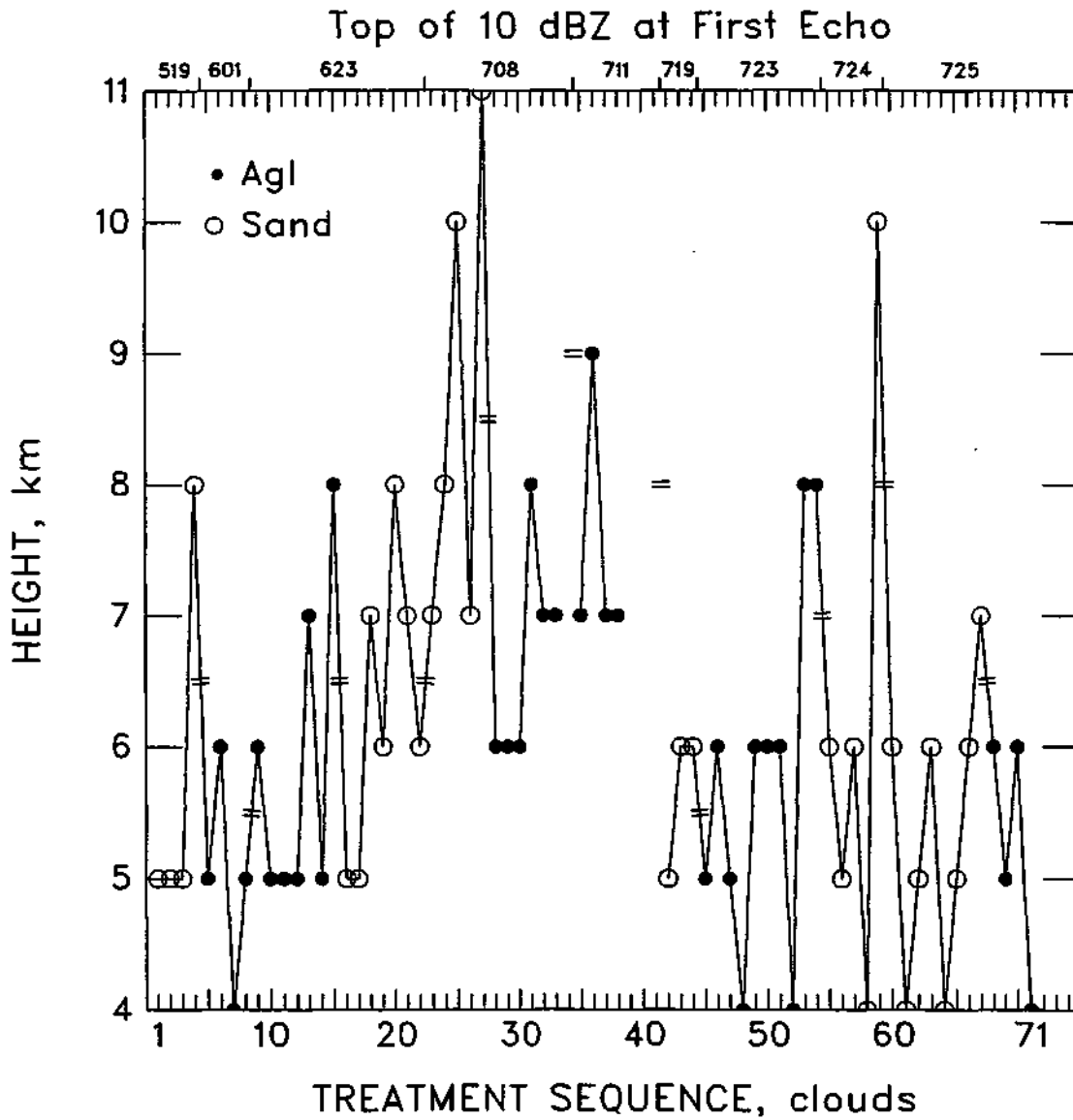


Figure 15. Top height of the 10-dBZ contour at first echo through the operational period

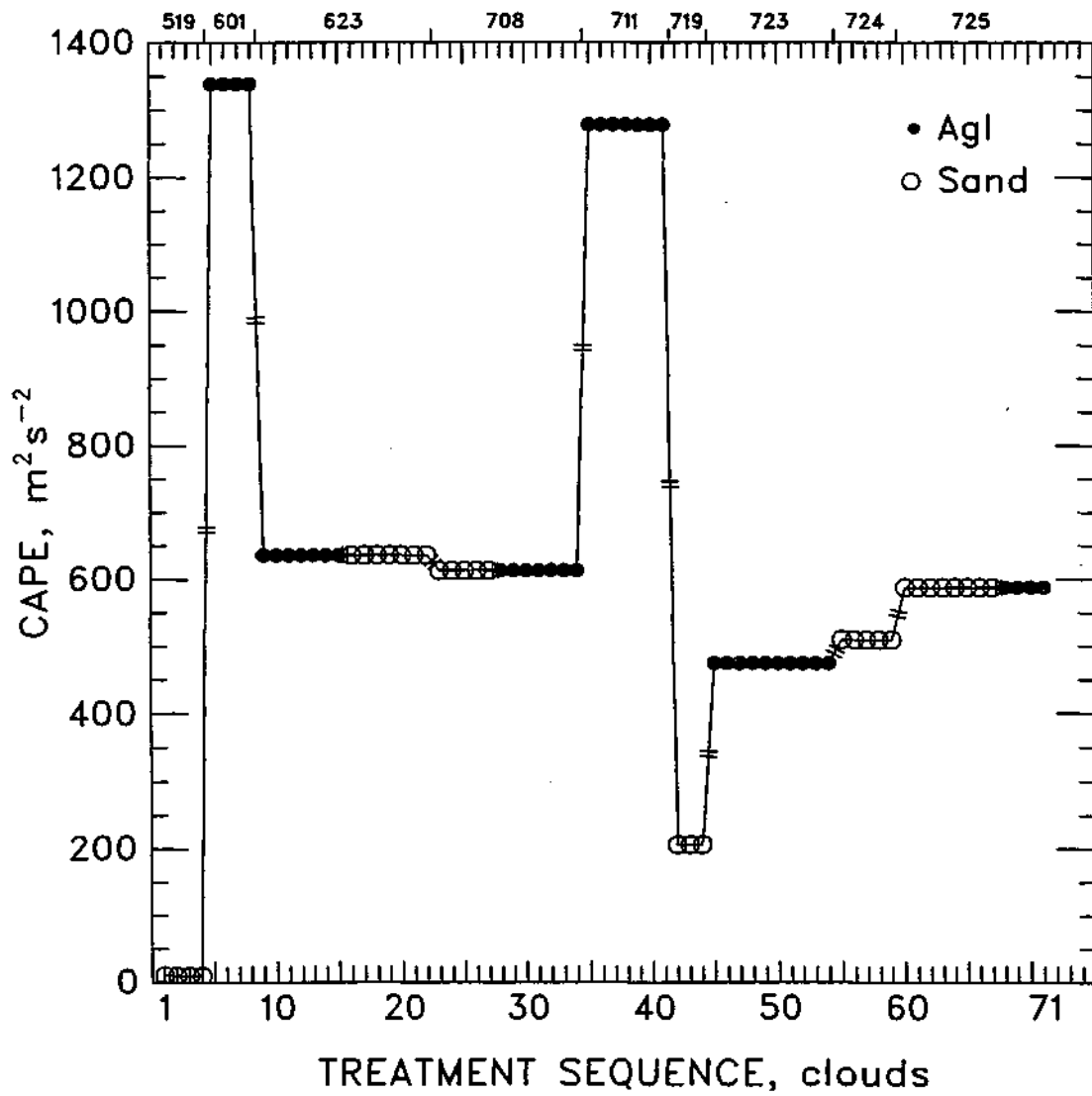


Figure 16. Bulk Richardson number through the operational period

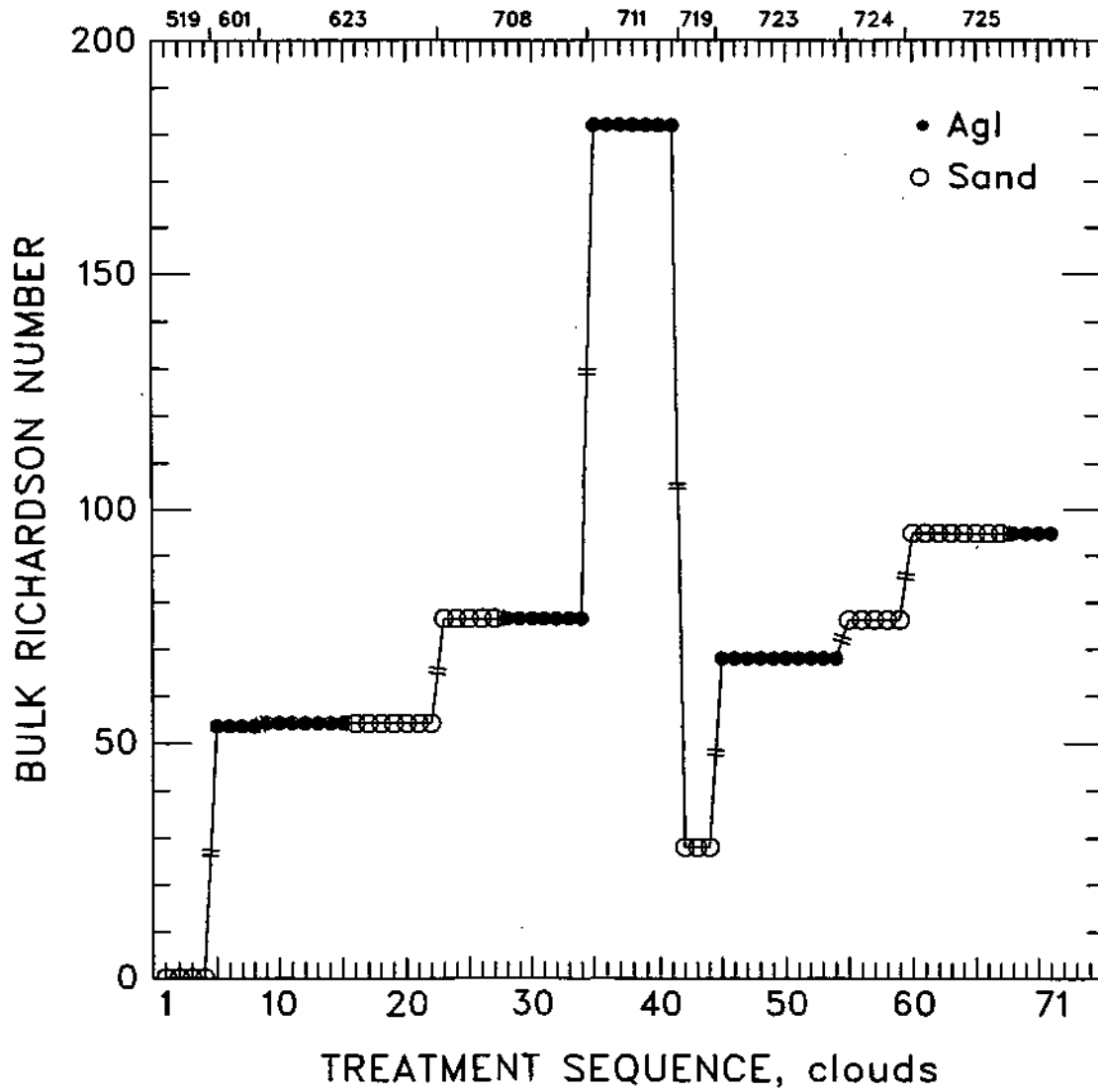


Figure 17. Convective available potential energy through the operational period

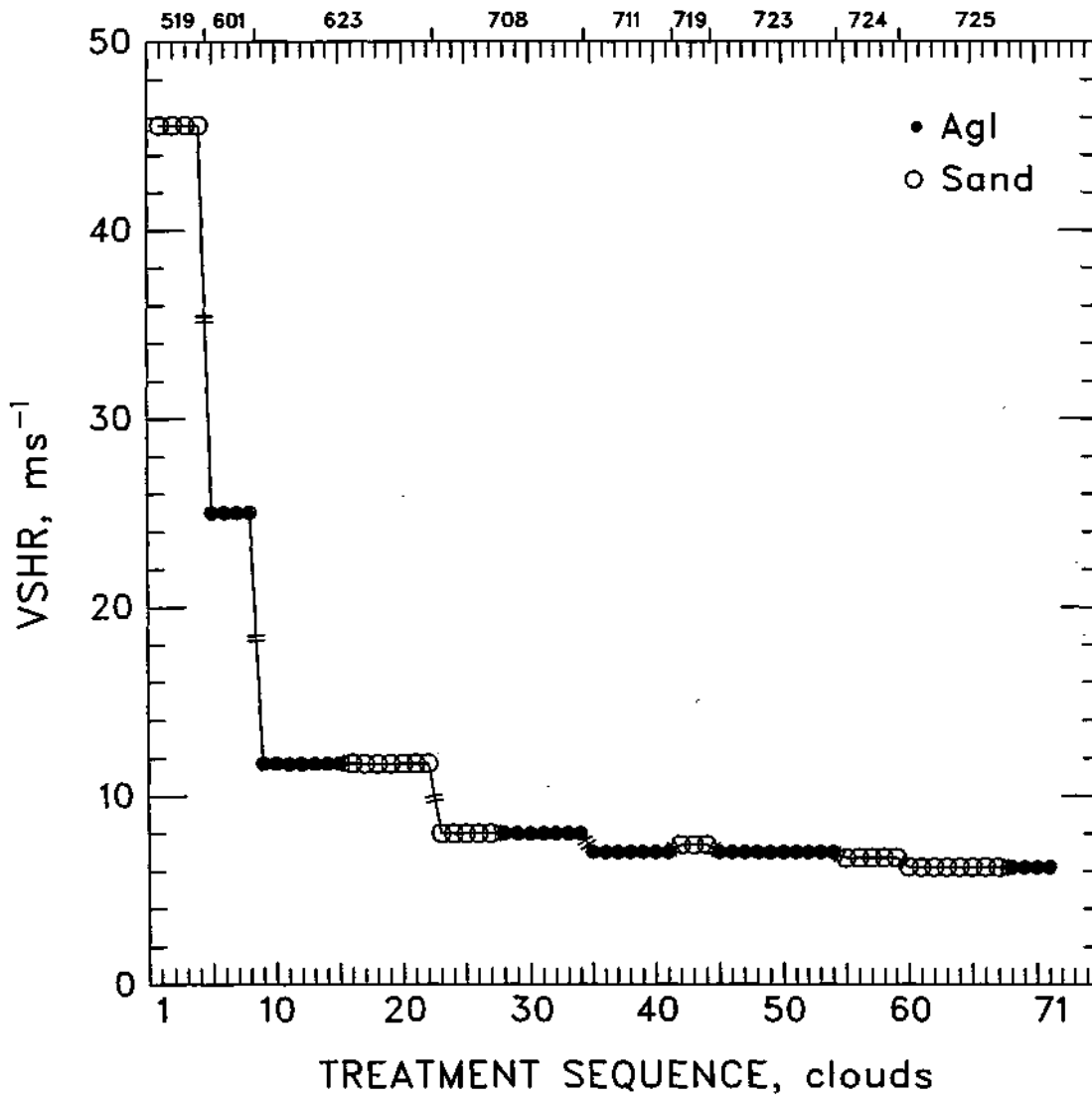


Figure 18. Vector difference in the wind at 4 km and the average wind in the lowest 500 m through the operational period

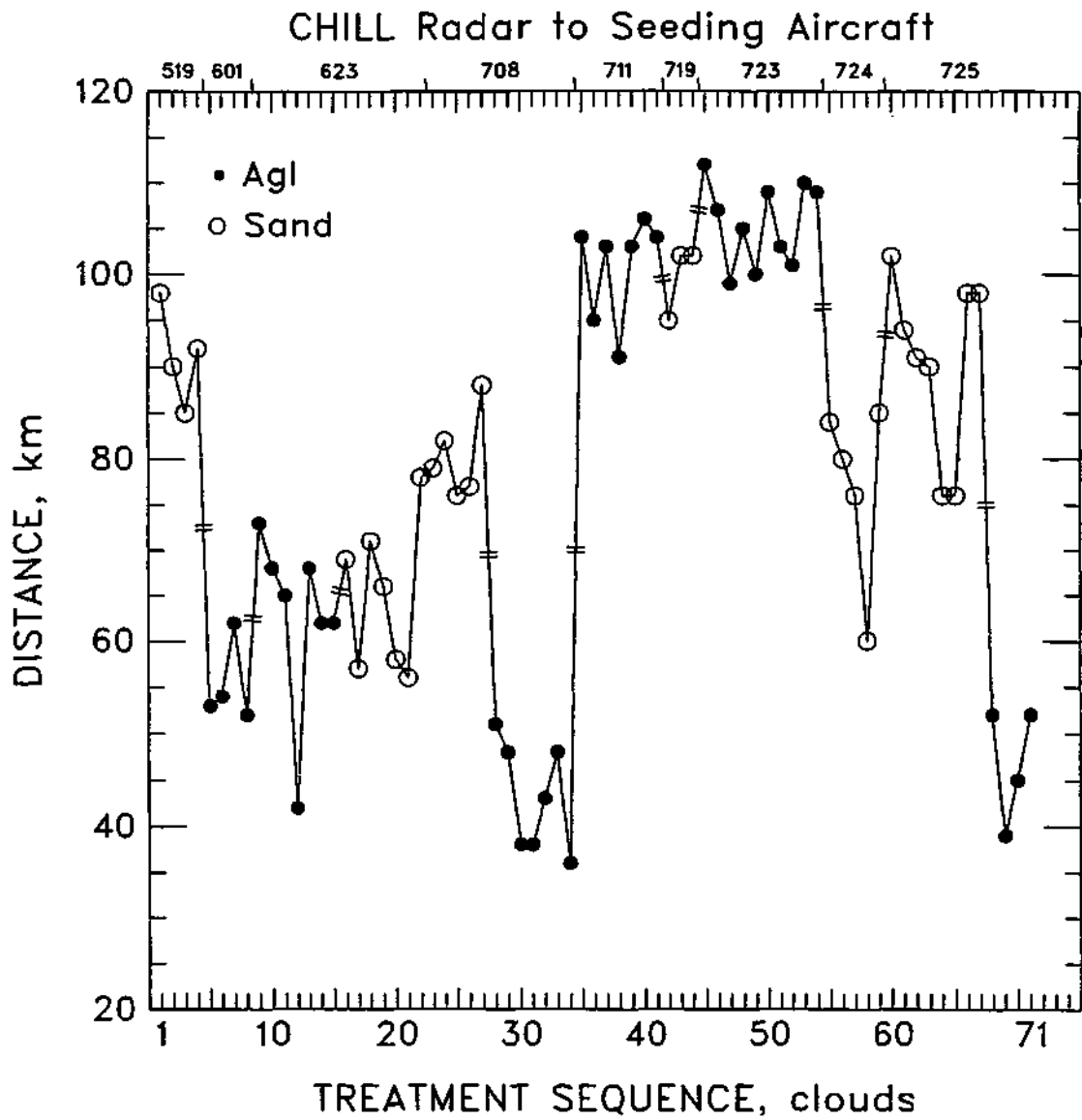


Figure 19. Distance from the CHILL radar to the seeding aircraft through the operational period

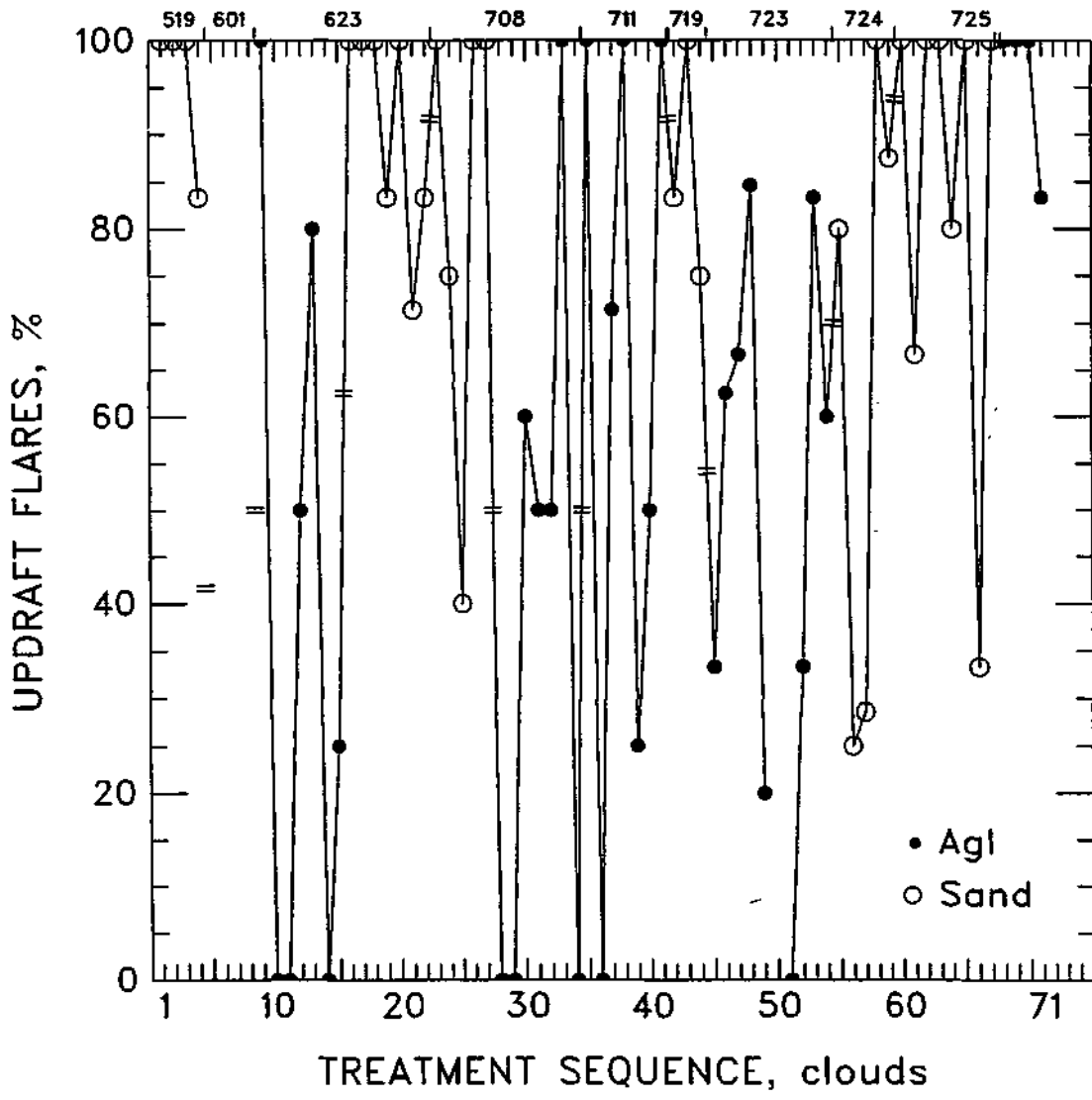


Figure 20. Percentage of flares released in (any) updrafts through the operational period

Table 3. Key Predictor Variables and Their Definitions

<i>Variables</i>	<i>Definition</i>
Synoptic	
pb	Synoptic (parcel) potential buoyancy (°C).
tccl	Temperature of CCL using averaged data in lowest 100 mb (°C).
Ri	Bulk Richardson number, calculated using CAPE and vs _{hr} .
Radar	
CPmndia	Mean diameter of echo at treatment, averaged in height (km).
CPHtp10	Top height of the 10 dBZ contour at treatment (km).
CPMxZ	Max reflectivity at treatment (dBZ).
FECPt	Time from first echo to treatment (min).
Aircraft	
NBuoy	Net buoyancy (°C) (= Mean_TBuoy - Load W _ Load_I)
Buoy_Enh	Buoyancy enhancement (°C).
Mean_VW	Mean vertical velocity (vertical wind) of the updraft (ms ⁻¹).
SWC_frac	Fraction of solid water content [SWCd / (Mean_JWC + LWCd + SWCd)].

Table 4. Key Response Variables and Their Definitions

<i>Radar variables</i>	<i>Definition</i>
MaxH10	Maximum top height of the 10-dBZ reflectivity contour (km).
MaxA10	Maximum area of the 10-dBZ reflectivity contour (km ²).
MaxZ	Maximum reflectivity (dBZ) of the echo core at any time.
MXCPdH10	Change in top height of the 10-dBZ contour from treatment to max height (km).
MXCPdA10	Change in area of the 10-dBZ contour from treatment to max area (km ²).
MXCPdZ	Change in max reflectivity from treatment to max reflectivity of the echo (dBZ).
CPMXtMxA	Time from treatment to max, 10-dBZ area of the echo (min).
FEMXtMxA	Time from first echo to max 10-dBZ area of the echo (min).

Table 5. Key Predictor Variables for All Clouds

Variables	Mean		Stan dev		Sample size		Method I		Method II	
	Sand	AgI	Sand	AgI	Sand	AgI	t	W	t	W
pb	4.1	5.6	2.2	1.9	32	39	0.11	0.08	0.07	0.00
tccl	16.3	16.4	2.1	1.6	32	39	0.81	0.82	0.81	0.83
Ri	62.1	88.8	31.0	45.8	32	39	0.37	0.60	0.43	0.63
CPmndia	4.8	3.2	2.5	2.4	32	39	0.08	0.03	0.04	0.01
CPHtp10	7.1	5.5	3.1	3.2	32	39	0.09	0.04	0.00	0.00
CPMxZ	43.2	30.4	19.7	19.9	32	39	0.11	0.06	0.06	0.01
FECPt	8.8	6.0	11.1	6.2	32	35	0.15	0.29	0.14	0.27
NBuoy	-1.3	-1.5	3.8	1.7	28	27	0.81	0.13	0.80	0.09
Buoy_Enh	0.5	0.5	0.04	0.06	28	27	0.02	0.03	0.03	0.03
Mean_VW	6.6	3.9	3.8	3.4	32	34	0.09	0.03	0.14	0.10
SWC_frac	0.22	0.17	0.33	0.27	28	27	0.63	0.80	0.54	0.77

Note: N = 71
t = student's t-test.
w = Wilcoxon sum rank test
= p-values significant at 0-5 percent
= p-values significant at 5-10 percent.
Variables are defined in table 3.

Table 6. Key Response Variables for All Clouds

Variable	Mean		Stan Dev		Sample Size		Method I		Method II	
	Sand	AgI	Sand	AgI	Sand	AgI	t	W	t	W
MaxH10	10.6	7.3	2.5	3.1	32	39	0.00	0.00	0.00	0.00
MaxA10	80.3	44.4	58.9	45.7	32	39	0.03	0.04	0.01	0.03
MaxZ	52.1	41.0	13.8	19.0	32	39	0.09	0.06	0.04	0.04
MXCPdH10	2.3	0.3	2.6	2.3	32	35	0.04	0.07	0.10	0.11
MXCPdA10	34.3	22.8	52.8	37.1	32	35	0.19	0.47	0.16	0.45
MXCPdZ	6.2	6.6	12.9	16.3	32	35	0.93	0.80	0.93	0.76
CPMxiMxA	9.0	7.2	13.0	6.9	32	35	0.51	0.55	0.39	0.45
FEMxiMxA	17.8	13.2	10.7	7.7	32	35	0.00	0.00	0.00	0.00

Note: N=71
t = student's t-test.
w = Wilcoxon sum rank test
= p-values significant at 0-5 percent
= p-values significant at 5-10 percent.
Variables are defined in table 4.

3. VISUAL ASSESSMENT OF SEEDING EFFECTS

by

Robert R. Czys and Stanley A. Changnon

Introduction

Many meteorologists and pilots experienced in flying cloud seeding aircraft have reported that they could see changes in the appearance of clouds shortly after seeding with AgI or dry ice. Typical reports noted that the seeding, which is intended to expedite the conversion of supercooled liquid to ice, causes rapid glaciation and/or cloud-top growth.

During the course of the 1989 work in Illinois, an experiment was conducted involving the visual assessment of seeding effects. At the end of each flight, the pilot of the meteorological/seeding aircraft, a 20-year veteran in cloud seeding, and the on-board meteorologist-cloud physicist, a relative novice, were asked to independently identify which type of treatment the experimental units had received, AgI or sand. Both personnel were totally blind as to the treatments used, and they could only judge the treatment effects by the appearances they expected to see in the rapidly growing upper portions of the cumulus congestus being sampled. Their individual decisions about the type of treatment were made after each flight, along with a record of their reasons for naming the treatment. If they could not show evidence of what they believed was either seeding or no seeding, they could indicate that they were unable to make a decision.

The project's senior radar meteorologist was involved in a similar experiment. During the radar data analysis, and after all treated echo cores had been completely measured, this analyst was asked to examine the data to identify which of the experimental units appeared to have been treated with AgI and which with sand. The analyst could also indicate inability to make a decision. This person was also totally blind to the treatment type. Decisions as to AgI treatment were based on perceptions that the seeded echo behavior, in particular horizontal growth and/or intensity, would conform to a standard reaction.

Analysis of the Results

The treatment identification made by the three individuals for each of the 25 experimental units are listed in table 7. In some cases, the observers and the analyst were unable to make a choice, and these cases are noted. Several instances of indecision occurred during May when rain systems were large and complex.

Table 8 summarizes each individual's choices based only on the cases when each person made a choice. Interestingly, the pilot picked 17 of 20 treatments correctly, or 85 percent. The on-board meteorologist also showed considerable skill, picking

13 of 19, or 68 percent. Thus, both observers on the aircraft were very skillful in detecting seeding effects in the clouds.

Conversely, the radar analyst picked only 5 of 18 cases correctly. The radar analyst's 28 percent rate of correct identification falls well below chance and reflects no skill in this area. This result suggests use of an incorrect perception of seeding effects, or an inverse cloud response due to seeding. Chapter 5, which will address the seedability of clouds, shows that an inverse outcome might be expected from examination of the radar data; that is, many seeded echoes appeared to grow less and seemed shorter than sand-treated echoes. Thus, the expected radar portrayal of the seeded echo behavior was reversed, and a low score by the analyst was in essence "correct," in that it was substantiated by the ensuing analysis.

Also shown in table 8 are the choices made for the large "A" experimental units, and the smaller "B" experimental units. This breakdown indicates that the pilot and the on-board meteorologist were both extremely skilled in identifying the treatment choices made with the smaller clouds. The pilot's score was perfect, nine for nine, and the meteorologist was 80 percent correct.

Both were less accurate on the large cloud choices. This may be attributed to the greater complexity of the large cloud experimental units, which are more difficult to track and observe during and after treatment. They represent much more complicated cloud conditions than the B experimental units. This is also expected because the B experimental units were penetrated two or more times, providing the pilot and the meteorologist with more information on B experimental units than on A experimental units.

The cases when neither the pilot, the meteorologist, nor the analyst could identify a treatment showed no preference for either seeded or nonseeded cases, and were almost evenly split for each individual. Inability to decide occurred for several reasons, including lack of aircraft contact with treated clouds and the complexity of the sky. In most such cases, the observers reported that they were unable to follow the cloud's elements after treatment.

Summary

This evaluation must be treated with caution due to the limited response variables and the relatively small sample size of visual impressions. Only two persons, well skilled in cloud studies and observation, were available to make such visual estimates. However, it is important to this assessment that both showed skill much above the level of chance (62 percent) in

identifying a seeded experimental unit. In fact, their success rate ranged from 68 percent to 85 percent correct for the 20 seeding decisions they made. Their choices were less correct with the large cloud conditions, but still better than chance, while their choices with small clouds were nearly perfect. There seems little doubt that seeding near cloud tops produced marked visual effects. Hence, skilled analysts and observers can qualitatively detect seeding effects.

These first-hand visual observations were not substantiated by the radar meteorologist. However, the radar meteorologist's apparent inverted skill was supported by the cloud echo-core analysis. The characteristics of the seeded echo cores, as perceived by radar analysis, were generally less indicative of expected behavior (rapid growth and larger tops) than were the sand-treated clouds. Thus, based on the expected primary echo reaction to seeding, the analyst's decisions were in a sense "correct" guesses.

A question remains about echo height when comparing the echo-core results described in chapter 5 with these visual

results. In general, the radar echo data indicated that the seeded echoes grew less, on the average, than did the sand-treated echoes. However, the pilot, who demonstrated considerable skill in detecting seeding and identified eight of the large cloud experimental units correctly, also indicated that rapid vertical growth increased with the AgI-treated clouds (on the cases he chose correctly). Thus, increased cloud growth was a key factor in his determination of seeding. The on-board meteorologist made correct choices of AgI treatment in the large clouds based not on observations of growth, but rather on the appearance of ice streamers, intercloud haze, mergers of feeder cells, and other forms of glaciation.

The unanswered question is why the growth of clouds appeared visually but not in the radar data. Were the cloud particles below the detection capability of the 10-cm wavelength radars? Regardless, one is led to believe from this admittedly small sample that skilled cloud observers can detect the effects of cloud seeding in and around treated clouds with reasonably high rates of success.

TABLES FOR CHAPTER 3

Table 7. Summary of Treatments and Estimated Treatments, 1989 Field Experiment

Number	Experiment unit			Estimations		
	Type*	Date	Treatment	Pilot	In-flight meteorologist	Radar meteorologist
1	B	5/19	AgI	**	**	**
2	A	5/19	P	**	**	AgI
3	B	5/25	P	**	AgI	**
4	B	5/30	P	**	AgI	**
5	A	6/1	AgI	**	AgI	P
6	B	6/3	P	P	P	AgI
7	B	6/3	AgI	AgI	AgI	**
8	B	6/12	AgI	AgI	AgI	AgI
9	B	6/12	P	P	P	P
10	B	6/18	P	P	P	**
11	A	6/23	AgI	AgI	**	P
12	A	6/23	AgI	AgI	AgI	**
13	A	6/23	P	P	AgI	AgI
14	B/A	6/27	P	P	P	AgI
15	B/A	6/27	AgI	AgI	AgI	P
16	B	7/2	P	P	**	P
17	A	7/8	P	P	**	AgI
18	A	7/8	AgI	AgI	AgI	P
19	A	7/11	AgI	AgI	P	P
20	A	7/19	P	P	P	AgI
21	B	7/19	AgI	AgI	AgI	**
22	A	7/23	AgI	P	P	AgI
23	A	7/24	P	P	P	P
24	A	7/25	P	AgI	P	AgI
25	A	7/25	AgI	P	**	P

Notes: * A = large clouds; B = small clouds.
 ** Unable to make a decision.
 [shaded box] = Incorrect guesses.

Table 8. Visual Identification of Seeding Effects, 1989 Field Experiment

	Pilot	In-flight meteorologist	Radar meteorologist
Total number of choices of treatment	20	19	18
Number correct	17	13	5
Percent correct	85	68	28
Number of A or large cloud choices	11	9	12
Number correct	8	5	2
Percent correct	73	56	17
Number of B or small cloud choices	9	10	6
Number correct	9	8	3
Percent correct	100	80	50

4. EVALUATION BASED ON SYNOPTIC WEATHER CONDITIONS

by
Nancy E. Westcott

Introduction

This chapter presents the results of the 1989 cloud seeding experiment in the context of synoptic weather conditions. The data were examined from this perspective for several reasons. As in past cloud modification projects, partitioning the data into groups collected during similar weather conditions should reduce the natural day-to-day variability of cloud behavior, thus enlarging the chance to detect a seeding signal. Under different weather conditions, cloud growth characteristics are apt to be different and thus, treatment effects may differ. Cloud histories were also examined to determine whether significant differences in growth existed under different synoptic conditions. This approach also provides a basis for the comparison of results with other projects conducted in the Midwest and elsewhere.

Use of Synoptic Variables in Midwestern Experiments

Summertime convection occurs under many synoptic weather conditions in the Midwest. These conditions can be described in many ways: by synoptic types, by thermodynamic indexes, by wind field parameters, by cloud model runs, by cloud characteristics in the study area, or by some combination of the above. All of these methods have been used to forecast like conditions for cloud development and also in subsequent data analysis in an attempt to reduce the natural variability of cloud growth characteristics.

In cloud seeding experiments of relatively short duration, such as a single summer season, it is especially important to examine the ambient conditions under which clouds form. It is possible for seeded clouds to develop under conditions in which clouds are expected to be large, while nonseeded clouds could develop during periods when clouds are expected to be small. This occurred during the 1986 PACE field program (Westcott, 1990). Thus data from the 1986 experiment were partitioned according to synoptic weather conditions during the analysis phase. As a result, clouds were segregated into categories of like behavior, drastically changing the interpretation of the 1986 seeding results. The time of day, type of forcing, amount of cloud cover, and first echo height were important in describing the different weather conditions.

Cloud modification projects relevant to the Midwest have partitioned their data according to various atmospheric conditions. During Project Whitetop, a cloud seeding experiment in south-central Missouri (1960-1964), precipitable water and wind direction were used to forecast acceptable days for treatment. In the analysis of the Whitetop results, wind direction (defined by the seeding plume motion), wind speed at 1.2

km above mean sea level (msl), the presence of precipitation in the nonplume area, the number of seeding hours, and the maximum echo-top height were used as criteria to partition the days for analysis of cloud seeding effects on daily rainfall (Braham, 1966). A slightly positive seeding effect was found on days with maximum echo tops between 6 and 12 km and on days with west winds. A negative treatment effect was observed on days with south winds, and a stronger negative effect was found on days with maximum echo tops of more than 12 km. On days with precipitation in the control area, modest increases in statistical significance were found for these positive and negative effects. When more seeding material was applied, the mean rainfall in the target area decreased, suggesting that overseeding had occurred. No effect was observed on dry days with maximum echo tops of less than 6 km (Flueck, 1971; Braham, 1979).

Two major inadvertent cloud modification projects of the 1970s examined summer rain periods. One was the Metropolitan Meteorological Project (METROMEX, 1971-1975) and the other was the Chicago Hydrometeorological Area Project (CHAP, 1976-1979). Rain events in METROMEX were partitioned by synoptic weather type, wind direction, and amount of precipitation (Vogel, 1977; Changnon, 1978a; Braham, 1981). CHAP employed the same stratification criteria (Changnon, 1980b). The duration, areal coverage, and total rainfall amounts were found to vary according to synoptic type.

In two cloud seeding experiments in the Dakotas [Rapid Project, 1964-1966; and the North Dakota Pilot Project (NDPP), 1969-1972] precipitable water, 850-millibar (mb) wind conditions, and vorticity advection were used to forecast suitable rain periods for seeding (Dennis and Kozielski, 1969; Dennis et al., 1975). Both projects partitioned their results according to storm type (shower and storm days). The Rapid Project data also were stratified by direction of flow (Dennis and Koscielski, 1969). The NDPP seeding results were examined in terms of the 500-mb temperature, cloud-base temperature, and cloud model-derived seedability. The Rapid Project results indicated increased daily rainfall on shower days and a negative treatment effect on storm (squall line) days. The NDPP results indicated a slightly positive seeding effect on both types of days. In addition, first echoes were observed to form at a lower height on seeded days (Dennis and Koscielski, 1972).

Elements Leading to the Design of the 1989 Experiment

The 1986 and 1989 Illinois field experiments were both designed to derive the largest possible sample of experimental units. In planning the 1986 seeding experiment, the randomiza-

tion of the treated rain periods (areas) was to be based on synoptic type. But unlike the multiyear projects mentioned previously, it was reasoned that a single six-week project might produce too few samples in each category. Thus no blocking was done (Changnon et al., 1987), and the clouds were simply randomized based on rain periods. Each rain period had to be separated by an hour or more from other rain periods. The analysis of the three experimental units treated in 1986 revealed the possibility of more than one discrete rain area for seeding within the rain periods.

In the 1989 experiment, however, the randomization was designed on a more localized scale, following the concept of the Southwest Texas Project (Rosenfeld and Woodley, 1989). An experimental unit was defined as a moving circle with a radius of 28 km, containing one or more echoes. The circle was defined by centering on the geometric mean of the treated cores. A mean unit motion was determined from the center of the unit at the time of the last treatment and then from its subsequent locations as noted in real time. The experimental unit's movement was then calculated by interpolating its position backward and forward in time. Only one type of treatment was applied to the echoes within an experimental unit, and none was applied in the 28-km buffer zone surrounding each circle (Czys et al., 1992). During the 1989 experiment, two or more large cloud experimental units occurred during a given convective period on three days. Thus, the experimental design was successful in increasing the number of experimental units over the number that would have been obtained using the 1986 rules.

The PACE 1986 cloud data were examined for criteria that might be useful in predicting convection suitable for modification in 1989. This was done in two ways, first using five standard thermodynamic criteria (Scott and Huff, 1987); and secondly using a combination of the temperature of the cloud condensation level and the potential buoyancy (Scott and Czys, 1992; Czys and Scott, 1993). These later parameters could successfully indicate the probability of convective occurrence; categorize the maximum daily echo-top height as short, medium, or tall; and indicate the presence or absence of supercooled drizzle and raindrops at the -10°C seeding levels.

The results of PACE 1986 and projects Whitetop and METROMEX suggested that the expected daily echo-top height was the appropriate blocking parameter for the 1989 experiment. A climatology of daily maximum echo tops was determined from METROMEX to be a bimodal distribution of echo-top heights in rural storms (Braham and Wilson, 1978; Braham, 1981). The major inflection point in the distribution was at 10 km, with peaks at 6 and 12 km. A seeding response would be especially difficult to detect and actually might differ for events when clouds typically reached 6 to 10 km, or when they grew to 12 km or higher. Thus, to maintain the largest possible sample of clouds within each randomized group, only two randomization blocks were used, based on cloud-top heights observed at the time the experimental unit was declared:

1. The large cloud experimental units were those in which clouds were actively growing through the flight level around 6 km above ground level (AGL), while other cloud tops in the area were exceeding 9 km.
2. The small cloud units were those in which clouds were just reaching the flight level (6 to 8 km).

The synoptic characteristics, and in particular the thermodynamic indexes were found to be very different for the large and small cloud units in 1989. An average of five suitable clouds per experimental unit were found on large cloud days, whereas the average was two per experimental unit on small cloud days. The radar analysis of the 12 large cloud experimental units included 67 clouds, but the eight small cloud units contained only 15 suitable clouds. Additionally, the large clouds units contained clouds with the greatest growth and were the largest rain producers.

The randomization procedure successfully provided a balanced number of AgI- and sand- treated units and clouds. Six of the 12 large cloud experimental units were treated with AgI and six with sand, for a total of 35 AgI-treated echo cores and 32 sand-treated echo cores.

Within the large cloud group, however, two distinct cloud populations were sampled based on synoptic weather conditions. These two populations of clouds were classified as "cold front" (CF) and "air mass" (AM), although various other synoptic characteristics could typify these days. The cloud data from 1989 were thus partitioned and analyzed based on these synoptic groupings.

The echo growth characteristics and apparent treatment responses of all the large clouds were compared with the responses observed within the two primary synoptic categories, and also with those echoes occurring during the same synoptic period but in different experimental units (thus having received different treatments). This allowed examination of the day-to-day variability, a comparison of the variability among events of common synoptic type, and study of the variability within a day. If the variability within a day and within synoptic type were as large as those observed for the whole population, the prospect of discerning a seeding signal would be small.

Data and Analysis

Radar Echo Data

Evaluation of the 1989 cloud seeding results was based primarily on reflectivity data collected using the CHILL 10-cm radar. A minimum reflectivity threshold of 10 dBZ was imposed on the analyzed data. The radar volumes were of 1.5- to 4-minute durations, and the echo cores were located within 30 to 110 km of the radar. The data were interpolated to a grid encompassing the experimental unit. The 1989 study focused on the early growth characteristics of individual cores, which in most cases merged with a multicelled cloud system. An inter-

active core tracking program, ICORT, was developed for use with the three-dimensional interpolated reflectivity data ($1 \times 1 \times 1$ -km resolution).

An echo core was defined as an identifiable maximum in reflectivity. Merging was determined to occur when a core became part of a multicored system. Nearly all of the echo cores were merged with other echoes at some point in their history. The only ones not merging had very short lifetimes. The echo cores at the time of first detection were classified as isolated, loosely joined, or strongly merged. For the loosely joined cores, a distinct core was observable at all heights, and typically they were joined at a single level. The lowest levels of each of the strongly merged cores were not distinct from their parent storms at the time of first detection, but they could be identified at low levels later in their history (chapter 7).

This breakdown of first echoes basically stratified the echo cores according to the distance of separation of new feeder clouds from the parent storm. Of the treated cores, the isolated cores typically formed within 5 km of another echo, and the loosely joined clouds about 1 km from an adjacent core, according to the resolution of the radar interpolation scheme. The strongly merged cores may be reminiscent of the weak evolution observed by Petersen (1984) and Westcott and Kennedy (1989). In these, the downdraft-induced outflow was so close to the existing echo in a multicelled storm under weak shear conditions, that the new core appeared as a bulge on the edge of the parent storm, and only became a distinct core later in its history.

The simpler cores generally followed a pattern of 1) formation at a height of 3 to 6 km, 2) vertical and horizontal expansion, and 3) descent of the echo core toward the surface. The expansion of the core and the drop in the altitude of its maximum reflectivity often occurred simultaneously. The same growth model was found in the mid to upper levels for the more complex merged cores, and that pattern was assumed in making the more subjective decisions on defining the beginning and ending of the cores at the lower levels. Echo cores were tracked until they dissipated or until they became indistinguishable from an adjoining echo at all levels. Reflectivity contour intervals of 2.5 dBZ were used. Loss of definition at all levels occurred after the core had reached its peak area, height, and reflectivity. Sixty-seven echo cores were tracked, and four additional clouds were treated but never echoed.

Various echo-core properties were determined for the individual cores at the time of first echo; at the time of treatment; and at the times of the peak height, area, and reflectivity. The amount of change and the rate of change of these properties were computed between the time of first echo and the time of treatment; and between the time of treatment and the time of the peak height, area, or reflectivity. The duration of the echo core was estimated as the time from first echo to the time of peak area. Area was chosen as a basis for the period of growth because the core typically continued to expand horizontally after the peak height was reached (Westcott, 1990).

Moreover, vertical growth computations were made 2 minutes prior to treatment, at the time of treatment and 4 minutes after treatment by fitting a polynomial to the 10-dBZ contour defining the echo top. Some values were missing in the vertical growth parameters because some cores did not echo until after treatment, some dissipated so rapidly that not enough data were available, and a few cores were poorly fit by the computer scheme. Definitions of the variables presented in this chapter are described in the appendixes.

The properties of echoes other than the treated ones have been employed to characterize convection within the units. Earlier projects, in particular Project Whitetop and the Florida Area Cumulus Experiment (FACE), found important covariates in the amount and duration of echo coverage or rainfall prior to treatment (Simpson and Woodley, 1971; Biondini et al., 1977) and in the rainfall in areas adjacent to the target area during and after treatment (Braham, 1966). In this analysis, the radar-estimated rainfall was computed for reflectivities of 30 dBZ or more over a 240 x 240-km area centered on the radar site near Champaign (CMI), and also for the area encompassing the experimental unit. Rainfall totals were accumulated from 15 minutes prior to treatment until treatment, from beginning to end of treatment, and in 15-minute periods after the last treatment pass. The maximum echo top observed within the unit and the maximum daily echo top also were determined.

First echo information was gathered on all of the isolated cores within and nearby each experimental unit. These data were grouped according to whether they occurred before or after the first treatment and whether they formed inside or outside the experimental unit. They were used 1) as indicators of cloud growth properties, 2) to corroborate the first echo properties from the smaller population of treated clouds, and 3) as points of comparison for projects elsewhere.

Cloud Updraft Properties at Time of Treatment

During PACE 1989, a well-instrumented aircraft was used both to seed clouds at about the -10°C altitude and also to sample the microphysical, thermodynamic, and kinematic properties of the treated cloud. (Changnon et al., 1991a; Czys et al., 1992). In particular, the updraft properties of each cloud were examined to confirm cloud conditions detected by radar.

Weather Forecast Parameters

The synoptic variables were computed from the 0700 central daylight time (CDT) Peoria (PIA) soundings. Peoria is located about 130 km northwest of CMI and is on the edge of the experimental area. Forecasting studies have indicated that the early-morning PIA soundings are useful for predicting convective conditions in the PACE target area (Scott and Czys, 1992; Scott and Huff, 1987). These same variables were computed for the 1900 CDT soundings, but many of these

soundings were disturbed by daytime convection and thus were difficult to assess. An NCAR CLASS sounding unit was operated at CMI, and soundings typically were made at midday. Due to mechanical/electrical problems, CLASS soundings in late July limited the rawinsonde data for certain days. However, these additional soundings were used to determine if conditions had changed significantly from the 0700 PIA sounding values.

Weather Conditions

Synoptic Weather Classifications

The six synoptic weather classifications used in this analysis were originally developed for project METROMEX. The classifications and their definitions are listed in table 9.

Many of the 1989 large cloud experimental units occurred in two synoptic conditions. Six units were cold frontal, and occurred on four days. Four units were air mass and occurred on three consecutive days. The other two units were classified as a squall zone and an upper level, low-pressure system. These two units both occurred on days when a second experimental unit had been declared as a small cloud unit. The PIA 0700 CDT sounding data on these days reflected some wetter conditions conducive to large clouds (table 10), and some common to small cloud systems (table 11).

Air-mass storms tend to occur later in summer and are generally smaller in area and duration than cold-front storms (Hiser, 1956). Earlier research has shown that air-mass storms make up only 7 to 33 percent of the total number of storms in various Midwest regions, and they contribute only about 0.5 to 20 percent of the total rainfall (Changnon, 1980b; Vogel, 1977; Hiser, 1956; Hudson et al., 1952). While air-mass storms are generally smaller in overall rainfall production, their relative importance has been found to increase during dry years (Huff, 1969). Air-mass storms also occur at a time in the growing season when rainfall increases due to cloud seeding would be most beneficial.

Cold fronts are a common type of forcing in the central Midwest, particularly in the spring and early summer (Hiser, 1956; Vogel, 1977; Changnon, 1980b). These events typically make up a higher percentage of the total number of summer rain periods (15 to 40 percent) and produce 12 to 40 percent of the total rainfall. However, only about 50 percent of the cold-front storms occur during daylight hours, when air-mass storms are at their peak and when cloud seeding is usually undertaken.

During METROMEX, hail was observed on both air-mass and cold-front days although it was more common on cold-front days. Hail occurred during 23 percent of the cold-front periods and during only 3 percent of the air-mass periods (Changnon, 1978b).

Table 9 also lists four other types of summer rain-producing conditions, which were either not sampled or were characteristic of only one rainstorm. These represent about 55 percent of all summer events and produce 60 percent of all the rainfall

(Vogel, 1977). Hence, the two categories considered here, cold front and air mass, represent less than half of the potential rainfall conditions. In addition, the four air-mass units occurred on three consecutive days in late July and originated from a common air mass. Caution should be used in extrapolating these data to all instances of air-mass storms.

Meteorological Conditions Sampled in 1989

Thermodynamic and kinematic parameters depicting the environmental conditions observed during the 1989 experimental days, and a brief description of the observed storms are presented for each experimental unit (table 10-13). The environmental parameters chosen have been found by earlier studies to be related to the presence and intensity of convection. Two estimates of buoyancy were computed: the convective available potential energy (CAPE), and potential buoyancy (pb). CAPE was evaluated from cloud base to the top of the positive area (between the sounding and a representative moist adiabat on a skew- t diagram). It serves as an estimate of the net work per unit mass done by the environment on an air parcel (energy per unit mass gained by the parcel), that rises from the cloud base to the lowest level of zero potential energy. Thus, CAPE is a measure of potential instability at middle and upper levels (Moncrieff and Green, 1972; Weisman and Klemp, 1982, 1984; Lemone, 1989; Bluestein and Jain, 1985).

Potential buoyancy was computed as the difference between the pseudoadiabat through the cloud base (estimated by the CCL) and the environmental temperature at 500 mb, the approximate treatment level. Thus pb is related to the average updraft from cloud base to 500 mb (Mather et al., 1986b). Lemone (1989) found that in the absence of other external forcing, CAPE is related to the cloud's vertical velocity and potentially to the cloud's depth. Both CAPE and pb were found to be larger for the cold-front days. Although there was external forcing on the cold-front days, the estimates of CAPE and pb suggest that in the absence of forcing, stronger updrafts and taller clouds might still be expected during these periods.

The lifted index (li), which is often used as a severe weather forecast parameter is similar in definition to pb. Lifted index was computed by lifting a parcel along the moist adiabat from the lifted condensation level to 500 mb, where the temperature, considered to be the updraft temperature of a developing cloud, is compared to that of the environment (Peppier, 1988). As found with pb and CAPE, the li differs greatly for the cold-front units, the air-mass units (table 10), and the small cloud units (table 12).

Cold-front and air-mass days were also contrasted according to the prevailing winds. Winds on the cold-front days were typically from the west, and on the air-mass days from the south (table 10). The vertical shear of the horizontal wind was computed in two ways. First it was computed for the Richardson number as the difference between the density-weighted mean wind through 6 km and the mean wind within a representative

surface layer of 500 m (Weisman and Klemp, 1984). Seasonal variation in shear was pronounced, with progressively less shear later in the convective season, as expected from the northward retreat of the polar front. The cold-front soundings showed somewhat stronger shear than the air-mass, particularly in May and June. The afternoon PIA and CMI soundings indicated shear values of more than 10 square meters per second squared (m^2s^{-2}) on the cold-front days, but no increase of shear on the air-mass days. Many studies have indicated that shear is essential to the development of severe storms (e.g., Marwitz, 1972; Weisman and Klemp, 1982; Fovell and Ogura, 1989).

More recently, the interaction of low-level shear with the cold surface outflow has been found to be important in the development of long-lived squall lines (Rotunno et al., 1988; Weisman et al., 1988). The low-level shear at 0700 CDT on three of the four cold-front days was stronger than on the air-mass days (table 10), even though the shear was of moderate intensity on some days. From the above discussion of the ambient weather conditions, one might expect the development of large clouds and possibly severe weather on cold-front days, as opposed to air-mass days. In fact, 16-km echo tops and hail were observed in the 160-km radius of the target area during the afternoon and early evening of each of the four cold-front days.

The height and temperature of the first echo formation on the cold-front and air-mass days also indicated differences in storm and precipitation growth (table 11). The cloud-base temperatures as estimated by the temperature of the convective condensation level were typically warmer on the air-mass days than on the cold-front days in this sample. The precipitable water (pw) also was greater for air-mass days. In this warmer and moister environment, first echoes could and did form at lower altitudes on the air-mass days. The first echo heights on cold-front days were higher and colder, with 16 percent forming above the freezing level, 33 percent below the freezing level, and 51 percent straddling the zero degree isotherm. First echoes on air-mass days formed completely below or just at the freezing level (51 and 49 percent, respectively), but none formed completely above the freezing level. The higher first echoes may indicate that raindrops took longer to form in an atmosphere with somewhat less moisture available, that the coalescence process was more active on the air-mass days, or that the updraft strength at the time of first echo was greater on cold-front days.

Other indexes indicated that while more intense convection might be expected on the cold-front days, clouds could reach 12 km during air-mass days as well. The Richardson number for the air-mass and cold-front days indicated that convection was favored on all large cloud-type days. Also, a relationship among pb, the tccl, and the maximum daily cloud-top height developed by Scott and Czys (1992), coupled with the air-mass and cold-front soundings, showed those days to have more than 60 percent probability for forming tall clouds. The other synoptic types fell into the category of less than 60 percent probability.

Large storms were also signaled on cold-front and air-mass days by several other indexes. The K index, the modified K index, the modified Showalter index, the Sweat index, and the Jefferson index have been found to correlate with rainfall in the Midwest (Peppier and Lamb, 1989). Scott and Huff (1987) found that if four out of five of these indexes exceeded a critical value at both PIA and Salem, IL, (SLO) at 0700 CDT, deep convection would likely occur in the target area. Except for June 23, 1989, the 0700 CDT PIA soundings alone indicated that deep convection could occur. (SLO no longer existed in 1989.)

On each of the two days that were not classified as cold-front or air-mass, a second unit was classed as a small cloud unit. The morning sounding on May 19 and July 19, 1989, indicated that the CAPE and pb were quite small (table 10), more similar to that on air-mass or small cloud days, while the tccl and pw were similar in value to those found on the cold-front days. The PIA sounding on May 19 indicated very strong shear, while shear was weak on July 19, as on the air-mass days. Late in the afternoon on May 19, when the vertical shear was strong, CAPE was small, and thus the RI was small. A "mini-tornado" was observed in the central Illinois area (Kennedy et al., 1989).

Small Cloud Experimental Units

To confirm that the small cloud experimental units were substantially different from the large cloud units, as suggested by earlier midwestern studies and the subjective forecasts made during PACE 1989, the small cloud units also were examined (table 12). Of the first echo heights of the relatively isolated cores, 86 percent formed completely below the zero-degree isotherm, similar to those for the air-mass storms. Coalescence must be an important factor in precipitation formation on these days. The maximum echo tops reached were considerably lower on the small cloud days as well. Values of pb, CAPE, and li indicated that substantially less energy was available for cloud growth, both in the middle and upper troposphere, during these units. These environmental buoyancy estimates appear to be most related to the echo-top height. The pb versus tccl relationship objectively forecasted less than a 60 percent chance of tall clouds forming on small cloud days.

The formation of large or small clouds does not depend on the type of forcing or the amount of vertical shear in low and mid-levels. None of the six small cloud units studied so far were air mass. The amount of rainfall produced in the small cloud experimental unit was generally less than that found for both cold-front and air-mass units. Rainfall over the extended area for the same period was comparable to that of large cloud experimental unit air-mass storms (table 13).

Comparison of Echo Properties of Cold-Front and Air-Mass Cases

Nearly equal samples of cold-front and air-mass echo cores were treated in large cloud units, as shown in table 14. Either

sand or AgI treatments were applied to 33 cold-front echo cores and to 27 air-mass cores. The four no-echo clouds were treated during the cold-front units. All air-mass clouds that were treated, echoed. Seven echoes from the other two large cloud units were treated with sand and are not considered here.

Cores at First Echo

First echo information from the large sample of echoes within and near the experimental units before, during, and after treatment (table 15) indicated that cold-front first echoes occurring on days with hail were taller, colder, and slightly deeper than the air-mass echoes. These results are consistent with earlier findings for days with more organized convection and hail (Towery and Changnon, 1970; Changnon and Morgan, 1976; Changnon, 1978b). The cold-front and air-mass first echo cores were characterized by similar areas and reflectivities at the time of first detection. The mean height of the freezing level was similar for the cold-front and the air-mass units.

The first echo information for the individually tracked and treated cores (table 14) likewise indicated that the cold-front cores were taller and colder than the air-mass cores. On cold-front days, 70 to 75 percent of the treated echo cores were isolated or loosely joined at the time of first echo. In contrast, 70 to 75 percent of the treated air-mass echo cores were strongly merged at the time of first echo. This suggests that stronger updrafts occurred on the cold-front days, and that stronger outflows initiated new core growth farther from the parent cores.

The 27 air-mass first echo cores were much more reflective than their cold-front counterparts (table 14). The initial reflectivity was probably greater for the more merged treated cores than for the large sample of isolated air-mass cores and the cold-front cores because they were already part of larger systems. Because the air-mass cores were joined with the more mature parent systems, their boundaries were somewhat indistinct, perhaps leading to larger values of area and reflectivity. However, the reflectivities might be expected to be greater since the tracked air-mass cores were taller and larger than the isolated air-mass cores.

Cores at Treatment

Several variables, either radar-derived or observed by the seeding aircraft at the time of treatment, have been deemed important indicators of subsequent cloud growth. These variables were examined to identify any distinction between the cold-front cores and the air-mass cores at the time of treatment.

The mean values of the cold-front cores reveal that they were younger, shorter in height, and smaller in diameter at the time of treatment (figures 21, 22). They also tended to have smaller reflectivities and contain smaller amounts of liquid water as measured two-dimensional (2D) precipitation and cloudprobes (table 16). The smaller sizes and lower reflectivities may be due in part to the fact that the cold-front cores were

younger at the time of treatment. The aircraft measurements confirmed that the cold-front clouds had smaller fractions of the total condensate in the solid phase at the time of treatment, which would be expected in younger clouds. Likewise, the change in height, area, and reflectivity from first echo to treatment should be greater for the older air-mass cores. These differences are statistically significant, using both the Student's *t*-test and the Wilcoxon sum rank test.

The horizontal growth rates of the cores were estimated from the time of first echo to the time of treatment (figure 22), and the air-mass cores were growing more rapidly in area than the cold-front cores. Aircraft measurements of mean net buoyancy indicated that the cold-front clouds were more negatively buoyant. Estimated vertical growth at the time of treatment, derived from the rate of change of the 10-dBZ reflectivity contour defining the height of the echo top, indicated that most echoes were growing slowly at the time of treatment, although a few were growing very rapidly. Ten cold-front cores indicated negative vertical growth, as compared to only three air-mass cores.

Updraft velocity was estimated using aircraft measurements. While most updrafts ranged from 0 to 7 ms^{-1} on cold-front days, they exceeded 10 ms^{-1} in about 25 percent of the cores. Updrafts ranged from 0 to 7 ms^{-1} in the air-mass clouds. The mean speed was greater for the cold-front clouds. This difference was statistically significant at the 5 percent level according to the Student's *t*-test (table 16).

The radar-estimated vertical growth and mean updraft speed were best correlated for cores with lower updraft speeds, which occurred on air-mass days. The mean vertical growth was lower than the mean updraft velocity, and the largest differences were found for updraft speeds greater than 10 ms^{-1} . The lower mean radar-derived vertical motions may have resulted from several factors:

1. The echoes formed at relatively high levels on cold-front days, with only 12 percent growing more than 1 km prior to treatment. On air-mass days, however, the first echoes generally formed 1 km lower, so a growth measurement could be made from a lower starting elevation. About 70 percent of the air-mass cores had grown more than 2 km by treatment time, and 33 percent had grown more than 3 km. Thus prior to treatment, the air-mass cores overall started lower and grew taller than the cold-front cores, allowing a better growth estimate.
2. The lower echo growth values on cold-front days could also have been caused partly by assigning a value of zero to the updraft speed of the clouds with no updraft, while the radar estimate of vertical growth used negative values.

The air-mass cores were larger at the time of treatment, and the radar-based estimates of horizontal and vertical growth indicated that they were growing more in height and area than the cold-front cores. This was corroborated by greater negative net buoyancy values for the cold-front cores.

Echo-Core Peak Values

Echo behavior characteristics after treatment were defined as response variables (figures 23,24, table 17). Between the cold-front and the air-mass cores, the latter were taller, larger in area, more reflective, and took longer to reach maximum area from first echo. However, only the differences in peak maximum reflectivity and the change in maximum reflectivity were statistically different by both the Wilcoxon and *t*-tests. The reflectivity of the cold-front cores may have changed greatly after treatment because they were younger at the time of treatment. In the mean, the cold-front cores were 3.3 minutes old at treatment, and peak reflectivity was 26.8 dBZ. The air-mass cores, however, were 11.2 minutes old at treatment, with mean reflectivities of 47.5 dBZ. But the air-mass cores attained higher peak reflectivities. The mean peak values of maximum reflectivity achieved for cold-front and air-mass cores were 41.6 and 54.4 dBZ, respectively.

Both types of cores experienced similar mean changes and rates of change in height and area after treatment, although the peak values were again larger for the air-mass cores (figure 25). Overall, the cold-front cores grew less and ended sooner, either through dissipation or merger. In fact, not even half (42 percent) of the cold-front cores grew in height at all during their history. On the other hand, 85 percent of the air-mass cores grew more than 2 km, and 74 percent grew more than 3 km in height during their life spans. Thus, the differences in peak values seem to be related to the echoes' behaviors before and at the time of treatment.

Cold-Front versus Air-Mass Echo Properties

The cold-front experimental units had the tallest daily echo tops; some of the tallest, largest, and most reflective echo cores; and the strongest updrafts. Hail was produced on these days, there was much potential buoyancy present in the atmosphere, and vertical shear was stronger than on air-mass days. In addition, past studies have shown that cold-front storms are longer lasting and generally produce more rain than air-mass storms (Changnon, 1980b; Vogel, 1977). This was largely the case for the 1989 storms: more mean rainfall was produced during cold-front periods within the experimental unit and for a 240 x 240-km area around CMI (table 18). In fact, three of the five cold-front experimental units produced more than $200 \times 10^4 \text{ m}^3$ of rain from 15 minutes before treatment to 15 minutes after treatment (table 11). Only one of the four air-mass cores produced comparable rain. The four largest rain-producing systems, whether cold-front or air-mass storms, were lines (table 12). From 15 minutes before treatment to 30 minutes after treatment, the cold-front units produced more rain than did the air-mass units (table 19).

Thus, in the mean, the cold-front cores could be expected to be larger than the air-mass cores. Instead, a broad, perhaps bimodal distribution was present in the vertical motion param-

eters at the time of treatment; in the peak height, area, and reflectivity; in the change in core area and reflectivity after treatment; and in the estimate of vertical growth 4 minutes after treatment. There were many small cold-front cores and a few large ones. On average, the air-mass cores were larger, longer lasting, and more reflective.

The smaller cold-front cores may be explained in part by the results of Newton and Newton (1959). The stronger vertical shear on cold-front days may inhibit the growth of the smaller cores, as the rapid entrainment of stronger horizontal winds into narrow clouds results in a cloud more prone to dissipate. The growth of the wider cores with stronger updrafts is enhanced by the kinetic energy drawn from the wind field under strong shear conditions. The air-mass cores were generally larger, taller, and more often merged with another air-mass core at the time of treatment. Moreover, they remained larger and taller following treatment. Even the small air-mass cores grew, having formed in a protected environment less affected by vertical shear than the small cold-front cores.

Evaluation of Potential Seeding Effects

Cold-Front Cores

During the six cold-front experimental units, 21 cores were treated with AgI and 12 with sand flares. At the time of first echo, the AgI-treated cores were smaller in horizontal area and shorter than the sand-treated cores (table 20). Significant differences, however, were only observed when the cores were treated as statistically independent entities. At the time of treatment, the sand-treated cores were generally younger than the AgI-treated cores. The mean height area, reflectivity, and fraction of solid water content of the AgI- and sand-treated cores were nearly the same. However, both the radar- and the aircraft-estimated rates of vertical growth were greater for the sand- than the AgI-treated cores. Larger changes and rates of change in height, area, and reflectivity between first echo and treatment were also noted for the younger sand-treated cores. Thus, even though the mean height, area, and reflectivity were similar at treatment for the AgI- and sand-treated cores, the sand-treated cores grew more vigorously. At treatment time, 11 clouds had not echoed. Four of the seven AgI-treated clouds never echoed, although the four sand-treated cores did eventually echo.

From the dynamic seeding hypothesis, it was expected that the AgI-treated cores would grow more after treatment and taller overall than the sand-treated cores. However, the sand-treated cores grew significantly taller than the AgI-treated cores (table 21). They also had significantly longer growth periods, requiring more time after treatment to go from first echo to peak areal extent. While this might be due in part to the younger age of the sand-treated cores at treatment, in the mean, they were growing more before treatment and continued to grow more after treatment in terms of height area, and reflectivity. That is,

the cores treated with sand were more vigorous both before and after treatment.

The tallest cold-front echoes, whether treated with sand or AgI, exhibited the largest radar-estimated vertical growth at treatment, and stronger and wider updrafts. Five of the tallest cores had mean core diameters greater than 4 km and were treated with sand. Aircraft measurements of updraft speed indicated that eight of the cold-front cores had updrafts of greater than 9 ms^{-1} , and six of the eight reached heights of more than 10 km. The other two cores had mean updraft diameters less than 1.5 km. Two cores with weaker updraft speeds, but with updraft diameters greater than 1.5 km, reached more than 10 km. Updraft diameter was better correlated with peak height (0.73) than was core diameter (0.41). None of the cold-front cores with updraft diameters less than 1.5 km grew more than 10 km in height. On the other hand, three cores with diameters less than 3 km grew to greater than 10 km.

Of the 18 cold-front cores with diameters less than 5 km that were echoing at treatment, 13 were treated with AgI. This bias towards smaller diameters at treatment for the AgI-treated cores renders it impossible to determine a seeding effect.

Rosenfeld and Woodley (1989) in west Texas and Gagin et al. (1986a) in Florida reported that cores that were young at the time of treatment and that were treated with many flares responded better to seeding in terms of duration and areal extent. In Texas, no difference was found in peak height; although in Florida, the AgI-treated clouds grew taller. The 1989 Illinois data showed little relationship between core age at treatment and the peak height of the echo core (figure 26c). Most cold-front cores were treated within 5 minutes of first echo, including the three tallest of the AgI-treated cores that echoed. However, eight others also treated with AgI within 5 minutes of first echo did not reach 10 km in height. It appears that for the cold-front cores, the size of the core at treatment is more important than its age.

For cloud seeding operations, these findings suggest that when the atmosphere is characterized by moderate to strong vertical shear and large values of potential buoyancy, the sample of clouds that are approachable by a seeding aircraft may be characterized by many small and a few large clouds, with the very large clouds growing regardless of treatment. On cold-front days, it may be more difficult to find a positive seeding effect, even without a sampling bias.

Air-Mass Cores

During the four air-mass experimental units, 14 cores were treated with AgI and 13 with sand. As there were only four air-mass units, only six unique rerandomization permutations were possible, resulting in a minimum p-value of about 0.17. At the time of first echo, the sand- and AgI-treated cores had similar mean heights, although the mean areas of the sand-treated cores were somewhat larger (table 22). Seven of nine cores with horizontal areas greater than 10 km^2 were treated with sand.

At the time of treatment, the air-mass sand-treated cores were slightly older, taller, and had larger reflectivities than the AgI-treated cores (table 22). However, the AgI- and sand-treated cores were similar in mean areal extent at treatment, rate of change in area from first echo to treatment radar-estimated vertical growth, and mean updraft velocity at treatment. The p-values indicate that none of the predictor variables was significantly different.

However, the sand-treated cores grew taller than the AgI-treated cores (table 23). They also demonstrated a greater mean change and rate of change in height after treatment although the values were not significant. The rate of change in area was somewhat larger for the AgI-treated cores, but again it was not significant. Since cloud seeding was expected to increase vertical growth, if a seeding effect was present it acted in a negative way. In terms of peak horizontal area and peak reflectivity, the sand- and AgI-treated cores were similar in mean value and in distribution, so no seeding effect was suggested. Because only height was different, it is not clear that AgI treatment was the cause of the lower maximum heights.

No relationship was found between core age at treatment and the maximum echo top for the air-mass cores treated with either AgI or sand (figure 26f). This result is consistent with that from west Texas, where no difference in the height of the sand- and AgI-treated cores was found (Rosenfeld and Woodley, 1989). The sand-treated cores were generally taller for any given age group, for any given range of core diameter (figure 26d), and for any given range of updraft velocity (figure 26e).

Variability within Day and within Synoptic Category

The variability of summertime clouds has long plagued the evaluation of cloud seeding experiments. Earlier projects partitioned their data into groups based on weather conditions, and relied on statistics to verify cloud seeding results (e.g., Flueck, 1971; Biondini et al., 1977). The premise for partitioning data into like groups is to limit the variability of the data from that of the population as a whole. If the "within-day" and the "within-synoptic class" variability equals or exceeds the variability of the sample as a whole, then the possibility of finding a seeding effect is reduced.

To examine the variabilities within a day or within a convective period, a comparison was made of the data from the three days when more than one experimental unit occurred in the same convective period. The data were compared with 1) the total sample of tracked cores and 2) the total sample broken down by synoptic conditions. The standard deviations of the predictor variables at treatment time were computed for the combined AgI and sand samples (table 24), and the standard deviations of the response variables were computed for the sand-treated cores alone (table 25).

The standard deviations of the predictor and response variables for the units occurring within the same day were about

equal or larger than those for the population as a whole. The AgI-sand differences likewise were equal or slightly larger. This suggests that even within a given convective period, core characteristics can vary greatly. The need for statistical tests was made obvious when the standard deviation of values was the same or larger than the magnitude of differences between the AgI- and sand-treated cores.

Grouping the cores by synoptic type, however, reduced the day-to-day variability of cloud characteristics at treatment time. For both the cold-front and air-mass cores, *the* standard deviations in core diameter and reflectivity at treatment were about the same or smaller than for the population as a whole. The AgI-sand differences for these parameters were smaller as well. The standard deviation of the predictor variables was generally smallest for the air-mass days, except for the age of the cores at treatment. The mean deviations in vertical growth and updraft velocity in particular were smaller for the air-mass cores and greater for the cold-front cores than for the population as a whole. These results, in conjunction with the significant differences between the air-mass and cold-front cores shown in table 16, suggest that the synoptic stratification was a useful way to segregate storms, although the bias in the values at the time of treatment was not eliminated.

Summary and Conclusions

The 1989 cloud data were partitioned according to synoptic weather conditions. Most rain cases were associated with either cold-front or air-mass conditions. These two conditions had different thermodynamic and kinematic properties, which were reflected in the characteristics of the cores at the time of first echo and at the time of treatment. Due to the small number of cores sampled (33 cold-front and 27 air-mass) and because of the small number of units sampled on these days (6 of 12 units were cold-front, 4 were air-mass, and the other 2 fell into other synoptic classes that were not included here), it is not clear how representative these results are for other summers.

The cold-front units had more potential energy available for growth and somewhat stronger shear than the air-mass units. On the cold-front days, clouds taller than 16 km were present somewhere in the study area, hail was observed, and in general, more rain was produced. However, in the mean, the air-mass cores were larger than the cold-front cores. The cold-front cores, with many small cores and a few large ones, had a broad range of values and possibly bimodal distributions in peak height, area, reflectivity, and vertical growth. At the time of first echo and at the time of treatment, the cold-front cores tended to be more separate from their parent cores, whereas the air-mass cores were already merged with their parent cores. Unlike the cold-front cores, all air-mass cores contained echoes at the time of treatment. The smaller cold-front cores, might have been more vulnerable to the detrimental effects of entrainment. The largest cold-front cores showed the strongest updrafts sampled and the greatest radar-estimated horizontal and vertical growth.

The cold-front and air-mass units were further stratified by treatment type. Of the cold-front clouds, a disproportionate number of small cores were treated with AgI, while the larger cores received sand. Also, before and at the time of treatment, the mean growth rates were larger for the cold-front sand-treated cores. Thus, it was not surprising that the sand-treated cores reached peak heights greater than the AgI-treated cores. No seeding effect could be deduced from the cold front sample.

At the time of treatment, the air-mass sand-treated cores, in the mean, were older, taller, and had larger reflectivities than the AgI-treated cores. However, these differences were not significant. In examining the peak core values, the air-mass sand-treated cores grew taller than did the AgI-treated cores. Since the cloud seeding was expected to increase the vertical growth of the echo cores, there may have been a negative effect on the height of the air-mass cores. In terms of core duration, peak horizontal area, and peak reflectivity, the sand- and AgI-treated cores were similar in their means and in their distributions. Thus, the air-mass population showed no seeding response for any parameter other than perhaps height.

FIGURES AND TABLES FOR CHAPTER 4

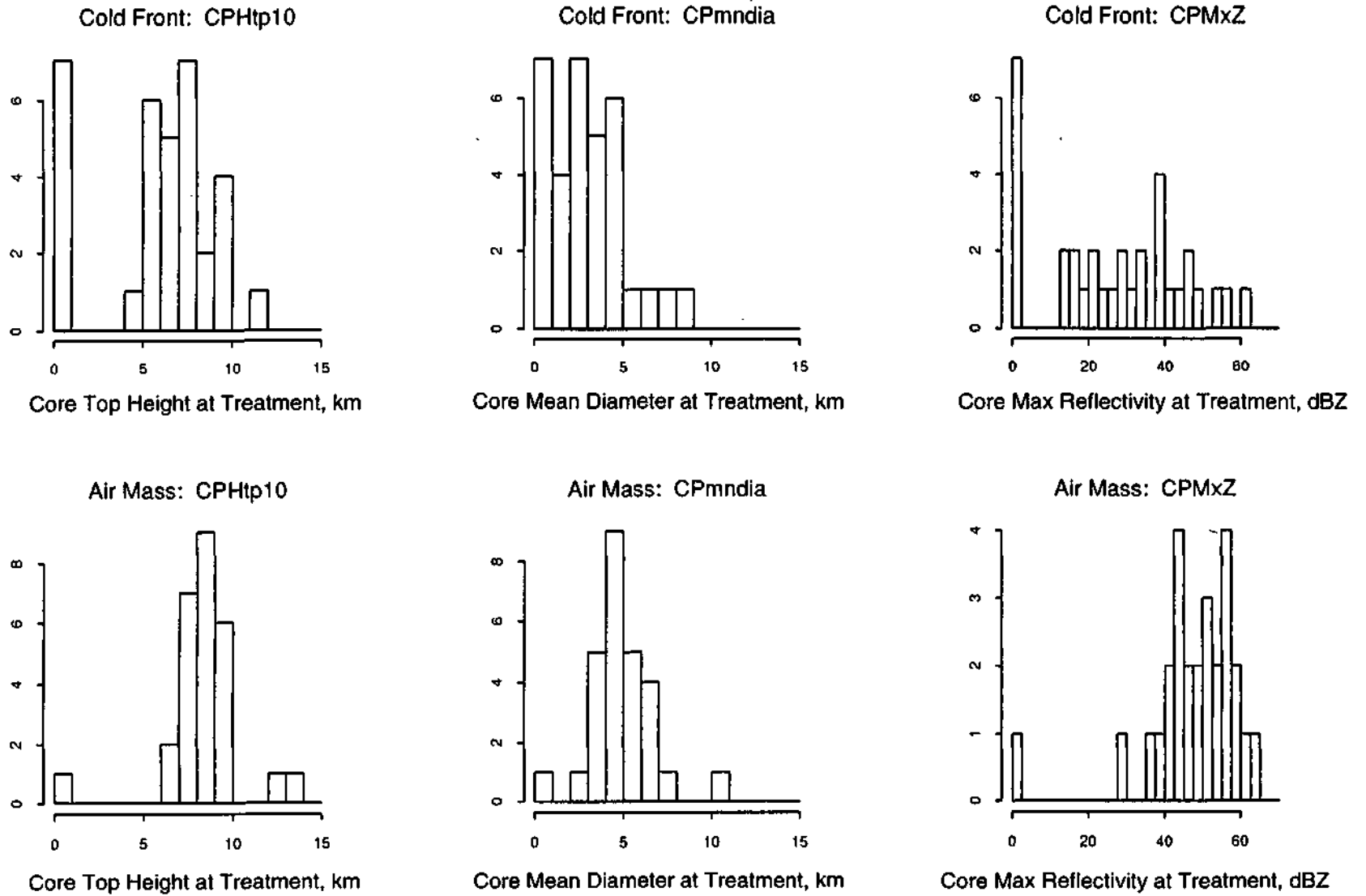


Figure 21. Frequency histogram of the echo-core top height, mean diameter, and maximum reflectivity at the time of treatment, stratified by synoptic weather conditions

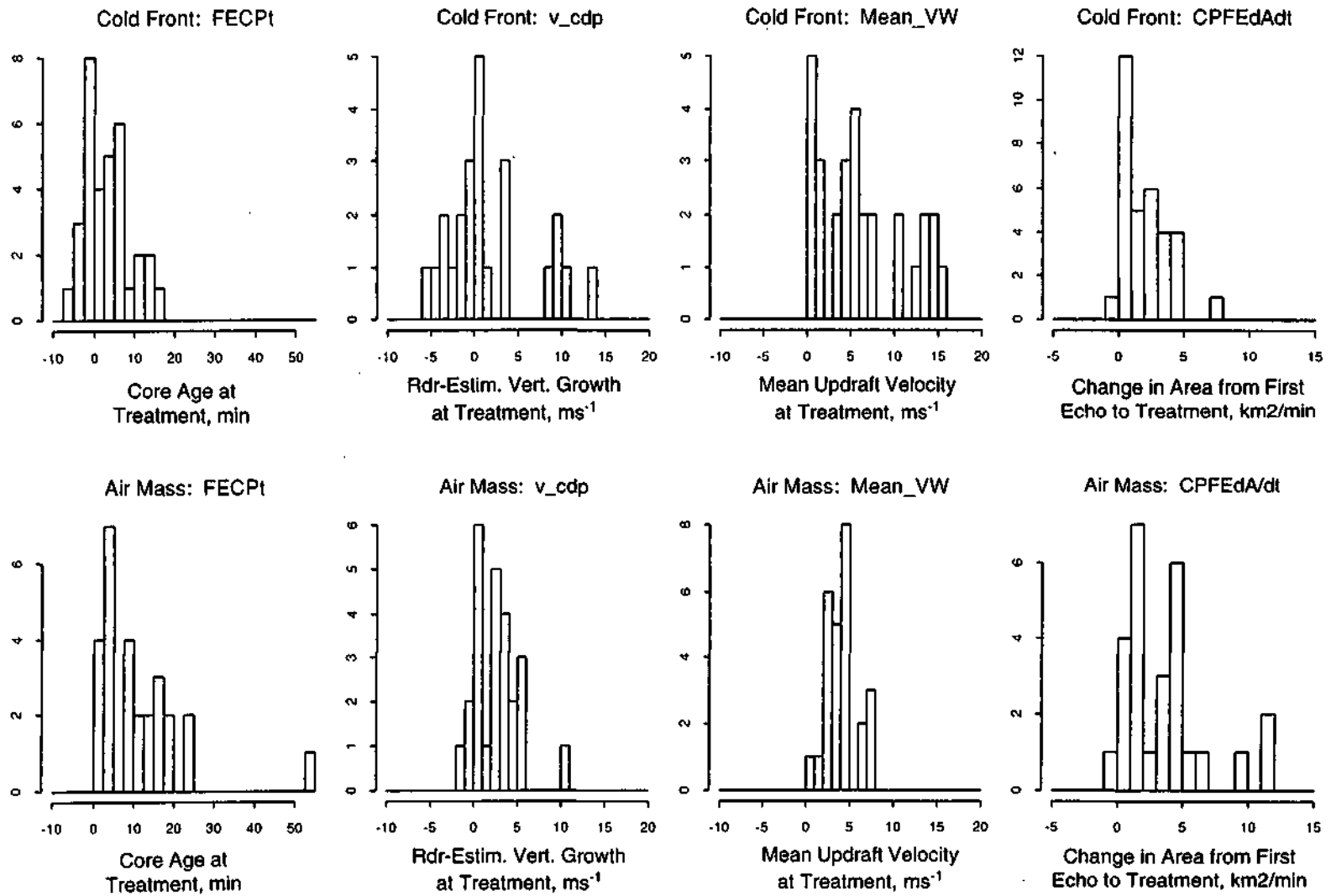


Figure 22. Frequency histograms of the echo-core age, radar-estimated vertical growth, aircraft-estimated vertical motion at the time of treatment, and the rate of change of horizontal area from the time of first echo to the time of treatment, stratified by synoptic weather conditions

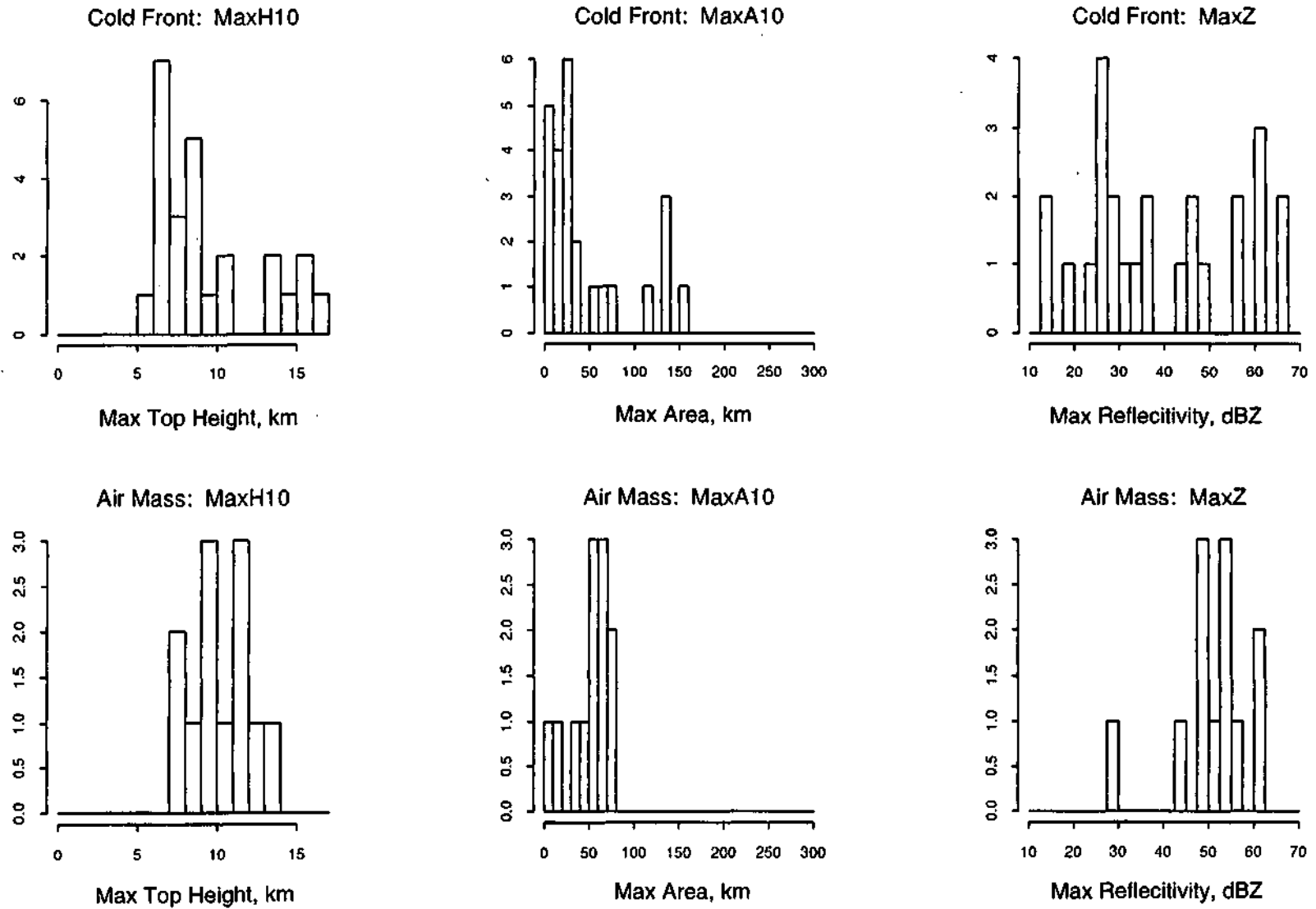


Figure 23. Frequency histograms of the peak height, peak area, and peak reflectivity of the echo cores, stratified by synoptic weather conditions

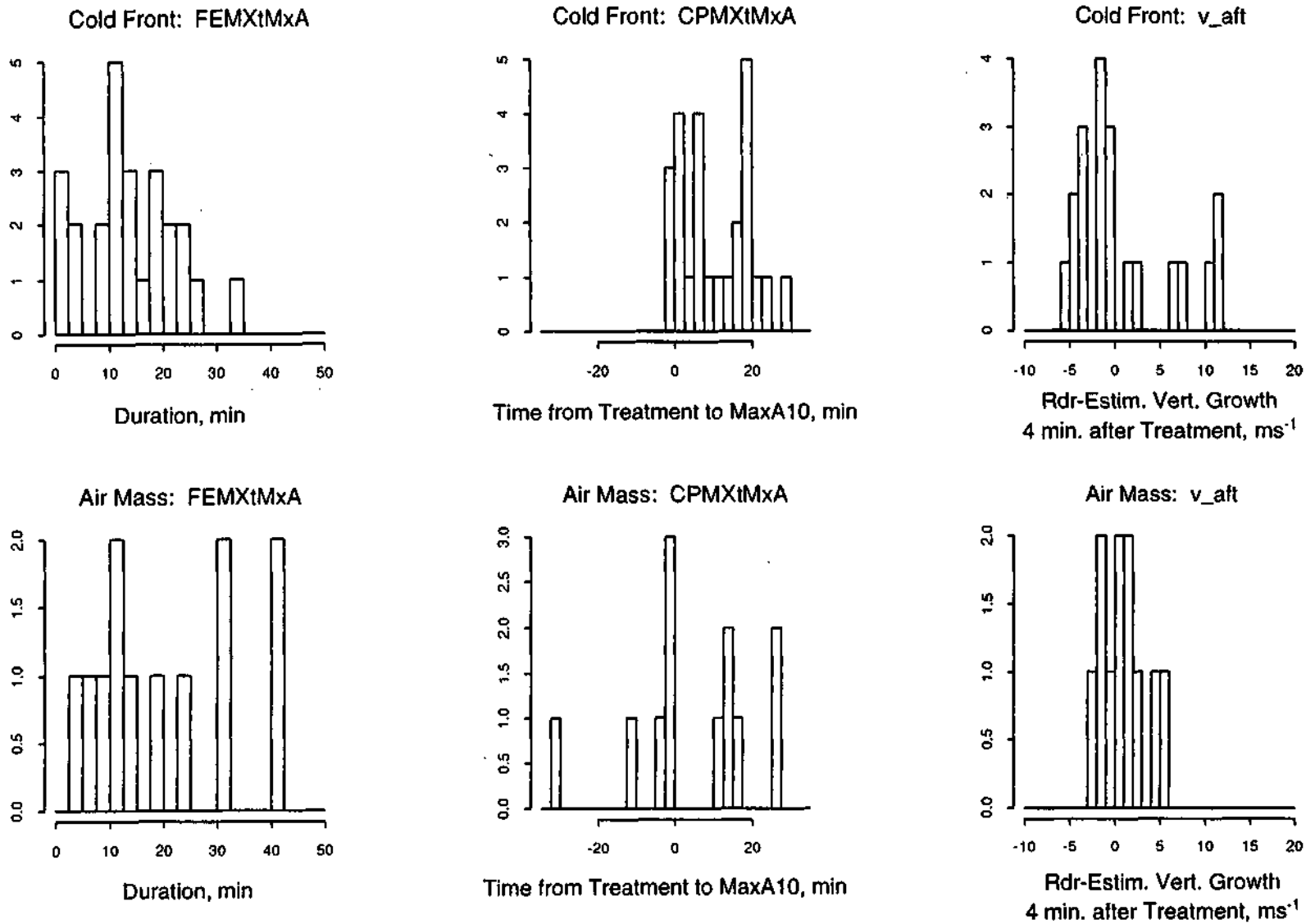


Figure 24. Frequency histogram of the echo-core duration, duration following treatment, and radar-estimated vertical motion 4 minutes after treatment, stratified by synoptic weather conditions

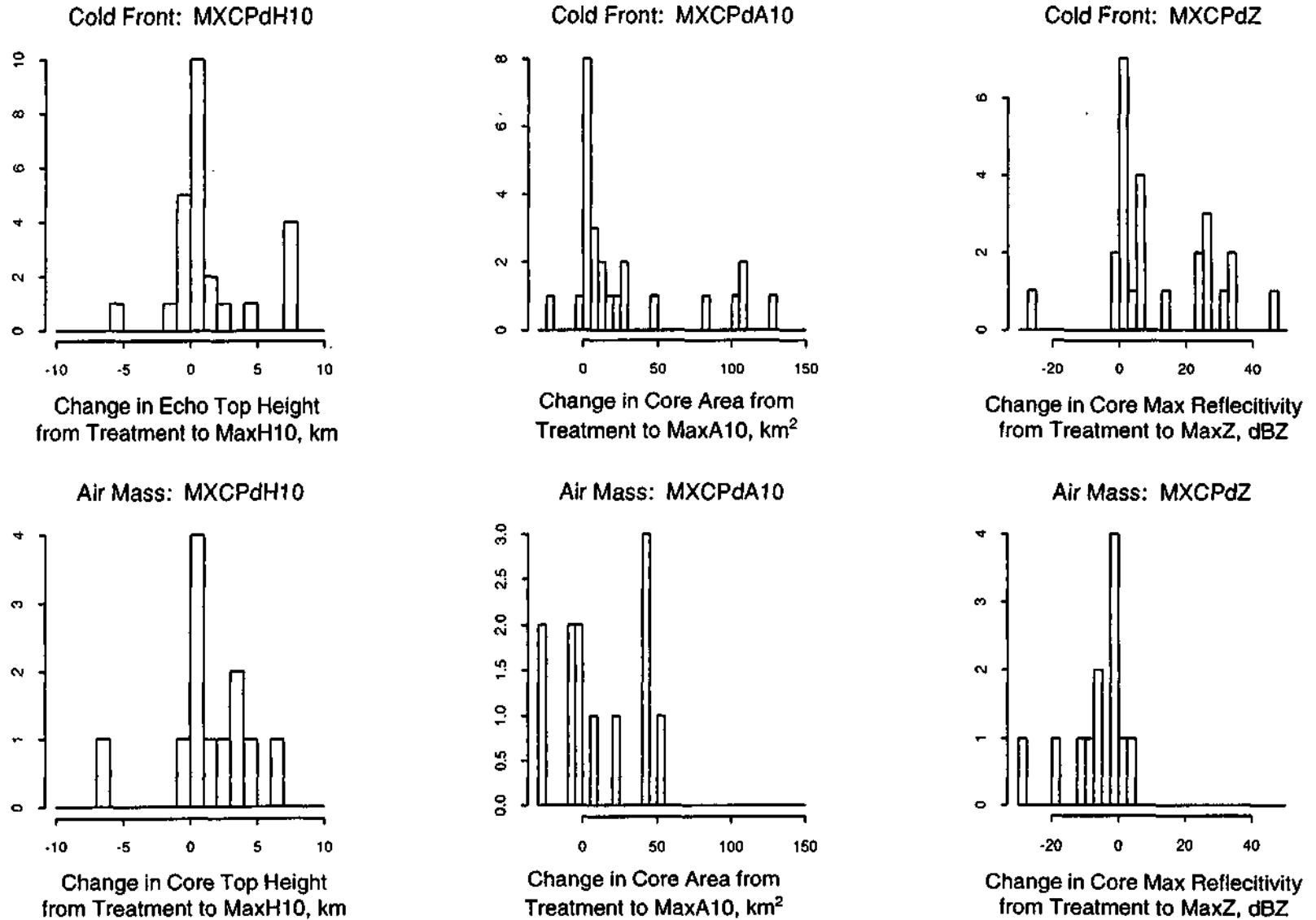


Figure 25. Frequency histograms of the change in height, area, and reflectivity following treatment, stratified by synoptic weather conditions

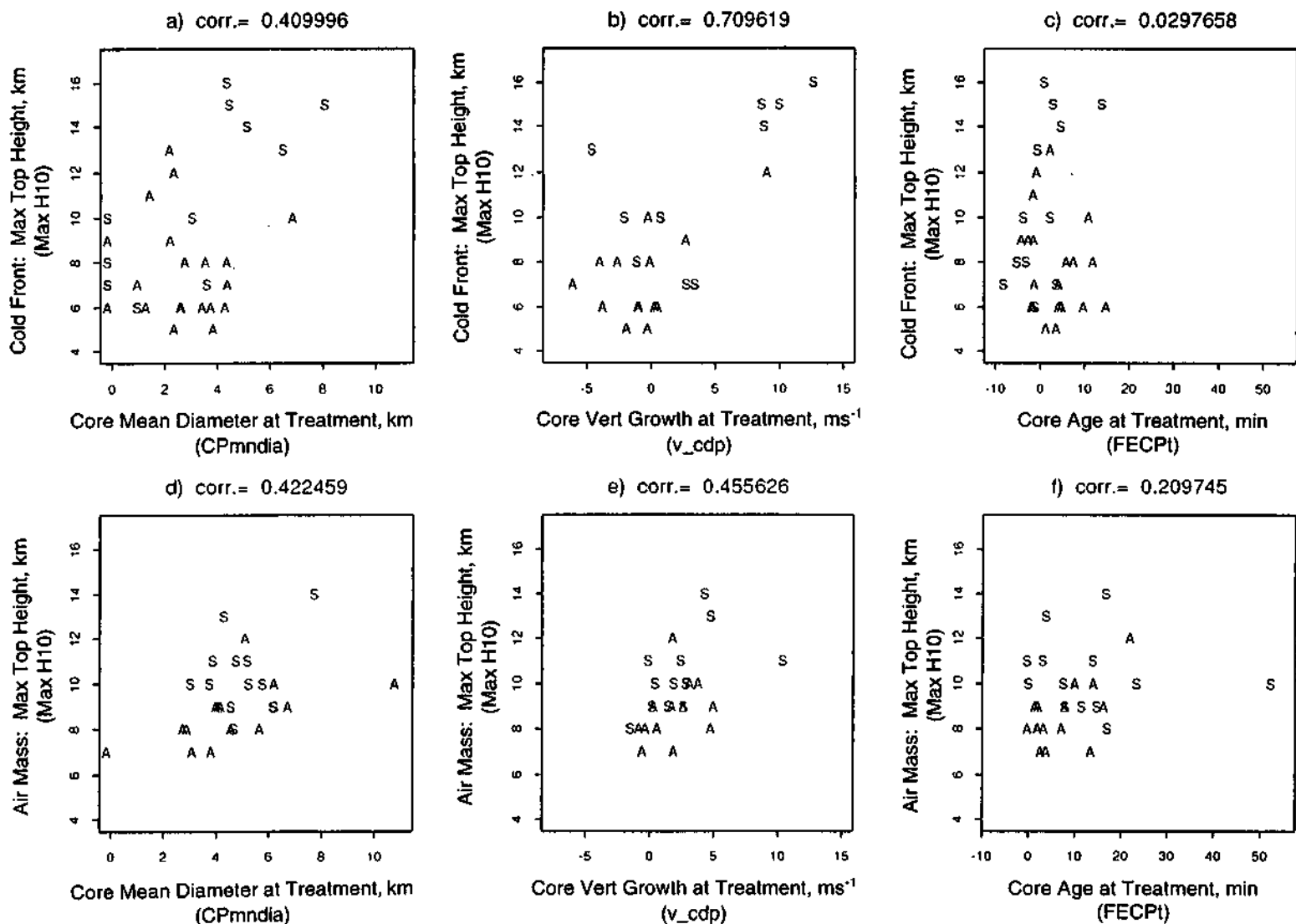


Figure 26. Scatter plots of the echo-core mean diameter, radar-estimated vertical growth, and age at treatment versus the peak height attained by the core. The data are stratified by synoptic weather conditions.

Table 9. Synoptic Classifications

<i>Rain event</i>	<i>Definition</i>	<i>Occurrences in 1989</i>
Squall-line	A nonfrontal group of thunderstorms accompanied by a trigger mechanism, usually a short wave trough. The convective activity associated with the storm systems is intense, well organized, and often arrayed in a narrow band or line of active thunderstorms.	0
Squall-zone	A mesoscale system of thunderstorms organized into an area or cluster and independent of a frontal zone. These storms, like squall lines, tend to move across large regions of the Midwest, and an upper-air impulse is usually discernible.	1
Frontal	Precipitation forms within 120 km (75 mi) of a surface front (cold, static, or warm). There is no synoptic evidence that this precipitation is associated with a squall zone, which on occasion moves 40 km (25 mi) or more ahead of the fronts.	6
Prefrontal and postfrontal	Precipitation associated with a frontal structure but at a distance of 120 to 140 km (75 to 150 mi) ahead or behind a front (cold, static, or warm).	0
Air-mass	A shower or thunderstorm generated within an unstable air mass. No large-scale or mesoscale synoptic causes are evident. The resulting convective activity is usually widely scattered to scattered and weak	4
Upper-level, low-pressure	A cyclonic storm situated so close to the research area that it is not possible to associate the precipitation with a frontal or mesoscale weather structure. The systems are rare during the summer.	1

Table 10. Large Cloud Experimental Unit Weather Indexes

<i>EU treatment</i>	<i>Date</i>	<i>Synoptic type</i>	<i>CAPE*</i> (m^2s^{-2})	<i>VShr</i> (m^2s^{-2})	<i>tccl*</i> <i>Ri*</i>	($^{\circ} C$)	<i>pw*</i> ($^{\circ} C$)	<i>pb*</i> ($^{\circ} C$)	<i>li*</i> ($^{\circ} C$)	<i>ki*</i> ($^{\circ} C$)	<i>mki</i> ($^{\circ} C$)	<i>jeff</i> ($^{\circ} C$)	<i>msh*</i> ($^{\circ} C$)	<i>swt</i> ($^{\circ} C$)
Cold-front experimental Units			852	11.9	82.5	15.9	3.7	6.7	-4.6	32.1	41.9	33.7	7.6	226
			354	6.7	50.1	1.9	0.5	1.8	4.3	3.9	3.1	4.7	3.0	125
5 a	6-01-89	cold fit	1339	25.0	53.5	18.0	4.4	6.4	-5.3	38.1	43.3	37.2	5.3	298.7
11 a	6-23-89	cold fit	636	11.7	53.2	15.8	3.1	5.0	-2.1	24.8	30.8	32.9	10.7	166.5
13 s		cold fit	636	11.7	53.2	15.8	3.1	5.0	-2.1	24.8	30.8	32.9	10.7	166.5
17 s	7-08-89	cold fit	613	8.0	76.5	13.8	3.8	8.2	-3.8	30.6	31.6	39.3	8.1	356.6
18 a		cold fit	613	8.0	76.5	13.8	3.8	8.2	-3.8	20.6	31.6	39.3	8.1	356.6
19 a	7-11-89	cold fit	1278	7.0	182	17.9	3.9	7.4	-5.4	30.8	36.8	36.0	9.1	237.5
Air-mass experimental units			540	6.5	83.5	18.0	4.2	3.6	-3.3	35.0	44.9	32.7	8.0	173
			57	0.4	13.7	1.2	0.8	0.1	0.5	1.7	0.6	1.5	0.3	20
22 a	7-23-89	air mass	475	7.0	68	16.2	4.1	3.6	-1.9	28.0	34.2	30.0	11.6	119.7
23 s	7-24-89	air mass	510	6.7	76	18.3	4.1	3.4	-2.4	30.2	36.3	33.1	10.4	180.7
24 s	7-25-89	air mass	588	6.2	95	18.8	4.8	3.6	-2.5	36.4	41.6	33.9	6.5	184.5
25 a		air mass	588	6.2	95	18.8	4.8		-2.5	36.4	41.6	33.9	6.5	184.5
Other synoptic type experimental units			108	26.5	14.1	14.6	3.5	1.6	-0.7	34.7	40.6	33.3	8.2	166
2 s	5-19-89	Sql Z	10	45.6	.2	13.2	3.3	0.8	0.3	33.8	40.1	32.9	8.5	180.9
20 s	7-19-88	LP	206	7.4	28	15.8	3.7	2.3	-1.6	35.5	41.2	33.6	7.8	151.9

Notes: EU = experimental unit.

All parameters were computed from the 0700 CDT Peoria soundings.

The means (above) and standard deviations (below) are provided for the cold-front and air-mass units. Only the mean is computed for the "other" synoptic category.

a and s = AgI and sand treatments, respectively.

* = variables are defined in appendix A.

Table 11. Large Cloud Experimental Unit Storm Descriptors

EU	Date	Surface to		Storm	FE top	FE top.	FE	Hail	Max top height		Storm type	RER	
		700- mb shear (deg ms ⁻¹)	500 mb winds deg.ms ⁻¹						motion (de.ms-1)	height (km)		temp (°C)	EU (km)
Cold-front experimental units					5.7	-8.90			14.5	16.6		255	47
					1.3	8.3			1.4	0.5		194	43
5	6-01-89	250 at 12	230 at 20	249 at 15	4.4	-2.2	28	Yes	14.5	16.0	line	405	60
11	6-23-89	189 at 9	205 at 12	270 at 9	4.3	-0.3	35	Yes	14.5	16.5	area	•	•
13	6-23-89	189 at 9	205 at 12	261 at 7	5.2	-5.4	37	Yes	15.5	16.5	line	233	53
17	7-08-89	289 at 10	340 at 14	321 at 10	7.1	-19.3	17	Yes	13.5	16.5	isol	82	53
18	7-08-89	289 at 10	340 at 14	314 at 10	7.4	-19.0	11	Yes	16.5	16.5	line	497	109
19	7-11-89	224 at 5	230 at 9	282 at 4	5.7	-7.0	32	Yes	12.5	17.5	area	58	7
Air-mass experimental units					3.8	3.8			13.3	13.8		93	13
					0.5	4.0			1.0	0.5		86	7
22	7-23-89	187 at 5	175 at 12	173 at 9	4.2	-0.7	14	No	13.5	13.5	line	206	20
23	7-24-89	193 at 6	190 at 11	158 at 8	3.8	3.0	10	No	14.5	14.5	area	114	16
24	7-25-89	189 at 5	165 at 4	171 at 4	4.0	3.9	22	No	12.5	13.5	area	28	13
25	7-25-89	189 at 5	65 at 4	130 at 4	3.0	9.1	25	No	12.5	13.5	area	25	4
Other experimental units (days with large and small clouds)					3.6	-0.8			13.0	13.0		162	127
2	5-19-89	202 at 19	180 at 23	235 at 15	3.0	1.8	5	No	11.5	11.5	line	146	156
20	7-19-89	240 at 5	265 at 8	280 at 7	4.2	-3.3	17	No	14.5	14.5	line	177	97

Notes: The mean (above) and standard deviation (below) are provided for the cold-front and air-mass units. Only the mean is computed for the other storm types.

EU = experimental unit.

Wind data are from the 0700 CDT Peoria soundings.

FE = first echo.

FE top height and FE top temp are indicated nearby and in the experimental unit, both before and after treatment.

EN = extended network.

Presence of hail is indicated within 150 km of CMI.

Max top height: EU during the period of treatment and EN for the afternoon; both within 150 km of CMI.

Storm type = line, area, or isolated.

EU and EN = a 240 x 240-km area centered on CMI.

RER = Radar-estimated rainfall accumulated from 15 min prior to the beginning of treatment to 15 min following the end of treatment.

Table 12. Small Cloud Experimental Unit Weather Indexes

<i>EU/ treatment</i>	<i>Date</i>	<i>Synoptic type</i>	<i>CAPE*</i> (m^2s^{-2})	<i>Vshr</i> (m^2s^{-2})	<i>Ri*</i>	<i>tccl*</i> (°C)	<i>pw*</i> (°C)	<i>pb*</i> (°C)	<i>li*</i> (°C)	<i>kt*</i> (°C)	<i>mki*</i> (°C)	<i>jef*</i> (°C)	<i>msh*</i> (°C)	<i>swt*</i> (°C)
Experimental units			19	10.9	1.3	13.3	3.4	0.1	1.7	25.5	31.6	30.9	9.5	160
			47	5.0	3.2	2.4	0.6	0.9	1.2	12.0	11.6	1.1	1.2	35
6 s	6-03-89	cold frt	11.5	14.6	7.9	9.1	2.4	-0.2	2.9	28.9	36.2	30.7	8.8	212.9
8 a	6-12-89	Sql Z	0	14.3	0	15.6	3.8	-0.6	0.8	33.9	39.7	32.0	8.6	164.6
9 s	6-12-89	Sql Z	0	14.3	0	15.6	3.8	-0.6	0.8	33.9	39.7	32.0	8.6	164.6
14 s	6-27-89	cold frt	0	11.5	0	12.9	3.7	0.1	2.6	27.4	32.5	30.9	9.6	156.5
15 a	6-27-89	cold frt	0	11.5	0	12.9	3.7	0.1	2.6	27.4	32.5	30.9	9.6	156.5
16 s	7-02-89	LP	0	9.4	0	13.5	2.8	1.8	0.2	1.8	8.7	29.1	11.8	103.5

Notes: All parameters were computed from 0700 CDT PIA soundings.

Means are noted above and standard deviations below.

a and s = AgI and sand treatments, respectively.

* = Variables are defined in appendix A.

Table 13. Small Cloud Experimental Unit Storm Descriptors

EU	Date	Surface to		Storm motion	FE top height	FE top temp	FE sample	Hail	Max top height		Storm type	RER	
		700-mb shear	500 mb winds						EU (km)	EN (km)		EU ($10^4 m^3$)	EN ($10^6 m^3$)
		deg ms^{-1}	(deg ms^{-1})	(deg ms^{-1})	(km)	(°C)							
					3.4	3.2			9.0	11.1		57.2	13.4
					0.5	3.7			0.9	2.1		26.5	9.0
6	6-03-89	155 at 13	-	271 at 17	3.9	-2.3	15	Yes	10.5	11.5	area	89.1	27.1
8	6-12-89	235 at 8	225 at 8	257 at 13	3.6	1.9	22	No	8.5	8.5	line	40.2	6.6
9	6-12-89	235 at 8	225 at 8	260 at 14	3.3	3.4	13	No	8.5	8.5	isol	62.6	3.2
14	6-27-89	189 at 6	245 at 15	289 at 11	2.8	7.8	23	No	8.5	13.0	isol	16.9	8.2
15	6-27-89	189 at 6	245 at 15	306 at 9	2.9	6.9	23	No	10.5	13.0	line	80.5	17.9
16	7-02-89	158 at 2	160 at 2	96 at 4	3.9	1.7	25	No	8.5	12.0	line	53.6	17.4

Notes: The mean (above) and standard deviation (below) are provided for the cold-front and air-mass units. Only the mean is computed for the other storm types.

EU = experimental unit.

Wind data are from the 0700 CDT Peoria soundings.

FE - first echo.

FE top height and FE top temp are indicated nearby and in the experimental unit, both before and after treatment.

EN = extended network.

Presence of hail is indicated within 150 km of CMI.

Max top height: EU during the period of treatment and EN for the afternoon; both within 150 km of CMI.

Storm type = line, area, or isolated;

EU and EN = a 240 x 240-km area centered on CMI

RER = Radar-estimated rainfall accumulated from 15 min prior to the beginning of treatment to 15 min following the end of treatment.

Table 14. First Echo Height, Temperature, Area, Depth, and Maximum Reflectivities for the Large Clouds, Stratified by Synoptic Type from the Sample of Treated Echo Cores

Variable	Cold front (N = 33)		Air mass (N = 27)		t	P-val		Other (N = 7)	
	Mean	Stan dev	Mean	Stan dev		W	Mean	Stan dev	
FEHtp10	6.6	15	5.7	1.4	.018	.013	5.7	1.1	
FEHMxZ	5.4	1.7	4.2	1.4	.005	.007	4.3	1.1	
FEtpTmp	-15.0	103	-7.6	8.9	.005	.001	-12.3	8.4	
FEmzTmp	-7.2	10.6	1.1	8.6	.002	.004	-4.5	6.2	
FEA10	8.1	8.7	8.7	6.4	.759	.414	15.4	12.0	
FEdpth10	2.5	1.6	2.0	1.5	.233	.256	2.1	1.1	
FEMxZ	23.2	10.6	31.0	12.5	.011	.020	28.8	6.2	

Notes: t = student's *t*-test probabilities for difference between cold-front and air-mass cores.
W = Wilcoxon rank sum test probabilities.
Other = squall-zone and low-pressure experimental units.

Table 15. First Echo Height, Temperature, Area, Depth, and Maximum Reflectivity for the Large Clouds, Stratified by Synoptic Type from the Large Sample of First Echoes Occurring Before and After Treatment, Within and Near the Experimental Units

Variable	Cold front (N = 160)		Air mass (N=71)		t	P-val		Other (N = 23)	
	Mean	Stan dev	Mean	Std D		W	Mean	Stan dev	
FEHtp10	5.3	1.5	3.7	1.0	<0.001	<0.001	4.0	1.0	
FEHMxZ	4.2	1.6	2.7	1.0	<0.001	<0.001	2.7	1.6	
FEHbsIO	3.0	1.6	1.8	0.8	<0.001	<0.001	1.6	0.9	
FEtpTmp	-6.5	9.1	4.7	6.2	<0.001	<0.001	-2.1	4.6	
FEmzTmp	0.05	9.7	9.8	6.2	<0.001	<0.001	5.0	6.0	
FEbsTmp	7.6	10.1	15.4	5.5	<0.001	<0.001	10.8	5.0	
FEA10	4.5	3.0	4.0	2.7	.227	.232	5.7	3.2	
FEdpth10	2.3	1.4	1.9	1.1	.018	.018	2.3	1.2	
FEMxZ	17.9	5.7	16.6	1.9	.105	.138	17.9	5.6	

Notes: t = student's *t*-test probabilities for difference between cold-front and air-mass cores.
W = Wilcoxon rank sum test probabilities.
Other = Squall-zone and low-pressure experimental units.

Table 16. Predictor Variables at the Time of Treatment for Echo Cores under Cold-Front and Air-Mass Conditions

<i>Predictor variable</i>	<u>Mean</u>		<u>Stan. dev.</u>		<u>P-val</u>		<u>Sample</u>	
	<i>CF</i>	<i>AM</i>	<i>CF</i>	<i>AM</i>	<i>(t)</i>	<i>(W)</i>	<i>CF</i>	<i>AM</i>
CPmndia ^b	2.9	4.9	2.2	2.0	<0.00	<0.001	33	27
CPHtp10 ^b	5.4	7.9	3.2	2.2	.001	<0.001	33	27
CPMxZ ^b	26.8	47.5	18.6	12.6	<0.00	<0.001	33	27
FECpt ^b	3.3	11.2	5.6	10.9	.001	<0.001	33	27
Mean_VW ^c	6.2	3.9	4.9	1.8	.033	.121	29	26
UP_dia ^c	1.4	1.3	1.0	0.8	.634	.859	29	26
SWC_frac ^c	.056	.306	.120	.350	.002	.029	24	25
LWCd ^c	.168	.264	.448	.535	.504	.003	24	25
NBuoy ^c	-1.38	-0.44	1.81	1.60	.059	.043	24	25
Buoy_Enh ^c	0.49	0.51	0.08	0.03	.121	.219	24	25
CPFEdH10 ^b	0.2	2.2	1.4	2.6	<0.001	<0.001	33	27
CPFEdA10 ^b	10.8	28.6	15.3	30.7	.005	.002	33	27
CPFEdZ ^b	10.4	16.4	10.9	15.6	.086	.117	33	27
V_cdp ^b	1.7	2.5	5.1	2.5	.456	.002	24	25
CPFEdA/dt ^b	1.97	3.55	1.90	3.21	.021	.029	33	27
CPFEdZ/dt ^b	2.41	1.98	2.87	2.30	.532	.911	33	27

Notes: t and W are probabilities that the samples are the same, using the student's t-test and the Wilcoxon rank sum test. b, c variables are defined in appendix B or C, respectively.

Table 17. Response Variables for Echo Cores under Cold-Front and Air-Mass Conditions

<i>Response variable</i>	<u>Mean</u>		<u>Stan dev</u>		<u>P-val</u>		<u>Sample</u>	
	<i>CF</i>	<i>AM</i>	<i>CF</i>	<i>AM</i>	<i>t</i>	<i>W</i>	<i>CF</i>	<i>AM</i>
MaxH10	8.8	9.5	3.2	1.7	.355	.080	33	27
MaxA10	46.7	72.0	45.0	58.3	.063	.015	33	27
MaxZ	41.6	54.4	15.4	8.1	<0.00	.001	33	27
MXCPdH10	1.2	1.0	2.9	2.2	.750	.349	33	27
MXCPdA10	28.3	26.3	40.5	49.0	.862	.988	33	27
MXCPdZ	12.6	-0.2	16.5	10.3	.001	.002	33	27
CPMXtMxA	10.1	6.3	8.5	12.5	.164	.196	33	27
FEMXtMxA	13.4	17.5	7.7	11.6	.111	.319	33	27
V_aft	1.7	1.3	5.7	1.9	.737	.285	28	25
MXCPdAdt	1.54	1.51	2.86	5.71	.982	.761	33	27
MXCPdZdt	1.48	2.09	0.77	1.30	.027	.086	33	27

Notes: t and W are probabilities that the samples are the same, using the student's t-test and the Wilcoxon rank sum test. Variables are defined in appendix B. CF = cold front; AM = air mass.

Table 18. Fifteen-Minute Rainfall Accumulations for the 1989 Illinois Experimental Units and the Extended Network Area

Time minutes	<u>Experimental unit</u>				<u>Extended network</u>			
	CF, N=5		AM, N=4		CF, N=5		AM, N=4	
	$(10^4 m^3)$		$(10^4 m^3)$		$(10^6 m^3)$		$(10^6 m^3)$	
	Mean	(Stan dev)	Mean	(Stan dev)	Mean	(Stan dev)	Mean	(Stan dev)
BT-15	34.1	(27.7)	23.6	(14.9)	11.8	(6.7)	4.2	(1.7)
BT-ET	64.6	(58.5)	24.4	(20.6)	14.5	(8.7)	4.4	(2.6)
ET+15	110.2	(91.6)	20.5	(23.3)	19.1	(12.4)	2.5	(3.0)
+15 to +30	117.3	(107.4)	16.1	(17.8)	19.6	(12.7)	1.6	(0.9)
+30 to +45	78.8	(61.3)	15.5	(14.0)	18.1	(10.6)	2.1	(2.0)
+45 to +60	70.4	(68.8)	9.9	(11.3)	16.9	(11.5)	1.5	(1.4)
+60 to +75	94.2	(124.6)	7.4	(8.1)	20.9	(13.6)	1.4	(1.3)
+75 to +90	108.6	(138.5)	20.7	(37.7)	20.8	(19.2)	3.3	(4.3)

Notes: Extended network = a 240 x 240-km area centered on the CMI radar near Champaign.
 BT = the beginning of treatment, and ET = the end of treatment. The treatment periods ranged from 10 to 48 minutes and have been normalized to 15-minute periods.
 CF = cold front; AM = air mass.
 BT-15 = the period from 15 minutes before treatment until the time of first treatment.
 ET+15 = the period from the end of treatment until 15 minutes later.

Table 19. Number of Illinois Units Increasing in Amount of Rainfall Accumulation from One Rain Period to the Next

Time (minutes)	<u>Experimental Unit</u>		<u>Extended Network</u>	
	CF	AM	CF	AM
BT - 15 through BT - ET	3/5	1/4	3/5	1/4
BT - ET through ET + 15	4/5	1/4	4/5	1/4
ET + 15 through ET + 30	3/5	2/4	2/5	1/4
ET + 30 through ET + 45	1/5	1/4	2/5	1/4
ET + 45 through ET + 60	2/5	1/4	2/5	0/4
ET + 60 through ET + 75	2/5	0/4	4/5	0/4
ET + 75 through ET + 90	3/5	0/4	2/5	1/4

Notes: BT = the beginning of treatment, and ET = the end of treatment.
 BT-15 = the period from 15 minutes prior to treatment to the time of first treatment.
 BT+15 = the period from the end of treatment until 15 minutes later.
 CF = cold front.
 AM = air mass.
 Extended network = a 240 x 240-km area centered on the CMI radar near Champaign.

Table 20. Predictor Variables at the Time of Treatment for Echo Cores under Cold-Front Conditions

<i>Predictor variable</i>	<u>Mean</u>		<u>Stan dev</u>		<i>t</i>	<i>TR</i>	<u>Sample</u>	
	<i>AgI</i>	<i>Sand</i>	<i>AgI</i>	<i>Sand</i>			<i>AgI</i>	<i>Sand</i>
FEHtp10 ^b	6.2	7.3	1.3	1.8	.069	.279	21	12
FEHMxZ ^b	5.0	6.0	1.5	1.8	.099	.279	21	12
FEA10 ^b	5.7	12.3	3.9	12.7	.033	.240	21	12
FEMxZ ^b	22.3	24.9	9.5	12.6	.578	.519	21	12
CPmndia ^b	2.8	3.1	1.7	2.9	.665	.298	21	12
CPHtp10 ^b	5.3	5.4	2.6	4.2	.911	.901	21	12
CPMxZ ^b	26.9	26.6	16.2	23.0	.972	1.00	21	12
FECpt ^b	4.3	1.5	5.4	5.7	.160	.279	21	12
Mean_VW ^c	4.4	8.8	4.5	4.5	.016	.519	17	12
UP_Dia ^c	1.1	1.9	1.1	0.8	.031	.375	17	12
SWC_frac ^c	.085	.027	.152	.070	.239	.760	12	12
LWCd ^c	.201	.136	.518	.387	.732	.625	12	12
NBuoy ^c	-1.38	-1.38	1.77	1.92	.993	1.00	12	12
Buoy_Enh ^c	0.45	0.52	0.08	0.06	.020	.144	12	12
CPFEdH10 ^b	-0.2	0.8	1.5	1.0	.037	.144	21	12
CPFEdA10 ^b	9.1	13.7	13.3	18.4	.421	.279	21	12
CPFEdZ ^b	7.7	15.3	8.8	12.9	.053	.048	21	12
V_cdp ^b	-0.2	4.3	3.6	5.8	.027	.346	14	10
CPFEdA/dt ^b	1.27	3.21	1.33	2.17	.003	.048	21	12
CPFEdZ/dt ^b	1.55	3.91	2.50	2.96	.021	.048	21	12

Notes: t = the probability that the sample means are the same, using the student's *t*-test.
 TR = the probability based on a rerandomization of the experimental units.
 b,c Variables are defined in appendix B or C, respectively.

Table 21. Response Variables for Echo Cores under Cold-Front Conditions

<i>Response variable</i>	<i>Mean</i>		<i>Stan dev</i>		<i>t</i>	<i>TR</i>	<i>Sample</i>	
	<i>AgI</i>	<i>Sand</i>	<i>AgI</i>	<i>Sand</i>			<i>AgI</i>	<i>Sand</i>
MaxH10	7.8	10.8	2.3	3.6	.007	.125	21	12
MaxA10	36.9	63.9	35.3	55.9	.098	.279	21	12
MaxZ	40.2	44.2	13.2	19.0	.479	.625	21	12
MXCPdH10	0.4	2.6	2.4	3.3	.036	.375	21	12
MXCPdA10	19.8	43.3	36.8	43.3	.108	.279	21	12
MXCPdZ	9.7	17.5	17.8	13.1	.195	.433	21	12
CPMXtMxA	7.2	15.3	7.5	8.0	.006	.125	21	12
FEMXtMxA	11.5	16.8	5.7	9.8	.058	.048	21	12
V_apt	.71	3.56	5.85	5.14	.210	.750	18	10
MXCPdA/dt	1.12	2.28	3.24	1.94	.419	.279	21	12
MXCPdZ/dt	1.60	1.26	0.77	0.75	.234	.510	21	12

Notes: *t* = the probability that the sample means are the same using the student's *t*-test.
TR = the probability based on a rerandomization of the experimental units.
Variables are defined in appendix B.

Table 22. Predictor Variables for Echo Cores under Air Mass Conditions

<i>Predictor variable</i>	<i>Mean</i>		<i>Stan dev</i>		<i>t</i>	<i>TR</i>	<i>Sample</i>	
	<i>AgI</i>	<i>Sand</i>	<i>AgI</i>	<i>Sand</i>			<i>AgI</i>	<i>Sand</i>
FEHtp10 ^b	5.6	5.7	1.3	1.6	.930	1.00	14	13
FEHMxZ ^b	4.5	3.8	1.5	1.2	.238	.385	14	13
FEA10 ^b	7.1	10.5	6.6	6.0	.184	.385	14	13
FEMxZ ^b	28.3	34.0	12.2	12.6	.240	.615	14	13
CPmndia ^b	4.7	5.2	2.5	1.2	.541	.385	14	13
CPHtp10 ^b	7.4	8.3	2.6	1.6	.308	.385	14	13
CPMxZ ^b	44.4	50.7	15.4	8.0	.201	.385	14	13
FECPt ^b	8.5	14.1	6.7	13.8	.182	.385	14	13
Mean_VW ^c	3.4	4.4	1.7	1.8	.175	.385	14	13
UP_Dia ^c	1.1	1.5	0.8	0.8	.275	.769	13	13
SWC_frac ^c	.287	.323	.341	.371	.807	1.00	12	13
LWCd ^c	.336	.197	.728	.275	.528	.615	12	13
NBuoy ^c	-1.04	0.11	1.40	1.64	.072	.385	12	13
Buoy_Enh ^c	0.51	0.51	0.03	0.02	.909	1.00	12	13
CPFEdH10 ^b	1.8	2.6	3.0	2.1	.416	.385	14	13
CPFEdA10 ^b	30.4	26.7	38.6	20.4	.763	1.00	14	13
CPFEdZ ^b	16.2	16.7	17.0	14.7	.929	1.00	14	13
V_cdp ^b	2.2	2.8	2.0	3.1	.543	.385	13	13
CPFEdAdt ^b	3.74	3.35	3.50	3.00	.760	.769	14	13
CPFEdZdt ^b	2.40	1.52	2.60	1.93	.334	.769	14	13

Notes: t = the probability that the sample means are the same using the student's *t*-test.
 TR = the probability based on a rerandomization of the experimental units.
 b, c Variables are defined in appendixes B or C, respectively.

Table 23. Response Variables for Echo Cores under Air-Mass Conditions

<i>Response variable</i>	<i>Mean</i>		<i>Stan dev</i>		<i>t</i>	<i>TR</i>	<i>Sample</i>	
	<i>AgI</i>	<i>Sand</i>	<i>AgI</i>	<i>Sand</i>			<i>AgI</i>	<i>Sand</i>
MaxH10	8.6	10.4	1.4	1.7	.007	.385	14	13
MaxA10	68.4	75.8	53.6	65.0	.748	.615	14	13
MaxZ	54.0	54.9	9.6	6.4	.794	1.00	14	13
MXCPdH10	0.2	1.8	2.2	2.0	.064	1.00	14	13
MXCPdA10	27.4	25.2	38.4	60.0	.910	.615	14	13
MXCPdZ	1.8	-2.3	13.1	5.9	.303	1.00	14	13
CPMXtMxA	7.3	5.3	6.2	17.2	.688	.615	14	13
FEMXtMxA	15.7	19.4	9.8	13.5	.423	.769	14	13
V_aft	1.3	1.4	1.5	2.4	.901	1.00	13	12
MXCPdA/dt	2.39	0.57	6.31	5.06	.419	.615	14	13
MXCPdZ/dt	2.40	1.75	1.32	1.23	.196	.769	14	13

Notes: t = the probability that the sample means are the same using the student's *t*-test.

TR = the probability based on a rerandomization of the experimental units.

^{b,c} Variables are defined in appendix B.

Table 24. Difference in Mean Values for AgI and Sand Treatments for all Large Cloud Cores; Cold-Front Cores; and Air-Mass Cores

Variable	All	Difference		All	P-val			Stan dev		
		CF	AM		CF	AM	All	CF	AM	
Sample	35 A 32 S	21 A 12 S	14 A 13 S							
CPmndia ^b	-1.3	-0.3	-0.5	.038	.065	.541	2.4	2.2	2.0	
CPHtp10 ^b	-1.0	-0.1	-0.9	.029	.911	.308	2.9	3.2	2.2	
CPMxZ ^b	-9.3	0.3	-6.3	.067	.972	.201	19.2	18.6	12.6	
FECpt ^b	-2.8	2.8	-5.6	.154	.160	.182	8.9	5.6	10.9	
V_cdp ^{b*}	-2.5	-5.5	-0.6	.163	.027	.543	3.9	5.1	2.5	
Mean_VW ^{c*}	-2.6	-4.4	-1.0	.231	.016	.175	3.9	4.9	1.8	

Afternoons with two experimental units

Variable	All	Difference		All	P-val			Stan dev		
		CF	AM		CF	AM	All	CF	AM	
Sample	17 A 20 S	13 A 12 S	4 A 8 S							
CPmndia ^b	-1.1	-0.6	-1.6	.202	.485	.092	2.1	2.2	1.6	
CPHtp10 ^b	-0.8	-0.3	-0.8	.375	.851	.667	3.3	3.4	2.7	
CPMxZ ^b	-9.0	-2.3	-12.5	.317	.767	.179	19.6	19.2	14.8	
FECpt ^b	0.1	3.2	-0.5	1.00	.141	.959	10.5	5.3	13.9	
V_cdp ^b	-4.2	-5.5	-1.9	.577	.021	.419	4.5	5.2	3.3	
Mean_VW ^c	-3.7	-5.6	-1.0	.202	.002	.397	4.1	4.8	1.8	

Sample from afternoons with two experimental units

	All	From total sample			Sample from afternoons with two experimental units		
		CF	AM	All	CF	AM	
V_cdp ^{b*}	27 A 29 S	14 A 10 S	13 A 12 S	11 A 18 S	8 A 10 S	3 A 8 S	
Mean_VW ^{c*}	32 S	30 A 12 S	17 A 13 S	13 A	none missing		

Notes: P-values are from the student's *t*-test.
 Only the "All" category p-values are rerandomized (208 runs).
 CF = cold-front cores.
 AM = air-mass cores.
 The standard deviations are for the combined AgI- and sand-treated cores.
 * Sample size for variables with missing data.
^{b, c} Variables are defined in appendix B or C, respectively.

Table 25. Difference in Mean Values for AgI and Sand Treatments for All Large Cloud Cores, Cold-Front Cores, and Air-Mass Cores

Variable	<u>Difference</u>			<u>P-val</u>			<u>Stan dev</u>		
	All	CF	AM	All	CF	AM	All	CF	AM
Sample	35 A 32 S	21 A 12 S	14 A 13 S						
MaxH10	-2.5	-3.0	-1.8	.019	.007	.007	2.5	3.6	1.7
MaxA10	-30.8	-27.0	-7.4	.019	.098	.748	58.9	55.9	65.0
MaxZ	-6.4	-4.0	-0.9	.087	.479	.794	13.8	19.0	6.4
FEMXtMxA	-4.6	-5.3	-3.7	.010	.058	.423	10.7	9.8	135
V_aft ^{b*}	-1.4	-2.8	-0.1	.596	.210	.901	5.1*	5.1	2.4

For two experimental units

Variable	<u>Difference</u>			<u>P-val</u>			<u>Stan dev</u>		
	All	CF	AM	All	CF	AM	All	CF	AM
Sample	17 A 20 S	13 A 12 S	4 A 8 S						
MaxH10	-3.0	-3.5	-1.5	.202	.007	.215	3.0	3.6	1.6
MaxA10	-35.3	-36.1	-34.1	.202	.064	.004	41.9	55.9	10.8
MaxZ	-8.5	-9.0	-5.0	.202	.181	.355	15.4	19.0	4.3
FEMXtMxA	-4.5	-6.0	2.3	.202	.086	.791	10.7	9.8	12.2
V_aft [*]	-3.7	-5.2	-0.9	.577	.034	.601	4.7	5.1	2.8

Sample from afternoons with two experimental

	<u>From total sample</u>			<u>units</u>		
	All	CF	AM	All	CF	AM
V_aft	31 A 29 S	18 A 10 S	13 A 12 S	13 A 18 S	10 A 10 S	3 A 8 S

Notes: P-values are from the student's *t*-test.
 Only the "All" category p-values are rerandomized (208 runs).
 The standard deviations are for the sand-treated cores only.
 A = AgI treatment.
 S = sand treatment.
 CF - cold-front cores.
 AM = air-mass cores.
^{*}Sample size for variable (V_aft) with missing data.
^bVariables are defined in appendix B.

5. EVALUATION ACCORDING TO A SEEDABILITY INDEX

by

Robert R. Czys, Mary Schoen Petersen, and Nancy E. Westcott

Introduction

This chapter discusses an attempt to address the problem of the "bad draw" in the sand versus AgI treatments, as revealed by predictor variable analysis (see chapter 2). The seedability index analysis (SIA) investigated cloud characteristics before and at treatment to identify a quasiobjective set of AgI- and sand-treated clouds that were similar at treatment. These clouds could be more directly compared for a fairer assessment of seeding effects.

Development of the Seedability Index

The seedability criteria were chosen after careful consideration of the most relevant physical conditions known to exist during the initial phases of the dynamic seeding hypothesis. Relevance was defined on the basis of past cloud modification research (for example, Rosenfeld and Woodley 1989; Smith et al., 1986; Woodley and Sax, 1976; Simpson and Dennis, 1974; and Woodley, 1970) and Illinois findings on the internal structure and development of cumulus congestus clouds (Czys, 1991; Westcott, 1990; Pohtovich and Reinking, 1987; Ackerman, 1986; Ackerman and Westcott, 1986; Ackerman et al., 1979). Some of the variables that compose the seedability index were chosen to characterize in-cloud conditions at the time of treatment that might be suitable for dynamic seeding (updraft size and velocity, buoyancy, amount of supercooled liquid water, and frozen condensate). Others were chosen to characterize early cloud behavior (radar-measured height defined by the 10-dBZ contour, growdi rates, reflectivity changes, and echo age at treatment). Mesoscale atmospheric variables, such as convective condensation level and instability parameters, which are relevant to summer cloud development and behavior, were also selected. Other variables defined seeding dosages, as well as potential measurement uncertainties that could be associated with radar.

The 20 variables that constitute the seedability index (SI) are listed in table 26. Again, based on past findings, "thresholds" were established for each criterion, depending on the level at which a negative or positive suitability was represented. These thresholds are also listed in table 26.

Broadest updraft diameter, its mean vertical wind, and the percentage of cloud with updraft (numbers 1-3) were chosen as the best indicators of the organization of a cloud's vertical circulation. The reasoning was that narrow clouds, clouds with many small updrafts, or clouds with weak updrafts had circulations that were poorly organized; therefore they would not respond too favorably to dynamic seeding. Net buoyancy of the

broadest updraft (4) was chosen because if a cloud was either too negatively or too positively buoyant, the forces acting on these clouds might be too large to be appreciably modified. Potential buoyancy enhancement (5), calculated according to the method of Orville and Hubbard (1973), was chosen as an indicator of the potential invigoration from latent heat release due to seeding.

The presence of supercooled drizzle and raindrops in the main (broadest) updraft (6), and the absence of ice, expressed as the fraction of the total condensate that was frozen (7), were chosen because they are required according to the dynamic seeding hypothesis for release of latent heat (Lamb et al., 1981) and beneficial loading of the updraft. Past research has shown that a cloud can occasionally develop "ultra-high" ice particle concentrations very early in the evolution of precipitation (see for example Hobbs, 1969; Hobbs and Rangno, 1985; Rangno and Hobbs, 1990; Mossop, 1970, 1985a,b; and Hallett et al., 1978). This is an unwanted condition for seeding, because the desired effect is to produce ice from supercooled water.

The time from first echo to treatment (8) was selected to include the effect of cloud age on seedability. Old clouds may have well-developed ice concentrations, or they may be past the stage where seeding can be effective. Although not directly related to the dynamic seeding hypothesis, the distance of the echo from the radar (9) was included to limit measurement errors related to spreading of the radar beam.

Maximum reflectivity at the time of treatment (10) and rate of change of maximum reflectivity from first echo to treatment (12) were chosen as indicators of the level of activity of rain production processes. Clouds with similar CPMxZ (10) can be considered to have initiated precipitation-size particles with the same intensity; and clouds with similar CPFE $\frac{dZ}{dt}$ (12) can be considered to have evolved the precipitation population at the same rate. Hence, these clouds potentially can reach final maximum reflectivity at about the same time and at about the same maximum level. Hence, differences in maximum reflectivity might be due to seeding.

Mean echo-core diameter (13) was selected as another indicator of the organization of a cloud's vertical circulation, and height of the maximum reflectivity at treatment (14) was chosen to lower the SI if a cloud was raining out at treatment. The acceleration of the cloud top at treatment time (11), defined by the 10-dBZ contour, was chosen because rapid acceleration of growdi or decline of the echo top might not be overcome by the seeding.

To establish similarity in the meteorological conditions for the development of deep convective clouds, variables 15-18

were selected: the temperature of the convective condensation level (15) was chosen as an indicator of cloud-base height; potential buoyancy (16) was selected as an indicator of the strength of mesoscale vertical motion; a coalescence activity index (17) was developed to indicate the suitability of the mesoscale environment for the production of clouds with a "warm" rain processes; and bulk Richardson number (18) was selected as an indicator of a cloud's vertical tilt.

Finally, two criteria relating to dosage were included to account for responses that may be related to the amount of seeding material released: dosage 1 (19) was defined to indicate the rate of seeding material released in the updraft, and dosage 2 (20) refers to the percentage of the flares that were released in the updraft.

Table 27 summarizes the individual seedability index criteria for each of the 71 clouds treated in 1989. Cloud sequence numbers (first column) range from 1 to 71. Sequence 1 was the first large cloud treated during the experiment, and sequence 71 was the last Individual clouds are identified in the second column. The first three or four characters indicate the month and date, the next four the experimental unit number, and the last four the echo-core number for the experimental unit. The treatment material is listed in the third column.

Each column thereafter lists a seedability criterion shown in the same order as in table 26. A dot in table 27 indicates that the seedability criterion was met according to the threshold levels given in table 26. A number in table 27 indicates that a specific criterion was *not* met, and the actual value has been provided to indicate its difference from the threshold value. The notation of "NA" in table 27 indicates that a certain parameter was not computable, either because of an instrument failure, or because a computational method could not be applied to determine the criterion. For example, if vertical wind in a cloud could not be measured, parameters such as net buoyancy, buoyancy enhancement, liquid water content, and fraction of solid water content could not be computed. Also note in table 27, the large number of NA notations listed for LWCd (liquid water in the drizzle and raindrop size distribution). Data for this criterion are limited because the 2D C probe did not function properly, particularly for clouds 1 through 8.

Clouds 10 and 11 had no updrafts. That is, the instrumentation operated properly, but the cloud was composed of all downdraft or didn't have a region with at least one meter per second (m s^{-1}) of upward-moving air for 3 continuous seconds. This occurred because flares were released according to the treatment strategy even in weak updraft situations. These clouds were assigned a zero updraft diameter and a zero percent updraft. Furthermore, because calculations of variables like net buoyancy, buoyancy enhancement, and liquid water content depend on the existence of an updraft, these values could not be computed. Hence, NAs appear when no updraft measurements were available.

In the analysis using seedability criteria, 19 of the 71 clouds had to be eliminated from consideration because of a lack of

data on the critical variables. Seven of the clouds had no updraft data whatsoever. One other cloud had no updraft data and did not produce an echo. Four more clouds had no updraft data and no 2D image data. Three more clouds never produced an echo, and another four clouds had no 2D image data. After these exemptions, 52 clouds remained: 24 that were treated with AgI and 28 with sand.

Determination of SI Ratings

The SI was computed only for the sample of 52 clouds with all available criteria information, with the exception of cloud-top acceleration. The number of times each cloud met each criterion was summed, and then the percentage of the total possible 20 was computed for each cloud. In the event that a value for cloud-top acceleration could not be computed, the SI was calculated on the basis of 19 criteria. These percentages were used as an index, indicating each individual cloud's suitability for seeding. Thus, any two or more clouds could be considered similarly suitable for seeding, even though individual criteria may not exactly correspond. The resulting values for the 52 clouds, plotted in the sequence that they were treated, appear in figure 27.

This "temporal" plotting of an empirical seedability index reveals two interesting features. First, a temporal shift occurred in "seedability," at least for the criteria selected and the threshold values established. To the extent that the selection of criteria and threshold values validly characterize a cloud's suitability for dynamic seeding, the results suggest that the seedability of the clouds decreased during June and early July (clouds 1-41), and thereafter leveled off and varied from approximately 70 to 90 percent (clouds 42-71). This SI trend points to the potential inadequacy of visual and real-time, in-cloud selection criteria.

The second important finding revealed in figure 27 relates to clouds 23-34. They were all treated on one day, July 8, when a pair of experimental units was obtained. Comparison of the sand and the AgI values according to the SI reveals considerable difference in the seedability of the two experimental units. The clouds in the initial unit on this day received sand treatments, and the SI shows that these clouds may have been more suitable for seeding than those of the second experimental unit, which was treated with AgI. These two experimental units were separated in space by roughly 50 km and in time by less than 40 minutes.

This example of potential storm differences in nearby experimental units further demonstrates the problem of obtaining comparable samples within storm periods. It is also worth noting that clouds 60-71 (in EU24 and 25), which occurred on July 25, showed no appreciable difference in seedability. These unaccountable likenesses and differences demonstrate one aspect of the great difficulty that natural variability imposes in evaluating cloud seeding experimentation.

Application of the Seedability Index

The SI was used as a mechanism to create subgroups of clouds that showed similarity at the time of seeding, thus providing a valid basis for comparison of responses. For example, this analysis could set a threshold of 90 percent on the SI, and then compare the properties of the sand-treated and AgI-treated echo cores at the time of seeding. If the comparisons show no differences in initial cloud characteristics, then comparison of AgI- and sand-treated cloud responses might reveal valid seeding effects if sample sizes are large enough. Thus, any differences discerned in responses might be attributed to the seeding material, assuming that sand truly has no effect on cloud dynamics, and that AgI has an effect at least somewhat consistent with the dynamic seeding hypothesis under testing.

Analyses were performed using SI levels of 90, 80, 70, 60, and 50 percent. *The 1989 PACE Data Book* (Czys et al., 1993) summarizes the results for each of these SI filter levels. Furthermore, clouds with low seedability indexes were also analyzed as a check against bias introduced by the subjective selection of the seedability criteria and thresholds.

Tables 28 and 29 summarize the number of sand- and AgI-treated clouds that met the varying SI levels. All 52 clouds met at least 50 percent of the criteria (table 28). Note that the sample sizes begin to diverge at the 70 percent level. Values in these tables show that fewer of the AgI-treated clouds had high SI levels. This occurred in spite of the randomization scheme. From the standpoint of clouds with low SI, table 29 shows that only two sand-treated clouds met fewer than 70 percent of the seedability criteria, while ten AgI-treated clouds met less than 70 of the criteria, again implying that fewer suitable clouds were treated with AgI.

Key Findings

Key results are presented for the most suitable clouds, defined as those with $SI \geq 70$ percent; and for less suitable clouds, defined as those with $SI < 80$ percent. These two subgroups were selected for analysis because they provide a fairly large sample of clouds for each SI filter level chosen. In general, the major findings for clouds in both subgroups are not contradicted by the other SI percentages. The data for these analyses are in *The 1989 PACE Data Book* (Czys et al., 1993).

Analysis of Clouds with High Seedability Indexes

Means, standard deviations, sample sizes, and significant levels of the key predictor variables for the clouds that met 70 percent or more of the seedability criteria appear in table 30. The values of the key predictor variables for the 40 clouds with $SI \geq 70$ percent were compared with those for all 67 clouds (table 31). Comparison revealed that the clouds with $SI > 70$ percent produced a subgroup of AgI-treated clouds with properties similar to the sand-treated clouds at the time of treatment:

1. Their mean diameters were greater than the diameters of the sample of all other AgI-treated clouds that had echoes.
2. They were taller, on average, than all other AgI-treated clouds at the time of treatment by nearly 1 km, as indicated by CPHtpLO.
3. They had maximum brightnesses about 8 dBZ higher at the time of treatment than all other AgI-treated clouds that echoed.
4. They had maximum reflectivities about 3 dBZ brighter at the time of treatment than all other AgI-treated clouds that echoed.
5. They had areas about 8 km^2 larger at the time of treatment than all other AgI-treated clouds that echoed.
6. Their time from first echo to treatment was longer, on average, than for all other AgI-treated clouds that echoed.
7. There was very little difference in net buoyancy between them and all other clouds; this was also true for buoyancy enhancement.
8. On average, the mean vertical wind was higher for them than for all clouds that echoed.
9. Their fraction of total condensate as ice was generally greater than the fraction of ice for all clouds that echoed.
10. Their potential buoyancy was, on average, lower than that of all clouds that echoed.
11. Their temperature of convective condensation level was about the same as that of all clouds that echoed.
12. Their bulk Richardson numbers were lower than those of all other clouds that echoed.

A similar comparison of the sand-treated clouds with $SI \geq 70$ percent to all sand-treated clouds that echoed showed very little difference between the two samples. Hence, the net effect of using the SI as a filter was to obtain subsamples of AgI- and sand-treated clouds that were very similar at the time of treatment, but at the expense of reduced sample size. This provided for a valid comparison of seeding responses.

Results in table 30 show that none of the predictor variables was significantly different. In contrast, table 31 shows that 9 of the 13 predictor variables for sand- and AgI-treated clouds were significantly different for either the *t*-test, the Wilcoxon test, or both. It should be noted that in testing 13 variables, approximately 10 to 15 percent can be expected to be significantly different from one another. Hence, at least one or possibly two predictor variables should be statistically different by chance. Therefore, with no significant differences shown in table 30, the sand- and AgI-treated clouds can be considered to be virtually identical at the time of treatment. Any differences discerned in the response variables could be cautiously attributed to the treatment, considering the small sample size.

Table 32 lists key response variables for clouds that met > 70 percent of the seedability criteria. Only one response variable showed a significant difference between the AgI and sand treatments: maximum height. Hence, to the extent that this

significant difference did not happen by chance, the response data suggest that the AgI-treated clouds may not have grown as tall as the sand-treated echo cores. Evidence of no other effects on parameters such as area, reflectivity, or brightness, whether from the time of treatment or from the time of first echo to maximum could be found in the data for clouds with SI ≥ 70 percent Examination of similar responses for clouds with SI ≥ 50 to 90 percent [*The 1989 PACE Data Book* (Czys et al., 1993)] also supports the conclusion that if AgI had any appreciable effect on cloud growth, it was a negative effect on maximum height. This conclusion is clearly opposite from that expected according to the dynamic seeding hypothesis.

Figure 28a was constructed using data for clouds with SI ≥ 70 percent, following methods that are similar to those presented in Rosenfeld and Woodley (1989). In figure 28a, mean echo-core height was computed for only those echo cores that existed at each interpolated observation time relative to treatment. Hence, sample size changes with time, as shown by the numbers along the bottom of figure 28a for either AgI- or sand-treated clouds. Thus, in figure 28a, the AgI-treated echoes observed 9 minutes prior to treatment are not necessarily the same AgI-treated echoes observed 24 minutes after treatment. Because figure 28a allows only for comparison of echoes that existed at the observation time, mean values were recomputed using the entire sample of clouds at each interpolated observation time, and these are shown in figure 28b. In this case, a zero height was used for every observation time at which no echo core existed.

Examination of both plots of figure 28 reveals two important features. First, both methods of computing mean maximum height reveal that for a period of time after treatment, the sand-treated clouds were taller than the AgI-treated clouds. Figure 28a suggests that this difference is greater than one standard measurement error

$$\frac{\sigma}{\sqrt{n}}$$

by 2 to 3 km, for a duration of approximately 30 minutes, beginning at about the time of treatment. The difference between the mean maximum heights of the sand- and AgI-treated clouds is much less dramatic when computed on the basis of a constant sample size (figure 28b). However, figure 28b suggests that there may have been a short period of time (~12 minutes) when the mean maximum height of the sand-treated clouds exceeded that of the AgI-treated clouds by one standard measurement error.

Differences that might be due to seeding are obscured somewhat in figure 28a because the growth trend, both for the sand- and AgI-treated clouds, appears to be nothing more than

an extension of expected echo-top behavior beginning almost 21 minutes prior to treatment. However, this conclusion is not supported by figure 28b, which indicates that the mean maximum echo-core tops for both the AgI- and sand-treated clouds begin to diverge from each other possibly as soon as 3 minutes after treatment. Therefore, evidence that AgI treatment had any effect on mean maximum echo-core height is extremely weak. To the extent that AgI treatment may have had an effect, it may have been negative and opposite to that expected according to the dynamic seeding hypothesis.

Figure 29 shows composite diagrams for mean maximum echo-core areas. As can be seen in figure 29a, mean area growth rates overlap one another beginning almost as early as 21 minutes prior to treatment, and they continue to be similar until about 12 minutes after treatment. After that time the AgI-treated echo cores suddenly decline in mean area, separating the means by more than one standard error.

On the other hand, mean areas computed on the basis of the entire sample of clouds (figure 29b) do not show a dramatic difference. Thus, although the "snapshot" of response variables that is offered in table 32 did not suggest an effect on area, figure 29 provides weak evidence that there may also have been a negative effect on echo-core area. This finding is also inconsistent with the results expected according to the dynamic seeding hypothesis.

Figure 30 shows mean maximum reflectivity with time before and after treatment. While figure 30b gives no indication of a seeding effect on reflectivity, figure 30a shows faint evidence that there may have been a reduction in reflectivity that roughly corresponds to the time in which figure 29a suggests a reduction in area. However, the decrease in reflectivity at about 21 minutes after treatment occurs only briefly, adding to the uncertainty with which a firm conclusion can be drawn.

Figure 31 shows composite diagrams for mean maximum rain flux for echo cores that met ≥ 70 percent of the seedability criteria. These plots are the "noisiest" of the composite diagrams, which makes interpretation difficult. However, the plots appear to indicate that both samples of echo cores had similar rain flux from approximately 18 minutes prior to treatment until about 15 minutes after treatment. After this time and corresponding to the decrease in mean echo-core area and reflectivity, rain fluxes for the sand-treated echoes become about one standard error greater than the AgI-treated echoes. This difference persists about 33 to 42 minutes after treatment.

In summary, the evidence presented in figures 28-31 and in table 32 provides no definitive conclusion about what effect, if any, AgI treatment may initially have had on the individual echo cores with SI ≥ 70 percent. However, if there was any effect at all, the evidence points toward reduction of echo core height, area, reflectivity, and rain flux.

All of these effects are contrary to those expected from the dynamic seeding hypothesis. Therefore, above all, these results warrant a reconsideration of the dynamic seeding hypothesis and call into question its applicability in Illinois.

Analysis of Clouds with Low Seedability Index

Comparative analysis was also performed on clouds with relatively low SI; that is, clouds with SI < 80 percent. Key predictor variables for clouds with SI < 80 percent are listed in table 33. The significance tests indicate that the subgroup of clouds with SI < 80 percent were similar at the time of treatment, noting that buoyancy enhancement had the highest significance levels. However, the mean and standard deviations for buoyancy enhancement are the same. Given the high likelihood of one significant difference in ten due to chance, the populations of sand- and AgI-treated clouds in this subgroup can be considered similar at treatment, thus allowing the responses to be compared to discern seeding effects.

Table 34 lists key response variables for clouds with low SI. The only variable with a weakly significant difference is change in area from treatment time to maximum. This indicates that the AgI-treated clouds may have undergone larger changes in area than the sand-treated clouds. However, if the general rule applies that 10-15 percent of a sample of variables will show significant differences, this one weak significance level is insufficient for a strong claim for a seeding effect. Therefore, the results in table 34 suggest that AgI may have had little or no initial effect on the echo cores with SI < 80 percent.

Figure 32 shows mean maximum heights for clouds with SI < 80 percent. In both graphs, the two traces are intertwined, and the behavior after treatment appears to be nothing more than an extension of that expected from the trends prior to and around the time of treatment. Thus on average, AgI seeding likely had no effect on maximum echo-core height.

Figure 33 indicates that the sand-treated clouds generally had larger areas prior to the time of treatment. But from about 6 minutes after treatment, their areas were generally smaller than the AgI-treated echo cores. However, the differences are barely more than one standard error, and in both the sand and AgI cases, trends after treatment do not appear to differ from those expected prior to treatment.

Figure 34 shows mean maximum reflectivity for the sand- and AgI-treated echo cores prior to and after treatment. Figure 34a shows that on average, the maximum reflectivity for sand-treated clouds declined from approximately 12 minutes prior to treatment to about 30 minutes after treatment while the mean maximum reflectivity of the AgI-treated echo cores follows an inverted parabolic curve, and reflectivities exceed those of the sand-treated cores for much of the time after treatment. However, as has previously been the case, the trends do not appear to be drastically different from those expected from pretreatment behavior.

The diagrams for rain flux (figure 35) show little difference, on average, between the sand- and AgI-treated clouds. However, rain flux among the AgI-treated clouds continues for approximately 15 minutes after the values for the sand-treated clouds decline to zero, weakly suggesting that the AgI-treated echo cores may have had a greater persistence of rain flux.

In summary, the evidence presented in figures 32-35 and in table 34 again does not provide a definitive conclusion about the effect that AgI treatment may initially have had on the individual echo cores with SI < 80 percent. However, the evidence for "less suitable" echo cores seems to point toward positive seeding effects on area, reflectivity, and rain flux.

These responses are consistent with those expected from the dynamic seeding hypothesis, but yet unexpected for "less" suitable echo cores. Thus, to the extent that these results indicate a valid seeding signal, the dynamic seeding hypothesis for Illinois is called into further question.

Discussion

The 1989 cloud seeding sample was initially small, and analysis by filtering according to a SI made the sample even smaller. This condition precluded strong statistical support for any conclusions. The analysis for echo cores with high SI, (i.e., those perhaps better suited for dynamic seeding than those with low SI) pointed toward a negative dynamic reaction, while evidence for echo cores with low seedability pointed toward a positive reaction. Both findings are contrary to expectations according to the dynamic seeding hypothesis.

These highly unexpected results are cause for extreme caution before taking the next step toward interpreting physical processes, rejecting and/or revising the hypothesis, and questioning results from previous dynamic seeding experiments. Such unusual and contrary results may only suggest that AgI and sand had little or no initial effect on echo-core behavior that could be used as a gauge to test some of the early steps of the dynamic seeding hypothesis. However, it may also be incorrect to ignore the contrary evidence, particularly because of its strong implications for future exploratory seeding in Illinois and possible impacts on other convective cloud seeding projects.

One possible explanation for a negative effect on echo-top height could be that seeding and consequent latent heat releases may have increased cloud turbulence, rather than strengthening and organizing the updraft, as Gayet and Soulage (1992) noted. Thus, uneven latent heat release may promote mixing of the updraft regions into downdraft and vice versa. Consequently, rather than achieving an invigoration of vertical cloud motion, vertical growth would dissipate, and AgI-treated cores would not grow to maximum heights greater than the sand-treated cores. This argument points to the need to properly target the seeding agent to the updraft regions.

At the microphysical scale, the seeding agent probably has its largest initial effect on the smallest supercooled cloud droplets because 1) the concentration of supercooled cloud droplets is several orders of magnitude greater than that of drizzle and raindrops, and 2) cloud droplets must be in much closer thermoequilibrium with the environment than supercooled drizzle and raindrops, which may be warmer than the environment.

Following the discussion in Dennis (1980), simple Brownian collection theory indicates that approximately 10,000 cloud droplets should capture an AgI particle in the same time it takes one raindrop to capture an AgI particle, assuming that the production of ice crystals directly from the AgI particles can be neglected without error. If this does occur, the net consequence would be to stunt the broadening of the particle spectrum by coalescence and riming processes, both of which depend on supercooled cloud droplets as a source for growth. Thus, processes that tend to move condensate into precipitation particle sizes would be restricted in the presence of enhanced latent heat release. This would promote the transport of condensate aloft and may aid internal mixing. All these issues can and should be addressed in future field programs to achieve a better theoretical and observational understanding of natural precipitation processes and how they may be altered at the in-cloud, cloud, and mesoscale.

Conclusions

This chapter covered the use of a seedability index to create subgroups of clouds with similar characteristics at the time of the treatment so that comparisons of responses could reveal a true seeding effect. The SI created subgroups of "suitable" and "unsuitable" clouds, thereby overcoming the "bad draw." However, the inherent reduction in sample size precluded obtaining conclusive evidence.

A detailed examination of the responses for "suitable" clouds (those with SI ≥ 70 percent) indicated that *if* AgI had any effect on cloud behavior, it was to reduce maximum echo-top

height. Composite diagrams showing average maximum echo-core height with time also suggested that AgI had a negative effect on vertical cloud growth. Similar composite diagrams for area, reflectivity, and rain flux indicate that AgI-treated clouds may have had, on average, smaller areas, lower reflectivities, and smaller rain fluxes than sand-treated clouds. However, it remains uncertain whether these responses were the result of seeding or merely extensions of expected echo behavior before and at treatment time. These results are not generally sensitive to the SI filter level used and are inconsistent with the dynamic seeding hypothesis.

Responses of clouds with low seedability indexes (those with SI < 80 percent) showed no conclusive evidence that AgI affected cloud behavior in terms of maximum height, area, reflectivity, or rain flux. Close examination of composite diagrams for average maximum height, area, and rain flux suggested that AgI may have had a positive effect on clouds that were "less suitable" for dynamic seeding. However, the extent to which this indicates a weak seeding signal cannot be entirely separated from expectations based on the clouds' behavior prior to treatment.

In general, the effect of AgI on echo cores within approximately 30 minutes of treatment was unappreciable according to radar observations. Possible effects opposite to those expected from the dynamic seeding hypothesis were found for clouds with both high and low seedability indexes. This calls into question the validity of the dynamic seeding hypothesis for Illinois, and draws attention to the need to improve basic understanding of natural cloud processes and interactions at different atmospheric scales.

FIGURES AND TABLES FOR CHAPTER 5

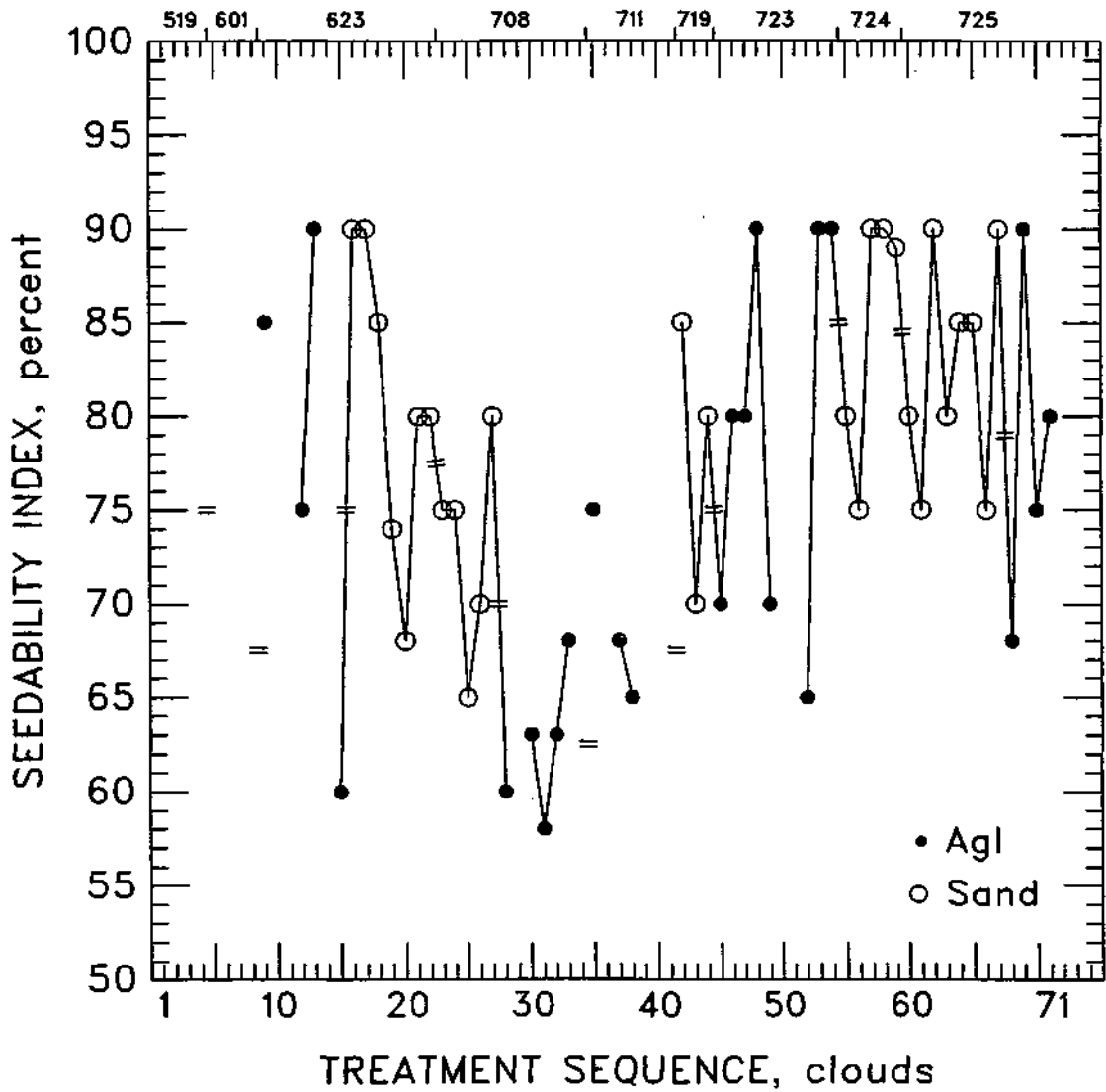


Figure 27. Temporal variation of the seedability index. Values not joined by a solid line indicate a missing intervening value.

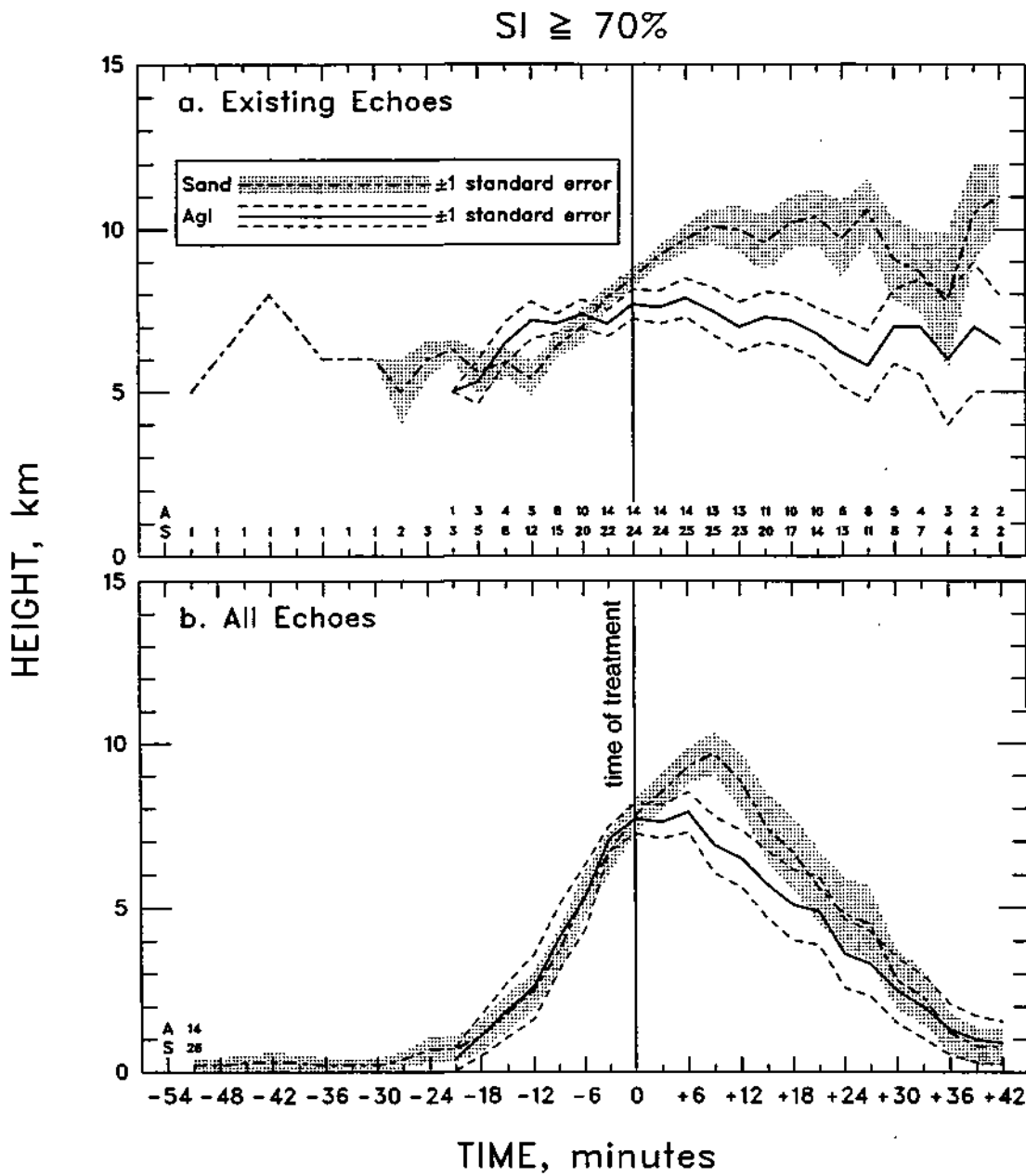


Figure 28. Variation with time of maximum echo-top height for sand- and AgI-treated echoes with $SI > 70$ percent in existence at each interpolated volume scan (a) and all treated echoes (b)

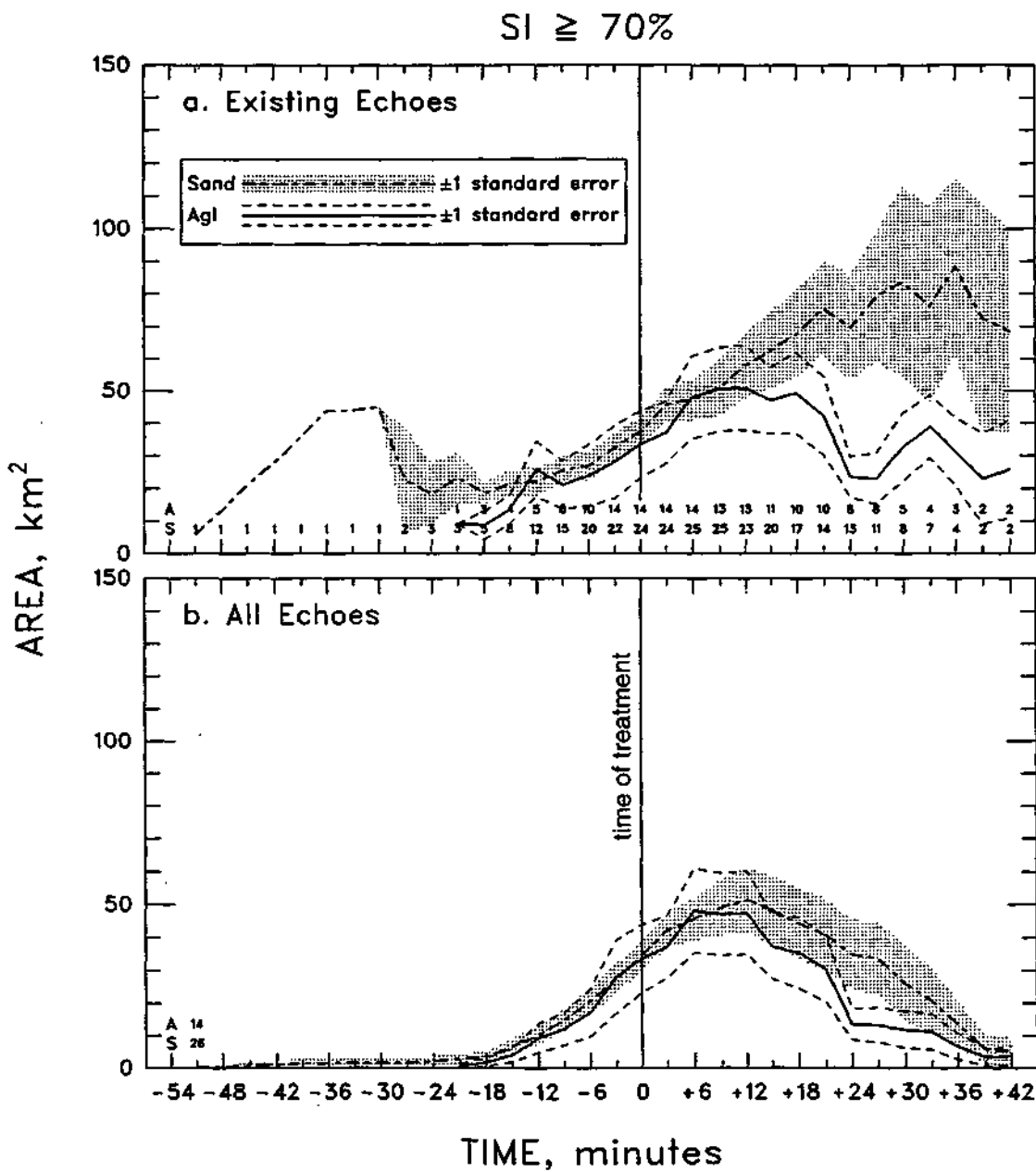


Figure 29. Variation with time of maximum echo area for sand- and Agl-treated echoes with $SI > 70$ percent in existence at each interpolated volume scan (a) and all treated echoes (b)

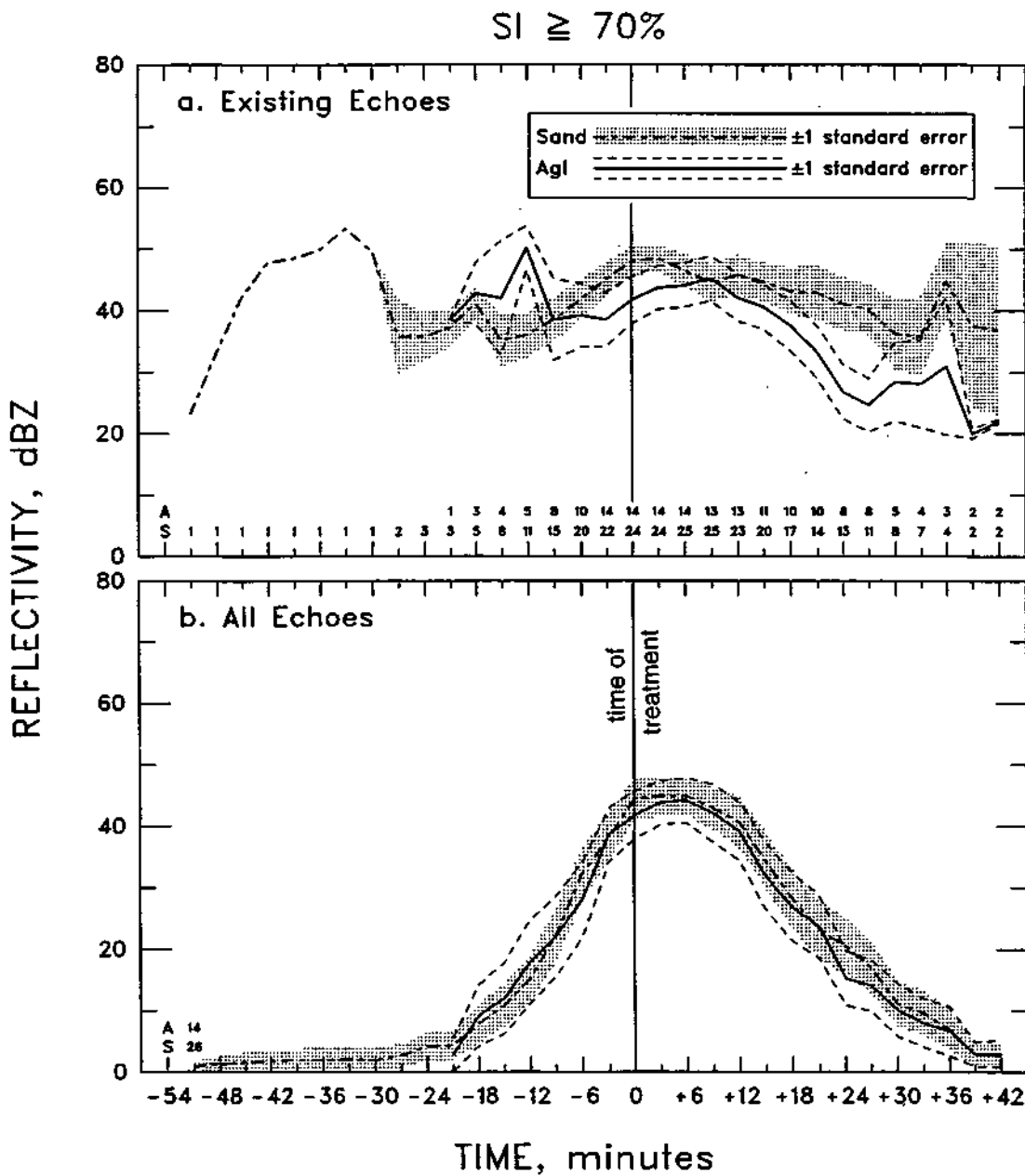


Figure 30. Variation with time of maximum echo reflectivity for sand- and AgI-treated echoes with SI >70 percent in existence at each interpolated volume scan (a) and all treated echoes (b)

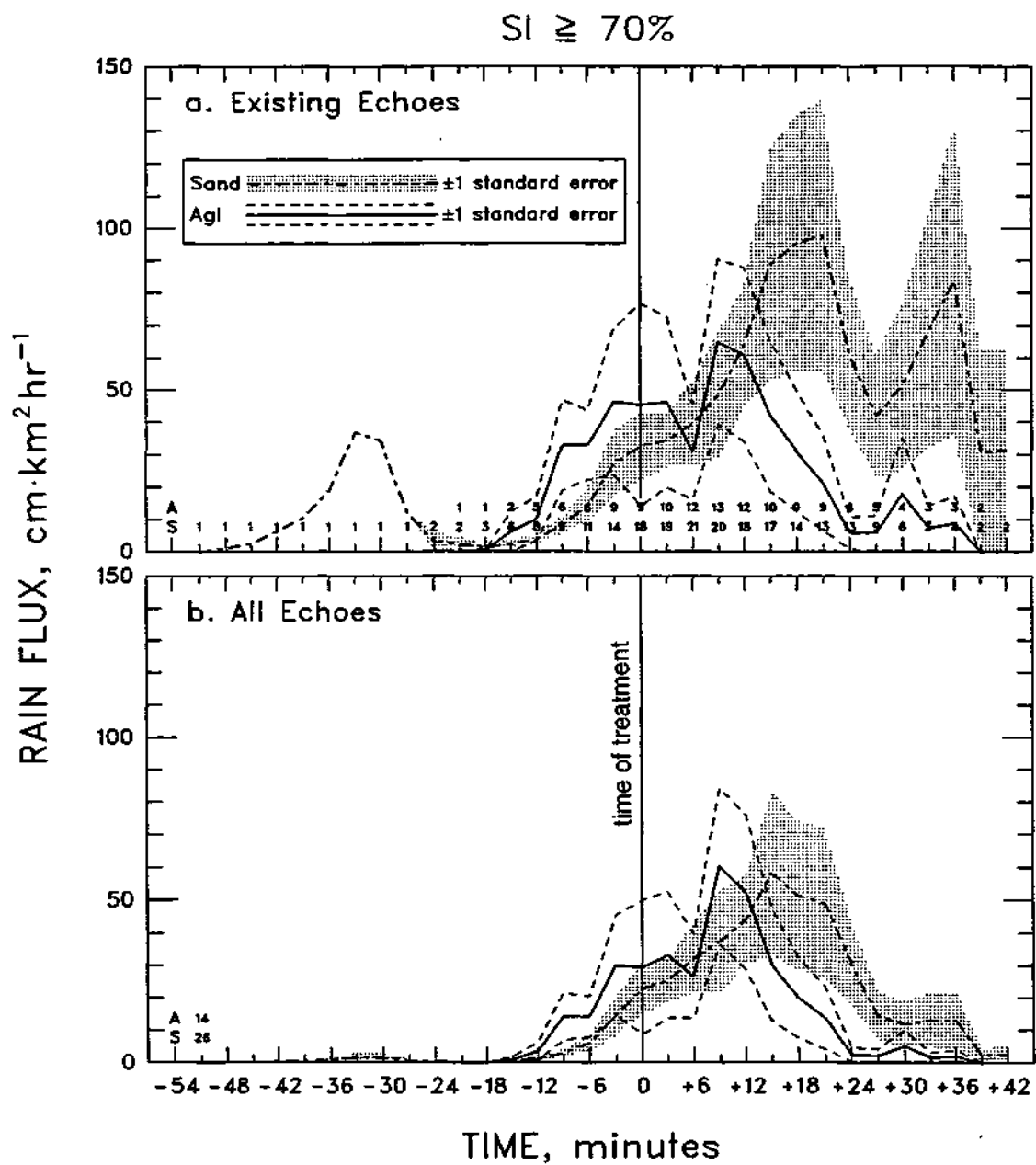


Figure 31. Variation with time of maximum rain flux for sand- and AgI-treated echoes with SI >70 percent in existence at each interpolated volume scan (a) and all treated echoes (b)

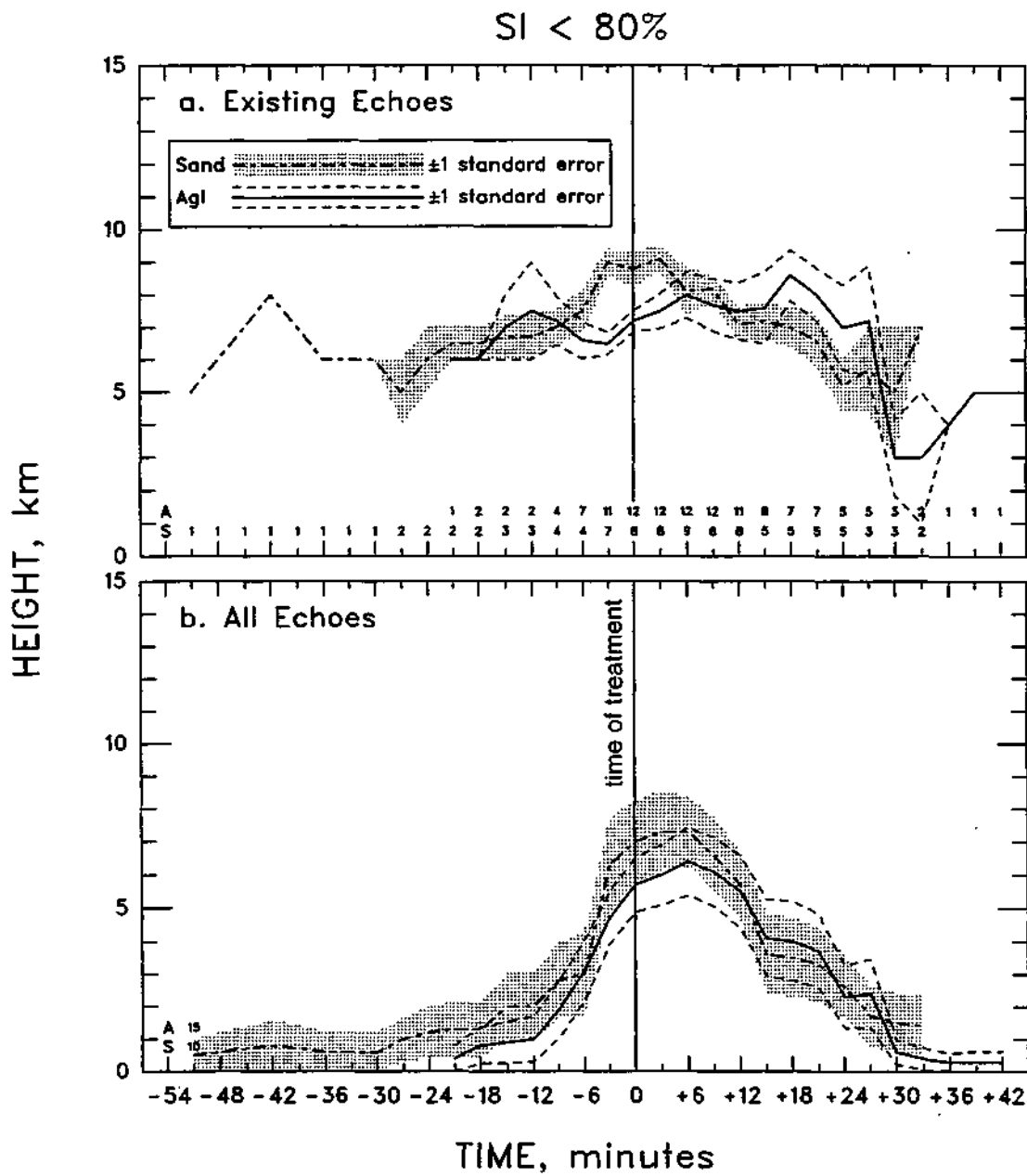


Figure 32. Variation with time of maximum echo-top height for sand- and AgI-treated echoes with SI <80 percent in existence at each interpolated volume scan (a) and all treated echoes (b)

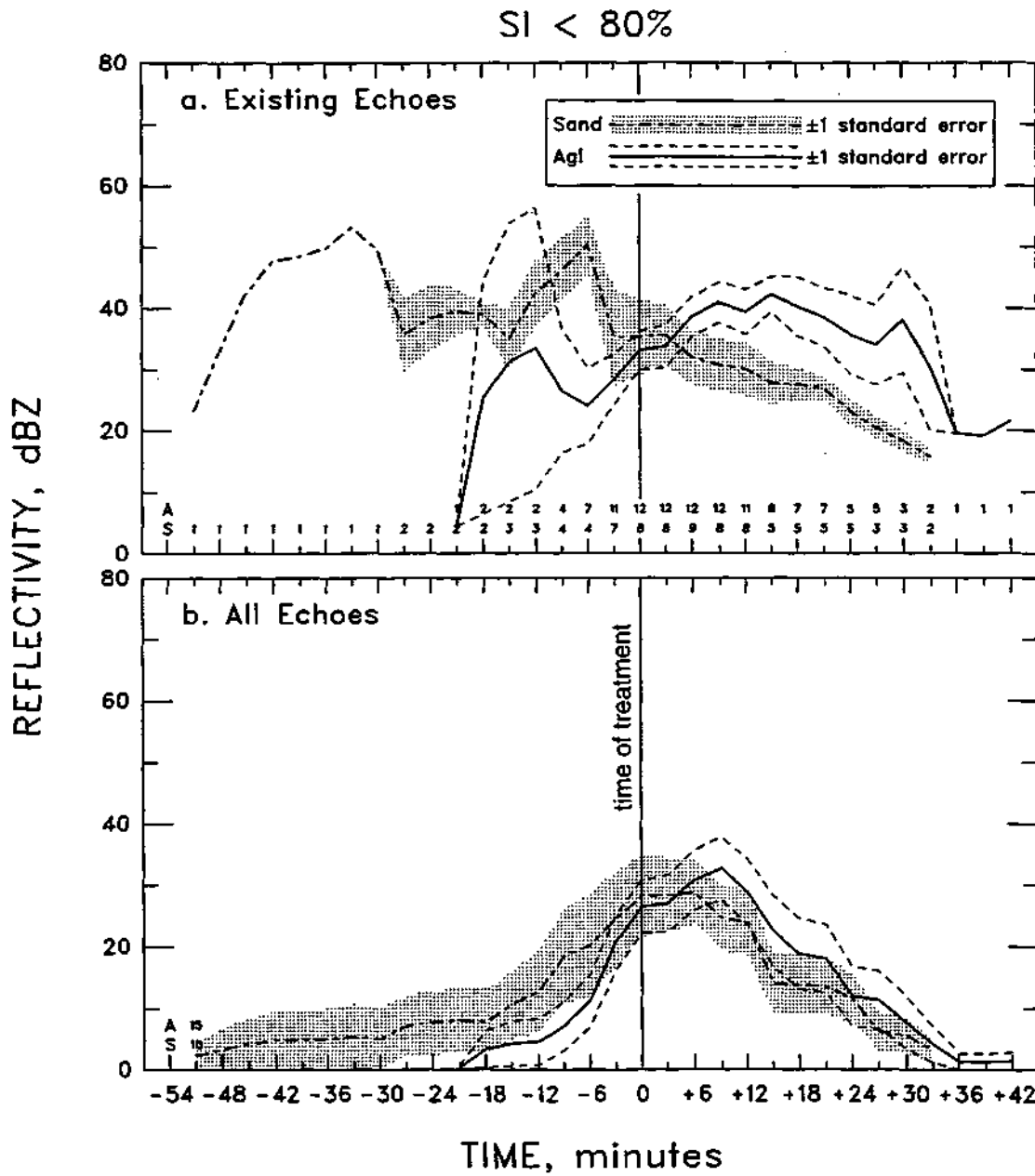


Figure 33. Variation with time of maximum echo area for sand- and AgI-treated echoes with SI <80 percent in existence at each interpolated volume scan (a) and all treated echoes (b)

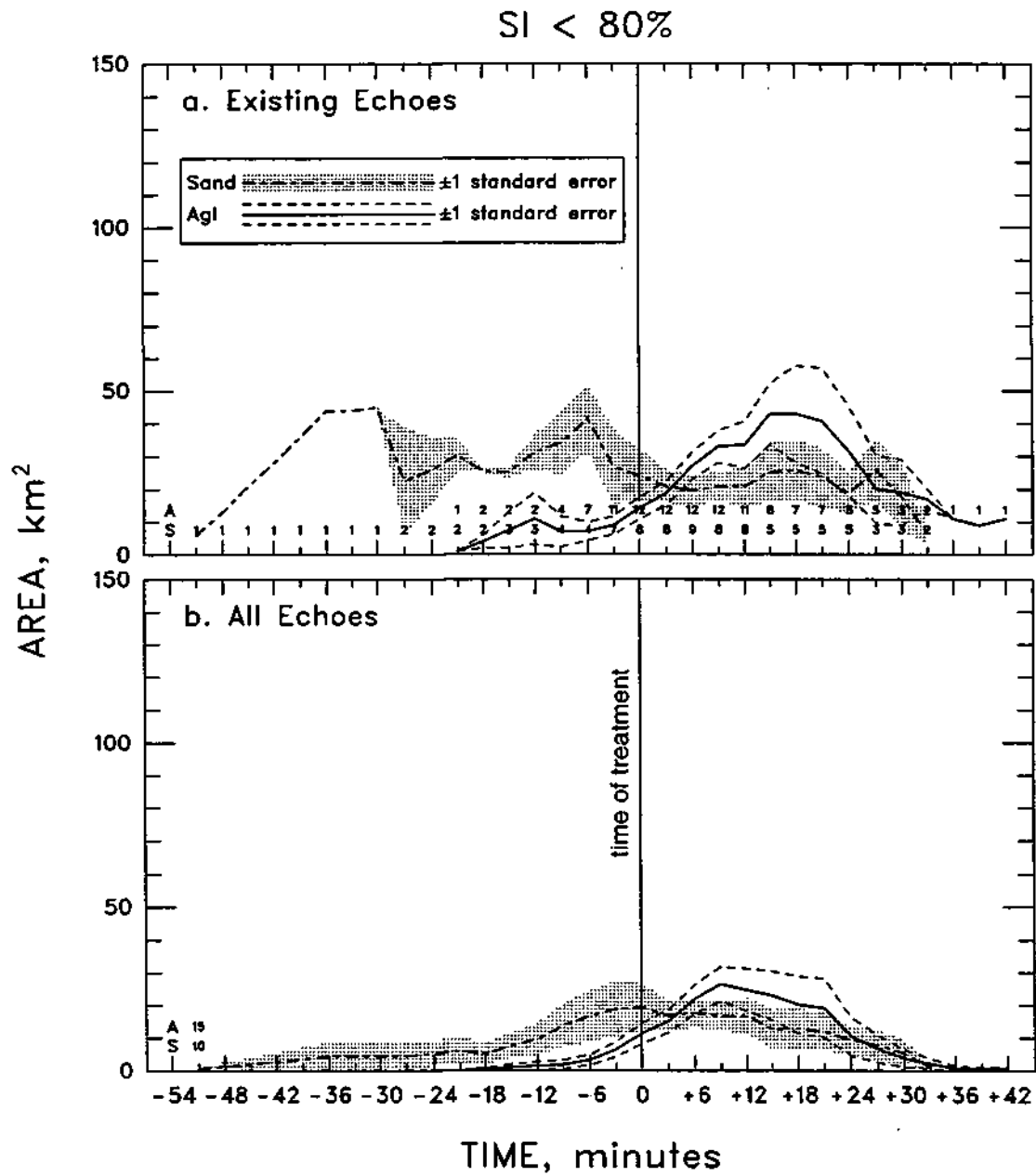


Figure 34. Variation with time of maximum echo reflectivity for sand- and AgI-treated echoes with SI <80 percent in existence at each interpolated volume scan (a) and all treated echoes (b)

SI < 80%

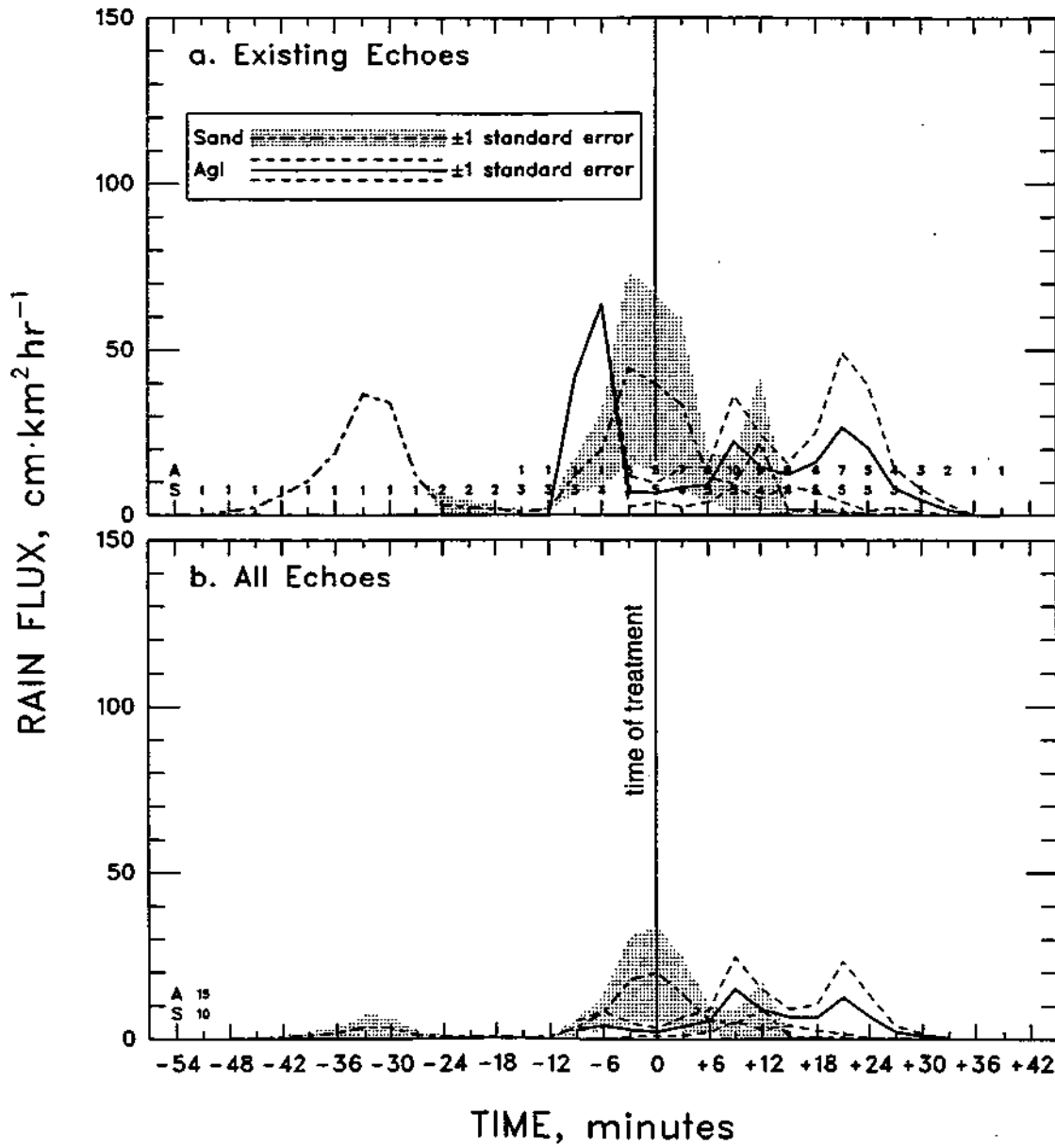


Figure 35. Variation with time of maximum rain flux for sand- and Agl-treated echoes with SI <80 percent in existence at each interpolated volume scan (a) and all treated echoes (b)

Table 26. Variables and Thresholds Limits Defining the Seedability Index.

<i>Number</i>	<i>Variable name</i>	<i>Threshold</i>
1	Up_Dia ^c	$x \geq 1000 \text{ m}$
2	Mean_VW ^c	$2 < x < 8 \text{ m s}^{-1}$
3	%_Updraft ^c	$x \geq 33\%$
4	NBuoy ^c	$-2 \leq x \leq +2 \text{ }^\circ\text{C}$
5	Buoy_Enh ^c	$x \geq 0.45 \text{ }^\circ\text{C}$
6	LWCd ^c	$x \geq 0.1 \text{ g m}^{-3}$
7	SWC_frac ^c	$x \leq 40\%$
8	FECPT ^b	$x < 15 \text{ min.}$
9	range ^b	$30 \leq x \leq 90 \text{ km}$
10	CPMxz ^b	$x > 20 \text{ dBZ}$
11	a_cdp ^b	$-0.02 < x < +0.02 \text{ km min}^{-2}$
12	CPFEdZ/dt ^b	$x \geq 0.0 \text{ dBZ min}^{-1}$
13	CPmndia ^b	$x \geq 1.0 \text{ km}$
14	CPHMxz ^b	$1 > x \geq 1.5 \text{ km}$
15	tccl ^a	$x > 14^\circ\text{C}$
16	pb ^a	$x \geq 3^\circ\text{C}$
17	L ^a	$x \leq 0$
18	Ri ^a	$x \geq 11$
19	Dosage 1	$1.5 \leq x \leq 3.5 \text{ flares km}^{-1}$
20	Dosage 2	$x \geq 50\%$

Notes: ^a, ^b, ^cVariables are defined in appendixes A, B, or C, respectively.

Table 27. Summary of Individual Seedability Index Criteria Outcomes

Number	CLD_ID	Treat	UP_Dia	Mean VW	% Updraft	NBuoy	Buoy Enh	LWC2	SWC - frac	FECPt	range	CPMz	a_cdp	CPFE dZ/dt	CPmn dia	CPHM xZ	tot	pb	L	Ri	U _{frst} U _{km}	% in Up	SI
1	519bEU02EC01	S	.	.	.	NA	NA	NA	NA	.	98	13.2	0.8	.	0.2	4.124	.	NA
2	519bEU02EC04	S	.	9.41	.	NA	NA	NA	NA	.	.	.	-0.0476	.	.	.	13.2	0.8	.	0.2	.	.	NA
3	519bEU02EC03	S	.	8.92	.	NA	NA	NA	NA	13.2	0.8	.	0.2	.	.	NA
4	519bEU02EC03	S	763.9	.	.	NA	NA	NA	NA	.	92	13.2	0.8	.	0.2	6.411	.	NA
5	601EU05EC01	A	NA	NA	NA	NA	NA	NA	NA	.	.	.	NA	1.7	.	NA	NA	NA
6	601EU05EC02	A	NA	NA	NA	NA	NA	NA	NA	.	.	.	0.0748	1.7	.	NA	NA	NA
7	601EU05EC03	A	NA	NA	NA	NA	NA	NA	NA	15.83	1.7	.	NA	NA	NA
8	601EU05EC04	A	NA	NA	NA	NA	NA	NA	NA	1.7	.	NA	NA	NA
9	623aEU11EC01	A	0.0015	.	.	.	16	1.4	.	.	.	85
10	623aEU11EC02	A	0	0	0	NA	NA	NA	NA	1.4	.	0	0	NA
11	623aEU11EC04	A	0	0	0	NA	NA	NA	NA	.	.	.	-0.0203	1.4	.	0	0	NA
12	623aEU11EC03	A	.	1.76	.	-2.56	0.43	0.0427	1.4	.	.	.	75
13	623aEU11EC06	A	1.4	.	.	.	90
14	623aEU11EC07	A	0	0	0	NA	NA	NA	NA	1.4	.	0	0	NA
15	623aEU11EC08	A	253.1	1.62	26.09	-2.9	.	0.0025	1.2	.	.	1.4	.	.	25	60
16	623bEU13EC08	S	.	15.28	1.4	.	.	.	90
17	623bEU13EC09	S	-0.0237	1.4	.	.	.	90
18	623bEU13EC10	S	.	14.28	.	.	.	0.0749	1.4	.	.	.	85
19	623bEU13EC11	S	.	10.02	.	.	.	0	.	.	.	14.24	NA	1.4	.	4.76	.	74
20	623bEU13EC12	S	.	13.9	.	.	.	0	.	.	.	0	NA	.	0	.	.	.	1.4	.	0.543	.	68
21	623bEU13EC13	S	.	.	.	-4.14	.	0.0021	1.4	.	1.45	.	80
22	623bEU13EC14	S	.	14.6	.	-3.07	.	0.0003	1.4	.	.	.	80
23	708EU17EC01	S	0	.	.	0	.	13.8	.	9	.	.	.	75
24	708EU17EC02	S	930.4	.	.	-5.41	.	0	13.8	.	9	.	.	.	75
25	708EU17EC03	S	0	.	.	.	0	.	.	0	.	13.8	.	9	.	0.607	40	65
26	708EU17EC05	S	0.39	0	.	.	.	0	.	.	0	.	13.8	.	9	.	.	.	70
27	708EU17EC06	S	0	13.8	.	9	.	0.865	.	80
28	708EU18EC07	A	884	1.7	27.03	.	.	.	0.5189	13.8	.	9	.	0	0	60
29	708EU18EC09	A	0	0	0	NA	NA	NA	NA	.	.	12.8	NA	.	.	.	13.8	.	9	.	0	0	NA
30	708EU18EC11	A	.	.	.	0.41	0	0	NA	-2.9807	0	.	13.8	.	9	.	.	.	63
31	708EU18EC13	A	968.6	.	26.92	.	0.39	0	.	.	.	0	NA	.	0	.	13.8	.	9	.	.	.	58
32	708EU18EC14	A	616.8	.	.	-3.74	.	0	.	.	.	19.24	NA	.	.	.	13.8	.	9	.	0.953	.	63
33	708EU18EC15	A	.	10.4	.	3.17	0.29	0.0498	NA	.	.	.	13.8	.	9	.	.	.	68
34	708EU18EC12	A	0	0	0	NA	NA	NA	NA	.	.	0	NA	NA	0	.	13.8	.	9	.	0	0	NA
35	711EU19EC02	A	.	13.32	.	.	.	0.0005	.	.	104	.	.	-0.875	3.4	.	.	.	75
36	711EU19EC03	A	0	0	0	NA	NA	NA	NA	.	95	3.4	.	0	0	NA
37	711EU19EC06	A	.	12.88	.	0.43	0	.	.	.	103	16.68	NA	3.4	.	.	.	68
38	711EU19EC09	A	.	.	.	-2.55	0.41	.	.	.	91	0	.	.	0	.	.	.	3.4	.	.	.	65
39	711EU19EC04	A	864	.	.	-4.39	.	0.009	.	NA	103	0	NA	NA	0	.	.	.	3.4	.	0.615	25	NA
40	711EU19EC05	A	420.8	.	32	-3.67	.	0.0028	.	NA	106	0	NA	NA	0	.	.	.	3.4	.	.	.	NA
41	711EU19EC08	A	.	.	.	-3.27	.	0.0008	.	NA	104	0	NA	NA	0	.	.	.	3.4	.	.	.	NA
42	719aEU20EC01	S	.	11.27	95	2.3	85
43	719aEU20EC02	S	.	.	.	-18.32	.	.	0.9679	16.35	102	2.3	.	.	3.597	.	70
44	719aEU20EC03	S	0.5117	.	.	102	1.1	.	2.3	80
45	723EU22EC02	A	486.1	.	20.69	.	.	0.0965	.	.	112	4.135	33.33	70
46	723EU22EC04	A	0.4767	.	15.02	107	4.262	.	80
47	723EU22EC05	A	937	.	.	-2.28	.	0	.	.	99	80
48	723EU22EC08	A	.	.	.	-3.15	105	90
49	723EU22EC09	A	407.9	1.9	6.94	-2.25	100	20	70
50	723EU22EC10	A	NA	NA	NA	NA	NA	NA	NA	.	109	NA	NA	NA
51	723EU22EC11	A	0	0	0	NA	NA	NA	NA	.	103	0	0	NA
52	723EU22EC14	A	589	.	30.43	-3.33	.	0.0048	.	.	101	3.511	33.33	65
53	723EU22EC01	A	0.4036	.	110	90
54	723EU22EC03	A	0.0179	.	.	109	90
55	724EU23EC07	S	.	.	.	2.47	.	.	0.8497	17.67	1.1	.	80
56	724EU23EC08	S	.	.	.	3.51	.	.	0.9536	24.4	0.62	23	75
57	724EU23EC09	S	1.318	28.57	90
58	724EU23EC11	S	0.0853	1.332	.	90
59	724EU23EC06	S	.	.	.	-2.68	NA	-1.2614	89
60	725EU24EC01	S	517.6	0.0028	.	.	102	4.691	.	80
61	725EU24EC03	S	0.0696	.	53.18	94	1.204	.	75
62	725EU24EC04	S	0.6296	.	91	90
63	725EU24EC05	S	0.7126	18.02	1.2	.	.	.	1.397	.	80
64	725EU24EC06	S	0.0824	.	15.75	1.4	85
65	725EU24EC07	S	275.3	0.0065	3.711	.	85
66	725EU24EC08	S	448	.	17.86	.	.	.	0.6386	.	98	33.33	75
67	725EU24EC09	S	98	90
68	725EU25EC10	A	380.6	.	11.43	.	.	0	.	.	.	0	NA	-4.5568	0	68	
69	725EU25EC11	A	0.0029	0.7719	90
70	725EU25EC12	A	0.0203	0.9076	17.27	1	.	.	.	0.621	.	75
71	725EU25EC3	A	0	0.6417	22.93	1.34	.	80

Note: a,b,c Variables are defined in appendixes A, B, or C, respectively.

**Table 28. Seedability of the Sand- and AgI- Treated Clouds
Expressed in Number of Clouds**

<i>Treatment</i>	<i>Number of clouds meeting $\geq X\%$ of the SI</i>					
	≥ 50	≥ 60	≥ 70	≥ 80	≥ 90	100
Sand	28	28	26	18	6	0
AgI	24	23	14	9	5	0

**Table 29. Nonseedability of the Sand- and AgI- Treated Clouds,
Expressed in Number of Clouds**

<i>Treatment</i>	<i>Number of clouds meeting $< X\%$ of the SI</i>					
	<50	<60	<70	<80	<90	100
Sand	0	0	2	10	22	28
AgI	0	1	10	15	19	24

Table 30. Population Statistics of Predictor Variables for Clouds with SI $\leq 70\%$.

Variable	<u>Mean</u>		<u>Standard dev</u>		<u>Sample size</u>		<u>P-values</u>	
	Sand	AgI	Sand	AgI	Sand	AgI	t	W
CPmndia ^b	4.8	4.4	2.1	2.3	26	14	0.62	0.13
CPHtp10 ^b	7.5	7.6	2.6	1.9	26	14	0.95	0.39
CPMxZ ^b	44.3	41.7	17.3	14.2	26	14	0.75	0.42
CPMxB ^b	23.1	22.1	8.7	5.8	26	14	0.78	0.29
CPA10 ^b	34.3	33.1	22.6	38.3	26	14	0.86	0.24
FECPI ^b	9.5	8.3	11.8	7.3	26	14	0.66	0.86
NBuoy ^c	-1.3	-1.2	3.9	1.2	26	14	0.92	0.21
Buoy_Enb ^c	0.5	0.5	0.0	0.0	26	14	0.20	0.20
Mean_VW ^c	6.3	4.7	3.8	3.0	26	14	0.50	0.29
SWC_frac ^c	0.2	0.3	0.3	0.3	26	14	0.83	0.72
pb ^a	4.4	4.2	1.8	1.1	26	14	0.79	0.71
tcc1 ^a	16.9	16.8	1.8	1.2	26	14	0.91	0.86
Ri ^a	71.3	78.9	21.9	32.9	26	14	0.62	0.88

Notes: N = 67

p $\leq 5\%$

5 < p $\leq 10\%$

p > 10%

^{a, b, c}Variables are defined in appendixes A, B, C, respectively.

t = student's *t*-test.

W = Wilcoxon sum rank test.

^{a, b, c}Variables are defined in appendixes A, B, or C, respectively.

Table 31. Population Statistics for all Clouds with Radar Data.

Predictor variable	Mean		Standard dev		Sample size		P-val	
	Sand	AgI	Sand	AgI	Sand	AgI	t	W
CPmndia ^b	4.787	3.544	2.459	2.246	32	35	0.034	0.006
CPHtp10 ^b	7.094	6.143	3.052	2.756	32	35	0.185	0.028
CPMxZ ^b	43.214	33.905	19.750	17.908	32	35	0.047	0.013
CPMxB ^b	22.388	18.235	9.974	8.550	32	35	0.071	0.008
CPA10 ^b	38.219	23.514	29.552	28.681	32	35	0.043	0.010
FECpt ^b	8.790	5.992	11.081	6.202	32	35	0.202	0.315
NBuoy ^c	-1.264	-1.210	3.798	1.569	28	24	0.948	0.212
Buoy_Enh ^c	0.525	0.483	0.047	0.065	28	24	0.010	0.017
Mean_VW ^c	6.589	3.993	3.783	3.563	32	30	0.007	0.003
SWC_frac ^c	0.215	0.186	0.332	0.278	28	24	0.737	0.971
pb ^a	4.122	5.423	2.181	1.827	32	35	0.010	0.005
tccl ^a	16.278	16.394	2.112	1.571	32	35	0.798	0.697
Ri ^a	62.066	81.120	31.024	38.862	32	35	0.031	0.526

Notes: N = 67

p ≤ 5%

5 < p ≤ 10%

p > 10%

a, b, c Variables are defined in appendixes A, B, C, respectively.

t = student's *t*-test.

W = Wilcoxon sum rank test.

Table 32. Population Statistics of Response Variables for Clouds with SI > 70%.

<i>Predictor variable</i>	<i>Mean</i>		<i>Standard dev</i>		<i>Sample size</i>		<i>P-values</i>	
	<i>Sand</i>	<i>AgI</i>	<i>Sand</i>	<i>AgI</i>	<i>Sand</i>	<i>AgI</i>	<i>t</i>	<i>W</i>
MaxH10	10.8	8.6	2.7	2.0	26	14	0.06	0.06
MaxA10	80.2	65.6	61.2	55.6	26	14	0.22	0.25
MaxZ	52.6	52.1	13.5	12.2	26	14	0.95	0.86
MaxB	27.7	28.2	6.4	6.5	26	14	0.82	0.69
MXCPdH10	2.5	0.7	2.7	1.5	26	14	0.22	0.17
MXCPdA10	37.0	26.9	57.5	46.0	26	14	0.46	0.72
MXCPdZ	5.0	6.6	12.2	12.8	26	14	0.78	0.83
MXCPdB	2.7	3.3	6.2	7.0	26	14	0.86	0.76
CPMXtMxA	9.5	8.3	14.1	7.7	26	14	0.80	0.41
FEMXtMxA	19.0	16.6	11.1	9.2	26	14	0.41	0.31

Notes: N = 67

p ≤ 5%

5 < p ≤ 10%

p > 10%

t = student's t-test.

W = Wilcoxon sum rank test.

Variables are defined in appendix B.

Table 33. Population Statistics of Predictor Variables for Clouds with SI < 80 %.

Variable	Mean		Standard dev		Sample size		P-value	
	Sand	AgI	Sand	AgI	Sand	AgI	t	W
CPmndia ^b	2.6	2.3	2.7	1.8	10	15	0.62	0.78
CPHtplO ^b	4.8	5.0	4.2	3.3	10	15	0.85	0.47
CPMxZ ^b	24.3	23.4	24.4	17.9	10	15	0.90	0.95
CPMxB ^b	13.5	13.2	12.7	9.3	10	15	0.97	0.82
CPA10 ^b	18.3	10.5	23.5	12.4	10	15	0.23	0.75
FECpt ^b	8.9	4.0	18.5	5.1	10	15	0.34	0.78
NBuoy ^c	-2.5	-1.3	6.0	1.7	10	15	0.64	0.71
Buoy_Enh ^c	0.5	0.5	0.1	0.1	10	15	0.12	0.12
Mean_VW ^c	5.6	5.2	3.8	4.0	10	15	0.71	0.56
SWC_rac ^c	0.3	0.1	0.4	0.3	10	15	0.30	0.79
pb ^a	5.6	6.1	2.4	2.1	10	15	0.42	0.44
tccl ^a	15.8	16.0	2.1	1.9	10	15	0.85	0.62
Ri ^a	70.8	95.3	20.3	46.2	10	15	0.56	0.56

Notes: N = 25

p ≤ 5%

5 < p ≤ 10%

p > 10%

t = student's *t*-test.

W = Wilcoxon sum rank test.

Variables are defined in appendix B.

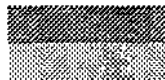


Table 34. Population Statistics of Response Variables for Clouds with SI < 80%.

Variable	Mean		Standard dev		Sample size		P-values	
	Sand	AgI	Sand	AgI	Sand	AgI	t	W
MaxH10	8.8	8.5	1.5	2.2	10	15	0.64	0.52
MaxA10	38.5	39.5	29.4	39.4	10	15	0.89	0.80
MaxZ	39.1	42.9	16.5	13.9	10	15	0.35	0.38
MaxB	21.6	23.6	7.7	7.4	10	15	0.36	0.53
MXCPdH10	0.7	0.0	0.8	3.3	10	15	0.52	0.55
MXCPdA10	2.8	27.8	25.1	39.2	10	15	0.62	0.23
MXCPdZ	9.3	10.9	17.6	22.9	10	15	0.82	0.72
MXCPdB	5.2	5.6	9.7	12.7	10	15	0.88	0.97
CPMXiMxA	3.2	8.8	15.2	7.2	10	15	0.33	0.53
FEMXiMxA	12.1	12.8	7.4	8.2	10	15	0.74	0.91

Notes: N = 67

p ≤ 5%

5 < p ≤ 10%

p > 10%

t = student's t-test.

W = Wilcoxon sum rank test.

Variables are defined in appendix B.

6. STATISTICAL SIGNIFICANCE OF THE EFFECTS OF SEEDING INDIVIDUAL ILLINOIS CLOUDS IN 1989

by

K. Ruben Gabriel and Stanley A. Changnon

Design of the 1989 Experiment

Seeding flights were initiated in 1989 when conditions seemed suitable for precipitation augmentation. Once a flight started, the first storm encountered with large cloud conditions was defined as an experimental unit. This was randomly designated to be seeded with either sand or AgI, based on independent draws with a 50/50 probability. Allocation and delivery were devised so that the crew in the plane was unaware of the type of treatment. If a second storm of that type was subsequently located on the same flight, it was defined as another experimental unit and received the alternate treatment, i.e., if the first was AgI-seeded, then the second was sand-seeded, and vice versa. Several flights and storms were excluded from the analysis for various reasons, but the remaining flights, treatments, and clouds are summarized in table 35.

The Data

Fifty-three large clouds were included in this analysis. Data available for these clouds include the date of seeding, storm (experimental unit), treatment (sand or AgI), a synoptic classification (cold front, air mass, or other), and 11 predictor and 8 response variables considered most important meteorologically. The predictor variables, which are defined in appendix A, B, or C as noted, are:

1. CPmndia^b
2. CPHtp10^b
3. CPMxZ^b
4. FECpt^b
5. NBuoy^c
6. Buoy_Enh^c
7. Mean_VW^c
8. SWC_frac^c
9. pb^a
10. tccl^a
11. Ri^a

The response variables, all of which are defined in appendix B, are:

1. MaxH10
2. MaxA10
3. MaxZ

4. MXCPdH10
5. MXCPdA10
6. MXCPdZ
7. CPMXtMxA
8. FEMXtMxA

Methods of Analysis

Comparison of data from AgI-treated units with control data from sand-seeded units involved the means of the variables. Without any evidence that transformations would have been preferable, it was difficult to judge this from so few observations. The test statistic was the Student's t for storms, as calculated from the ten units and weighted according to the number of clouds in each unit. An alternative statistic would have been the Student's t for the clouds, calculated without weights for all 53 clouds, irrespective of the units. The storm t is preferable to the cloud t since randomization was based on the units, and the clouds within a single unit could not be assumed to constitute independent observations.

Because the seeding was allocated randomly to the eight "first units," while the "second units" received the alternate seeding, each resulting experimental allocation was one of 2^8 or 256 possible randomizations — each of the eight first units having had two possible allocations). Significance could be calculated for each of these statistics by referring them to the appropriate t distributions (with 9 and 52 degrees of freedom, respectively). But the more reliable method of establishing significance was to compare the unit t statistic observed in the experiment with the values it could have taken under the other 255 possible randomizations ($=2^8-1$). All 256 possible allocations were equally probable under the randomization scheme, so *rerandomization analysis* assessed significance by referring the statistic calculated from the experimental results to the set of its 256 rerandomizations. Thus, significance was obtained by calculating the same statistic with each of the 256 possible treatment allocations.

Tables 36-38 show this randomization P-value for each variable, as well as the P-values computed from the r -tables. The latter are somewhat precarious because of the dubious assumptions on which their distributions are based. Thus, the *unit means analysis*, which uses the t for units, requires assumptions of normality and independence that may be misleading for such a small number of observations. Furthermore, the *individual clouds analysis*, which uses the t for clouds, treats the 53 clouds as though they were independent observations and

ignores their grouping into ten experimental units. The latter analysis has a sample large enough to make normality assumptions acceptable, but it is extremely dubious since it ignores the similarities of clouds in the same experimental unit.

Further analyses of the response variables were made after covariance adjustment for certain predictors. Unit analyses used standard analysis of covariance techniques and referred the resulting statistics to the t distribution with eight degrees of freedom. To obtain more reliable rerandomization tests, each response's mean was adjusted for its regression in the entire sample, and rerandomization tests were then applied to the adjusted means. An alternative procedure would have recalculated the analysis of covariance t for each rerandomization. The present procedure uses the same overall regression adjustment for all 256 permutations. This is valid, though possibly less sensitive than the alternative procedure would have been.

Analysis of Individual Predictors and Responses

Table 37 shows the difference between the mean of each variable under AgI seeding and under sand seeding, as well as the approximate level of significance assessed by the individual cloud analyses, unit means analyses, and rerandomization tests.

It is evident from table 36 that there were some differences between AgI and sand for the predictor variables. The clouds analysis suggests that the differences in buoyancy enhancement are highly significant, whereas those on mean diameter and maximum reflectivity of the echo at treatment, mean vertical velocity of the updraft, and bulk Richardson number have P-values of about 10 percent. The analysis of the units is more conservative, showing a P-value of about 10 percent for buoyancy enhancement, and nothing remotely significant for any other variable. This is confirmed by the rerandomization analysis. Multiplicity would have led one to expect a type-I error of about one 9-percent significant result among 11 predictors, so one must conclude that there is little evidence that the random allocation of seeding was selective of particular storms.

For the response variables, all three methods of analysis indicate some significant reductions under AgI seeding. The evidence is clear for maximum height of the 10-dBZ reflectivity contour, but equivocal for change in height from treatment to maximum and time from first echo to maximum area. There is no evidence of seeding effects on any of the other responses.

Analysis of Responses Adjusted for Some of the Predictors

More sensitive analyses were sought by adjusting the response differences for differences in predictor variables. Two predictors with relatively high correlations with the response, buoyancy enhancement and mean vertical velocity, were used for covariance adjustment of the experimental unit data, as shown in tables 37 and 38, respectively.

The unit analyses, with covariance adjustment for either buoyancy enhancement or mean vertical velocity, suggest a possibly significant effect only on maximum height and time from first echo to maximum area. Multiple covariance adjustment for both predictors essentially confirms these results, at least for maximum height, although it is a weaker significance: unit analysis P-values are 0.070 for maximum height, 0.189 for change in height from treatment to maximum, and 0.497 for time from first echo to maximum area. It was not considered necessary to verify these analyses by rerandomization.

Conclusions

The tentative conclusion from all these analyses is that AgI seeding, compared to sand seeding, was not related to the predictor values, but had a negative effect on the maximum echo height, possibly on change in height of the 10-dBZ contour from treatment to maximum height, and on the time from first echo to maximum echo-core area. AgI seeding had no effect on the other response variables. In view of the moderate P-values, and taking into account the multiplicity of responses tested, the conclusion must be regarded as tentative, rather than as strong evidence against the null hypothesis of no seeding effect.

TABLES FOR CHAPTER 6

Table 35. Experimental Units and Seeding Allocations

<i>Serial number</i>	<i>Date</i>	<i>Experimental unit</i>	<i>Seeding</i>	<i>Number of clouds</i>
11	6/23	First	AgI	4
13	6/23	First	Sand	7
17	7/8	First	Sand	5
18	7/8	Second	AgI	5
19	7/11	First	AgI	3
20	7/19	First	Sand	3
22	7/23	First	AgI	9
23	7/24	First	Sand	4
24	7/25	First	Sand	8
25	7/25	Second	AgI	4
Totals	10		5 and 5	53

Table 36. Significance Tests on Unadjusted Variables

<i>Variable</i>	<i>Difference of means under AgI and sand</i>	<i>P-value cloud analysis</i>	<i>P-value unit analysis</i>	<i>P-value re-randomization</i>
Predictor				
CPmndia ^b	-1.18	.080	.295	.176
CPHrp10 ^b	-0.76	.390	.491	.262
CPMx2 ^b	-8.86	.114	.413	.207
FECpt ^b	-2.83	.292	.500	.258
NBuoy ^c	+0.035	.966	.977	.973
Buoy_Enh ^c	-0.041	.008	.113	.090
Mean_VW ^c	-1.652	.104	.402	.418
SWC_Frac ^c	-0.037	.665	.783	.648
pb ^a	+0.604	.261	.664	.352
tccl ^a	-0.458	.349	.718	.406
RC ^a	+14.54	.090	.513	.359
Response				
MaxH10	-2.12	.002	.009	.043
MaxA10	-23.05	.143	.191	.133
MaxZ	-4.13	.287	.480	.289
MXCPdH10	-2.23	.003	.052	.121
MCXPdA10	-9.06	.509	.458	.289
MXCPdZ	+1.17	.794	.888	.777
CPMXtMxA	-1.72	.580	.561	.477
FEMXtMxA	-4.56	.106	.044	.074

Notes: The predictor variables are defined in appendixes A, B, and C, respectively.
The response variables are defined in appendix B.

Table 37. Significance Tests on Responses Adjusted for Predictor e

<i>Variable</i>	<i>Adjusted difference of means under AgI and sand</i>	<i>P-value unit analysis</i>	<i>P-value re-randomization</i>
MaxH10	-1.81	.051	.148
MaxA10	-8.23	.652	.535
MaxZ	+3.03	.554	.551
MXCPdH10	-1.70	.1992	.254
MCXPdA10	-8.98	.560	.434
MXCPdZ	-4.99	.599	.484
CPMXtMxA	-2.80	.448	.438
FEMXtMxA	-2.35	.242	.2737

Notes: The variables are defined in appendix B.

Table 38. Significance Tests on Responses Adjusted for Predictor v

<i>Variable</i>	<i>Adjusted difference of means under AgI and sand</i>	<i>P-value unit analysis</i>	<i>P-value rerandomization</i>
MaxH10	-1.79	.010	.062
MaxA10	-33.32	.102	.172
MaxZ	+1.34	.798	.234
MXCPdH10	-1.84	.036	.172
MCXPdA10	-8.52	.4226	.734
MXCPdZ	+4.82	.5311	.277
CPMXtMxA	-0.43	.870	.953
FEMXtMxA	-4.56	.079	.074

Notes: The variables are defined in appendix B.

7. COMPARISON OF CLOUD SEEDING RESULTS FROM ILLINOIS AND TEXAS

by
Nancy E. Westcott

Introduction

Recent, similar weather modification projects were conducted in Illinois and Texas. Both sought to determine if a seeding effect could be distinguished in warm-season convective clouds and in ensuing cloud systems. The Precipitation Augmentation for Crops Experiment carried out two field programs in east-central Illinois, one in 1986 and one in 1989 (Changnon et al., 1991a). The Southwest Texas Cooperative Experiment of Texas and Oklahoma (SWCP) carried out field programs in west Texas in 1986, 1987 (Rosenfeld and Woodley, 1989), 1989, and 1990. This chapter compares the cloud characteristics of the two geographic areas, identifies the similarities and differences in the design and evaluation of these two projects, and discusses their results. The Texas results are used to help interpret the Illinois findings. Discussion will focus on individual cloud and echo-core behaviors and areal rainfall estimates for the multicelled systems in which the individual clouds were treated. The results of the PACE 1989 field year and the SWCP 1987 field year will be emphasized. Most of the details concerning SWCP were determined from Rosenfeld and Woodley (1989), hereafter referred to as "RW89."

Experimental Design, Data, and Analysis

Project Design

Both PACE 1989 and SWCP 1987 were randomized cloud seeding experiments. While individual clouds were sampled, the projects' experimental units were essentially circles moving with time and containing a multicelled cloud system, rather than individual clouds. A single treatment type was applied to the clouds in each experimental unit, and all clouds within an experimental unit were considered potential targets. In Texas, the experimental unit was a moving circle with a 25-km radius centered on the "qualification cloud" (RW89). It was surrounded by a 10-km buffer zone. In Illinois, the unit was a moving circle with a 28-km radius, centered on the geometric mean position of all the treated clouds in the unit (see figure 3). Randomization in both experiments was based on the experimental unit, while the primary cloud analysis emphasized the behavior of the individual echo cores within it.

The dynamic seeding hypothesis was the basis of both projects. This hypothesis starts with the concept of enhancing the vertical growth of individual clouds through the release of latent heat by the rapid freezing of supercooled water. In later

steps, this enhancement should enlarge the horizontal extent of a cloud system, ultimately leading to increased precipitation (Changnon et al., 1991a; RW89). The limited results of the 1986 Illinois experiment suggested that the buoyancy added to the cloud tower might reduce the net deceleration of the updraft in many cases; on the other hand, it also accelerated the updraft in a few cases (Politovich and Reinking, 1987; Czys, 1991; Westcott, 1990). In addition to updraft enhancements, the invigorated cloud would presumably have enhanced downdrafts, helping to trigger new neighbor growth. Thus, the cloud system would be expanded through the growth of more clouds and more cloud mergers.

The dynamic seeding hypothesis is based on the premise that the subject clouds contain adequate supercooled water and low ice concentrations. Thus, both the Texas and Illinois projects required initial sampling of a candidate cloud to determine if the clouds in the area were suitable for treatment. The "initial qualification" cloud was required to have cloud liquid water in excess of 0.5 grams per cubic meter (g m^{-3}), a moderate updraft, and a top extending to about -10°C or about 6 km above ground level (AGL). In Texas a peak updraft speed of $> 5 \text{ ms}^{-1}$ was desired, and in Illinois (RW89) an updraft of 2 to 4 ms^{-1} was preferred (Changnon et al., 1991a). Subsequent cloud treatments in the experimental unit were made at about 6 km AGL and temperatures of -8 to -12°C . Twenty-gram AgI flares were ejected from the aircraft into the updraft regions of clouds. In Illinois, placebo sand flares were dropped into control clouds. In Texas, the control clouds were sampled by the aircraft, but no placebo flares were released.

Properties of the clouds in Illinois and Texas at the time of treatment are presented in table 39, along with the mean number of flares ejected into the clouds. Liquid cloud water in both projects was measured using a Johnson-Williams Hot Wire Meter. The Illinois AgI-treated clouds had greater maximum liquid water content at treatment than both the Illinois control clouds and the Texas clouds. But the Illinois control clouds had slightly more than the Texas control clouds. The Illinois AgI-treated clouds had mean maximum updraft values comparable to those in Texas, but the Illinois control clouds had larger maximum updraft speeds than those in Texas. In comparing the time in updraft to the time in cloud, it appears that the Illinois AgI-treated clouds had less updraft per cloud than the Illinois control clouds.

On average, the Illinois AgI-treated clouds received flares every 6.8 seconds, and the control clouds got sand flares every 8.0 seconds. In Texas, the AgI-treated clouds received flares

about every 4.4 seconds, and RW89 estimated that the control clouds would have received flares about every 3.3 seconds, making the Texas seeding rate about 50 percent greater than that in Illinois. The intention was to deposit the seeding material into updraftair. If all of the flares were dropped into updraftair, then in the mean, the Illinois and Texas updrafts received AgI-treated flares every 2.2 seconds, the Illinois control updrafts every 3.7 seconds, and the Texas control updrafts every 1.8 seconds. In Illinois about two-thirds of the flares were dropped into the updrafts (chapter 2). If one considers the whole cloud, the Texas seeding rates were larger. However, the types of flares used were different. The flares used in Illinois in 1989 were obtained from the Weather Modification Group, and laboratory tests performed at Colorado State University showed them to be two to three times more effective in producing ice nuclei than those used in Texas (Personal communication, R.P. Sellers, Weather Modification Group, Alberta, Canada).

Thus, for the clouds sampled during both experiments, the maximum cloud water content values and maximum updraft speeds were generally comparable, and the clouds in both Texas and Illinois seem to have met the physical criteria required by the dynamic seeding hypothesis. If only the approximate number of flares dropped in the cloud updrafts is considered, the number of flares ejected is also comparable.

Distinctions between the Designs of the Projects

While the basic goals and hypotheses of the Illinois and Texas projects were quite similar, there were some differences in operational procedures, and these might have impacted the results. These distinctions probably are in large part a result of climatological differences.

Based on historical cloud studies, the Illinois experiment was divided into two parts, a large cloud and a small cloud experiment, each with a separate randomization scheme (Changnon et al., 1989, 1991a). The weather conditions on days with large clouds and those with small clouds were sufficiently different to believe that the clouds could react differently to AgI treatment, and that a seeding effect reflected in the height of the cores would be particularly difficult to detect. In the 1989 field season, data were collected from 25 experimental units that included 15 large cloud units on 16 days between May 15 and July 31. Three of these units were beyond useful radar range, so only 12 large cloud units could be compared with 15 experimental units in Texas. In Illinois, no two units on a given flight could receive the same treatment. On three of the eight days with large clouds, more than one unit was treated, two different treatment types were deployed.

In Texas, no blocking was done based on weather conditions. The 15 experimental units occurred on nine days between June 1 and August 15, 1987. Five of the days had two or more units, and on three of them, both a control and an AgI treatment were applied. On one other day two units received AgI flares, and on the other day the two units were not seeded. In both Texas

(RW89) and Illinois (Westcott, 1990; chapter 4), it has been found that clouds vary within a single day as much as they do from day to day. Thus treating two units with two different materials on one day does not necessarily provide comparable seeding conditions for a control and seed comparison (Changnon et al., 1991b; Czyns et al., 1992).

The Texas design stipulated that no echo top could exceed 10 km AGL within the area of the potential experimental unit prior to the first treatment. The objective of this rule was to reduce the impact of larger systems on the treated cores. In Illinois there was no such restriction, so that readily accessible, common storm systems would be treated. In 7 of the 12 Illinois units, a 10-km echo top existed within 25 km of the first treated core. However, no difference was found between the echo-core properties of the clouds with or without a 10-km echo top nearby. For all Illinois experimental units sometime during the treatment period, at least one of the treated cores was within 25 km of an echo top ≥ 10 km.

In Texas, it was further stipulated that the first treated cloud must be at least 40 km away from echoes with reflectivities of ≥ 50 dBZ. In Illinois, earlier field programs found that high reflectivities could be associated with small to moderate cloud systems, and it was believed that such a limitation was too restrictive. This Texas-Illinois difference may reflect a major difference in summertime conditions that produce clouds with tops > 10 km. However, not enough information is currently available to ascertain a climatological difference. For safety reasons, seeding in Illinois was terminated within 95 km of a severe weather warning area, or if the warning area was within the same convective system even if the clouds were farther than 95 km away. This rule reduces the number of candidate events by 35 percent (Changnon, 1993).

Evaluation Methodology

Evaluation of the results of both projects was based primarily on radar reflectivity measurements. The CHILL 10-cm radar was employed in the 1989 Illinois project. The analyzed data were based on a minimum reflectivity threshold of 10 dBZ. The data were interpolated to 1 x 1 -km constant-altitude plane-position indicator displays (CAPPIS) and from 1 to 19 km in altitude. The echo-core data were flagged using an interactive core tracking program, and all echo information was extrapolated on the fly from the interpolated grids. The volume scans were of variable length, ranging from 1.5 to 4 minutes. Echoes included in the study were within 110 km of the radar.

In Texas, the Sky water 5-cm radar was used, and attenuation and height corrections were applied to the data. A 12-dBZ minimum reflectivity threshold was applied to the data. A complete volume scan of the whole target area was made every 5 minutes. Seven levels of echo data were examined: the lowest elevation scan, a cloud base scan, and CAPPIS at elevations of 3.5, 5.5, 7.5, 10, and 12.5 km. In addition, the echo-top and base

heights were recorded, as well as the value of maximum reflectivity in the vertical cross section and the altitude of the reflectivity maximum.

In both Illinois and Texas, the aircraft positions were located on the radar fields using Loran-C positioning information from aircraft navigational systems. In Illinois, the Loran-C measurements appeared to position the aircraft within 1 to 2 km of the target echo core, although a Radar Aircraft Tracking System (RATS) was also used to locate the aircraft. In Illinois several clear air flights were conducted during which the aircraft was "painted" by radar to intercompare radar, LORAN, and RATS positioning. In Texas, VHF omni-directional range/distance measuring equipment (VOR/DME) readings were used to provide backup location measurements.

Definitions of Echo Cores and Echo Merging

Both programs were designed to examine individual clouds, many of which were part of multicelled systems. In order to analyze the cloud echo data, it was necessary to assume that the individual radar cores nearest to the treated cloud were associated with the visible cloud. In the early stages of cloud growth, this is considered to be a safe assumption (Kingmill and Wakamoto, 1991; Knight and Miller, 1992). A comparison of the Illinois aircraft locations with the radar echo locations supported this basic assumption, at least in the upper levels of the radar echoes, where all cloud passes were within 2 km of a core. The next step in the analysis procedure was to track the treated echoes over time.

In Illinois, the cores were first identified at their upper levels at the time of treatment. Then they were examined through all heights at the time of treatment. Then they were tracked backward in time to the first echo, and then forward in time until they could no longer be identified or until they dissipated. Many radar cores were already merged with another echo at the time of treatment (78 percent); and even at the time of first echo, 72 percent of the treated cores were joined to an adjacent echo. For 69 percent of the cores merged at first echo (50 percent of all cores), the echo-core base could not be distinguished from the parent echo.

At first echo, the Illinois cores were classified as isolated, loosely joined, or strongly merged to assist in modeling echo growth of the more complex cores. A schematic portrayal of these classifications is given in figure 36. All three classes of cores were sampled during most experimental units, but the loosely joined cores were more typical of frontal days with moderate to strong shear, while the strongly merged cores were more common on the weak shear air-mass days (chapter 4).

The loosely joined core was typically connected at a few locations with another echo, but its base and top were clearly defined. The strongly merged core appeared as a bulge on an existing echo; only later in its history, perhaps only for 5 to 10 minutes, was it clearly defined through its entire height. These cores often were terminated just after peaks in maximum

reflectivity and area were attained at the surface. Tracking was discontinued if the cores could no longer be identified through most levels, and after they had reached maximum height, area, and reflectivity. The Illinois cloud seeding results were briefly examined with regard to the merger type. While the classification of cores aided tracking efforts, little difference in subsequent echo behavior was attributable to the first echo being loosely joined or strongly merged.

In the Texas experiment, convective cells were tracked, and like the Illinois echo cores, the cells were representative of individual clouds. The Texas cells were defined and tracked using data at cloud base. Reflectivity data above the cores at cloud base were examined, but not used in tracking decisions.

Tracking Methods

In Illinois, an interactive core tracking program was used by a meteorologist to trace the histories of the echo cores (Changnon et al., 1990, 1991b). The ICORT program utilized three-dimensional interpolated reflectivity data. A reflectivity field for a given height and time was displayed on a computer terminal screen, and keystrokes were used to rapidly display reflectivity fields at previous and subsequent times, and at higher and lower elevations. One could quickly move from one echo to another on the screen, compute cell motions, and identify the treated cores. The flagged echo-core data were later accessed by other computer software to calculate echo-core properties.

In Texas, a computerized tracking program was used to trace the history of the echo cores (Rosenfeld, 1987). Merging of echo cores also was a problem for tracking echo histories in Texas. Two tracking procedures were developed, at least in part to address the merger problem. The short-track method tracked cells until they dissipated or merged with other cells (at the cloud-base level). This method worked well for cells that could be tracked through most of their lifetime. About 30 percent of the short-track cores lost their identities by merging or splitting within 5 minutes of their first detection by radar.

The Illinois echo-tracking procedure and the Texas short-track method are similar in that they measured the individual cores through what is considered to be a period comparable to the life of individual cloud cells (Byers and Braham, 1949; Kingmill and Wakamoto, 1991). Both methods discontinued tracking the cores when they merged with an adjacent echo to the extent that the core was no longer identifiable.

In Texas, as in Illinois, many cells merged with their neighbors before the echo system achieved its peak height, area, reflectivity, and rainfall rate. A long-track method was developed to extend the tracking of the short-track cells through some or all of the cells with which they subsequently merged. The Texas cores were tracked until they disappeared off the radar scope, in some cases for two to three hours. The cell histories were discontinued when a running mean rainfall reached a minimum at the same time the cell merged or split. One

difficulty with this method is that when two or more short-track cells merged into one long-track cell, the ensuing portion of the cell history was appended to both of the merging short-track cells. Nevertheless, the long-track method appears appropriate for cloud seeding evaluation in that it may account for more of the treatment effect if seeding material is spread within a multicelled system. However, the method probably does not address single cloud cells.

Thus, the Illinois clouds will be compared with the Texas short-track cells, although the long-track results also will be discussed. In spite of certain differences that exist in the echo analysis of the two projects, the similarities in the objectives, cloud types, designs, and evaluations provide a meaningful basis for comparison of the results.

Sample Size

During the 1987 Texas field experiment, 115 clouds were penetrated by aircraft, identified in the radar data, and subsequently tracked. Some of these did not meet the treatment requirements and did not receive AgI flares or simulated treatment. Thus, there were 95 short-track cells and 98 long-track cells.

During the 1989 Illinois field program, 81 clouds were penetrated and treated, but only 67 clouds were tracked. Four clouds were treated but never echoed. The radar appeared to alias four additional clouds when the airplane passed through the edge of a large parent storm, so that no individual core could ever be identified. No tracking was performed on these four clouds. On six occasions, clouds were penetrated twice and received second treatments.

Echo Characteristics at Treatment

In Texas, the data were analyzed as a function of 1) the number of flares dropped and 2) cell age at treatment. Results of a similar evaluation of the Florida FACE II echo data had indicated that one could expect the largest seeding effect when the youngest, most vigorous clouds received the most treatment (Gagin et al., 1986b). Most Texas clouds were treated within 5 minutes of first echo (figure 37). Values in table 40 show that about half (48 to 59 percent) of all treated cores in Texas were treated with more than eight flares, and nearly half (41 to 49 percent) were treated early with more than eight flares.

In Illinois, 47 to 57 percent of the cores were sampled within 5 minutes of first echo detection, as compared to 88 to 91 percent for the Texas short-track cells. Very few Illinois cores (9 to 14 percent) were treated with more than eight flares. And only two Illinois cores were treated within 5 minutes of first echo with more than eight flares. Thus, not enough Illinois cases were available to compare seeding effects of the young, heavily seeded cores.

In Texas, an echo was present at treatment time for all cells. No echo was present 15 minutes before treatment, and only 10

to 15 percent of the cells were observed prior to treatment. In contrast, five of 67 Illinois echo cores were first observed only after treatment, and four other treated clouds never echoed. These nine clouds occurred on frontal days (chapter 4). Even more striking is the fact that many Illinois cores (15 percent) were observed more than 15 minutes prior to treatment. Most of these occurred in experimental units associated with air-mass convection (chapter 4). A third of the Illinois cores were observed more than 10 minutes prior to treatment. This corroborates the 1986 observation that Illinois clouds often form low in the atmosphere and grow upward, likely because of the importance of coalescence in the growth of precipitation. By the time an Illinois cloud is treated at the -10°C level, it often already contains high reflectivities at mid-levels, though usually below the flight level (Westcott, 1990).

The Illinois cores and the Texas short-track cells were tracked for similar lengths of time following treatment. About 50 percent of the cores were still being tracked 20 minutes after treatment, and about 33 percent of the cores at 30 minutes (figure 37). This further suggests that the Texas short-track and the Illinois tracked cores may be more representative of individual clouds. The distinctions in echo age at the time of treatment between the Illinois and Texas cores could result from climatological differences in ambient weather conditions, or they could be due to differences in the core definitions and echo tracking methods. While the mean values of the echo-core dimensions from the Texas short-track data and the Illinois ICORT data are generally comparable (tables 41 and 42), the particulars of echo growth were difficult to compare.

The Texas long-track method approximately doubled the time that an echo was tracked, again suggesting that the long-track cells encompassed several cores. The long-track clouds may have benefited from the greater period for the seeding material to mix into the cloud system, and they could be suitable units for studying treatment effects in Texas. It is not clear that the long-track method would be appropriate in Illinois, however. The Illinois air-mass cores, for example, generally formed below or straddled the freezing level and then grew upward. Often they were strongly merged even at the time of first echo. Nevertheless, the long-track method would probably have extended the life of the Illinois echo cores both forward and backward in time. While this would probably provide useful information regarding the life of the echo system, extending the life backward in time would have made the seeding effects more difficult to detect. That is, the individual first echo times of the strongly merged cores would probably be invalid if they were subjected to the long-track method, because they would probably be for the first echo in the complex rather than for the treated clouds.

Assessment of Sampling Bias

Both projects attempted to determine if the AgI-treated cores and the controls were similar in character at the time of

treatment. In Texas, a vigor index was used. Vigor, defined as the product of updraft speed and hot wire cloud liquid water, was computed for each second of an aircraft pass. The untreated qualification clouds from the AgI-treated units in Texas were found to be more vigorous than the untreated clouds from the Texas control units. The treated clouds from the AgI-treated units were slightly less vigorous than those from the control units. It was concluded that no human biases entered into the conduct of the experiment. This was an important finding in that the treatment was made known to the seeding operators after an experimental unit was declared.

In Illinois, the control and AgI-treated cores were found to be markedly different at the time of treatment. The control cores were significantly larger than the AgI-treated cores. This bias occurred in spite of the facts that treatment decisions were made known only after all of the basic radar and aircraft analyses had been performed (Czys et al., 1992), and that the units were blocked by the expected height of the clouds within it.

In Illinois, two separate studies have attempted to eliminate the bias from the cloud sample by selecting like groups of echoes. A seedability index was computed, taking into account the microphysical properties of the clouds at treatment, the radar properties of the clouds before and at the time of treatment, and the synoptic environment at 0700 CDT (chapter 5). The SI is the percentage of 20 criteria that fell into a range of values indicating a favorable chance of continued cloud growth. Stratifying the data by the SI appeared to eliminate the natural bias at the time of treatment, though it was found that fewer AgI-treated cores had large SI values. Additionally, the data were partitioned by synoptic weather conditions to attempt to identify the bias and to select like populations of clouds. It was found that the bias was most apparent on the frontal days. On the air-mass days, the bias was still present but not as pronounced at the time of treatment (chapter 4).

In this analysis, no attempt was made to normalize the cloud differences at treatment. Thus, in examining the following results, it must be remembered that at the time of treatment, the Illinois control cores were generally larger in diameter than the AgI-treated cores.

Comparison of Echo Responses to Treatment

The echo-core data from Illinois and Texas were examined in two ways. First, composite time plots of the control and AgI-treated cores were constructed for the core height, area, reflectivity, and rain flux histories. All of the tracked echo-core data were incorporated into these plots. For the Illinois data, this includes values beyond the time of peak height, area, and reflectivity and are presented below.

Second, the mean values of the six Texas response variables examined in RW89 were compared. These variables are described in table 4.1, and the closest corresponding variables computed for the 1989 Illinois evaluation are described in table 4.2. There were two major differences in parameter definitions:

1. For the Illinois study, the life span of the echo core and the time over which total rain volumes were summed were reconciled to a common point in time for each core. The total duration of the echo core was taken from the time of first echo to the time at which the echo reached its maximum areal extent, even though the echo core often was tracked beyond this time. The total rain volume was computed through the time of the maximum rain flux. This was done so that all echo cores were examined in the same fashion, regardless of how long an individual core could be identified. The mean duration of the Illinois cores was 7 minutes less than that of the Texas short-track cores.
2. The second difference in the parameters is related to the location of the peak values of area and reflectivity in the echo core. The maximum reflectivity and area were computed at the cloud-base level for the Texas cores, but the maximum value could be located at any height for the Illinois cores.

Composite Plots

Based on the entire tracked history, data from Illinois show that the mean heights and horizontal extents of the control cores were larger than for the AgI-treated cores 6 minutes prior to treatment (figure 38). The height of the control cores increased more rapidly than that of the AgI-treated cores. After treatment, the rate of increase of height diminished for both types of composited cores. However, the mean control core reached its peak height about 20 minutes after treatment, while the AgI-treated core attained its peak height about 6 minutes following treatment. The horizontal area of the control and AgI-treated cores increased in extent at about the same rate. However, the composited control core, larger in area even 9 minutes prior to treatment, remained larger than the AgI-treated core. The control core typically reached its peak area for the first time about 20 minutes after treatment, and the AgI core about 12 minutes after treatment. Values beyond 24 minutes were based on only a few cores.

The mean age of the Illinois control cores (11 minutes) was greater than that of the AgI-treated cores (6 minutes) at the time of treatment, but their relative ages seemed to have had little effect on the treatment outcome. The percentage of AgI-treated cores was largest at the time of treatment, and the largest percentage of control cores present occurred 6 minutes after treatment. The older control cores might have been expected to dissipate earlier, but instead, they lasted longer than the AgI-treated cores. A stratification of echo cores by their age at treatment (not shown) indicated that differences between the AgI-treated and control cores were largest for those cores older than 5 minutes at the time of treatment. However, even for those cores younger than 5 minutes at the time of treatment, the control cores were still larger than the AgI-treated cores.

The composite plots of the Texas short-track cores (figure 5 in RW89) show that in terms of the cell height, area, and rain

flux histories, the AgI-treated and control cells remained very similar 10 minutes beyond treatment time, when the control cells reached their peak areas and rain fluxes. The AgI-treated cells subsequently grew wider and produced more rain. After 20 minutes, the AgI-treated cells became taller and more reflective. As the AgI-treated cells increased in area, their rainfall contribution also increased. Additionally, more control cells were present up to 25 minutes after treatment; after 25 minutes, more AgI-treated cells remained. The longer duration of the larger AgI-treated cells obviously contributed to the larger rainfall volume as well.

The Texas long-track plots showed a similar trend in values (figure 6 in RW89). After 5 to 10 minutes, the AgI-treated and control cells began to diverge in behavior, although their areas and rain flux curves remained very similar until 15 minutes after treatment, when the control cores reached their peak values. In terms of height, the AgI-treated and control cells were very similar until 25 minutes beyond treatment. The maximum reflectivity values for the composited cells continued to be very similar until 45 minutes after treatment. The larger areas of the composited AgI-treated cells again appears to have contributed to larger rain volumes. Later in the cell history, the AgI-treated cells became taller than the control cells.

The experimental results from the composited plots for the Illinois and the Texas short-track method are contrasted in figure 39 for the period when most cells were sampled. The height, area, and rain flux plots show that in the Texas experiment, the AgI-treated cores grew steadily larger than the control clouds, beginning about 10 minutes after treatment. The differences are smaller and opposite to the Illinois cores. The Illinois sand-treated cores, though generally larger than the Illinois AgI-treated cores, also became steadily larger beginning about 10 minutes after treatment.

Mean Values

If only the mean values of the response variables of the Illinois cores were examined, one would infer a negative seeding effect (table 42). However, as shown in Changnon et al. (1991b), Czys et al. (1992), in chapters 2, 4, and 5 of this report, and by the composite plots, a bias existed at the time of treatment so that the control cores were already larger than the AgI-treated cores. However, it remains clear that the effects of cloud seeding on maximum echo characteristics did not overcome the bias in the Illinois sample.

The results of the two Illinois studies that attempted to eliminate the bias at the time of treatment also detected no appreciable seeding effect. In looking at cores with updrafts and high seedability values (chapter 5), the means and distributions of the maximum echo tops, maximum echo areas, and durations of the control cores were found to shift toward larger values. Mean values for the other response variables were also larger for the control cores, but the differences were not statistically significant.

In looking at the cores that occurred during air-mass conditions (chapter 4), the control clouds were found to be slightly larger at treatment. The air-mass results were mixed: the control cores were taller, wider, and longer lasting than the AgI-treated cores, but they also had lower maximum rain fluxes and total rain volumes.

In all Illinois stratifications, the control cores achieved larger mean echo heights than did the AgI-treated cores. The height difference was present in the sample of 67 Illinois cores from 1989, whether the echo top was defined by the 20-, 35-, or 10-dBZ contour. This suggests that for Illinois, the height difference was not caused by limitations of the radar in measuring small particles, as suggested by RW89. However, why the sand-treated clouds were taller throughout their lifetime remains unexplained.

While temporal values for the Texas short-track cells indicate that the AgI-treated cells had larger area and maximum rain flux values beginning 10 minutes after treatment, the overall mean values do not show the same difference in peak values (table 42). In the mean, the short-track cells' peak height, area, reflectivity, rain flux, and duration were about the same for both treatments. Only the total rain volumes of the AgI-treated cells were larger. However, when the early, more heavily treated cells (AgI) are considered alone, their mean areas, durations, and maximum rain fluxes were larger (table 43).

Examination of the long-track results reveals that the peak height and reflectivity values were the same for the control and the AgI-treated cells (table 42). However, the AgI-treated cells lasted 15 to 20 minutes longer, attained larger peak areal coverages, and had larger peak rain fluxes than the control cells. The longer durations, larger areas, and greater maximum rain flux values together resulted in larger total rain volumes for the long-track cells. The differences between the control and AgI-treated Texas cells in area, duration, and peak rain flux became larger and more significant when the young, heavily treated cells were examined alone (table 44). Additionally, the number of mergers of a long-track core with another core were examined. It was found that the AgI-treated long-track cells were more likely to merge than the control cells. Merging is one way in which echoes expand in area. The cells treated with more (AgI) flares, which were likely to be larger at the time of treatment, were found to merge even more than the control cells that received more than eight flares.

The results of the Texas short-track method suggest that at least 10 minutes are required for the seeding effect to become apparent on the increased areal extent of individual clouds for the AgI-treated population as a whole. The long-track method suggests that a seeding effect transferred to adjacent cells becomes apparent 5 to 10 minutes later, some 15 to 25 minutes after treatment. Both methods produced small differences in height that became apparent 20 and 45 minutes after treatment, well after the AgI-treated and control area values began to diverge. The mean values indicated no difference in height for either of the Texas tracking methods. Thus, neither the Illinois

nor the Texas project supported the initial steps of the seeding hypothesis, in which the clouds were expected to increase in height due to the release of latent heat as a result of seeding.

Comparison of Experimental Unit Rainfall

As stated previously, the Illinois and Texas programs also were designed to examine the rainfall properties of the experimental units. Because of the small samples sizes involved, the results must be treated with caution.

In Illinois, radar-estimated rainfall was computed for reflectivities ≥ 30 dBZ, using the Z/R relationship, in which $Z=300 R^{1.35}$ (Changnon et al., 1980). Reflectivities > 56 were set to 56 dBZ. Rainfall was computed for every volume scan. The data were accumulated in 15-minute intervals beginning 15 minutes before the first treatment (BT-15) to 90 minutes after the last treatment (ET + 90). After 90 minutes, the number of units with rainfall began to decrease rapidly. Rainfall also was accumulated between the time of the first and last treatments.

Only five of the AgI-treated units were included in the analysis, since no post-treatment radar data were available for one AgI-treated unit. The rainfall histories for the other units were considered to continue until the echoes dissipated or until 90 minutes after the last treatment. The Illinois radar-estimated rainfall data are shown in table 44. Because of the small sample, the number of experimental units that had an increase in rainfall volume from one period to the next is also indicated in table 45. The rainfall from one AgI-treated unit was underestimated, as the storm moved out of radar range 45 minutes after the end of treatment. Thus the AgI mean values are underestimated for periods beyond 45 minutes.

In Texas, a Z/R relationship of $383 R^{1.62}$ was used to compute rainfall (Smith et al., 1977). The experimental unit rainfall history in the 1987 Texas experiment was considered to continue until:

1. The treated system merged with other echoes from outside the unit.
2. One hour had passed.
3. The echoes dissipated.
4. The cloud system that contained the unit expanded to more than 100 km in horizontal extent.

From the data presented in RW89 and from additional data made available to us by Dr. William Woodley, rainfall totals were accumulated in 30-minute increments from the first qualification pass to 150 minutes after the qualification pass (table 46).

The average duration of the treatment periods in the Illinois experiment was 30 minutes, not including the qualification pass. In the six AgI-treated experimental units, 249 flares were dropped, for an average of 42 flares per experimental unit. A total of 404 AgI flares was ejected into the six 1987 Texas AgI-treated experimental units, resulting in an average of 67 flares

per experimental unit. The Texas treatment periods typically lasted 60 minutes. Thus, the Texas units were generally treated over a longer period of time and received more flares than the Illinois units.

As discussed in more detail in chapter 8, the accumulated rainfall values for the 1989 Illinois experiment indicated that on average, the AgI-treated units produced more rain than the control units, even before the time of treatment (table 44). Comparison of the mean values also shows that the amount of rain in the experimental unit increased during the first 30 minutes after treatment. The amount of rain decreased during the next half hour, and then increased again during the period 1.0 to 1.5 hours after treatment. Accumulated rainfall values in the extended network showed the same trend for the AgI-treated units. Table 45, however, shows that the mean values were dominated by heavy rainfall amounts in two of the five periods. The control units increased in rain volume during the 15 minutes following treatment, and rainfall values remained high through the next 15 minutes. A slight increase in rain was observed from 75 to 90 minutes after treatment. In the mean, the AgI-related rain values were larger than the sand-related values within the experimental units, but smaller when considering the network as a whole.

In Texas, during the first hour after the qualification pass, which was the mean length of the treatment period, the control units produced more rainfall in the mean (tables 46 and 47). Following this time, the AgI-treated units began to produce more rainfall than the control units, as is shown in the increasing sample size of units with accumulated rainfall greater than 10^5 m^3 (table 46). Overall, the 1987 Texas control units produced more rainfall than the AgI-treated units. Rainfall totals prior to the onset of treatment were not computed for the Texas units. This sample includes two AgI-treated and two control units that did not meet project criteria.

During the 1986, 1987, 1989, and 1990 Texas experiments, radar-estimated rainfall from 17 AgI-treated units and 17 control units was computed. Five units were excluded from this analysis since the rainfall integrations were cut off, and another five did not meet project criteria. This eliminated four of the seven units producing greater than 3×10^6 m^3 of rain overall. Data from the remaining 24 units are presented in tables 48 and 49. The AgI-treated units were observed to produce nearly twice as much rain as the control units during the period when treatment was first occurring. It is unknown if more rain had been occurring in the experimental unit area prior to the onset of treatment. The peak in mean AgI-treated unit rainfall accumulation came in the periods 60 to 90 minutes after the qualification pass. For the control units, the mean rainfall accumulation peaked from 90 to 120 minutes after the treatment pass. For both the AgI-treated and control units, only one or two of the twelve units increased in rainfall between the periods 60 to 90 and 90 to 120 minutes after treatment.

In summary, the five AgI-treated Illinois units produced more rain overall than the six control units. However, ancillary

data indicate that the AgI-treated units may have produced heavier rain regardless of treatment because heavier rain was occurring prior to treatment. While more rain occurred in the AgI-treated experimental units than in the control units, more rain overall occurred in the extended network during the control periods than during the AgI treatment periods. Thus, the data do not show clear evidence of a positive effect on rainfall. Nevertheless, the results indicate that in spite of the AgI-treated cores being smaller, and in spite of more rain in the control extended network, the AgI-treated units did produce more rain overall.

In Texas, the control units produced more rain overall in 1987, particularly during the treatment period. After the mean treatment period, the AgI-treated units began to produce more rain, however. Considering the Texas rainfall from four summer experiment seasons, the AgI-treated units produced more rain early and overall (table 48). As more rain was occurring early in the AgI-treated units, more rain might have been expected overall. In both Texas and in Illinois, the possibility of a positive seeding effect may be present. However, sufficient data are not available to provide explicit evidence of a positive treatment effect. Huff and Schickedanz (1970) estimated that some 500 storms would be required to obtain significance for a 20 percent increase in precipitation.

Conclusions

The results of two similar cloud seeding experiments, one based in central Illinois and one in west Texas, were compared to gain insight into the Illinois findings. The design and operation of the two experiments were similar. Both projects addressed the initial response of clouds to AgI seeding and the possibility of enhancing rainfall over an area roughly corresponding to that of mesoscale rain system. Several differences between the two projects may have affected the results. These include echo-core definitions and tracking approaches, seeding rates, operational criteria, climatological differences in cloud growth, and the conditions under which seeding was accomplished. However, these differences did not apparently materially affect the interpretation and comparison of echo-core behavior and rainfall results.

Cloud Effects

In Illinois, the initial response to treatment was masked by a bias in the data: the control cores were initially larger than the AgI-treated cores and remained so after treatment. Dynamic seeding did not overcome this initial difference; that is, after treatment the behavior of the AgI-treated cores did not differ from what might have been expected to occur naturally.

In Texas, when considering the cloud-scale results (short-track cells), there also was little evidence of a positive treatment effect on the total population of treated cells. However, a positive seeding effect was present in the mean values when only the clouds treated early and with many flares (thus large clouds) were considered. These amounted to about half of the

population of treated cells. The seeding effect on these cells was most obvious in terms of cell duration, area, peak rain flux, and total rain volume. The seeding effect was not observed in terms of echo height.

According to the dynamic seeding hypothesis, the height of the echo cores should increase due to enhanced buoyancy caused by the rapid release of latent heat from the rapid freezing of supercooled water. This was not observed in either experiment. If the most observable seeding effects are found 20 minutes after treatment, the earliest steps of the dynamic seeding hypothesis may be difficult to document with current technology and analysis tools.

Area Rainfall Effects

Radar-estimated rainfall values were examined using 11 experimental units in both Illinois and Texas. In Illinois, the AgI-treated units produced more rain on average than the control units. This result was influenced significantly by two of the five AgI-treated units. During these two units, heavy rain was occurring prior to treatment, and the extended network rainfall showed a similar trend in rainfall amounts for the corresponding periods. Thus, heavier rain might have been expected regardless of treatment. However, in the mean, heavier rain fell in the AgI-treated units in spite of the observation of larger seed-treated cores and larger rainfall values in the extended control network.

In Texas, the control experimental units produced more rain overall in 1987 than did the AgI-treated units, particularly during the treatment period. However, in the hour following the end of the average treatment period, the AgI-treated units produced more rain than the control units. In addition, the Texas long-track results suggest that seeding effects may become more apparent 20 minutes following treatment. The four seasons of Texas data indicate that the seeded units produced peak rainfall in the 30-minute period following treatment, and the control units in the period 60 minutes following treatment. The AgI-treated units produced more rain overall. Although the data available in Texas and Illinois are not sufficient to provide definitive evidence of a positive treatment effect on area rainfall, the results are more favorable than might be expected from the individual cloud studies.

Implications

These results have implications for future cloud seeding projects. First, in spite of design precautions in the Illinois study, a biased sample of clouds was drawn during a 2.5 month cloud seeding experiment. Even in Texas, only certain of the clouds (large clouds treated early) appeared to react positively to AgI treatment (~ 50 percent). This percentage of suitable clouds would be closer to 35 to 30 percent had the study included other clouds that were sampled but did not qualify for treatment according to the liquid water and updraft criteria. Thus, in both Illinois and Texas, it was difficult to select suitable

clouds in real time based on visual and penetration criteria.

The rain comparison was encouraging, particularly in light of the Illinois cloud-scale results. However, these results were based on a small sample of experimental units, and the sample size may have greatly influenced the results presented. More cases must be collected and studied in detail before the total effect of cloud seeding on areal rainfall can be determined. With the difficulties and costs involved in obtaining a large sample, it is unclear if the results of these studies warrant further experimentation.

The aircraft properties indicate that the Illinois and Texas clouds were both suitable for treatment based on the dynamic seeding hypothesis. Nevertheless, some differences in cloud properties between the Illinois and Texas regions may have led to differences in the response to treatment. Illinois had few cases of early and heavily treated cores. In fact, many were already merged at the time of treatment. It could be that the echo growth properties evidenced by the age of the echo at treatment were different, at least for this sample of clouds. Also in Illinois, an echo with reflectivities >40 dBZ was often present prior to treatment at altitudes below the flight level. This was not the case in Texas, where echoes generally formed at or just before the time of treatment. Some clouds in Illinois also were observed to form after treatment occurred. The variations in echo formation in Illinois is related in part to differences in synoptic weather conditions. The variation in Illinois echo-growth properties, as well as the complexity of individual echo-core growth, make it difficult to detect the response of the clouds to AgI seeding.

Another possible difference between the two studies could be the level of treatment. A comparison of seeding material concentrations per unit time was made. The Texas AgI-treated clouds received more flares overall and more flares per second than the Illinois clouds. The percentage of updraft area within the Illinois AgI-treated clouds was smaller than for the Texas clouds, however. If only the updraft area were considered, and assuming that most of the flares were ejected into updraft air,

then the number of flares per second was comparable in Illinois and Texas. More importantly, the Illinois flares were some two to three times more effective in producing ice nuclei, according to laboratory tests performed at Colorado State University. The Illinois aircraft scientist and pilot could visually observe a seeding signal (apparent glaciation of cloud material) during most experimental units (chapter 3). They believed that the clouds were not underseeded and in fact worried that in some instances they were overseeded. Project Whitetop (1960 to 1964 in Missouri) indicated that overseeding could occur (Braham, 1979; Flueck, 1971). Future work should examine the Illinois clouds in which second passes were made to determine if a treatment signal could be detected in the microphysical measurements and in echo-growth properties. The question of seeding amounts, at least for Illinois, needs to be addressed.

In yet another distinction, the Texas project selected only experimental units in which no cloud top exceeded 10 km within 25 km of the cloud selected. In Illinois, use of this rule would have greatly restricted the number of units. Over half of the PACE 89 units exceeded this 10-km limit. Even more restrictive would have been the Texas rule that no unit be declared within 40 km of a ≥ 50 -dBZ echo. Often, even the treated Illinois clouds had high reflectivities below the flight level, even at the time of treatment. This suggests that the cloud systems suitable for multicell rain system development in Illinois and Texas may be substantially different. Obviously, such results lead to concern over the transfer of seeding technologies among different climatological locations.

Thus in Illinois, the manner and concentration in which cloud seeding material is dispersed throughout a cloud system should be considered. Additionally, the failure to detect a difference in height soon after treatment is one indication that the dynamic seeding hypothesis should be reevaluated. Finally, the impact of the differences in cloud and storm properties on seeding effects, possibly through the use of numerical models, should be examined more thoroughly before embarking on further experimentation.

FIGURES AND TABLES FOR CHAPTER 7

Vertical Slice through Idealized Echo Cores

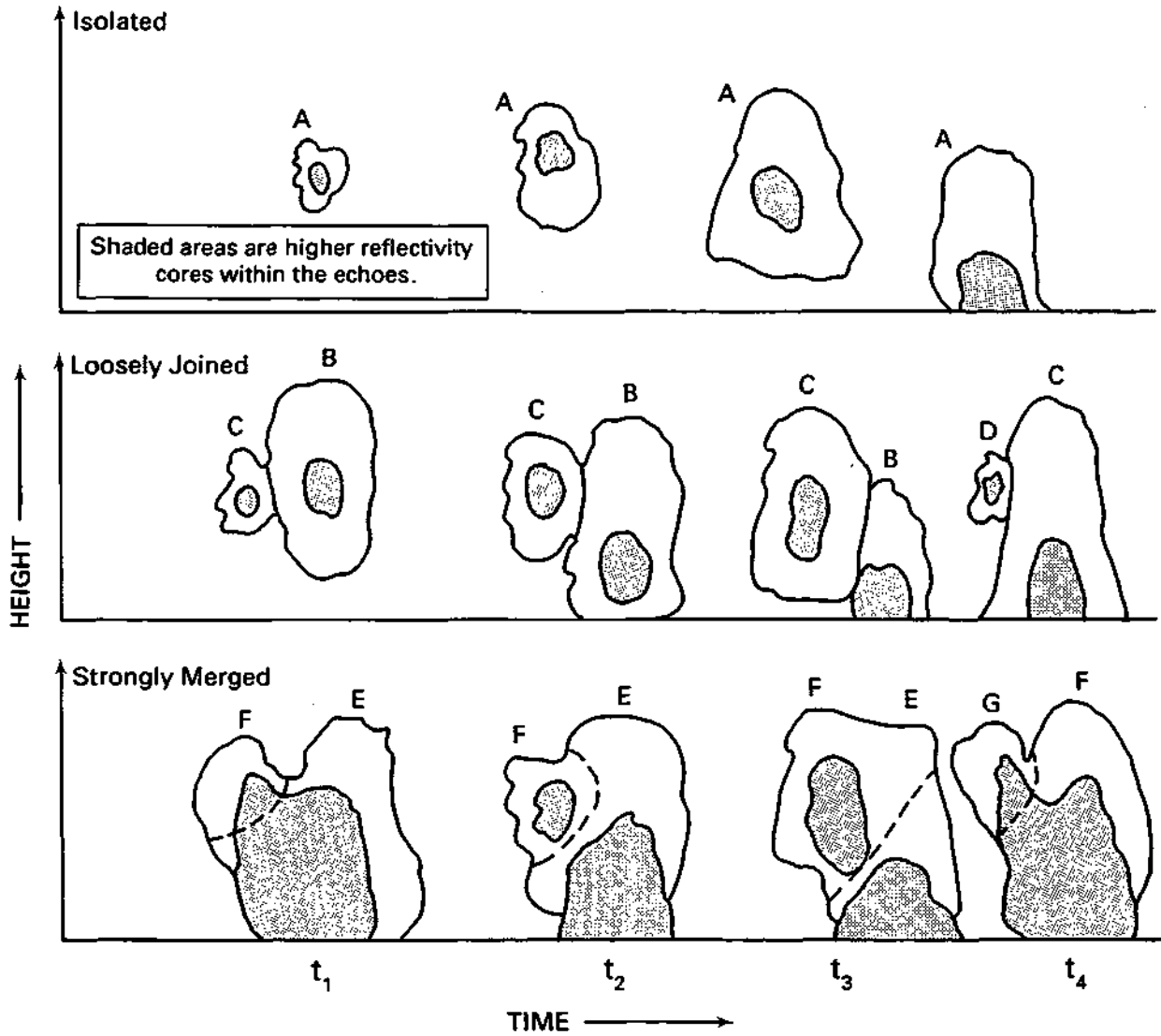


Figure 36. Schematic of typical Illinois echo cores during their lifetimes

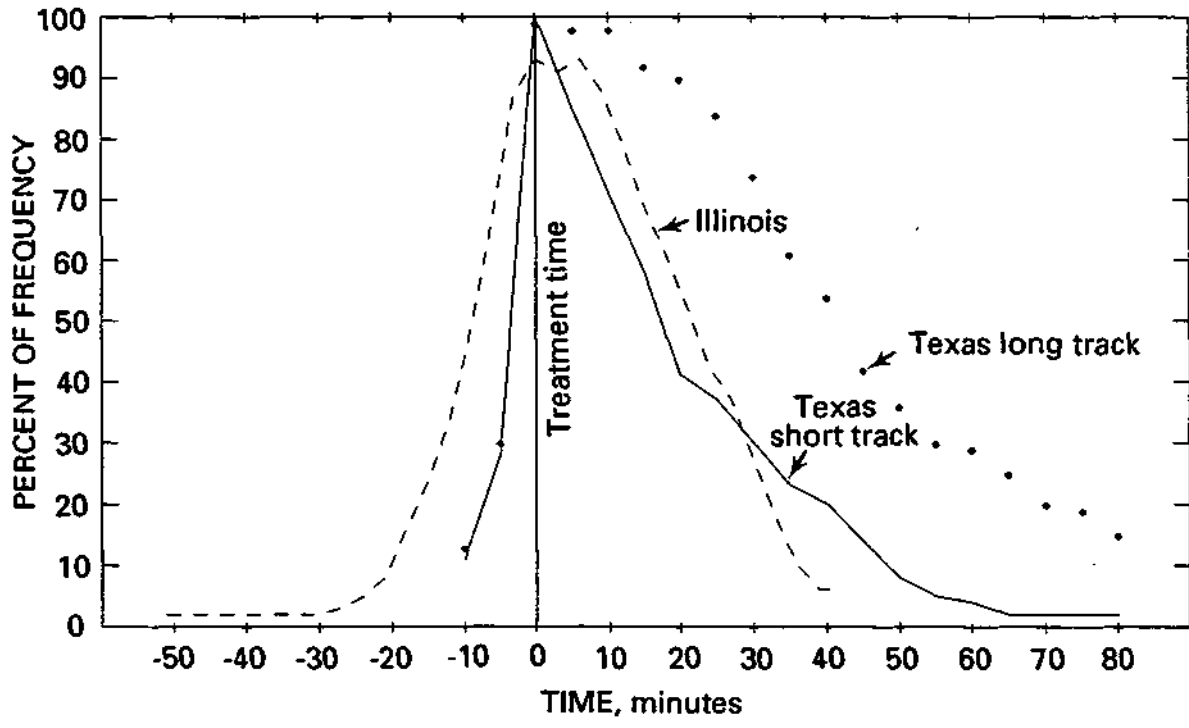


Figure 37. Percentage of frequency of treated and tracked echo cores for Illinois and Texas

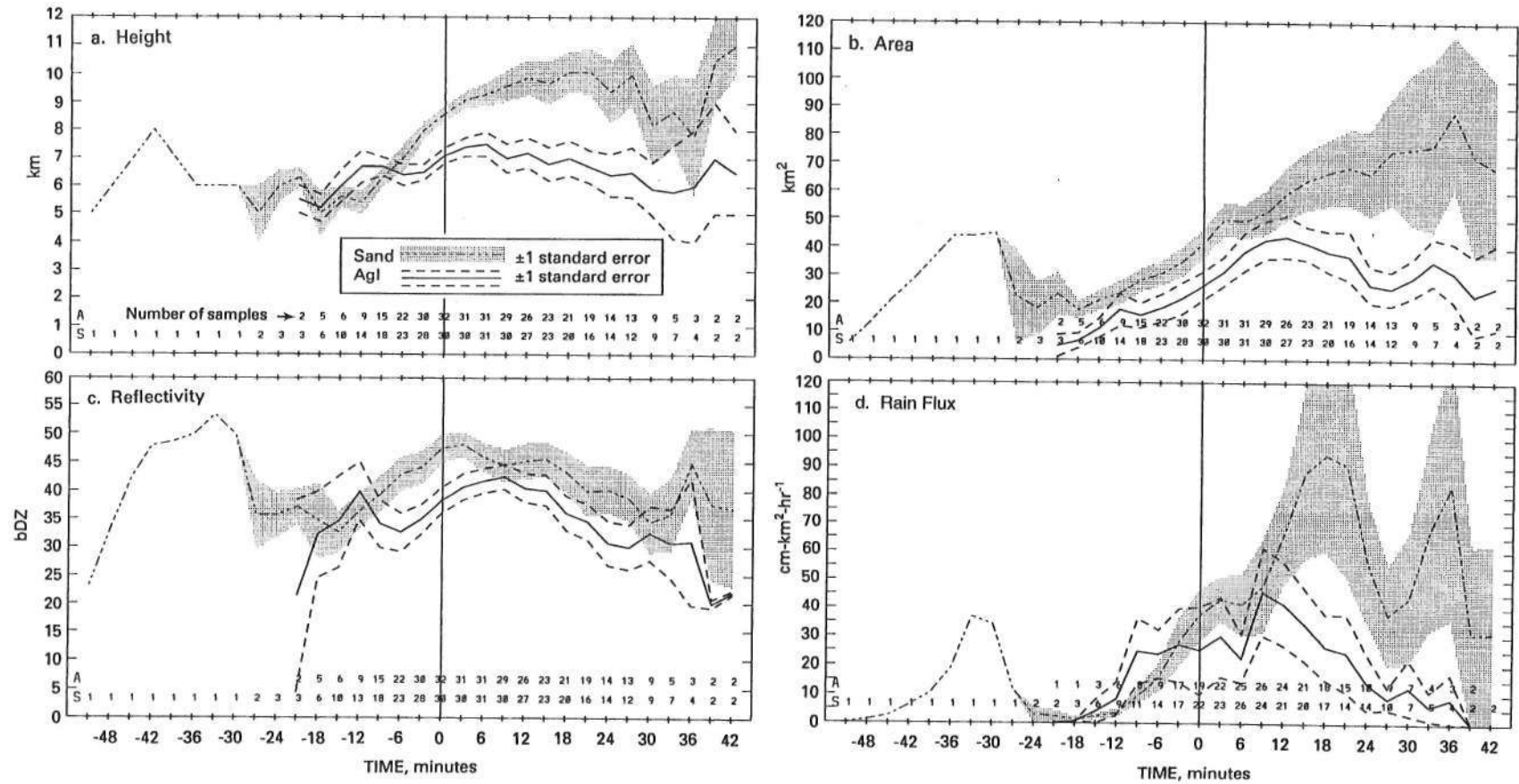


Figure 38. Mean echo-core heights, areas, maximum reflectivities, and rain volumes relative to the time of treatment for the total Illinois echo-core sample. Data are interpolated to 3-minute Intervals. Zero values are not included.

Table 39. Mean Cloud Properties at the Time of First Treatment for the Treated and Tracked PACE 1989 Clouds and the SWCP 1987 Clouds

<i>Property</i>		<i>Illinois (N=67)</i>		<i>Texas (N=124)</i>	
		<i>AgI</i>	<i>Sand</i>	<i>AgI</i>	<i>Sand</i>
Max_JWC ^c (gm ⁻³)	Sample	24	32	60	64
	Median	2.60	1.88	1.61	1.74
	Mean	2.38	1.97	1.68	1.67
	Stan dev	1.34	1.19	0.58	0.46
Max_VW (ms ⁻¹)	Sample	30	32	60	64
	Median	5.4	9.3	5.3	7.3
	Mean	7.2	11.3	6.1	7.3
	Standev	6.9	7.1	3.8	4.0
#_SECS ^o (sec)	Sample	30	32	60	64
	Median	11.0 (34.0)	18.5 (38.0)	15.5 (30.5)	15.0 (28.0)
	Mean	12.6 (38.8)	20.5 (40.0)	16.0 (32.8)	15.8 (29.4)
	Standev	10.9 (16.1)	12.7 (28.0)	10.2 (16.8)	9.2 (14.7)
C_fls flares	Sample	35	32	60	64
	Median	5.0	5.0	7.0 *	8.0
	Mean	5.7	5.5	7.5 *	8.9
	Stan dev	3.7	2.8	4.1 *	5.8

Notes: The cloud and updraft widths are expressed in terms of seconds in-cloud and seconds in updraft. The updraft durations are in parentheses.

* flare counts were included from a day in which only half the flares were ejected (RW89), and also includes passes in which no flares were dropped as the treatment criteria were not met.

In Illinois, the maximum updraft and liquid cloud water content data were unavailable for five clouds, and the max LWCD was unavailable for six other clouds without updrafts.

Variables are defined in appendix C.

Table 40. Percentage of Frequency of Cores Treated and Tracked in Dlinois and Texas

<i>Echo cores</i>	<i>AgI</i>	<u>Treatment</u> <i>Control/sand</i>
Total sample of treated and tracked echo cores		
Illinois ICORT method	44	48
Texas short-track method	46	49
Texas long-track method	35	32
a. Cores treated within 5 minutes of first echo		
Illinois ICORT method	57	47
Texas short-track method	91	88
Texas long-track method	87	86
b. Cores treated with more than 8 flares		
Illinois ICORT method	14	9
Texas short-track method	48	54
Texas long-track method	52	59
c. Cores treated early with more than 8 flares		
Illinois ICORT method	6	0
Texas short-track method	41	46
Texas long-track method	46	49

Notes: a = cores treated early.
b = cores treated with many flares.
c = cores treated early with many flares.

Table 41. Means, Standard Deviation, and P-values for the 67 Tracked Echoes, Illinois, 1989

	<i>AgI</i> <i>mean</i>	<i>Sand</i> <i>mean</i>	<i>AgI</i> <i>std dev</i>	<i>Control</i> <i>std dev</i>	<i>t</i>	<i>P-val</i>	<i>W</i>
Rvol	88.1	116.7	358.7	374.6	.385		.010
Hmax	8.1	10.6	2.0	2.5	.019		.019
Zmax	45.7	52.1	13.6	13.6	.087		.067
Amax	49.5	80.3	45.6	58.9	.019		.058
Dur	13.2	17.8	7.7	10.7	.010		.010
RVRmax	87.5	125.1	177.7	192.8	.471		.134
Sample	35	32					

Notes: P-values were computed for the student's *t*-test and Wilcoxon rank sum test from 208 rerandomized runs.

Dur = time in minutes from first echo to the time of maximum area of the echo core.

Hmax = maximum echo height (km AGL) of the core.

Zmax = maximum reflectivity (dBZ) in the echo core.

Amax = maximum horizontal area (km²) in the echo core.

RVRmax = maximum rainflux (10³m³ h-1) of the echo core, through the 1-km level.

Rvol = total rain volume yield (10³m³) of the echo core, through the time of the max rainflux.

Table 42. Means Values, Single Ratios, and Percentage of Probability of the Significance Levels for the Differences in the AgI and Control Cell Properties for the 1987 Texas project.

	<i>AgI</i>	<i>Texas short-track</i>			<i>AgI</i>	<i>Texas long-track</i>		
		<i>Control</i>	<i>SR</i>	<i>SL %</i>		<i>Control</i>	<i>SR</i>	<i>SL %</i>
Rvol	94.6	63.0	1.50	13.7	267.8	107.9	2.44	4.9
Hmax	8.5	9.0	0.95	53.7	10.5	10.3	1.03	36.4
Zmax	37.4	42.0	0.89	64.1	48.0	49.7	0.97	56.1
Amax	48.1	46.4	1.04	36.7	79.7	66.1	1.21	19.9
Dur	21.4	23.7	0.90	52.8	58.1	41.3	1.41	2.7
RVRmax	278.4	259.6	1.07	32.5	626.7	441.2	1.52	9.3
Sample	44	48			46	49		

Notes: SR - single ratios.

SL^x.01 = P-values.

Dur = time in minutes after the first scan until the cell lost its identity.

Hmax = maximum echo height (km msl) of the cell.

Zmax = maximum reflectivity (dBZ) of the cell at the cloud base level.

Amax = maximum area (km²) of the cell at cloud base.

RVRmax = maximum rain volume rate (10³m³ h-1) of the cell through cloud base.

Rvol = total rain volume yield (10³m³) of the cell.

Table 43. Mean values, Single Ratios, and Percentage of Probability of the Significance Levels for the Differences in the AgI and Control Cell Properties for the Young, Heavily Treated 1987 Texas cells

	<i>Texas short-track</i>				<i>Texas long-track</i>			
	<i>AgI</i>	<i>ContrOl</i>	<i>SR</i>	<i>SL %</i>	<i>AgI</i>	<i>ContrOl</i>	<i>SR</i>	<i>SL %</i>
Rvol	158.0	77.3	2.04	10.7	330.0	126.5	2.61	5.1
Hmax	9.5	10.2	0.93	59.4	11.6	11.1	1.04	30.3
Zmax	45.8	45.0	1.02	32.7	52.6	52.7	1.00	40.6
Amax	72.2	45.0	1.61	5.8	97.0	63.9	1.52	6.9
Dur	30.5	245	1.25	14.0	68.1	42.6	1.60	0.7
RVRmax	449.2	315.5	1.42	145	789.3	475.6	1.66	10.2
Sample	18	22			21	24		

Notes: SR = single ratios.

SL^x.01 = p-value.

Includes cells treated within 5 minutes of first echo with more than eight flares.

P-values were computed for the student's *t*-test and Wilcoxon rank sum test from 208 rerandomized runs.

Dur = time in minutes from first echo to the time of maximum area of the echo core.

Hmax = maximum echo height (km AGL) of the core.

Zmax = maximum reflectivity (dBZ) in the echo core.

Amax = maximum horizontal area (km²) in the echo core.

RVRmax = maximum rainflux (10³m³ h⁻¹) of the echo core, through the 1-km level.

Rvol = total rain volume yield (10³m³) of the echo core, through the time of the max rainflux.

Table 44. Fifteen-Minute Rainfall Accumulations for the Illinois Experimental Units and for the Extended Network Area

<i>Time (minutes)</i>	<i>Experimental unit</i>				<i>Extended network</i>			
	<i>AgI, N=5 (10⁴ m³)</i>	<i>N=6 (10⁴ m³)</i>		<i>AgI, N=5 (10⁶ m³)</i>	<i>Sand, N=6 (10⁶ m³)</i>			
	<i>Mean (σ)</i>	<i>N (>10⁵m³)</i>	<i>Mean (σ)</i>	<i>N (>10⁵m³)</i>	<i>Mean (σ)</i>	<i>N (>10⁷m³)</i>	<i>Mean (a)</i>	<i>N (>10⁷m³)</i>
BT - 15	37.5 (275)	4	25.0 (16.8)	6	8.3 (7.9)	2	17.9 (153)	4
BT - ET	60.4 (59.0)	3	36.0 (25.6)	4	9.7 (10.8)	2	17.8 (13.2)	4
ET + 15	89.3 (1075)	4	52.1 (37.2)	5	12.9 (165)	2	17.9 (13.2)	4
+15 to +30	95.0 (118.0)	4	50.2 (42.4)	6	13.1 (15.8)	2	14.8 (115)	4
+30 to +45	66.9 (65.6)	4	44.7 (43.1)	4	10.9 (11.6)	2	16.7 (13.7)	2
+45 to +60	64.0 (74.0)*	3	25.0 (205)	4	10.5 (11.9)	2	12.1 (10.9)	3
+60 to +75	91.4 (127.0)*	3	23.6 (30.4)	3	13.4 (14.7)	2	15.3 (14.0)	3
+75 to +90	77.4 (148.2)*	3	36.3 (35.0)	4	14.4 (21.0)	2	12.5 (95)	3

Notes: The extended network area is defined as a 240 x 240-km area centered on the CMI radar.

BT = the beginning of treatment, and ET to the end of treatment.

The treatment periods ranged from 10 to 48 minutes and have been normalized to 15-minute period.

* = rainfall values were estimated as one AgI-treated unit was moving out of radar range.

σ = standard deviation.

Increases are counted in increments of > 5 x 10⁴ m³ for the experimental unit, and by > 10⁶m³ for the extended network area.

BT15 = the period from 15 minutes prior to first treatment to the time of first treatment.

Table 45. Number of Illinois Units Increasing in Rainfall Accumulation from One Accumulated Rain Period to the Next

<i>Time (minutes)</i>	<u><i>Experimental unit</i></u>		<u><i>Extended network</i></u>	
	<i>AgI</i>	<i>Sand</i>	<i>AgI</i>	<i>Sand</i>
BT - 15 through BT - ET	2 / 5	3 / 6	2 / 5	1 / 6
BT - ET through ET + 15	2 / 5	5 / 6	3 / 5	3 / 6
ET + 15 through 15 - 30	2 / 5	4 / 6	2 / 5	1 / 6
15 - 30 through 30 - 45	1 / 5	2 / 6	1 / 5	3 / 6
30 - 45 through 45 - 60	2 / 4	1 / 6	2 / 5	0 / 6
45 - 60 through 60 - 75	2 / 4	1 / 6	3 / 5	3 / 6
60 - 75 through 75 - 90	1 / 4	3 / 6	2 / 5	1 / 6

Notes: Increases are counted in increments of $> 5 \times 10^4 \text{ m}^3$ for the experimental unit, and by $> 10^6 \text{ m}^3$ for the extended network area.
BT15 = the period from 15 minutes prior to first treatment to the time of first treatment

Table 46. Accumulated Rainfall for the 1987 Texas Experimental Units

<i>Time from beginning of treatment (min)</i>	<u><i>AgI units, N = 6</i></u>		<i>1987 sample (10^4 m^3)</i>	<u><i>Control units, N = 5</i></u>		<i>1987 sample ($> 10^5 \text{ m}^3$)</i>
	<i>Mean (10^4 m^3)</i>	<i>Stan dev</i>		<i>Mean (10^4 m^3)</i>	<i>Stan dev</i>	
+ 30	38.2	(43.1)	1	46.7	(56.3)	
+ 30 to + 60	53.4	(57.6)	1	72.4	(104.7)	
+ 60 to + 90	66.7	(79.4)	2	81.8	(151.6)	
+ 90 to + 120	78.6	(89.7)	3	61.2	(125.7)	
+ 120 to + 150	82.4	(97.1)	3	21.9	(47.4)	

Note: The data were provided by Dr. William Woodley.

Table 47. Number of 1987 Texas Units Increasing in Amount of Rainfall Volume from One Accumulated Rain Period to the Next by $> 5 \times 10^4 \text{ m}^3$

<i>Time from beginning of treatment (min)</i>	<i>AgI</i>	<i>Control</i>
+ 30 through 30-60	3/6	3/5
30-60 through 60-90	1/6	1/5
60-90 through 90-120	2/6	0/5
90-120 through 120-150	1/6	0/5

Notes: Increases are counted in increments of $> 5 \times 10^4 \text{ m}^3$.

Table 48. Accumulated Rainfall for the 1986, 1987, 1989, and 1990 Texas Experimental Units with Complete Rainfall Histories and which had Qualified for Treatment According to the SWCP Project Criteria

<i>Time from beginning of treatment (min)</i>	<i>AgI units</i>			<i>Control units</i>		
	<i>Mean ($10^4 m^3$)</i>	<i>Stan dev</i>	<i>Sample ($>10^5 m^3$)</i>	<i>Mean ($10^4 m^3$)</i>	<i>Stan dev</i>	<i>Sample ($>10^5 m^3$)</i>
+30	37.1	(37.9)	1	19.31	(19.0)	0
+30 to +60	40.9	(47.0)	1	19.19	(16.1)	0
+60 to +90	45.1	(58.4)	3	20.71	(28.8)	0
+90 to +120	32.4	(61.3)	1	34.89	(58.3)	1
+120 to +150	27.6	(58.7)	2	31.83	(62.2)	2

Notes: There were a total of 12 AgI-treated and 12 control units.
The data were provided by Dr. William Woodley.

Table 49. Number of Texas Experimental Units Increasing in Rainfall Volume from One Accumulated Rainfall Period to the Next

<i>Rainfall period after beginning of treatment</i>	<i>AgI</i>	<i>Control</i>
+30 through 30-60	4/12	3/12
30-60 through 60-90	4/12	4/12
60-90 through 90-120	2/12	2/12
90-120 through 120-150	1/12	2/12

Notes: Rainfall increases are counted in increments of $> 5 \times 10^4 m^3$.

8. RAINFALLASSESSMENT

by

Stanley A. Changnon and K. Ruben Gabriel

Introduction

This chapter presents rainfall data relevant to the PACE experimentation from mid-May through the end of July 1989, including 24-hour totals on flight days and monthly conditions as compared to normal conditions. This chapter also includes an assessment of the radar-indicated rainfall that occurred during the 1989 large cloud experimental units. Both sections of this chapter help put the results into a climatological perspective.

Data and Analyses

The raingage data for the study area were taken from NWS observer stations and reported in 24-hour amounts. They thus integrate rainfall from experimental units and from all other rain systems occurring during the 24-hour sampling period. They do not represent values considered useful for a direct assessment of seeding effects.

The radar-indicated rainfall associated with the large cloud experimental units was subjected to an analysis that compared the AgI- and sand-related rainfall amounts. Each experimental unit was divided into time segments of 15 minutes. The amount of rainfall accumulated during 15-minute segments before treatment (BT-15) and after treatment ended (ET+15) was measured using a radar-rainfall equation explained in chapter 7. The treatment period itself was the only portion of time not fixed in a 15-minute interval during the lifetime of an experimental unit. Because the treatment period for each experimental unit ranged from 15 to 40 minutes, and averaged 30 minutes, a discrete time breakdown was not possible. The rainfall produced in a unit was stated in relation to the time treatment began and ended, however long this period took. Thus, the rainfall "clock" was set to begin with a measurement 15 minutes before treatment and then at 15-minute intervals after the treatment of the unit ended. Note that determination of rainfall using a radar equation is subject to errors of up to ± 100 percent of the indicated amount. The radar-indicated values for the experimental units were not "calibrated" to surface raingage data since recording raingages in the study area were insufficient to accomplish such a calibration. Thus, the results of the radar-indicated rainfall amounts are subject to large uncertainty and must be used with caution.

Regional Rainfall Conditions

Daily rainfall data were accumulated for the dates of the experimental units from mid-May to the end of July 1989. The

distribution of the 46 raingages in and immediately adjacent to the study area is shown in figure 40. Data from these stations, measured on a 24-hour basis at 0700 each day, helped develop a variety of rainfall statistics, as shown in table 50. The station values were utilized to calculate daily mean rainfall and point maximum and minimum values throughout the study area. Values ranged from a low of 0.4 millimeters (mm) for the day ending at 0700 on June 19, to a high of 29.5 mm for May 26. On many days, the point maximum values reached or exceeded 26 mm (1.0 inch), and on most dates at least one or more stations in the study area had no rain, as shown by the minimum values. Also shown in the table are the number of stations recording measurable rain and the number with no rain for each date. On ten of the rain days, fewer than half the 46 stations, or less than half of the area, had no measurable rain. Also shown in the table are dates with crop-damaging hail, which further indicates the regional aspects of precipitation conditions. In general, the hail days were also days with heavy point rainfall maxima.

Daily rainfall values were classified as light (less than 2.0 mm), moderate (2.1 to 15 mm), and heavy (greater than 15 mm) to examine conditions in different experimental units. The large cloud experimental units were associated with a wide range of regional rainfall conditions. They occurred with light regional rainfall on June 1 and 27, and on July 8, 23, 24, and 25 (the latter three days were all air-mass conditions). Moderate rains fell with large cloud experimental units on June 23 and July 11; and regionally heavy rain occurred with the experimental units on May 19 and July 19, both dates with damaging hail. On nine of the ten large cloud dates, the maximum point rainfall recorded in the study area exceeded 26 mm (1 inch), and on five dates the maximum exceeded 58 mm (2.3 inches). Six of the ten days with large clouds had damaging hail within the study area, and five of these six were associated with cold-front conditions.

Most small cloud experimental units occurred with light regional rainfall, although moderate to heavy rains occurred during the 24-hour period of May 25 and July 2. Recall that all experimental units occurred during the afternoon and are not related to rainfall in the other 18 hours of the day.

Examples of the regional rainfall isohyetal patterns associated with the last series of four experimental units studied in 1989 (July 19, 23, 24, and 25) are shown in figure 41. Readings for each of the 24-hour rainfall patterns were taken at 0700 on the day following the date noted. For figure 41, this period includes two experimental units that occurred during the afternoon and evening of July 19 (one seeded with AgI and one with sand). As shown in table 50, the area mean rainfall was 20.7 mm, and the isohyetal pattern shows that measurable rainfall covered the entire network, while two large areas received 20 mm

or more. The other three isohyetal patterns in the figure depict the rainfall associated with the July 23 unit, the July 24 unit, and two units on July 25. These patterns all illustrate similar rainfall, extremely localized within the study area, and very typical of Illinois (Changnon and Huff, 1980). As shown in table 50, the peak amounts on these three days of very isolated rainfall were 27, 30, and 59 mm, respectively.

A basic question about the 1989 season of operations concerns the normality of the surface weather conditions. This was investigated using the May, June, and July rainfall totals and mean temperatures for stations in the study area. This comparison revealed that May, June, and July rainfall totals at all stations were within 21 percent of their long-term averages. In all locations, May rainfall varied from 9.4 to 13.0 cm; values in June ranged from 8.9 to 11.9 cm; and those in July ranged from 8.5 to 10.7 cm. The mean monthly temperatures also were near normal. Values were $\pm 0.3^{\circ}\text{C}$ in all three months. In essence, the May-July period of 1989 when the experiment was conducted was a fairly typical weather period.

Evaluations of Seeded Rainfall Amounts

Rainfall production from the PACE experimental units was determined using radar reflectivity data. Rainfall values were calculated beginning with the amounts occurring 15 minutes before treatment, generally when rain was just beginning to fall from most experimental units, until 90 minutes after treatment ended in the unit, when most experimental units were quite mature and beginning to dissipate. The amount of rainfall accumulated over this period was determined for each experimental unit, as shown in table 51, and rainfall generated by the units treated with AgI was compared with that from the units treated with sand.

Post-treatment rainfall values of one AgI-treated unit were missing due to problems with radar operations. Inspection of the unit values for both the AgI- and the sand-treated units reveals widely different rainfall amounts. A few units produced very heavy rainfall, and a few produced very little. Note for example that by 90 minutes after treatment, the July 8 (2) unit had produced $1,770 \times 10^6 \text{ m}^3$ of rain, whereas the July 25 (2) AgI-treated case produced only about $25 \times 10^6 \text{ m}^3$ of rain.

The amount of rainfall occurring in the extended area, 240 x 240 km around the radar, was also determined for the same periods. The rainfall values for the extended area reflect unseeded conditions (table 52).

A comparison of the rainfall totals from the eleven complete experimental units (at 90 minutes after treatment) is presented in table 53. The values reveal that two AgI-treated units, July 8 (2) and June 1, produced rainfall totals considerably higher than the highest sand-treated unit which was $554 \times 10^6 \text{ m}^3$ on June 23 (2). However, rainfall totals for the AgI-treated units range from 282 to $7 \times 10^6 \text{ m}^3$ overall, from the highest to the lowest production. Three of the four lowest rain totals

were from experimental units treated with sand. However, more high-ranked sand treatments appear in the top four values in tables 52, showing the extended area, than in table 53, which shows the experimental units only.

Comparison of the rankings in table 53 for the experimental units and their extended areas shows that area rainfall was not always directly correlated with unit rainfall, a condition to be explored later. Three of the AgI-treated units dropped in rank when the extended area total rain was considered. Three of the four sand-treated units increased in rank in relation to the extended area rain, and two AgI and two sand treatments maintained their ranks.

The units' widely ranging rain production is not atypical of convective rainfall in Illinois (Changnon and Huff, 1980), and this situation affected the approaches used for comparing the AgI- and sand-related rainfall amounts. First, the median values were determined for the six AgI treatments and the six sand treatments for each of the time segments. The resulting median values are plotted in the upper portion of figure 42. The units' median values at treatment minus 15 minutes were identical, and they were still similar when treatment began: AgI= $30.8 \times 10^4 \text{ m}^3$ and sand = 24.7. However, during the 30 minutes of treatment (the average value), the AgI-related median rainfall value increased rapidly over the median sand value. At the end of the treatment, the median rainfall value for the AgI cases was $182.9 \times 10^4 \text{ m}^3$, as compared to $78.8 \times 10^4 \text{ m}^3$ for sand, which was 2.3 times higher, as shown in table 54. In the 30 minutes after treatment ended, the rainfall medians of both AgI- and sand-treated units increased in a generally similar direction, followed by a relative decrease in the rainfall production of the AgI-treated units. As shown in table 54, the ratios of their differences decreased from 1.47 at ET+30, to 1.2 by ET+60, and to 1.1 by ET+90.

Comparison of the medians of the extended area values is also revealing. First, the median sand values at BT-15 were higher than the AgI values, $3.95 \times 10^6 \text{ m}^3$ versus $1.15 \times 10^6 \text{ m}^3$, respectively. Further, the sand median values remained higher throughout their duration to ET +90, as shown in figure 42. The accumulated rainfall of the sand-treated cases was linear, with a slope similar to that of the experimental units associated with sand shown in the plot above.

The median value of the AgI cases for the extended area did not increase at the same rate as the sand cases (ratio all much less than 1.0), indicating that the sand-related rain accumulations at all times relative to treatment were greater than the AgI-related rain accumulations (column 5 of table 54). However, the ratios for the experimental units (column 4) were all greater than 1.0, consistent with a positive seeding effect. When viewed in combination, columns 4 and 5 provide evidence that AgI seeding enhanced rainfall on days with low regional rain productivity. The time distribution of the rainfall in the extended areas for the AgI cases is markedly different from that exhibited by the experimental units, as shown in figure 42. In essence, the rainfall medians for the AgI-treated units increased

rapidly during treatment time compared to the sand-treated units. Furthermore, rainfall from the AgI-treated units increased at a rate apparently much greater than the associated rainfall in the extended area.

To further examine the relationships between the area and the unit, the ratios of the medians for both AgI and sand were computed. The AgI ratios (column 2) show the unit rainfall, growing from 5 to 9.6 percent relative to area rainfall during the treatment period. Then the unit-to-area ratios for AgI remained at 10 to 11 percent until 75 minutes after treatment. Conversely, the sand-related rainfall medians for the units (column 3), which were 1.5 percent of the area values at the beginning of treatment, increased only slightly to 2.2 percent at the end of treatment and remained at 2 to 2.4 percent for the duration.

A second analysis also compared the accumulated rainfall values of the experimental units and the extended areas associated with the units. It was based on a transformation of the logarithms of the individual rainfall values to minimize the effect of the wide extremes in the rainfall amounts. The logs of the rainfall values for the AgI-treated units and extended areas and of the sand-treated units and extended areas were tested for the significance of the differences in rain accumulated at three time periods after the beginning of treatment: 1) at the end of treatment, 2) at ET+30, and 3) at ET+90.

The mean differences for ET versus BT for the experimental units were 4.04 for AgI and 3.39 for sand. The *t*-test of their differences, based on the experimental units, showed that the ET-BT values, under the hypothesis that $AgI > sand$, yielded a *t*-statistic of 0.837, which has a probability of 0.21. The Wilcoxon nonparametric summed rank test of the two sets of values produced a P-value of 0.11 for $AgI > sand$. The experimental unit tests for ET+30 versus BT produced P-values of 0.45 (*t*-test) and 0.27 (Wilcoxon). The tests of differences, $AgI > sand$, for rain at ET+90 versus BT produced P-values of 0.22 for the *t*-test and 0.12 for the Wilcoxon summed rank test. Twice the Wilcoxon P-values approximated the 0.1 significance level. Nevertheless, the question of the multiplicity of the tests tends to limit their value.

The extended area values were tested for a different hypothesis, since the sand values exceeded the AgI values at all time intervals, as shown in figure 42. The hypothesis tested was that the rain values for the sand-treated units were significantly greater than the rain values for the AgI-treated units. The *f*-test for ET versus BT values yielded a P-value of 0.15, and the *f*-test for ET+90 versus BT revealed a difference with a probability of 0.33.

The general conclusion is that the median rainfall values show marked differences, but they are not significant at the 0.05 to 0.1 levels. The sample size is too small, and the spread of the individual unit values is high, both of which reduce the significance of the differences.

The accumulated rainfall produced by the AgI- and sand-seeded units was also compared on the basis of synoptic weather conditions. The sample size is very small, so only very general

indications can be drawn. The median rainfall values of the AgI- and sand-treated units with cold-front and with air-mass conditions are listed in table 55. The cold-front cases (four AgI and two sand) show that at BT-15, the sand-treated units were producing four times more rainfall than the AgI-treated units. By the time treatment began, the AgI-sand rainfall ratio was 1.17, showing that the AgI-seeded units were then producing slightly more rain than the sand-treated units. During treatment, typically lasting 30 minutes, the AgI-related rainfall increased very rapidly relative to the sand-related rain; at ET, AgI-related rainfall was 2.47 times greater. And at ET+90, the AgI-related rainfall remained much higher than the sand-related rainfall, ranging from 2.3 to 2.6 times higher. Thus, the cold-front comparison suggests that rainfall increases were achieved through AgI treatment.

The relationships of AgI- versus sand-related rainfall in units produced under air-mass conditions, also shown in table 55, were quite different than the cold-front findings. The ratios reveal that the median rainfall from the AgI-treated units was consistently heavier than from the sand-treated units from their beginning to ET+45. Values were 1.57 to 1.65, except at the end of treatment, when the ratio soared to 2.5, suggesting some short-lived rainfall increase in the AgI-treated units. From ET+60 to ET+90, the ratios rapidly declined, suggesting that the rainfall from the AgI-treated units was not increasing at the rate of the sand-treated units. The ratios for the air-mass units suggest that AgI seeding in these conditions produced an abrupt, short-lived increase at the end of treatment, and a relative decrease in rainfall later in the life of the units.

Summary

It is not possible to draw firm conclusions about the seeding effect on rainfall from an exploratory experiment in which the comparisons are limited to only a few cases, six AgI-treated units and six sand-treated units. Only general tendencies can be inferred.

Given this caveat, the rainfall results suggest *different conclusions* than did the echo core/cell results described in prior chapters. The accumulated rainfall data for the experimental units treated with AgI showed: 1) an abrupt increase over the sand-treated unit rainfall just after treatment, given that the units started with about the same rainfall amount at BT-15; and 2) a generally decreasing difference between AgI- and sand-related rainfall up to ET+90. This result alone may suggest an enhancement due to AgI treatment, although tests of the differences show probability values of 0.11 to 0.27 for a seeding effect. Hence, this assessment points to the possibility that AgI *may* have had a positive effect on *system* rainfall, in spite of a possible negative effect on the growth of *individual* clouds that eventually merge with the parent rain system.

The second comparison relates to the rainfall occurring in the area around the existing experimental units. Comparison of

the AgI and sand values for these extended areas showed opposite outcomes: the sand-related area rainfall values were consistently higher than the AgI-related area values from BT-15 to ET+90. This means, in general, that the AgI-treated units were occurring in convective rainfall situations less favorable for heavy rainfall production than were the sand-treated units. Thus, comparison of rainfall distribution in the units against that in their areas reveals that the rainfall in the AgI-seeded units apparently grew rapidly, while that in the extended area did not. Conversely, rainfall from the sand-treated units grew at the same rate, approximately 2 percent, as rainfall in the extended area, and this relationship held throughout the lifetime of the units. Two indications in the data suggest that rainfall from the units treated with AgI may have been enhanced. First is the heavier (median) rainfall in the AgI-seeded units at the end of treatment, and second is the relatively greater rainfall in these units as compared to their extended area values.

Rainfall comparisons based on synoptic weather conditions revealed that much of the observed difference in the AgI-

and sand-seeded unit rainfall (table 55) was due to heavier rainfall in the seeded units associated with cold fronts. These cases included the two units that produced the highest rainfall accumulations (rank 1 and 2, table 53). The synoptic condition comparisons suggest that the overall apparent rainfall enhancement found in the units (table 54, column 4) was associated with cold-front situations, and not with rain enhancement in the air-mass cases.

Part of the AgI-versus-sand difference reflecting enhancement also relates to the fact that two of the six AgI-seeded units produced extremely heavy rainfall, higher than any sand-treated unit. Such an outcome is similar to findings from St. Louis (Changnon et al., 1981) and Chicago (Changnon, 1984). In both those locations, urban influences on summer convective rainfall systems were found to occur in cases of already existing convective rainfall, with increases found in a few heavier rainfall regimes. This points to the possibility that AgI seeding may be most effective when it is applied to well-organized rainfall systems.

FIGURES AND TABLES FOR CHAPTER 8

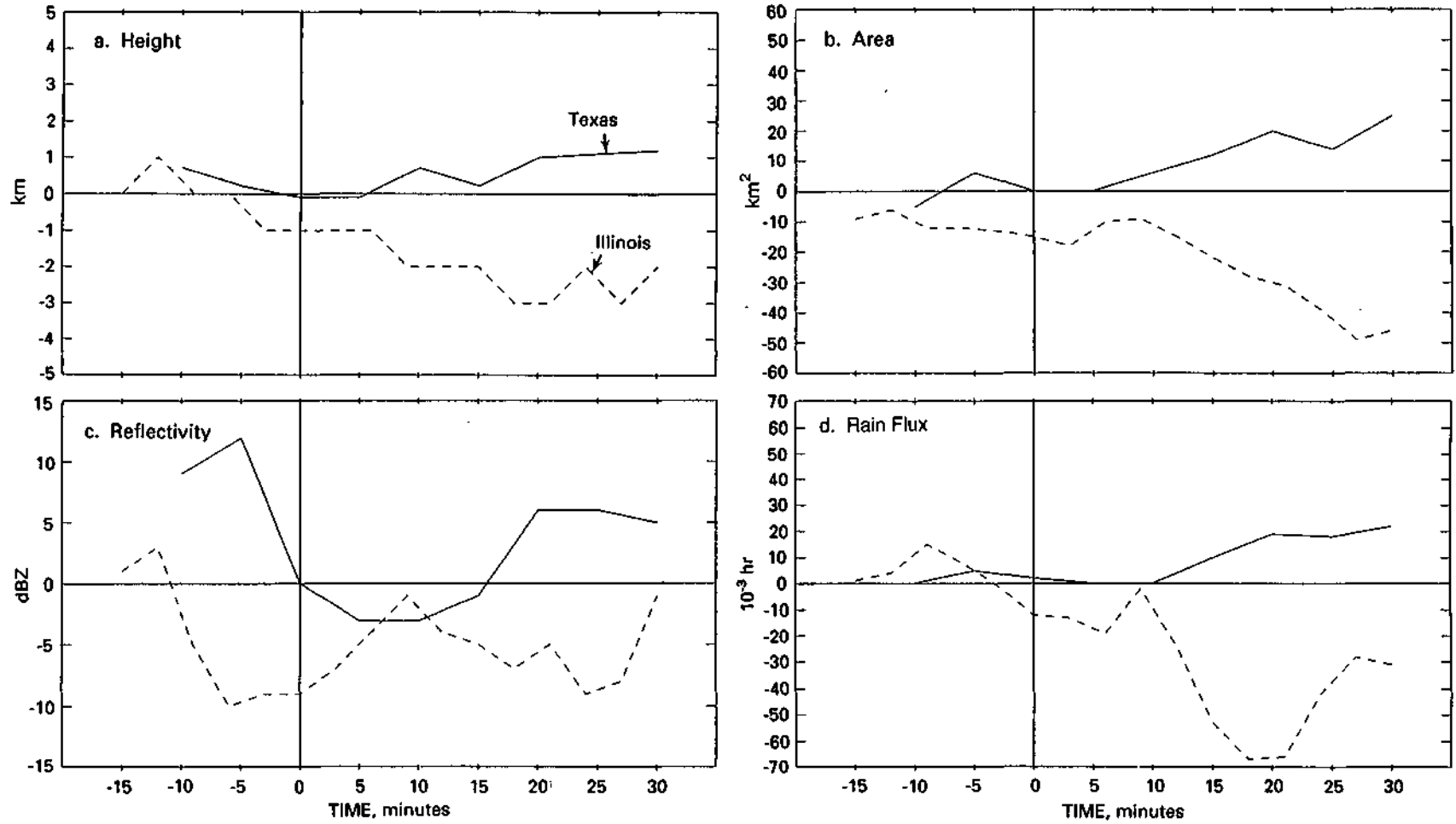


Figure 39. Mean differences between Agl and sand treatments on mean echo-core height, area, maximum reflectivity, and rain volume relative to the time of treatment, Illinois and Texas short-track echo cores

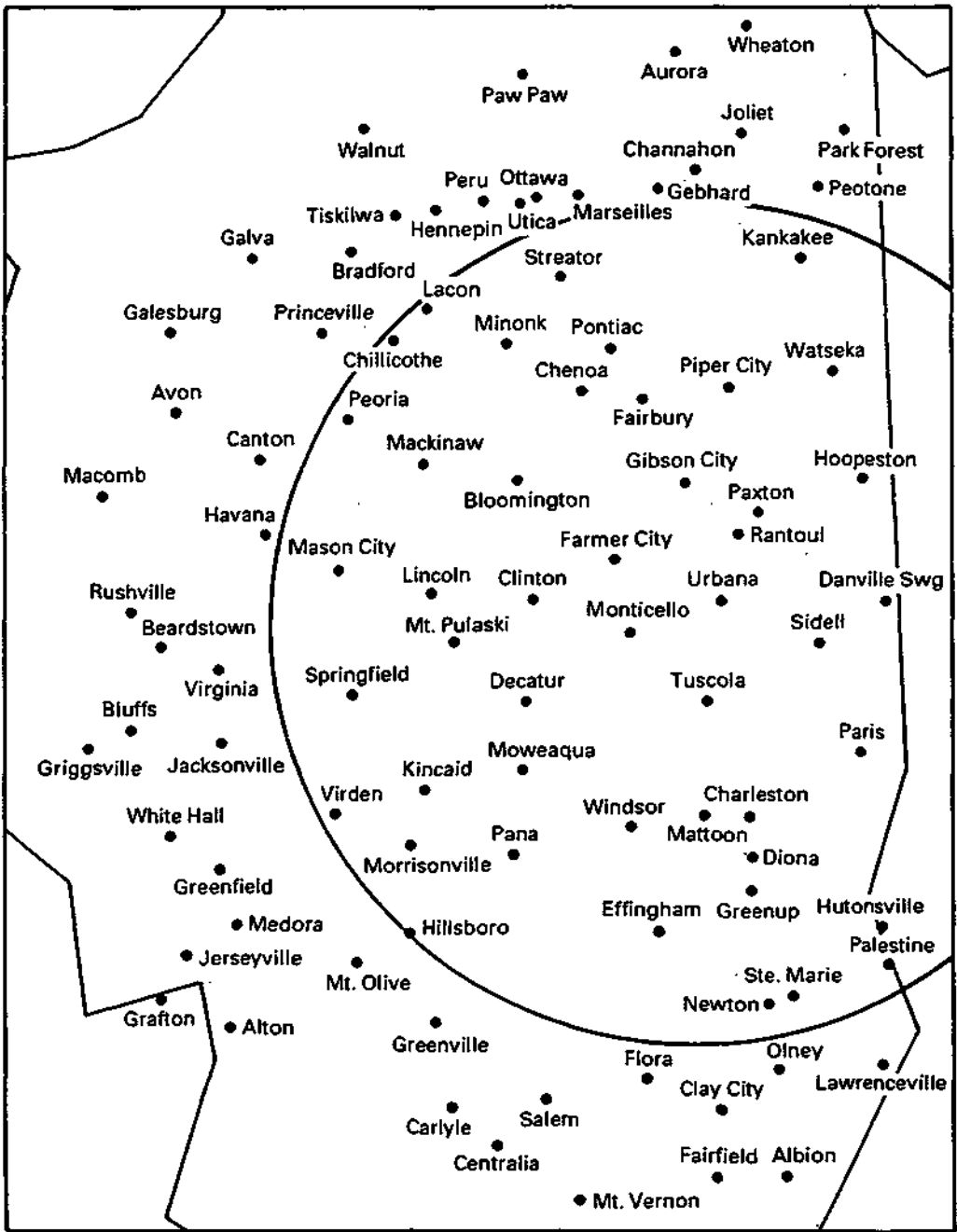


Figure 40. National Weather Service Cooperative rain gauge sites within and around the PACE target area, 1989

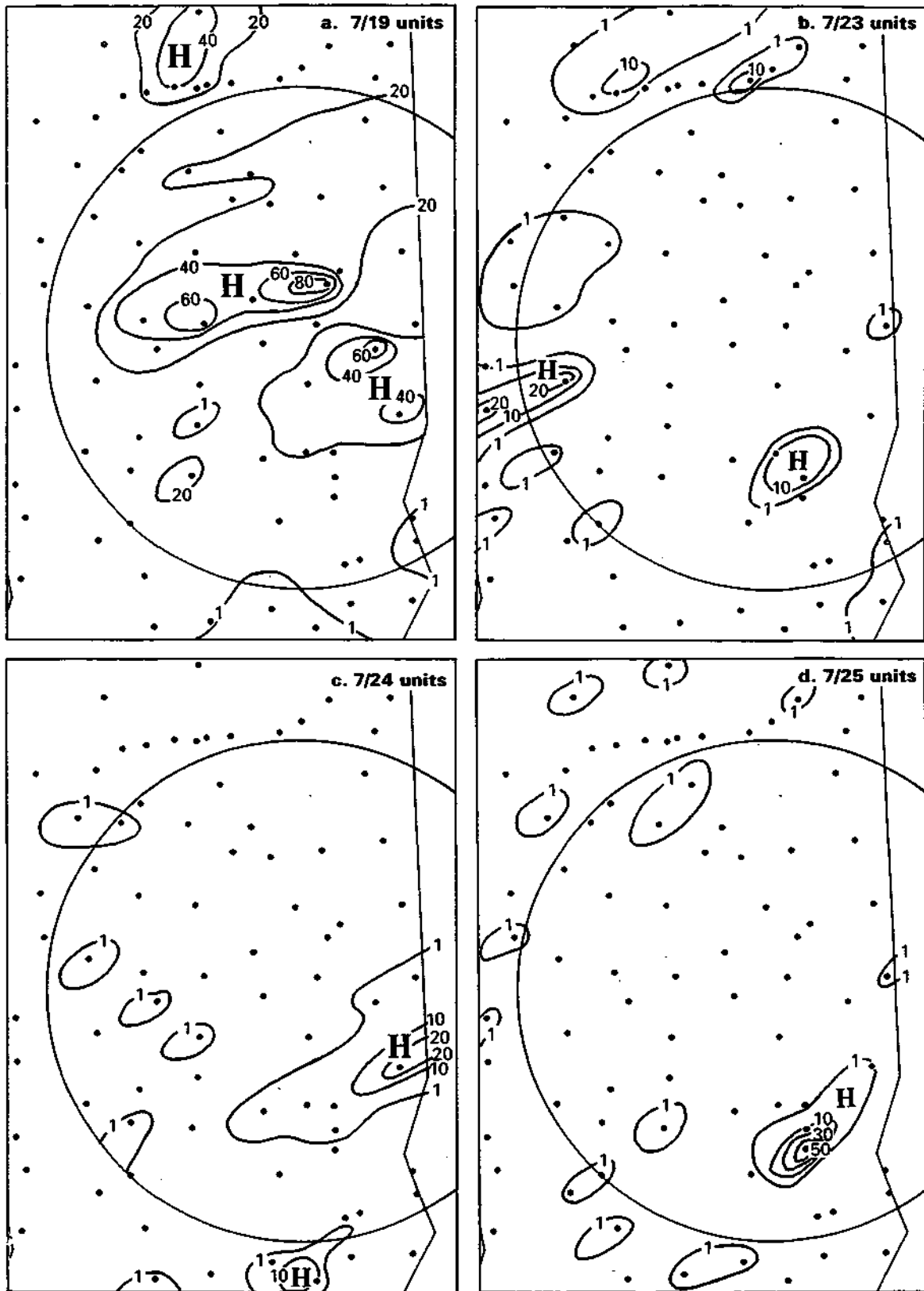


Figure 41. Daily rainfall associated with 1989 experimental units (mm)

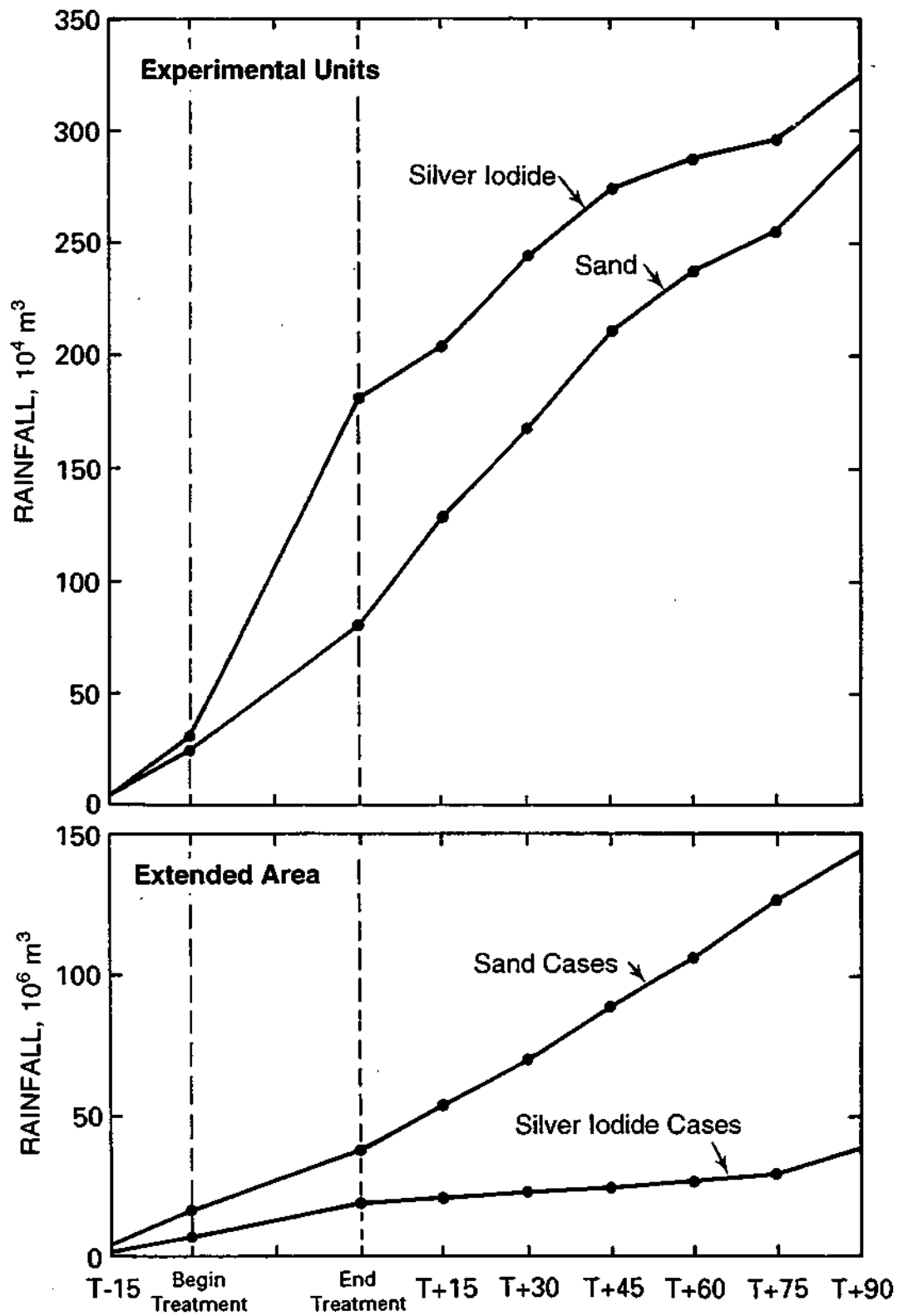


Figure 42. Accumulated rainfall for experimental units and the extended area, 1989

Table 50. Rainfall Values Based on 46 Raingage Stations in the Study Area, PACE Experimental Units, 1989

Date	Mean (mm)	Point maximum (mm)	Point minimum (mm)	With no rain	<i>Number of Stations</i>	
					With measurable rain	With damaging hail
5/20	22.6	64	0	3	43	Yes
5/26	29.5	59	3	0	46	-
5/31	0.8	9	0	36	10	-
6/2	3.8	26	0	21	24	Yes
6/4	3.7	21	0	17	28	Yes
6/13	2.1	12	0	23	22	-
6/19	0.4	6	0	40	5	-
6/24	7.2	58	0	27	18	Yes
6/28	2.8	29	0	29	16	-
7/3	8.1	55	0	18	28	-
7/9	1.0	21	0	39	7	Yes
7/12	8.3	75	0	24	22	Yes
7/20	20.7	82	0	3	43	Yes
7/24	1.8	27	0	36	10	-
7/25	1.8	30	0	32	14	-
7/26	2.0	59	0	38	8	-

Notes: Rainfall values are 24-hour amounts based on 0700 measurements. Thus, the rain associated with a unit on May 19 is shown for May 20.

Raingages are located within 160 km of Champaign radar.

Table 51. Accumulated Rainfall Amounts During Each Experimental Unit (10⁴ m³)

Interval	<u>AgI</u>							<u>Sand</u>				
	6/1	6/23 ⁽¹⁾	7/8 ⁽²⁾	7/11	7/23	7/25 ⁽²⁾	5/19	6/23 ⁽³⁾	7/8 ⁽¹⁾	7/19 ⁽¹⁾	7/24	7/25 ⁽¹⁾
BT-15	17.4	0.8	2.8	3.2	5.0	2.8	2.6	2.3	22.8	13.8	2.8	1.9
BT	95.9	10.0	44.5	13.1	48.3	17.1	20.1	14.9	51.0	69.9	29.2	12.1
ET	261.9	M	242.9	30.6	182.9	24.8	95.9	118.5	58.3	111.6	61.7	21.1
ET+15	404.9	M	496.7	57.8	205.5	24.5	145.7	232.9	82.0	177.2	113.9	28.1
ET+30	536.1	M	782.3	75.2	246.1	24.8	203.6	355.0	112.0	245.7	129.3	40.6
ET+45	647.9	M	940.4	107.2	278.5	24.8	312.2	441.8	117.3	283.7	144.5	49.9
ET+60	743.9	M	1118.1	146.6	285.6	24.8	369.6	479.0	119.3	304.7	170.6	56.2
ET+75	823.0	M	1428.1	208.8	291.2	24.8	452.1	495.2	122.8	310.0	199.5	61.4
ET+90	840.6	M	1770.1	331.7	295.5	24.8	519.1	554.0	125.2	320.9	276.7	62.8

Notes: (1) and (2) refer to the first or second experimental unit on these dates.
M = Missing data.
BT = Beginning of treatment.
ET = End of treatment.

Table 52. Accumulated Rainfall Amounts (10⁶ m³) Over the Extended Area During Each Unit

Interval	<u>AgI</u>						<u>Sand</u>					
	6/1	6/23 ⁽¹⁾	7/8 ⁽²⁾	7/11	7/23	7/25 ⁽²⁾	5/19	6/23 ⁽³⁾	7/8 ⁽¹⁾	7/19 ⁽¹⁾	7/24	7/25 ⁽¹⁾
BT-15	3.6	1.3	3.6	.02	1.0	0.6	9.2	3.8	4.1	7.1	0.8	1.1
BT	16.5	5.3	23.2	1.1	7.0	2.5	50.7	17.1	16.2	39.1	5.5	5.1
ET	35.0	M	73.1	4.0	19.0	4.0	126.0	39.2	34.9	61.2	9.2	10.9
ET+15	59.7	M	109.1	6.6	20.4	4.4	156.2	53.3	52.9	97.3	16.1	12.9
ET+30	87.5	M	142.0	8.9	22.7	4.8	180.6	63.9	78.0	122.3	18.4	14.1
ET+45	109.7	M	166.6	13.8	24.8	5.4	213.8	73.0	107.9	144.7	23.2	14.8
ET+60	123.6	M	196.2	20.5	26.5	5.9	227.5	78.9	136.3	165.5	26.6	15.2
ET+75	145.0	M	231.3	29.3	27.9	6.3	248.1	84.6	169.8	193.7	29.9	15.7
ET+90	152.7	M	282.5	40.1	30.1	6.9	261.8	90.0	197.0	210.3	39.6	16.3

Notes: (1) and (2) refer to the first or second experimental unit on these dates.
M = Missing data.
BT = Beginning of treatment.
ET = Ending of treatment.

Table 53. Rank Distributions of Experimental Unit Rainfall Totals and Extended Area Totals at 90 Minutes after Treatment

Rank	<u>Experimental unit</u>			<u>Extended area</u>		
	Value (10 ⁶ m ³)	Treatment	Date	Value (10 ⁶ m ³)	Treatment	Date
1	1,770	AgI	7/8(2)	282	AgI	7/8(2)
2	840	AgI	6/1	261	S	5/19
3	554	S	6/23(2)	210	S	7/19
4	519	S	5/19	197	S	7/8(1)
5	331	AgI	7/11	153	AgI	6/1
6	321	S	7/19	91	S	6/23(2)
7	295	AgI	7/23	40	AgI	7/11
8	276	S	7/24	40	S	7/24
9	125	S	7/8(1)	30	AgI	7/23
10	63	S	7/25(1)	16	S	7/25(1)
11	25	AgI	7/25(2)	7	AgI	7/25(2)

Table 54. Ratios of Seeded to Nonseeded Accumulated Rainfall Medians for Experimental Units and Their Extended Areas over time

Time intervals (minutes)	Seeded ratio, % (unit divided by area)	Nonseeded ratio, % (unit divided by area)	AgI/sand ratio for units	AgI/sand ratio for extended area
(1)	(2)	(3)	(4)	(5)
BT-15	2.4	0.7	1.02	0.29
BT	5.0	1.5	1.25	0.37
ET	9.6	2.2	2.32	0.53
ET+15	10.0	2.4	1.58	0.38
ET+30	10.8	2.4	1.47	0.32
ET+45	11.3	2.4	1.33	0.27
ET+60	10.8	2.2	1.20	0.25
ET+75	9.9	2.0	1.14	0.23
ET+90	8.3	2.1	1.11	0.28

Notes: BT = beginning of treatment.
ET = end of treatment.

Table 55. Comparison of Experimental Unit Rainfall Accumulated over the Duration, AgI and Sand Treatments

<i>Time</i>	<u><i>Cold front units</i></u>		<i>Ratio (AgI/Sand)</i>
	<i>AgI (4)</i>	<i>Sand (2)</i>	
-15 BT	23	105	0.22
Treatment begins (BT)	38.7	33.0	1.17
Treatment ends (ET)	242.9	98.3	2.47
+15 ET	404.0	1575	2.57
+30 ET	536.0	2325	2.31
+45 ET	648.0	2795	2.32
+60 ET	744.0	299.0	2.49
+75 ET	823.0	3085	2.67
+90 ET	840.0	3395	2.47
	<u><i>Air mass units</i></u>		
	<i>AgI (2)</i>	<i>Sand (2)</i>	<i>Ratio AgI/Sand</i>
BT-15	3.9	2.35	1.65
BT	32.7	20.65	1.58
ET	103.8	41.4	2.50
ET +15	114.5	70.5	1.62
ET +30	135.5	84.5	1.60
ET +45	151.5	96.5	1.57
ET +60	155.0	113.0	1.37
ET +75	158.0	130.0	1.22
ET+90	160.0	169.0	0.95

Notes: BT = beginning of treatment; BT-15 = 15 minutes before the beginning of treatment.
 ET = end of treatment; ET + 30 = 30 minutes after the end of treatment.

9. SUMMARY, CONCLUSIONS, AND RECOMMENDATIONS

by

Stanley A. Changnon and Robert R. Czys

Summary

A randomized cloud seeding experiment was conducted in Illinois from mid-May through July 1989. The purpose was to discover whether AgI seeding, applied according to the dynamic seeding hypothesis, altered either a) cloud conditions during their early life, as measured by radar, b) the rainfall from the cloud group in which the clouds were embedded, which was defined as the experimental unit, or both. Randomization was based on experimental units that were typically cloud groups of three or more cumulus congestus. These experimental units typically lasted two or more hours.

During the 2.5-month experiment, treatments were applied to 12 experimental units. Each unit contained large clouds, which were defined as those in which the cloud tops grew beyond 30,000 feet (9,100 m). The randomization of the experimental units was based on a 50/50 design. Six of the units were treated with AgI flares and six were treated with placebo flares containing sand. The flares were ejected into the updraft regions of young growing cumulus congestus clouds at the -10°C level. The dynamic seeding hypothesis states that following such applications, the added release of heat from the conversion of water to ice should increase cloud growth and enlarge the clouds, producing cloud-to-cloud interactions which, in the net, will allow a cloud system to produce more rainfall than it would otherwise.

During the 1989 experiment, 82 large clouds were treated, 36 with sand (in six units) and 46 with AgI (in six units). However, only 71 of these 82 clouds produced trackable radar echoes. Therefore, the radar evaluation was based on these 71 clouds, of which 32 received sand treatments and 39 AgI. The sample size was further reduced in some analyses to compensate for missing data due to aircraft or radar operational problems, or to address special studies based on certain cloud criteria. The experiment was conducted during a summer of near-normal rainfall amounts, near-normal temperatures, and on clouds and cloud systems that were typical of Illinois.

The synoptic weather conditions in the region, coupled with aircraft data on in-cloud conditions and pretreatment radar data, collectively produced 154 predictor variables. Analysis of synoptic conditions indicated that the experiment was conducted during a transition in meteorological conditions from those typical of late spring/early summer to those typical of late summer. Hence, many clouds treated early in the experiment were associated with cold-front circulations, while those treated later in the experiment were associated with vertical motions induced in air mass by the interaction of surface convergence and short-wave advection.

Many meteorological conditions and cloud properties were closely interrelated, and they all indicated various measures of instability in the mesoscale or cloud-scale atmosphere prior to treatment. Analysis of radar and aircraft data revealed that properties at the echo and in-cloud scales changed with the transition through the seasonal regimes. Hence, careful monitoring of meteorological conditions and associated cloud properties is warranted in other cloud seeding experiments.

The interrelated nature of many of the predictor variables from the mesoscale environment and the in-cloud characteristics necessitated the selection of a set of key predictor variables to describe the atmosphere on different spatial scales prior to and at treatment. Eleven key predictor variables were identified. These included three synoptic weather variables (potential buoyancy, CCL temperature, and bulk Richardson number); four radar-indicated variables (mean echo diameter at treatment, echo height at treatment, maximum reflectivity at treatment, and time from first echo to treatment); and four aircraft-measured, in-cloud variables (net buoyancy, buoyancy enhancement, mean updraft velocity, and fraction of solid water content). In this and any other cloud seeding experiment conducted in accord with the dynamic seeding hypothesis, these variables serve well as predictors of future cloud growth.

Comparison of the means and extremes of these 13 predictor variables for the randomly selected sand- and AgI-treated clouds revealed several significant differences. The number of significant differences was more than could be expected by chance. Every attempt had been made to select congestus clouds of extremely similar character, based on visual appearance, size, and in-cloud characteristics. Nevertheless, four key radar variables and three of the aircraft variables showed significant differences between the sand- and AgI-treated populations. This became a classic example of a "bad draw." These major differences at the time of treatment nullified any hope of defining differences due to a seeding effect. On the average, the AgI-treated clouds selected were smaller and less intense than the sand-treated clouds at the time of treatment. Thus, it was considered improper to directly compare the post-treatment characteristics of the AgI-treated clouds with those of the sand-treated clouds. As a result of the bad draw, several analyses were pursued in an attempt to make cloud comparisons based on similar pretreatment conditions.

Several major findings from the 1989 exploratory cloud seeding experiment in Illinois relate to visual effects (chapter 3), effects on individual echo cores (chapters 4 and 5), or to system rainfall (chapter 8).

As discussed in chapter 3, many scientists and pilots experienced in cloud seeding have reported the ability to

identify clouds seeded with AgI based on visual inspection of post-treatment behavior. The treatment, which seeks to convert water to ice rapidly, is often reflected in a "glaciated appearance" or rapid growth in the upper portions of a cumuliform cloud. A test in the 1989 experiment attempted to validate this ability. After each experimental unit, the pilot and the project meteorologist, both of whom flew aboard the seeding aircraft, were asked if they thought the clouds in the unit had been treated with AgI or sand. This two-person analysis revealed very high skill: the pilot correctly identified the treatment in 85 percent of the events, and the meteorologist was correct with 68 percent, both scores above chance. Neither had any information before, during, or after the experiment on the true nature of the treatment type. Although the sample size is small, it supports the hypothesis that the AgI dosage was sufficiently large to enhance glaciation and thus alter the outward appearance of the clouds.

In chapter 4, the results were examined in the framework of different known synoptic weather types that produce rain. For the analysis, the experimental units were classified by synoptic weather conditions to isolate the unexpected bias found in the total cloud selection and discern seeding effects. Past studies of urban effects on summer clouds at St. Louis and Chicago found that effects varied greatly among synoptic weather conditions (cold fronts, squall zones, air mass, etc.). Six of the twelve 1989 experimental units occurred under cold-front system conditions, four were associated with unstable air-mass conditions, and the others included a squall zone and low pressure. The analysis focused on the cold-front and air-mass cases. As expected, the cold-front clouds (echoes) grew taller and produced more rain than did the air-mass clouds (Changnon and Huff, 1980). However, the air-mass clouds (echo cores) were found to be generally larger at the time of treatment and already merged with surrounding clouds to a much greater extent than cold-front cores. The cold-front cores were separated more from other clouds at treatment time, and not all had developed echo cores at treatment. On the other hand, all air-mass clouds had echo cores at treatment. Thus, there were substantial differences in the characteristics of cells within the two synoptic classes sampled in 1989.

The differences between AgI- and sand-treated clouds, based on the cold-front and air-mass cases, were investigated. Unfortunately, the pretreatment aircraft and radar variables for the cold-front cases revealed that a strong bias still existed in this synoptic classification. The AgI-treated cloud sample included many small cores at treatment, whereas the sand-treated sample in cold fronts had many larger echo cores. This bias, which carried over into the total sample, negated any assessment of differences between AgI and sand treatments in the six cold-front cases. Contrary to the cold-front units, the air-mass units showed less evidence of a bias. The predictor variables of the clouds in the two AgI-treated and the two sand-treated units were generally alike.

To help measure cloud reactions to seeding, 36 response variables were defined for the radar echoes of the cores of the

treated clouds. These included fixed measures of echo heights, reflectivities, and areas (i.e., maximum values attained and growth rates). Echo cores were tracked from their origins (first echo) until they merged with others and became indistinguishable. Our analysis of the response variables after treatment revealed no material difference between the AgI- and sand-treated air-mass clouds as to sizes, heights, or reflectivities.

A second major analysis compared subgroups of clouds on the basis of their suitability for dynamic seeding. A "seedability index" was developed, based on 20 predictor variables selected to represent conditions before and at treatment. All clouds meeting these 20 seedability criteria were examined, but only 52 had sufficient data to be analyzed. The individual cloud's seedability criteria, expressed as the percentage of the 20 variables that qualified, ranged from a low of 55 percent up to 100 percent. A subgroup of 29 clouds was classed as having "high seedability," with indexes equal to or greater than 70 percent. A "less seedable" category was based on 27 clouds with SI less than 80 percent.

The comparison of the AgI- and sand-treated clouds in the higher seedability category, greater than 70 percent, revealed that they were alike before treatment and could be compared. Analysis of the response variables for this group revealed that their means differed only slightly. Only one of the means for the AgI-treated clouds, maximum height attained, was smaller and was rated significantly different from the sand-treated cloud values. Another comparison revealed that in addition to lesser heights, the AgI-treated clouds appeared smaller in area than the sand-treated clouds 10 minutes after seeding. In essence, the comparisons of the more seedable clouds indicated little evidence of a positive seeding effect according to dynamic seeding, and possibly weak evidence of a negative seeding effect.

Comparison of the less seedable clouds, those with indexes less than 80 percent, revealed that they too were sufficiently alike prior to seeding to permit comparison of their responses. Interestingly, the response variables for the AgI-treated clouds showed relatively larger echoes, somewhat higher reflectivities, and greater rain flux than did the sand-treated "less seedable" clouds. This outcome and that for the "more seedable" group raises serious questions about the validity of the dynamic seeding hypothesis for Illinois and whether the radars used were capable of detecting the seeding effects. In combination, the results suggest reconsideration of the dynamic seeding hypothesis and point to the possible need to modify or develop a new seeding hypothesis for summer cloud modification in Illinois.

In chapter 6, the 52 echo cores with complete data (from ten experimental units) were statistically compared according to the 11 key predictor variables and 8 primary response variables (echo height, area, intensity, and rates of change). The values for each were rerandomized 240 times to assess the statistical significance of the differences, if any, based on the mean values of the experimental unit and the echo core. One of the predictor variables, buoyancy enhancement, was smaller for the AgI-treated clouds and significantly different from that for the sand-

treated clouds. The response variable comparisons revealed that the only difference of consequence was that the AgI-treated clouds attained lower maximum heights than the sand-treated clouds. However, interpretations of such statistical outcomes are considered limited because the exploratory analysis included much multiplicity in these comparisons.

The 1989 cloud and rain results for the units were compared with those from an experiment conducted in west Texas during the late 1980s (chapter 7), with hopes that a comparative analysis might reveal other information about seeding effects. The Texas flare release rate was 50 percent higher than that in Illinois, but the increased activity of the AgI seeding agent used in Illinois may have partially offset this difference, as evidenced by the visible alteration of cloud appearances (chapter 3). Congestus clouds treated in Texas and Illinois were similar in cloud water content and updraft characteristics. Comparison of seeding effects at the cloud (echo-core) scale revealed that neither the Texas nor the Illinois AgI-treated clouds showed the expected growth in height predicted by the dynamic seeding hypothesis. However, the Texas echo cores did show enhanced areal growth after seeding. Comparison of area rainfall results, based on rain from the experimental units in Texas and Illinois (which were very similar in definition) showed that the experimental units treated with AgI may have produced more rain than the sand-treated units in both experiments. The time of the increased rainfall differed between the two experiments: rainfall in Illinois occurred sooner after treatment than it did in Texas. However, the sample of treated units in both states was small, and the findings must be interpreted with great caution.

Rainfall conditions during the 1989 experiment were near average, and area rainfall production on the days of the treated units varied considerably. But on most days, 2.6 mm (1 inch) or more occurred at one or more locations. In an analysis of total rainfall production (chapter 8), values were compared for the five AgI-treated units with complete radar data and the six units treated with sand. The median rainfall of the AgI-treated units was much greater at the end of treatment and 90 minutes thereafter than that of the sand-treated units. At 15 minutes prior to treatment, the median rainfall production of the AgI- and sand-treated units was the same, but rainfall increased during AgI treatment. Also, the rain production of the AgI-treated units was relatively higher than that in the surrounding area (~10 percent), or that of the sand-treated units (~2 percent), suggesting that the rainfall increase in the AgI cases was relatively large with respect to its rain-producing system. But since the sample size was small, the differences were not significant at the 0.05 level. Nevertheless, the results do suggest a positive AgI effect on experimental unit rainfall.

The result of the rainfall analysis showing possible increases in spite of a possible negative cloud effect (if at all) points to the need for improved understanding of multiscale interactions between cloud microphysics processes and cloud-scale kinematics, and the interaction of individual clouds with the larger parent cumulonimbus system. It also points to certain

inadequacies in the single-cloud focus of the dynamic seeding hypothesis and a need to modify the hypothesis for Illinois.

A Possible Alternative Hypothesis

On the basis of the preliminary results of the 1989 PACE field program, an attempt was made to develop a modified hypothesis. A factor to be taken into consideration in addition to the field results is the difficulty of perfectly restricting delivery of the seeding material to the main updraft (i.e., some of the seeding agent inevitably is deposited in downdraft regions or transition zones from downward- to upward-moving air or vice versa). If this is in fact the case, seeding of individual clouds (echo cores) may result in an uneven release of latent heat accompanied by increased turbulence, as Gayet and Soulague (1992) suggested. The effect of uneven latent heat release would be to mix updraft and downdraft regions. Consequently, upward vertical motion would become disorganized rather than being invigorated, as expected from the dynamic seeding hypothesis. The result would be that AgI-treated cores would not reach the maximum height that they would with no seeding.

At the microphysical scale, the seeding agent may have a large initial effect on the smallest supercooled cloud droplets, because 1) the concentration of supercooled cloud droplets is several orders of magnitude greater than that of drizzle and raindrops, and 2) cloud droplets must be in much closer thermoequilibrium with the environment than supercooled drizzle and raindrops, which may be warmer than the environment. Following the discussion in Dennis (1980), estimates based on simple Brownian collection theory indicate that approximately 10,000 supercooled cloud droplets should capture an AgI particle in the same time it takes one raindrop to capture an AgI particle, assuming that the production of ice crystals directly from the AgI particles can be neglected without error. If this does occur, the net consequence would be to stunt the broadening of the particle spectrum by coalescence and riming processes, both of which depend on supercooled cloud droplets as a source for growth. Thus, processes that tend to move condensate into precipitation particle sizes would be restricted in the presence of enhanced latent heat release. This is a critical issue that can and should be addressed in future field programs, and should also be considered in light of the modeling work that pointed to the importance of supercooled drizzle and raindrops as a suitability criterion for dynamic seeding (Lamb et al., 1981).

Thus, with these physical considerations as background, the following revised hypothesis for Illinois is proposed as a basis for future discussion:

- Retain all the cloud selection criteria in the revised seeding hypothesis, and target the updraft regions of clouds with "dropable" 20-g AgI flares at a rate equal to one every 500 to 1000 m of cloud transect, just as it was in the 1989 Illinois field program.

- Upon seeding an individual echo core, supercooled water is rapidly converted to ice in a lower location and earlier than would have occurred naturally.
- The conversion of supercooled water causes a latent heat release.
- Updraft regions cannot be perfectly targeted.
- Imperfect targeting of the seeding agent promotes uneven latent heat release and mixing of updraft and downdraft air, ultimately weakening the cloud's vertical motion and perhaps its overall vertical circulation.
- Consequently, any positive invigorating effect from latent heat release is lost by the negative effect of mixing.
- Mixing has a positive effect in dispersing the seeding material throughout the cloud volume when it is above 0°C before or as the echo core begins its final stage of merger with the main rainstorm.
- The feeder echo core acts as a surrogate for the seeding material, "seeding" the main rain system.
- In turn, seeding of the main rain system may increase rainfall by: 1) introducing graupel embryos into the main storm cloud system earlier and lower than would have occurred naturally, and 2) enhancing conversion of supercooled water to ice in the main rain cloud system.
- Rain production in the main cloud system may benefit microphysically from the advantage that graupel growth has over liquid raindrop growth (Johnson, 1987), and perhaps dynamically from the earlier and lower release of latent heat related to enhanced conversion of liquid to ice.
- Rain enhancement continues as long as AgI treated echo cores seed the main system; upon cessation of treatment, processes in the main system return to their natural course. Thus, rain enhancement occurs only while treatments are delivered.

Therefore, future field programs should be mindful not only of the physical chain of events that occurs at the scale of individual clouds (echo cores), but also those at the scale of the cumulonimbus system and the inherent scale interaction between the two.

Conclusions

In interpreting the many analyses of the 1989 experiment in Illinois, two facts should be kept in mind:

1. The experiment was exploratory and not confirmatory. It was designed primarily to examine the initial steps of the dynamic seeding hypothesis and to gain information relating to further field experimentation and analyzing the data obtained therefrom. The data were examined from many directions, which in essence invalidates decision making based on statistical significance. Results are better considered as guidelines and indications.
2. The 1989 experiment was more successful than the 1986 experiment in gaining a relatively large data sample for

a ten-week period. However, with 12 experimental units, the sample size was not large, and it is certainly unrealistic to attempt to draw significant conclusions, statistically or otherwise. The reader is urged to interpret the various findings with caution. A general interpretation of the total findings is of value nonetheless, particularly for providing guidance for further experimentation and research.

This general assessment of potential seeding effects was based on three different sets of measurements of the treated clouds and the cloud groups with which they were related. First was the assessment of visual cloud characteristics after treatment; second was the extended analysis of the characteristics of echo cores before, during, and after treatment; and third was the investigation of rainfall production from the units.

The visual assessment suggests that AgI applied to cumulus congestus growing above the -10°C level frequently produced changes that were visually detectable by meteorological observers. These results are consistent with the idea that AgI somehow affected cloud behavior.

The echo-core analyses, after considerable adjustment for an unfortunate bad draw, essentially indicated little or no effect in AgI-treated echoes, at least of the type expected after invigoration by dynamic seeding. Even after adjusting for bias, the reactions in echo height, reflectivity, and area did not indicate the expected seeding effect. The major difference occurred in the mean maximum heights of the AgI-treated cores, which were found to be less than those of the sand-treated cores in several analyses. This is contrary to expectations from the dynamic seeding hypothesis.

The third analysis concerned rain yield based on radar measurements of the experimental units and their surrounding areas. Radar-indicated rainfall measurements are limited in their accuracy, a factor that must not be ignored. Further, the comparison of rain yield was based on a small sample, five AgI- and six sand-treated units. The results suggest that the experimental units treated with AgI produced more rain, on the average, than did the sand-treated units. Furthermore, the AgI-related increases occurred at times when the regional rainfall was notably less than that associated with the sand-treated units, further suggesting enhancement effects.

Recommendations

The results of the 1989 field experiment, and those from other PreCCIP/PACE research involving the agricultural effects of added water on crops, leads to certain major recommendations for future research. These recommendations assume that the visual cloud effects noted were correct, that the results for individual echo cores were negative, and that the apparent rainfall enhancement from experimental units did not happen totally by chance. Our recommendations fall into two broad categories: 1) future atmospheric research into the origin and

evolution of growing-season rain clouds and systems, and 2) the practical use of cloud seeding to increase rainfall for crops.

Recommendations for Future Atmospheric Research

Recommendation 1. Future field research should focus on the multiscale nature of cloud and rain systems in Illinois, using AgI not only as a seeding agent that may augment rainfall, but also as a tracer to test and refine conceptual models about natural precipitation mechanisms and cloud and rain system development. Because of limitations in aircraft performance in 1986 and 1989, it was not possible to directly measure the physical effect of the AgI seeding agent on the microphysical and kinematic scale. Therefore, in other field programs on appropriate occasions, the research aircraft should follow the vertical transport of the seeding agent under both seed and placebo conditions to better define internal effects and natural and modified in-cloud processes.

Recommendation 2. While the multiscale nature of cloud and rain systems in Illinois is central to understanding how natural systems may be modified to produce more rain, the result of possible enhanced system rainfall also points to the need to focus on rain production from experimental units. One option would be to design a field program around the use of a high-resolution radar system and a network of raingages to calibrate the radar-estimated rainfall signal. Two specific questions to address might be:

1. Is there a rapid increase in rain during AgI treatment, as noted in 1989?
2. Is the difference in the amount of rain between seeded and placebo rain units 25 percent or more?

The second question addresses a key finding from the corn and soybean research, in that increases of 25 percent or more were required to materially increase crop yields (10 percent was not enough).

Recommendation 3. Future field experimentation should extend beyond the measurement capabilities of radar and aircraft. An alternative interpretation of the 1989 results is that the echo cores and their characteristics were not adequately measured. At the present level of advanced measurement technology, signal-to-noise ratios are still low. Perhaps the radars were too insensitive to measure critical conditions, or the proper in-cloud conditions were not analyzed.

Recommendation 4. Data collected as part of the PACE field programs should continue to be utilized. Because negative findings on echo cores do not agree with the more positive outcome on unit rainfall, conditions not analyzed may reveal explanations for the outcomes. A further analysis of the radar data for the core interactions and the relationship of these cores (both seeded and placebo) should be conducted. Two related analyses of the radar data are warranted, one into the frequency and type of cell mergers, and another into the total number of

cores within areal units. Prior research involving urban effects on summer clouds and precipitation development in St Louis and Chicago found that the areas of locally increased rainfall were strongly related to zones where radar echoes merged more frequently. The former is recommended because merger of convective elements (cells) has long been considered an important feature in rainfall development of convective clouds and is a part of the middle stages of the dynamic seeding hypothesis. Cloud-to-cloud interactions have been enhanced through seeding. This could be a "chemical" effect, in which the seeding material is rapidly shared among several adjacent cores (similar to the findings from the St. Louis tracer experiments), and/or a physical effect, with an increased number of cell mergers and possible cell interactions at levels critical to rainfall development. Future questions to be addressed are:

1. Did the AgI-seeded experimental units produce more cores than the sand-treated units?
2. Did the AgI-seeded units have more cell mergers?
3. How did differences in cores and mergers relate to cold-front and air-mass conditions?
4. How did the cloud system within the treated experimental unit behave in relation to other units that can be identified as control clouds and systems?

Several results indicated that seeding can have drastically different effects under different environmental situations and rainfall rates. Thus, further assessment should be made of experimental units producing light, moderate, and heavy rainfall.

Recommendation 5. Consideration of seeding agents and methods other than those specified by the dynamic seeding hypothesis may be worthy. One option would be to devote some exploratory experimentation to the relative advantages and disadvantages of different seeding agents and delivery systems (AgI flares, wing-tip burners, dry ice, ground-based seeding, cloud-based seeding, hygroscopic seeding, etc.). Moreover, an alternate hypothesis should be developed to recognize more fully simultaneous seeding effects on cloud microphysics and kinematics. Computer modeling studies should also be considered, as well as many other aspects of cloud seeding research.

Recommendation 6. Although PreCCIP/PACE research has advanced forecasting procedures for rain cloud occurrence and some aspects of their suitability for seeding (Scott and Czys, 1992; Czys and Scott 1993), further improvements to short- and long-term forecasting are still needed. Of particular value would be improvements in short-term and long-range (perhaps a week or a month) quantitative precipitation forecasting for areas equivalent to the 1989 PACE study area.

Recommendations on the Practical Use of Cloud Seeding in Illinois

Recommendation 1. If rainfall augmentation for crop production were the objective, a seeding system should be developed to function at night. This is needed because nearly

half of all summer rain falls at night (Changnon 1993), and the current seeding technology initially involves visual selection of suitable clouds.

Recommendation 2. The results from studies of corn and soybean yields from field plot experiments during 1987-1991 (Changnon, 1993) are not encouraging as to the economic benefits from rain enhancement (ten levels were tested, including no increase, and 10, 25, and 40 percent increases). The only added water treatment found better than "no increase" for enhancing yields was a 25 percent increase on days with moderate and heavy rains.

The ability to produce 25 percent rain increases was not demonstrated from the 1986 and 1989 experimental research, although certain commercial cloud seeders claim this level of modification can be attained. Past projects in Illinois do not support this claim (Changnon and Hsu, 1981). Regardless, if this rain enhancement had been applied in central Illinois during 1987-1991, it would have increased average annual income by \$3.60 per hectare, which is only 0.4 percent of the total hectare income (\$671).

These studies nevertheless showed the value of using summer rainfall predictions with varying rain modification levels, if they existed. For example, if existing predictions of summer rainfall had been employed (they have a 60 percent skill level) to decide what level of rain enhancement to apply (since some summers are too wet, some need moderate added amounts, and others need large increases), and if a seeding technology existed to increase rain amounts between 1 and 40 percent in any given summer, the expected financial gain would have been \$22.70 per hectare. However, this gain is still only 3.4 percent of the hectare production without a rain increase. Thus, even with a fairly sophisticated enhancement technology capable of targeting summer rainfall increases up to 40 percent, the economic value of the technology is marginal.

Recommendation 3. If cloud seeding is used to enhance summer rainfall, regardless of the economic considerations, certain past findings should be considered:

1. There is no evidence that rainfall enhancement over a sizable area will diminish the rainfall in downwind areas. Extensive Water Survey studies of the summer cloud and rainfall conditions at Chicago and St. Louis

have revealed that these cities both enhance rainfall in certain convective rain situations, producing an average increase of 10 to 25 percent in the total summer rainfall over areas of up to 2000 square miles (Changnon et al., 1981; Changnon, 1984). Importantly, the areas east and beyond these areas of urban-induced increase obtained rainfall matching that west of the cities, and no decrease was detectable, despite the atmosphere's inefficiency in converting available moisture to rainfall.

2. The 1986 and 1989 results are not encouraging about rainfall enhancement from use of the dynamic seeding approach. However, the results did suggest enhancement from dynamic seeding conducted during certain cold-front conditions. These frontal conditions would seem most amenable to enhancement, both from the 1989 results and from the urban results (Changnon et al., 1981). The effects of the static, cloud-base seeding approach have not been tested on Illinois rainfall, believing the dynamic seeding approach was superior for several reasons (Ackerman et al., 1979, 1980). The cloud-base tracer experiments conducted at St. Louis as part of METROMEX revealed that the tracer materials, which were not seeding materials, entered the in-cloud rain process, and 10 to 50 percent of the injected material was found in the rain from the cloud (Changnon and Semonin, 1975a,b). Static seeding may be a choice to consider if cloud seeding is used to enhance summer rain in Illinois.
3. Rainfall enhancement in summer droughts would have value if it could be achieved. However, climatic studies of summer droughts and cloud conditions (Huff and Vogel, 1977) reveal that the number of cloud opportunities for modification are limited. The crop field tests of ten different water additions to actual rainfall during the dry summers of 1988 and 1991 (Hollinger and Changnon, 1993; Changnon and Hollinger, 1993) revealed that the highest addition tested, 40 percent, provided sizable yield increases. The 1988 yield increases were 42 percent to corn and 16 percent to soybeans. Those in 1991 were 10 percent to corn and 5 percent to soybeans.

APPENDIX A. SYNOPTIC VARIABLES, ABBREVIATIONS AND DEFINITIONS

The synoptic variables are all from 0700 CDT Peoria soundings.

An-buff	80-100 nm radius area (not including Indiana, centered on CMI) 24-hr (80-85% 0700obs) station-averaged precipitation on the day prior to the experimental unit (mm).	li	Lifted index (measure of latent instability).
An-targ	80nmradiusarea(notincluding Indiana, centered onCMT) 24-hr (80-85% 0700obs) station-averaged precipitation on the day prior to the experimental unit (mm).	m80	Tallest max radar echo top within 80 nm of CMI observed between 1130 and 1830 CDT at the NWS site (MMO, STL, E W) closest to the echo (kft).
CAPE	Convective available potential energy (m^2s^{-2}).	m100	Tallestmaxradarechotopwithin 100 nm of CMI observed between 1130 and 2030 CDT at the NWS site (MMO, STL, E W) closest to the echo (kft).
cpe	Coalescence precipitation efficiency; relative size of L (%).	mki	Modified K-index.
ct	Convective temperature using average mixing ratio in lowest 100 mb ($^{\circ}C$).	msh	Modified Showalter index (measure of instability).
dbar	Average dewpoint temperature in lowest 100 mb layer ($^{\circ}C$).	pb	Synoptic (parcel) potential buoyancy ($^{\circ}C$).
dh38	Height difference between $-3^{\circ}C$ level and $-8^{\circ}C$ level (m).	pbot	Pressure at the bottom of "positive" area of rawinsonde (mb).
dir50	500-mb wind direction (degrees).	pccl	Pressure of convective condensation level (CCL) using averaged data in lowest 100 mb (mb).
dir85	850-mb wind direction (degrees).	plcl	Pressure of lifting condensation level (LCL) using averaged data in lowest 100 mb (mb).
dpt	Surface dew-point temperature ($^{\circ}C$).	pres0	Pressure of $0^{\circ}C$ level (mb).
EU-buff	80-100 nm radius area (not including Indiana, centered on CMI) 24-hr (80-85% 0700obs) station-averaged precipitation on the experimental unit day (mm).	pres10	Pressure of $-10^{\circ}C$ level (mb).
EU-targ	80nmradiusarea(notincludingIndiana, centered onCMT) 24-hr (80-85% 0700obs) station-averaged precipitation on the experimental unit day (mm).	ptop	Pressureat the top of "positive" area of rawinsonde (mb).
hccl	Height of CCL using averaged data in lowest 100 mb (m).	pw	Precipitable water between the surface and 500 mb (cm).
hgt0	Height of $0^{\circ}C$ level (m).	Ri	Bulk Richardson number, calculated using CAPE and vshr.
hgt10	Height of $-10^{\circ}C$ level (m).	spd50	500-mb wind speed (ms^{-1}).
hlcl	Height of LCL using averaged data in lowest 100 mb (m).	spd85	850-mb wind speed (ms^{-1}).
jef	Jefferson index (measure of instability).	swt	Sweat index (measure of instability).
ki	K-index (heat differential and moisture depth in the lower levels of the atmosphere).	tccl	Temperature of CCL using averaged data in lowest 100 mb ($^{\circ}C$).
L	Index of coalescence activity (raindrop size discriminant function based on tccl and pb).	temp	Surface temperature ($^{\circ}C$)
		tlcl	Temperature of LCL using averaged data in lowest 100 mb ($^{\circ}C$).
		vshr	Vector difference in wind at 4 km and average wind in lowest 500 m (ms^{-1}).

APPENDIX B. RADAR VARIABLES, ABBREVIATIONS AND DEFINITIONS

The synoptic variables are all from 0700 CDT Peoria soundings.

a_aft*	Acceleration of echo top 4 minutes after treatment (km min ⁻²).	CPFEdZ	Change in max reflectivity from first echo to treatment (dBZ).
a_bef	Acceleration of echo top 2 minutes before treatment (km min ⁻²).	CPFEdZ/dt	Rate of change of max reflectivity from first echo to treatment (dBZ min ⁻¹).
a_cdp	Acceleration of echo top at treatment (km min ⁻²).	CPHMxZ	Height of max reflectivity at treatment (km).
ADifeu	Change in experimental unit echo areal coverage from a) 15 minutes prior to first treatment to b) first treatment (km ²).	CPHtp10	Top height of the 10-dBZ contour at treatment (km).
ADiftn	Change in extended area echo areal coverage from a) 15 minutes prior to first treatment to b) first treatment (km ²).	CPmndia	Mean diameter of echo at treatment (Cloud Pass), averaged in height (km).
At-15eu	Experimental unit echo areal coverage 15 minutes prior to first treatment (km ²).	CPMxB	Max brightness at treatment (dBZ).
At-15tn	Extended area echo areal coverage 15 minutes prior to first treatment (km ²).	CPMxMxA*	Time from treatment to max 10-dBZ area (min).
AtCPEu	Experimental unit echo areal coverage at first treatment (km ²).	CPMxMxH*	Time from treatment to max 10-dBZ top height (min).
AtCPTn	Extended area echo areal coverage at first treatment (km ²).	CPMxMxZ*	Time from treatment to max reflectivity (min).
CPA10	Max area of the 10-dBZ contour at treatment (km ²).	CPMxZ	Max reflectivity at treatment (dBZ).
CPA56	Area at flight level at treatment (km ²).	CpStat	Indicator of core merging at treatment (0 = no echo at that time, 1 = isolated, 2 = merged, 4 = no echo ever).
CPA.L1	Area at 1-km level at treatment (km ²).	CPtoFR*	Time from treatment to first rain (min).
CPA.L6	Area near flight level (6 km) at treatment (km ²).	CPZ56	Max reflectivity at flight level at treatment (dBZ).
CPdia.56	Diameter of echo at flight level at treatment (km).	CPZ.L1	Max reflectivity at 1-km level at treatment (dBZ).
CPdia.L6	Diameter of echo near flight level (6 km) at treatment (km).	CPZ.L6	Max reflectivity near flight level (6 km) at treatment (dBZ).
CPFEdA10	Change in area of the 10-dBZ contour from first echo to treatment (km ²).	dA/dt-PO/PR*	Ratio of rates of change of echo area from a) treatment to time of max area and b) first echo to treatment (a/b).
CPFEdA/dt	Rate of change of 10-dBZ area from first echo to treatment (km ² min ⁻¹).	dA-PO/PR*	Ratio of max area changes from a) treatment to time of max area and b) first echo to treatment (a/b).
CPFEdB	Change in max brightness from first echo to treatment (dBZ).	dH/dt-PO/PR*	Ratio of rates of change of echo height from a) treatment to time of max height and b) first echo to treatment (a/b).
CPFEdH10	Change in top height of the 10-dBZ contour from first echo to treatment (km).	dH-PO/PR*	Ratio of echo height changes from a) treatment to time of max height and b) first echo to treatment (a/b).
CPFEdH/dt	Rate of change of 10-dBZ top height from first echo to treatment (km min ⁻¹).	dZ/dt-PO/PR*	Ratio of rates of change of max reflectivity from a) treatment to time of max reflectivity and b) first echo to treatment (a/b).

* Response variable

dZ-PO/PR*	Ratio of changes of max reflectivity from a) treatment to time of max reflectivity and b) first echo to treatment (a/b).	MaxH10*	Maximum top height of the 10-dBZ reflectivity contour (km).
FEA10	Max area of the 10-dBZ contour at first echo (km ²).	MXCPdA10*	Change in area of the 10-dBZ contour from treatment to max area (km ²).
FEbsTmp	Temperature at base of echo at first echo (°C).	MXCPdA/dt*	Rate of change of echo area from treatment to max area (km ² min ⁻¹).
FECPt	Time from first echo to treatment (min).	MXCPdB*	Change in max brightness from treatment to max brightness (dBZ).
FEdpth10	Depth of the 10-dBZ contour at first echo (km).	MXCPdH10*	Change in top height of the 10-dBZ contour from treatment to max height (km).
FEHbs10	Base height of the 10-dBZ contour at first echo (km).	MXCPdH/dt*	Rate of change of echo-top height from treatment to max height (km min ⁻¹).
FEHMxZ	Height of max reflectivity at first echo (km).	MXCPdZ*	Change in max reflectivity from treatment to max reflectivity (dBZ).
FEHtp10	Top height of the 10-dBZ contour at first echo (km).	MXCPdZ/dt*	Rate of change of max reflectivity from treatment to max reflectivity (dBZ min ⁻¹).
FEmndia	Mean diameter of echo at first echo, averaged in height (km).	MXFEdA10*	Change in area of the 10-dBZ contour from first echo to max area (km ²).
FEMxB	Max brightness at first echo (dBZ).	MXFEdA/dt*	Rate of change of 10-dBZ echo area from first echo to max area (km ² min ⁻¹).
FEMXtMxA*	Time from first echo to max 10-dBZ area (min).	MXFEdH10*	Change in the 10-dBZ top height from first echo to max height of core (km).
FEMXtMxB*	Time from first echo to max brightness (min).	MXFEdH/dt*	Rate of change of echo-top height from first echo to max height (km min ⁻¹).
FEMXtMxH*	Time from first echo to max height (min).	MXFEdZ*	Change in max reflectivity from first echo to max reflectivity (dBZ).
FEMXtMxZ*	Time from first echo to max reflectivity (min).	MXFEdZ/dt*	Rate of change of max reflectivity from first echo to max reflectivity (dBZ min ⁻¹).
FEMxZ	Max reflectivity at first echo (dBZ).	MxRFx*	Max rain flux of echo core (10 ¹⁰ cm ³ hr ⁻¹).
FEmZTmp	Temperature at the height of the max reflectivity at first echo (°C).	pdeg	Degree of polynomial used to determine velocities and accelerations of echo top before, at, and after treatment.
FeStat	Indicator of core merging at first echo (0=no echo at that time, 1 = separate at all levels, 2 = joined at some levels but can see base and top, 3 = joined at lower levels but can see top, 4 = no echo ever).	range	Distance from airport (radar site) to echo/treatment (km).
FEtoFR	Time from first echo to first rain (min).	RFxt-15eu	Experimental unit rain flux at 15 minutes prior to first treatment (10 ¹⁰ x cm ³ hr ⁻¹).
FEtpTmp	Top of echo temperature at first echo (°C).	RFxt-15tn	Extended area rain flux 15 minutes prior to first treatment (10 ¹⁰ x cm ³ hr ⁻¹).
FEVol10	Volume of the 10-dBZ contour at first echo(km ³).	RFxtCPeu	Experimental unit rain flux at first treatment (Cloud Pass) (10 ¹⁰ x cm ³ hr ⁻¹).
FltAltA	Aircraft-derived aircraft flight level at treatment (km).	RFxtCPTn	Extended area rain flux at first treatment (10 ¹⁰ x cm ³ hr ⁻¹).
FltAltR	Radar (RATS)-derived aircraft flight level at treatment (km).		
FRtoMxRFx*	Time from first rain to max rain flux of echo core (min).		
MaxA10*	Maximum area of the 10-dBZ reflectivity contour (km ²).		
MaxB*	Maximum brightness (dBZ).		
MaxZ*	Maximum reflectivity (dBZ).		

* Response variable

RFxDifeu	Change in experimental unit rain flux from a) 15 minutes before first treatment to b) first treatment ($10^{10} \text{ cm}^3 \text{ hr}^{-1}$).	TotRNVOL*	Total accumulated rain volume of echo core (10^{10} cm^3).
		v_aft*	Velocity of echo top 4 minutes after treatment (km min^{-1}).
RFxDiftn	Change in extended area rain flux from a) 15 minutes prior to first treatment to b) first treatment ($10^{10} \text{ cm}^3 \text{ hr}^{-1}$).	v_bef	Velocity of echo top 2 minutes before treatment (km min^{-1}).
		v_cdp	Velocity of echo top at treatment (km min^{-1}).

* Response variable

APPENDIX C. AIRCRAFT VARIABLES, ABBREVIATIONS AND DEFINITIONS

The synoptic variables are all from 0700 CDT Peoria soundings.

#_SECs	Number of seconds of the longest updraft.	LWCc	Liquid water content by method II (i.e., continuous; area under the line defined by NO_W and lamda_W) (gm^{-3}).
#_Ups	Number of updrafts in cloud (updraft $\geq 1 \text{ ms}^{-1}$ for at least 3 consecutive seconds).	LWCd	Liquid water content by method I (i.e., discrete) (gm^{-3}).
%_in_Up	Percentage of flares released in any updraft.	Max_Conc	Max concentration of cloud droplets in the updraft (cm^{-3}).
%_Updraft	Percent of cloud that is updraft.	Max_Dia	Max diameter of cloud droplet particles (pm).
2DfCnt	Total 2D probe particle count (of ice fragments) in Tconc_f.	Max_FWC	Max liquid water content during updraft from the FSSP probe (gm^{-3}).
2DgCnt	Total 2D probe particle count (of graupel) in Tconc_g.	Max_JWC	Max liquid water content during updraft from the JW probe (gm^{-3}).
2DiCnt	Total 2D probe particle count (of ice crystals) in Tconc_i.	Max_TBuoy	Maximum thermal buoyancy ($^{\circ}\text{C}$) (= Max_ThV - Env_ThetaV).
2DICnt	Total 2D probe particle count (of graupel, fragments, and crystals) in Tconc_I.	Max_ThV	Maximum virtual potential temperature during the updraft (K).
2DPoCnt	Total 2D probe particle count (of particles with depolarization > 0) in Tconc_Po.	Max_VW	Maximum vertical velocity during the updraft (ms^{-1}).
2DW3Cnt	Total 2D probe particle count in Tconc_W3.	Mean_Conc	Mean concentration of cloud droplets in the updraft (cm^{-3}).
2DWCnt	Total 2D probe particle count in Tconc_W.	Mean_Conc_D<13	Mean concentration of cloud droplets $< 13 \mu\text{m}$ in the updraft (cm^{-3}).
Buoy_Enh	Buoyancy enhancement ($^{\circ}\text{C}$) (see Orville and Hubbard, 1973).	Mean_Conc_D>25	Mean concentration of cloud droplets $\geq 25 \mu\text{m}$ in the updraft (cm^{-3}).
C_firs	Number of flares in the cloud.	Mean_Dia	Mean diameter of cloud droplet particles (from FSSP data) (μm).
Cld_Dia	Diameter of cloud (m).	Mean_FWC	Mean liquid water content of the updraft from the FSSP probe (i.e., cloud droplets $\rightarrow D < 45 \mu\text{m}$) (gm^{-3}).
Dmax_I	Maximum diameter of ice particles ($D > 150 \mu\text{m}$) in the updraft (mm).	Mean_JWC	Mean liquid water content of the updraft from the JW probe (i.e., cloud droplets) (gm^{-3}).
Dmax_W	Maximum diameter of supercooled liquid rain/drizzle drop particles (i.e., water with $D > 150 \mu\text{m}$) in the updraft (mm).	Mean_TBuoy	Mean thermal buoyancy ($^{\circ}\text{C}$) (= Mean_ThV - Env_ThetaV).
Env_TC	Temperature of the environment ($^{\circ}\text{C}$) (i.e., 10-consecutive-second mean within 1 minute prior to cloud).	Mean_ThV	Mean virtual potential temperature of the updraft (K).
Env_ThetaV	Mean virtual potential temperature of the environment (K) (i.e., 10-consecutive-second mean within 1 minute prior to cloud).	Mean_VW	Mean vertical velocity (vertical wind) of the updraft (ms^{-1}).
lamda_I	Ice size distribution slope.		
lamda_W	Water size distribution slope.		
Load_I	Loading from ice, solid ($^{\circ}\text{C}$) ($1^{\circ}\text{C} / 2.5 \text{ gm}^{-3}$).		
Load_W	Loading from water, liquid ($^{\circ}\text{C}$) ($1^{\circ}\text{C} / 2.5 \text{ gm}^{-3}$).		

NBuoy	Net buoyancy ($^{\circ}\text{C}$) (= Mean_TBuoy - Load_W - Load_I)	Tconc_I	Total concentration of ice particles in the updraft (L^{-1}).
N0_I	Ice size distribution intercept.	Tconc_Po	Concentration of particles with depolarization signal > 0 in the updraft (L^{-1}).
N0_W	Water size distribution intercept.	Tconc_W	Total concentration of water particles (L^{-1}).
PBuoy	Potential buoyancy ($^{\circ}\text{C}$) (= NBuoy+Buoy_Enh).	Tconc_W3	Total concentration of water particles > 300 μm (L^{-1}).
SWCc	Solid water content by method II (i.e., continuous; area under the line defined by N0_I and lamda_I) (gm^{-3}).	Thres_Dia	Threshold diameter \rightarrow defined such that the total concentration of droplets with diameters \geq Thres_Dia is 3 cm^{-3} , as measured by the FSSP probe (μm) (see Hobbs and Rangno, 1985).
SWCd	Solid water content by method I (i.e., discrete) (gm^{-3}).	U_flrs	Number of flares in the updraft
SWC_frac	Fraction of solid water content [SWCd / (Mean_JWC + LWCd + SWCd)].	U_tem	UP_Dia/1000
Tconc_f	Concentration of ice fragment particles in the updraft (L^{-1}).	UP_Dia	Diameter of the main (broadest or longest) updraft (m) (aircraft's mean airspeed X the number of seconds of updraft).
Tconc_g	Concentration of graupel particles in the updraft (L^{-1}).		
Tconc_i	Concentration of ice crystal particles in the updraft (L^{-1}).		

REFERENCES

- Ackerman, B. 1986. Hypotheses and Cloud Physics Studies. *In Precipitation Augmentation for Crops Experiment: Pre-Experimental Phase Studies*, Illinois State Water Survey Contract Report 404.
- Ackerman, B., Changnon, S.A., and R.G. Semonin. 1980. *Design of the Pre-experimental Phase of the Precipitation Augmentation for Crops Experiment*. Illinois State Water Survey Miscellaneous Publication 54.
- Ackerman, B., R.C. Grosh, and R.Y. Sun. 1979. *Assessing Midwest Cloud Characteristics for Weather Modification*. Illinois State Water Survey Contract Report 216.
- Ackerman, B., and N.E. Westscott. 1986. Midwestern Convective Clouds: A Review. *J. Wea. Mod.* 18:28-35.
- Ackerman, W.C., S.A. Changnon, and R.J. Davis. 1974. The New Weather Modification Law for Illinois. *Bulletin AMS* 44:745-750.
- Battan, L.J. 1953. Observation on the Formation and Spread of Precipitation in Convective Clouds. *J. Meteor.* 10:311-324.
- Beth wait, F.D., E. J. Smith, J.A. Warburton, and K. J. Heffernan. 1966. Effects of Seeding Isolated Cumulus Clouds with Silver Iodide. *J. Appl. Meteor.* 5:513-520.
- Biondini, R., J. Simpson, and W.L. Woodley. 1977. Empirical Predictors for Natural and Seeded Rainfall in the Florida Area Cumulus Experiment (FACE), 1970-1975. *J. Appl. Meteor.* 16:585-594.
- Bluestein, H.B., and M.H. Jain. 1985. Formation of Mesoscale Lines of Precipitation: Severe Squall Lines in Oklahoma during the Spring. *J. Atmos. Sci.* 42:1711-1732.
- Braham, R.R. 1966. *Final Report of Project Whitetop: Part I-Design of the Experiment; Part II-Summary of Operations*. University of Chicago.
- Braham, R.R. 1979. Field Experimentation in Weather Modification. *J. Amer. Statist. Assoc.* 74:57-104.
- Braham, R.R. 1981. *Urban Precipitation Processes*. In *METROMEX: A Review and Summary*. Meteorological Monograph 18, AMS, Boston: 75-116.
- Braham, R.R., and M.J. Dungey. 1978. A Study of Urban Effects on Radar First Echoes. *J. Atmos. Sci.* 17:644-654.
- Braham, R.R., and D. Wilson. 1978. Effects of St. Louis on Convective Cloud Heights. *J. Appl. Meteor.* 17:587-592.
- Byers, H.R., and R.R. Braham. 1949. *The Thunderstorm: Report of the Thunderstorm Project*, U.S. Government Printing Office, Washington DC.
- Changnon, S.A. 1973. Weather Modification in 1972: Up or Down? *Bulletin AMS* 54:642-646.
- Changnon, S.A., 1976: Testimony of Stanley A. Changnon. Weather Modification Hearings, Subcommittee on Environment and the Atmosphere of the Committee on Science and Technology, U.S. House of Representatives, 94th Congress, U.S. Government Printing Office, Washington, D.C., 337-367.
- Changnon, S.A. 1978a. Urban Effects on Severe Local Storms at St. Louis. *J. Appl. Meteor.* 17:578-586.
- Changnon, S.A. 1978b. Vertical Characteristics and Behavior of Radar Echoes. In *Summary of METROMEX, Vol. 2: Causes of Precipitation Anomalies*. Illinois State Water Survey Bulletin 63:274-279.
- Changnon, S.A. 1979. History of Planned Weather Modification Activities and Research at the Illinois State Water Survey, *J. Wea. Mod.* 18:156-165.
- Changnon, S.A. 1980a. The Rationale for Future Weather Modification Research. *Bulletin AMS*. 61:546-551.
- Changnon, S.A. 1980b. Evidence of Urban and Lake Influences on Precipitation in the Chicago Area. *J. Appl. Meteor.* 19:1137-1159.
- Changnon, S.A., 1984: Urban and Lake Effects on Summer Rainfall in the Chicago Area. *Physical Geography* 4:1-23.
- Changnon, S.A. 1993. The Potential Use of Summer Rainfall Enhancement in Illinois. Part II: Integration of Factors Affecting Enhancement Projects and Future Research. *J. Appl. Meteor.* 32:455-461.
- Changnon, S.A., D. Brunkow, R.R. Czys, A. Durgunoglu, P. Garcia, S.E. Hollinger, F.A. Huff, H.T. Ochs, R.W. Scott, and N.E. Westcott. 1987. *Precipitation Augmentation for Crops Experiment: Phase II, Exploratory Research, Year 1*. Illinois State Water Survey Contract Report 430.
- Changnon, S.A., Czys, R.R., S.E. Hollinger, F.A. Huff, K.E. Kunkel, M.S. Petersen, R.W. Scott, D.W. Staggs, and N.E. Westcott. 1991b. *Analysis and Planning for Precipitation Augmentation for Crops Experiment*. Illinois State Water Survey Contract Report 558.

- Changnon, S.A., R.R. Czys, S.E. Hollinger, F.A. Huff, M.S. Petersen, R.W. Scott, D.W. Staggs, and N.E. Westcott. 1990. *Analysis and Planning for Precipitation Augmentation for Crops Experiment*. Illinois State Water Survey Contract Report 557.
- Changnon, S.A., R.R. Czys, F.A. Huff, E.A. Mueller, J.B. Nespor, R.W. Scott, and N.E. Westcott. 1989. *Operations Manual: The Precipitation Augmentation for Crops Experiment - 1989, Phase II: Exploratory Modification Phase*. Illinois State Water Survey Miscellaneous Publication 143.
- Changnon, S.A., R.R. Czys, R.W. Scott and N.E. Westcott. 1991a. The Illinois Precipitation Modification Program. *Bulletin AMS* 17:587-604.
- Changnon, S.A., and S.E. Hollinger. 1993. The Potential Use of Summer Rainfall Enhancement in Illinois. Part I: A Field Experiment to Define Responses of Crop Yields to Increased Rainfall. *J. Appl. Meteor.* 32:445-54.
- Changnon, S.A., and C.F. Hsu. 1981. *Evaluation of the Illinois Weather Modification Projects, 1976-1980*. Illinois State Water Survey Circular 148.
- Changnon, S.A., and F.A. Huff. 1980. *Review of Illinois Summer Rain Conditions*. Illinois State Water Survey Bulletin 64.
- Changnon, S.A., and H. Lambright. 1987. Rise and Fall of Federal Weather Modification Policy. *J. Wea. Mod.* 19:1-12.
- Changnon, S.A., and G. Morgan. 1976. *Design of an Experiment to Suppress Hail in Illinois*. Illinois State Water Survey Bulletin 61.
- Changnon, S.A., and R.G. Semonin. 1975a. METROMEX: Lessons for Precipitation Enhancement in the Midwest. *J. Wea. Mod.* 7:77-87.
- Changnon, S.A., and R.G. Semonin. 1975b. *Studies of Selected Precipitation from METROMEX*. Illinois State Water Survey Report of Investigation 81.
- Changnon, S.A., R.G. Semonin, A.H. Auer, R.R. Braham, and J. Hales. 1981. *METROMEX: A Review and Summary*. Meteorological Monograph 18, AMS, Boston.
- Changnon, S.A., J.L. Vogel, F.A. Huff, and D.A. Brunkow. 1980. *Hydrometeorological Studies Addressing Urban Water Resource Problems*. Illinois State Water Survey Contract Report 238.
- Cooper, W.A., and R. P. Lawson. 1984. Physical Interpretation of Results from the HIPLEX-IE Experiment. *J. Appl. Meteor.* 23:523-540.
- Czys, R.R., 1991: A Preliminary Appraisal of the Microphysical Nature and Seedability of Warm Based Midwest Clouds at -10°C. *J. Wea. Mod.* 23:1-17.
- Czys, R.R., S.A. Changnon, M.S. Petersen, R.W. Scott, and N.E. Westcott. 1992. Initial Results from the 1989 Cloud Seeding Experiment in Illinois. *J. Wea. Mod.* 24:13-18.
- Czys, R.R., S.A. Changnon, M.S. Petersen, R.W. Scott, and N.E. Westcott. 1993. *The 1989 Precipitation Augmentation for Crops Experiment (PACE) Data Book*. Illinois State Water Survey Miscellaneous Publication 144.
- Czys, R.R., and R.W. Scott. 1993. A Simple Objective Method Used to Forecast Convective Activity during the 1989 PACE Cloud Seeding Experiment. *J. Appl. Meteor.* 32:996-1005.
- Dennis, A.S. 1980. *Weather Modification by Cloud Seeding*. Academic Press, New York.
- Dennis, A.S., and A. Koscielski. 1969. Results of a Randomized Cloud Seeding Experiment in South Dakota, *J. Appl. Meteor.* 8:556-565.
- Dennis, A.S., and A. Koscielski. 1972. Height and Temperature of First Echoes in Unseeded and Seeded Convective Clouds in South Dakota. *J. Appl. Meteor.* 11:994-1000.
- Dennis, A.S., J.R. Miller, E.I. Boyd, and D.E. Cain. 1975. *Effects of Cloud Seeding on Summertime Precipitation in North Dakota*. Bureau of Reclamation Report 75-1, South Dakota School of Mines, Rapid City.
- Flueck, J.A. 1971. *Final Report of Project Whitetop: Part V - Statistical Analysis for the Ground Level Precipitation Data*. The University of Chicago.
- Fovell, R.G., and Y. Ogura. 1989. Effects of Vertical Shear on Numerically Simulated Storm Structure. *J. Atmos. Sci.* 46:3144-3176.
- Gagin, A., D. Rosenfeld, and R. Lopez. 1986a. The Relationship between Height and Precipitation Characteristics of Summertime Convective Cells in South Florida. *J. Atmos. Sci.* 42:84-94.
- Gagin, A., D. Rosenfeld, W.L. Woodley, and R.E. Lopez. 1986b. Results of Seeding for Dynamic Effects on Rain-Cell Properties in FACE-2. *J. Appl. Meteor.* 25:3-13.
- Garcia, P., M. Pinar, and S.A. Changnon. 1990. Economic Effects of Precipitation Enhancement in the Com Belt. *J. Applied Meteor.* 29:63-75.
- Gayet, J.-F., and R.G. Soulage. 1992. Observation of High Ice Particle Concentrations in Convective Cells and Cloud Glaciation Evolution. *Quart. J. Roy. Meteor. Soc.* 118:177-190.
- Hallett, J., R.I. Sax, D. Lamb, and A.S. Ramachandra Murty. 1978. Aircraft Measurements of Ice in Florida Cumuli. *Quart. J. Roy. Meteor. Soc.* 104:631-651.
- Hiser, H.W. 1956. Type Distribution of Precipitation at Selected Stations in Illinois. *Trans. AGU* 37:421-424.

- Hobbs, P.V. 1969. Ice Multiplication in Clouds. *J. Atmos. Sci.* 26:315-318.
- Hobbs, P.V., and A.L. Rangno. 1985. Ice Particle Concentrations in Clouds. *J. Atmos. Sci.* 43:2523-2549.
- Hollinger, S.E., and S. A. Changnon. 1993. *Response of Corn and Soybean Yields to Precipitation Augmentation, and Implications for Weather Modification in Illinois*. Illinois State Water Survey Bulletin, in press.
- Hudak, D.R., and R. List 1988. Precipitation Development in Natural and Seeded Cumulus Clouds in Southern Africa. *J. Appl. Meteor.* 27:734-756.
- Hudson, H.E., G.E. Stout, and F.A. Huff. 1952. *Studies of Thunderstorm Rainfall with Dense Raingage Networks and Radar*. Illinois State Water Survey Report of Investigation 13.
- Huff, 1969: Climatological Assessment of Natural Precipitation Characteristics for Use in Weather Modification. *J. Appl. Meteor.* 8:401-410.
- Huff, F.A., and S.A. Changnon. 1972. Evaluation of Potential Effects of Weather Modification on Agriculture in Illinois. *J. Appl. Meteor.* 11:376-384.
- Huff, F.A., and P.T. Schickendanz. 1970. *Sampling Requirements in the Verification of Precipitation Modification Experiments In Rainfall Evaluation Studies, Part 2*. Illinois State Water Survey Contract Report 114.
- Huff, F.A., and J. Vogel. 1977. *Assessment of Weather Modification in Alleviating Agricultural Water Shortages during Droughts*. Illinois State Water Survey Contract Report 195.
- Johnson, D.B. 1987. On the Relative Efficiency of Coalescence and Riming. *J. Atmos. Sci.* 44:1671-1680.
- Kennedy, P.C., N.E. Westcott, and R.W. Scott. 1989. *Single Doppler Radar Observations of a Mini-Tornado*. Preprint, 16th Conf. on Severe Local Storms. AMS, Boston:209-212.
- Kingsmill, D.E., and R.M. Wakamoto. 1991. Kinematic, Dynamic, and Thermodynamic Analysis of a Weakly Sheared Severe Thunderstorm over Northern Alabama. *Mon. Wea. Rev.* 119:262-297.
- Knapp, V., A. Durgunoglu, and S.A. Changnon. 1988. Effects of Added Summer Rainfall on the Hydrologic Cycle of Midwestern Watersheds. *J. Wea. Mod.* 20:67-74.
- Knight, C, and L.J. Miller. 1992. CP-2 Radar in CAPE Solves Cloud Echo Puzzle. *ATD Observer*, Atmos. Tech. Division, NCAR:1-3.
- Kraus, T.W., R.T. Bruintjes, and J. Verlinde. 1987. Microphysical and Radar Observations of Seeded and Nonseeded Continental Cumulus Clouds. *J. Appl. Meteor.* 26:585-606.
- Lamb D., J. Hallett, and R.I. Sax. 1981. Mechanistic Limitations to the Release of Latent Heat during the Natural and Artificial Glaciation of Deep Convective Clouds. *Quart. J. R. Met. Soc.* 107:935-954.
- Lemone, MA. 1989. The Influence of Vertical Wind Shear on the Diameter of Cumulus Clouds in COPE. *Mon. Wea. Rev.* 117:1480-1491.
- Marwitz, J.D. 1972. The Structure and Motion of Severe Hailstorms. Part II. Multi-Cell Storms. *J. Appl. Meteor.* 11:180-188.
- Mather, G.K., B.J. Morrison, and G.M. Morgan. 1986a. A Preliminary Assessment of the Importance of Coalescence in Convective Clouds. *J. Atmos. Sci.* 20:29-47.
- Mather, G.K., B.J. Morrison, and G.M. Morgan. 1986b. A Preliminary Assessment of the Importance of Coalescence in Convective Clouds of the Eastern Transvaal. *J. Appl. Meteor.* 25:1780-1784.
- Montcrieff, M.W., and J.S.A. Green. 1972. The Propagation and Transfer Properties of Steady Convective Overtuning in Shear. *Quart. J. Roy. Meteor. Soc.* 98:336-352.
- Morrison, B.J., G.K. Mather, and G. Morgan. 1986. *Aircraft Observations of Target Turrets on Multicellular Storms Showing Radar Response to Dry Ice Seeding*. Preprint, 10th Conf. on Weather Modification, AMS, Boston:204-209.
- Mossop, S.C. 1970. Concentrations of Ice Crystals in Clouds. *Bulletin AMS* 51:474-479.
- Mossop, S.C. 1985a. The Origin and Concentration of Ice Crystals in Clouds. *Bulletin AMS* 66:264-273.
- Mossop, S.C. 1985b. Microphysical Properties of Supercooled Cumulus Clouds in which an Ice Particle Multiplication Process Operated. *Quart. J. Roy. Meteor. Soc.* 111:183-198.
- Newton, C.W., and H.R. Newton. 1959. Dynamical Interactions Between Large Convective Clouds and Environment with Vertical Shear. *J. Meteor.* 16:483-496.
- Orville, H.D. 1986. *A Review of Dynamic Mode Seeding of Summer Cumuli in Precipitation Enhancement-A Scientific Challenge*. Meteorological Monograph 21, AMS, Boston: 43-62.
- Orville, H.D., and K. Hubbard. 1973. On the Freezing of Liquid Water in a Cloud. *J. Appl. Meteor.* 12:671-676.
- Peppier, R.A. 1988. *A Review of Static Stability Indices and Related Thermodynamic Parameters*. Illinois State Water Survey Miscellaneous Publication 104.
- Peppler, R.A., and P.J. Lamb. 1989. Tropospheric Static Stability and Central North American Growing Season Rainfall. *Mon. Wea. Rev.* 117:1156-1180.

- Petersen, R. 1984. Triple Doppler Radar Analysis of Discretely Propagating Multicell Convective Storms. *J. Atmos. Sci.* 41:2973-2990.
- Politovich, M.K., and R.F. Reinking. 1987. *Characteristics of Updrafts in Central Illinois Cumuli*. Preprint, 11th Conf. on Weather Modification. AMS, Boston:68-71.
- Rangno, A.L., and P.V. Hobbs. 1990. Rapid Development of High Ice Particle Concentrations in Small Polar Maritime Cumuliform Clouds. *J. Atmos. Sci.* 47:2710-2722.
- Rosenfeld, D. 1987. Objective Method for Analysis and Tracking of Convective Cells as Seen by Radar. *J. Atmos. Oceanic Technol.* 4: 422-434.
- Rosenfeld, D., and W.L. Woodley. 1989. Effects of Cloud Seeding in West Texas. *J. Appl. Meteor.* 28:1050-1080.
- Rotunno, R., J.B. Hemp, and M.L. Weisman. 1988. A Theory for Strong, Long-Lived Squall Lines. *J. Atmos. Sci.* 45:463-485.
- Scott, R.W., and R.R. Czys. 1992. Objective Forecasting of Some Individual Cloud Characteristics in the 1989 Illinois Cloud Seeding Experiment *J. Wea. Mod.* 24:1-12.
- Scott, R. W., and F.A. Huff. 1987. *PACE 1986 Forecasting Program Design, Operations, and Assessment*. Preprint, 11th Conf. on Weather Modification. AMS, Boston:102-105.
- Simpson, J., 1980: Downdrafts as Linkages in Dynamic Cumulus Seeding Effects. *J. Appl. Meteor.* 19:477-487.
- Simpson, J., G.W. Brier, R.H. Simpson. 1967. Stormfury Cumulus Seeding Experiment. 1965. Statistical Analysis and Main Results. *J. Atmos. Sci.* 24:508-521.
- Simpson, J., and A.S. Dennis. 1974. Cumulus Clouds and their Modification. In *Weather and Climate Modification*, W.N. Hess, Ed. John Wiley and Sons, New York.
- Simpson, J., and W. L. Woodley. 1971. Seeding Cumulus in Illinois: New 1970 Results. *Science* 172:117-126.
- Smith, P.L., J.R. Miller, J.H. Hirsch. 1986. *Dynamic versus Microphysical Effects of Seeding: Some Cloud Model and Radar Observations*. Preprints 10th Conf. on Weather Modification, AMS, Boston: 175-178.
- Smith, T.B., R.L. Peace, and S.N. Howard. 1977. *Radar Evaluation of Big Spring Weather Modification Program*. LP-5. Texas Dept. of Water Res., Austin.
- Towery, N.G., and S.A. Changnon. 1970. Characteristics of Hail Producing Radar Echoes in Illinois. *Mon. Wea. Rev.* 98:346-353.
- Vogel, J.L. 1977. *Synoptic Weather Relations. In Summary of METROMEX, Volume 1: Weather Anomalies and Impacts*, Illinois State Water Survey Bulletin 62.
- Weather Modification Advisory Board (WMAB). 1978. *The Management of Weather Resources: Proposals for a National Policy and Program*. NOAA/Dept. of Commerce, Washington, DC.
- Weisman, M.L., and J.B. Klemp. 1982. The Dependence of Numerically Simulated Convective Storms on Vertical Wind Shear and Buoyancy. *Mon. Wea. Rev.* 110:504-520.
- Weisman, M.L., and J.B. Klemp. 1984. The Structure and Classification of Numerically Simulated Convective Storms in Directionally Varying Wind Shears. *Mon. Wea. Rev.* 112:2479-2498.
- Weisman, M.L., J.B. Klemp, and R. Rotunno. 1988. Structure and Evolution of Numerically Simulated Squall Lines. *J. Atmos. Sci.* 45:1990-2013.
- Westcott, N.E. 1990. Radar Results of the 1986 Exploratory Field Program Relating to the Design and Evaluation of PACE. *J. Wea. Mod.* 22:1-17.
- Westcott, N.E., and P.C. Kennedy. 1989. Cell Development and Merger in an Illinois Thunderstorm Observed by Doppler Radar. *J. Atmos. Sci.* 46:117-131.
- Woodley, W.L. 1970. Rainfall Enhancement by Dynamic Cloud Modification. *Science* 170:127-131.
- Woodley, W.L., and R.I. Sax. 1976. *The Florida Area Cumulus Experiment: Rationale, Design, Procedures, Results and Future Course*. NOAA Tech Rep. ERL 354-WMP06.

